

In compliance with the
Canadian Privacy Legislation
some supporting forms
may have been removed from
this dissertation.

While these forms may be included
in the document page count,
their removal does not represent
any loss of content from the dissertation.

**HYPER-SPECTRAL REMOTE SENSING FOR WEED AND
NITROGEN STRESS DETECTION**

by

Pradeep Kumar Goel

Department of Agricultural and Biosystems Engineering
Macdonald Campus of McGill University
Montreal, Canada

April, 2003

A thesis submitted to the Faculty of Graduate Studies and Research in partial
fulfillment of the requirements for the degree of

Doctor of Philosophy

© Pradeep Kumar Goel, 2003



National Library
of Canada

Bibliothèque nationale
du Canada

Acquisitions and
Bibliographic Services

Acquisitons et
services bibliographiques

395 Wellington Street
Ottawa ON K1A 0N4
Canada

395, rue Wellington
Ottawa ON K1A 0N4
Canada

Your file *Votre référence*

ISBN: 0-612-88478-3

Our file *Notre référence*

ISBN: 0-612-88478-3

The author has granted a non-exclusive licence allowing the National Library of Canada to reproduce, loan, distribute or sell copies of this thesis in microform, paper or electronic formats.

L'auteur a accordé une licence non exclusive permettant à la Bibliothèque nationale du Canada de reproduire, prêter, distribuer ou vendre des copies de cette thèse sous la forme de microfiche/film, de reproduction sur papier ou sur format électronique.

The author retains ownership of the copyright in this thesis. Neither the thesis nor substantial extracts from it may be printed or otherwise reproduced without the author's permission.

L'auteur conserve la propriété du droit d'auteur qui protège cette thèse. Ni la thèse ni des extraits substantiels de celle-ci ne doivent être imprimés ou autrement reproduits sans son autorisation.

Canada

ABSTRACT

This study investigated the possibility of using data, acquired from airborne multi-spectral or hyper-spectral sensors, to detect nitrogen status and presence of weeds in crops; with the ultimate aim of contributing towards the development of a decision support system for precision crop management (PCM).

A 24-waveband (spectrum range 475 to 910 nm) multi-spectral sensor was used to detect weeds in corn (*Zea mays* L.) and soybean (*Glycine max* (L.) Merr.) in 1999. Analysis of variance (ANOVA), followed by Scheffe's test, were used to determine which wavebands displayed significant differences in aerial spectral data due to weed treatments. It was found that the radiance values were mainly indicative of the contribution of weeds to the total vegetation cover in various plots, rather than indicative of changes in radiance of the crops themselves, or of differences in radiance between the weed populations and the crop species.

In the year 2000, a 72-waveband (spectrum range 407 to 949 nm) hyper-spectral sensor was used to detect weeds in corn grown at three nitrogen levels (60, 120 and 250 kg N/ha). The weed treatments were: no control of weeds, control of grasses, control of broadleaved weeds and control of all weeds. Imagery was acquired at the early growth, tassel, and fully-mature stages of corn. Hyper-spectral measurements were also taken with a 512-waveband field spectroradiometer (spectrum range 270 to 1072 nm). Measurements were also carried out on crop physiological and associated parameters. ANOVA and contrast analyses indicated that there were significant ($\alpha=0.05$) differences in reflectance at certain wavebands, due to weed control strategies and nitrogen application rates. Weed controls were best distinguished at tassel stage. Nitrogen levels were most closely related to reflectance, at 498 nm and 671 nm, in the aerial data set. Differences in other wavebands, whether related to nitrogen or weeds, appeared to be dependent on the growth stage. Better results were obtained from aerial than ground-based spectral data.

Regression models, representing crop biophysical parameters and yield in terms of reflectance, at one or more wavebands, were developed using the maximum r^2 criterion. The coefficients of determination (r^2) were generally greater than 0.7

when models were based on spectral data obtained at the tassel stage. Models based on normalized difference vegetation indices (NDVI) were more reliable at estimating the validation data sets than were the reflectance models. The wavebands at 701 nm and 839 nm were the most prevalent in these models.

Decision trees, artificial neural networks (ANNs), and seven other classifiers were used to classify spectral data into the weed and nitrogen treatment categories. Success rates for validation data were lower than 68% (mediocre) when training was done for all treatment categories, but good to excellent (up to 99% success) for classification into levels of one or the other treatment (i.e. weed or nitrogen) and also classification into pairs of levels within one treatment. Not one classifier was determined best for all situations.

The results of the study suggested that spectral data acquired from airborne platforms can provide vital information on weed presence and nitrogen levels in cornfields, which might then be used effectively in the development of PCM systems.

RÉSUMÉ

Cette étude vise l'évaluation du potentiel d'un système de télédétection en surface ou par spectromètre imageur aéroporté soit multispectral ou en hyperspace spectral, pour la détection de mauvaises herbes lors des cultures sous divers régimes de fertilisation azotée. La finalité de cette étude serait de contribuer au développement d'un système de surveillance des cultures dans un cadre de l'agriculture de Précision.

Durant la première année de l'étude (1999), un système d'aérophotogrammétrie multispectral (24-gammes d'ondes de 475 à 910 nm) servit à détecter les mauvaises herbes dans des champs de maïs (*Zea mays* L.) et de soja (*Glycine max* Merr.). Une analyse de variance suivie d'un test de Scheffe furent choisis pour déterminer laquelle des gammes d'ondes a présenté une différence significative quant aux représentations spectrales aériennes causées par les traitements de désherbage. L'analyse de cette saison de culture propose que les valeurs de radiance ont démontré la contribution des mauvaises herbes à la couverture végétative de plusieurs parcelles plutôt que d'être indicateur d'un changement de la radiance spectrale des cultures ou d'un changement de radiance entre les mauvaises herbes et les différentes cultures.

En 2000, un imageur spectrographique compact aéroporté fut employé pour acquérir des données dans un hyperspectrales de 72 bandes étroites dans les régions du visible et de l'infrarouge proche (409 nm à 947 nm), à trois stades phénologiques durant la saison de croissance (début de la croissance, stade de la panicule et à pleine maturité), afin de détecter les mauvaises herbes dans une culture de maïs sous quatre stratégies de gestion des mauvaises herbes: aucun contrôle, contrôle des graminées, contrôle des dicotylédones et contrôle complet des mauvaises herbes, et ce à des niveaux de fertilisation azotée de 60, 120, et 250 kg ha⁻¹. La collecte des données dans un hyperspectrales se fit aussi sur le terrain avec un spectroradiomètre mobile à 512 bandes étroites, d'une gamme de 270 nm à 1072 nm. De plus, divers paramètres physiologiques du maïs et paramètres associés à la croissance furent mesurés. L'analyse de variance et l'analyse des contrastes indiquent une différence significative

($\alpha = 0.05$) du facteur de réflexion à certaines gammes d'ondes en raison des différentes stratégies de contrôle de la mauvaise herbe et des régimes de fertilisation azotée. Le contrôle des mauvaises herbes s'est mieux distingué au stade de croissance de la panicule. Les niveaux d'azote ont été plus justement associés à la réflectance à 498 nm et 671 nm. Les différences notées à différentes gammes d'ondes, reliées aux mauvaises herbes ou au taux d'azote, semblent être directement influencées par le niveau de maturité de la culture. De meilleurs résultats ont été obtenus des données spectrales aériennes plutôt que des observations au sol.

Plusieurs relations fonctionnelles furent établies entre les paramètres biophysiques de la culture et les données spectrales en se basant sur les valeurs du coefficient de détermination multiple. Les coefficients de détermination (r^2) furent en général supérieurs à 0.7 pour les modèles basés sur des données spectrales prises au stade de croissance de la panicule. Les modèles basés sur l'indice de végétation normalisé se sont avérés plus fiables pour l'estimation des données de validation que les modèles basés sur la réflectance. Les gammes d'ondes de 701 nm et 839 nm ont été les plus courantes. Des arbres décisionnels, des réseaux neuronaux artificiels et sept autres classificateurs ont été utilisés pour classifier les données spectrales suivant les catégories de traitement des mauvaises herbes et de fertilisation azotée. La validation des résultats a donné des taux de moins de 68% (médiocre) pour l'ensemble des catégories de traitement, alors que des taux de succès allant jusqu'à 99% ont été obtenus pour la classification de l'un ou l'autre des traitements. Aucun des classificateurs ne s'est démarqué.

Les résultats ont démontré que les données spectrales aériennes peuvent servir les besoins de gestion de l'agriculture de précision en fournissant des données essentielles sur la présence de mauvaises herbes et sur les concentrations en azote des sols en culture.

ACKNOWLEDGEMENTS

I wish to express my sincere gratitude to my thesis supervisor, Dr. Shiv O. Prasher, for his guidance, stimulating suggestions and continuous encouragement throughout this study, and his assistance in the preparation of this manuscript. I appreciated his enthusiasm, patience, humor, and most remarkably, his extraordinary skill in simultaneously conducting research on diverse topics. I very much appreciate the confidence he showed in me for undertaking this research topic.

I would also like to thank the members of my committee, Drs. C. A. Madramootoo, D. L. Smith, J.-A. Landry, and R. B. Bonnell, for their suggestions in the course of this study. Thanks are extended to Dr. G. S. V. Raghavan, Professor and Chairman, Department of Agricultural and Biosystems Engineering, for extending support and encouragement during the entire period of the study. I am indebted to all the secretarial staff, past and present, and students in the Department of Agricultural and Biosystems Engineering, who extended their help and support in carrying out this work and making my stay at Macdonald campus a memorable period of my life.

I sincerely acknowledge the Graduate Studies and Research Office, McGill University, and J.W. McConnell Foundation, the donor agency of the fellowship, for awarding me a McGill Major fellowship for the years 2000-01 and 2001-02.

Two years of research in this project were carried out under the broad framework of a Canadian GEOIDE (Geomatics for Informed Decisions) network-funded research project. I am very thankful to all the team members of this project, especially Dr. A. A. Viau, project leader, Université Laval, for his overall support of the project; Dr. John Miller, York University, for providing hyper-spectral images; Dr. Nicola Tremblay, Agriculture and Agri-Food Canada, for helping in the collection and analysis of plant and soil samples. I would also like to thank the Natural Science and Engineering Research Council (NSERC) of Canada and GEOIDE for funding the project.

I extend my thanks to the Indian Council of Agricultural Research (ICAR), and the Central Soil and Water Conservation Research and Training Institute (CSWCRTI), Dehradun, India, for allowing me to pursue Ph.D. studies at McGill

University. My sincere gratitude goes to Dr. J. S. Samra, Deputy Director General, ICAR, and Dr. V. N. Sharda, Director, CSWCRTI, for their help and encouragement in completing this study and shaping my professional career. In addition, I am thankful to my colleagues and friends, and their families in India, especially for extending their wholehearted support to my family during those ten critical months when I left my wife Reena alone to take care of two little children.

My special thanks are due to Dr. R. M. Patel, who has accompanied me since the inception of the project and not only helped me on many research aspects of the study, but also provided much needed support to overcome many difficulties in my personal life during this period. I would like to extend my sincere thanks to Mr. Yousef Karimi, Miss. P. Bera, Mr. Venkatesh Meda, Dr. R. Bassi, Dr. Kamran Davary, Mr. Marc-David Andrade, Mr. Yoji Yuno, Dr. M. Rashed, Dr. C.-C. Yang, and Mr. Jamshid for their assistance throughout the conception of the project, fieldwork, and preparation of manuscripts.

My great appreciation is also due to Mr. P. Kirby, Mr. James, and Mr. Scott Couture for their assistance in carrying out fieldwork, and to Dr. Xiaomin Zhou for teaching me how to operate many instruments. Appreciation is also expressed for the contribution of all the summer students, who worked in the field during these years. I want to thank Mr. Peter Alvo, Mrs. Olive Moss and Dr. G. T. Dodds for their critical review of the manuscripts presented in the thesis.

I would like to thank my parents, my brother and sisters, and their families, for their support in giving me the courage to follow my dreams throughout these years. Appreciation is also extended to my wife's brother and sisters, and their families, for their support and help during this period.

Finally, I want to specially thank my lovely wife Reena, daughter Pratyasha, and son Pratyush for their love, understanding, forbearance, and support, without which I would have been unable to carry out my Ph.D. studies.

I wish to devote this thesis to my mother, Late Gayatri, whose love, sacrifice, and devotion towards her family is described inadequately by words.

CONTRIBUTION OF AUTHORS

In accordance with the regulations of the faculty of Graduate Studies and Research of McGill University, the following statement from the Guidelines for Thesis Preparation is included.

As an alternative to the traditional thesis format, the dissertation can consist of a collection of papers of which the student is an author or co-author. These papers must have a cohesive, unitary character making them a report of a single program of research. The structure for the manuscript-based thesis must conform to the following:

- 1. Candidates have the option of including, as part of the thesis, the text of one or more papers submitted, or to be submitted, for publication, or the clearly-duplicated text (not the reprints) of one or more published papers. These texts must conform to the "Guidelines for Thesis Preparation" with respect to font size, line spacing and margin sizes and must be bound together as an integral part of the thesis. (Reprints of published papers can be included in the appendices at the end of the thesis.)*
- 2. The thesis must be more than a collection of manuscripts. All components must be integrated into a cohesive unit with a logical progression from one chapter to the next. In order to ensure that the thesis has continuity, connecting texts that provide logical bridges between the different papers are mandatory.*
- 3. The thesis must conform to all other requirements of the "Guidelines for Thesis Preparation" in addition to the manuscripts.*

The thesis must include the following:

- (a) a table of contents;*
- (b) an abstract in English and French;*
- (c) an introduction which clearly states the rationale and objectives of the research;*
- (d) a comprehensive review of the literature (in addition to that covered in the introduction to each paper);*
- (e) a final conclusion and summary;*

4. *As manuscripts for publication are frequently very concise documents, where appropriate, additional material must be provided (e.g., in appendices) in sufficient detail to allow a clear and precise judgment to be made of the importance and originality of the research reported in the thesis.*

5. *In general, when co-authored papers are included in a thesis the candidate must have made a substantial contribution to all papers included in the thesis. In addition, the candidate is required to make an explicit statement in the thesis as to who contributed to such work and to what extent. This statement should appear in a single section entitled "Contributions of Authors" as a preface to the thesis. The supervisor must attest to the accuracy of this statement at the doctoral oral defense. Since the task of the examiners is made more difficult in these cases, it is in the candidate's interest to clearly specify the responsibilities of all the authors of the co-authored papers.*

Manuscripts based on the thesis:

1. Goel, P. K., S. O. Prasher, R. M. Patel, J.-A. Landry, R. B. Bonnell, and A. A. Viau. Classification of hyperspectral data by decision trees and artificial neural networks to identify weed stress and nitrogen status of corn. *Computers and Electronics in Agriculture* 39(2): 67-93.
2. Goel, P. K., S. O. Prasher, J.-A. Landry, R. M. Patel, R. B. Bonnell, A. A. Viau, and J. R. Miller. 2003. Potential of airborne hyperspectral remote sensing to detect nitrogen deficiency and weed infestation in corn. *Computers and Electronics in Agriculture* 38(2): 99-124.
3. Goel, P. K., S. O. Prasher, R. M. Patel, D. L. Smith, and A. DiTommaso. 2002. Use of airborne multi-spectral imagery for weed detection in field crops. *Transactions of the ASAE* 45(2): 443-449.
4. Goel, P. K., S. O. Prasher, J.-A. Landry, R. M. Patel, and A. A. Viau. 2003. Estimation of crop biophysical parameters through airborne hyper-spectral remote sensing. *Transactions of the ASAE* (In press).
5. Goel, P. K., S. O. Prasher, J.-A. Landry, R. M. Patel, and A. A. Viau. Hyperspectral image classification to detect weed infestations and nitrogen status

in corn. *Transactions of the ASAE* (In press).

6. Goel, P. K., S. O. Prasher, J.-A. Landry, R. M. Patel, and A. A. Viau. 2003. Assessment of corn growth parameters through hyperspectral field measurements. (Under preparation).

All the fieldwork, analysis of data, and preparation of above manuscripts were completed by the candidate, P. K. Goel, under the supervision of Dr. Shiv O. Prasher. Dr. Prasher provided the necessary funds, supervisory guidance, and assistance to carry out this research.

Dr. R. M. Patel of the Department of Agricultural and Biosystems Engineering, who helped the conduction of field experiments, was associated with the study during the entire period. The contributions of Dr. D. L. Smith and Dr. A. DiTommaso, from the Department of Plant Science, are recognized for their critical suggestions and help in the collection and interpretation of data, related to crop and weeds during the first year of the study.

Dr. A. A. Viau of the Université Laval was the GEOIDE (Geomatics for Informed Decisions) project leader. He arranged and managed necessary financial and technical resources for the second year of the study. Dr. J.-A. Landry from McGill University helped at various levels in the planning and conducting of the study in the second year. Dr. J. R. Miller of York University, and also members of GEOIDE project, provided the aerial hyper-spectral data for the second year of the study.

TABLE OF CONTENT

ABSTRACT	I
RÉSUMÉ	III
ACKNOWLEDGEMENTS	V
CONTRIBUTION OF AUTHORS	VII
TABLE OF CONTENT.....	X
LIST OF FIGURES.....	XIV
LIST OF TABLES.....	XVI
LIST OF SYMBOLS	XXII
CHAPTER 1	1
INTRODUCTION	1
1.1 Objectives.....	5
1.2 Scope.....	6
1.3 Thesis Organization.....	7
CHAPTER 2	9
LITERATURE REVIEW	9
2.1 Spectral Properties of Vegetation.....	9
2.2 Remote Sensing for Weed Detection.....	12
2.2.1 Weed detection in agricultural fields.....	12
2.2.2 Weed detection in rangelands/grasslands.....	16
2.3 Remote Sensing of Nitrogen Stress in Plants.....	18
2.3.1 Leaf-nitrogen level studies.....	19
2.3.2 Canopy-nitrogen level studies.....	20
2.3.2.1 Studies with ground-based canopy-scale spectral data acquisition systems.....	20
2.3.2.2 Studies with airborne field-scale data acquisition systems.....	24
2.4 Estimation of Vegetation Biophysical Parameters and Yield.....	25
2.5 Vegetation Index	28
2.6 Application of Decision Trees and Artificial Neural Networks (ANNs) in Remote Sensing.....	29
2.6.1 Decision trees.....	29
2.6.2 Artificial neural networks (ANNs)	33
2.7 Current Status and Concluding Remarks	37
PREFACE TO CHAPTER 3	38

CHAPTER 3	39
MULTI-SPECTRAL AIRBORNE REMOTE SENSING FOR WEED DETECTION	39
3.1 <i>Abstract</i>	39
3.2 <i>Introduction</i>	40
3.3 <i>Materials and Methods</i>	41
3.3.1 Study site and experiment details	41
3.3.2 Airborne spectral data acquisition	41
3.3.3 Plant parameters.....	42
3.3.4 Observations on weeds	44
3.3.5 Data analysis	46
3.4 <i>Results and Discussion</i>	46
3.4.1 Ground-based observations.....	46
3.4.1.1 Observations on weeds	46
3.4.1.2 Crop physiological parameters	47
3.4.2 Spectral response	50
3.4.3 Suitable wavebands for detection of weeds.....	53
3.4.4 Ratios of wavebands in the red and NIR	57
3.4.5 Relationship between crop physiological parameters and spectral data	60
3.5 <i>Conclusions</i>	65
PREFACE TO CHAPTER 4	67
CHAPTER 4	69
HYPER-SPECTRAL REMOTE SENSING TO DETECT NITROGEN AND WEED STRESSES	69
4.1 <i>Abstract</i>	69
4.2 <i>Introduction</i>	70
4.3 <i>Materials and Methods</i>	71
4.3.1 Experimental design and layout.....	71
4.3.2 Spectral measurements.....	72
4.3.3 Plant parameters.....	77
4.3.4 Observations on weeds	79
4.3.5 Data analysis	83
4.3.5.1 Selection of suitable wavebands	83
4.3.5.2 Estimation of crop biophysical parameters.....	83
4.4 <i>Results and Discussion</i>	86
4.4.1 Selection of wavebands.....	86
4.4.1.1 Early-growth stage	91
4.4.1.2 Tassel stage	98
4.4.1.3 Fully-mature stage	102
4.4.2 Estimation of crop biophysical parameters.....	104
4.4.2.1 Early-growth stage	104
4.4.2.2 Before tassel stage.....	121
4.4.2.3 Tassel stage	121
4.4.2.4 Fully-mature stage	128

4.5 Conclusions.....	135
PREFACE TO CHAPTER 5	138
CHAPTER 5.....	139
APPLICATION OF DECISION TREES AND ARTIFICIAL NEURAL NETWORKS TO CLASSIFICATION OF HYPER-SPECTRAL DATA.....	139
5.1 Abstract.....	139
5.2 Introduction.....	139
5.2.1 A brief overview of decision tree and artificial neural networks.....	141
5.3 Materials and Methods	141
5.3.1 Experimental details.....	141
5.3.2 Acquisition of spectral data	141
5.3.3 Data analysis	141
5.3.3.1 Decision trees.....	142
5.3.3.2 Artificial neural networks	143
5.4 Results and Discussion	143
5.4.1 Decision tree approach.....	143
5.4.1.1 Results based on reflectance at each waveband (sub-plot average)	144
.....	144
5.4.1.2 Results based on twenty randomly selected points in each sub-plot	148
.....	148
5.4.2 Comparison of the decision tree models with ANN models.....	154
5.5 Conclusions.....	159
PREFACE TO CHAPTER 6	161
CHAPTER 6.....	162
IMAGE CLASSIFICATION FOR MAPPING WEEDS AND NITROGEN LEVELS.....	162
6.1 Abstract.....	162
6.2 Introduction.....	162
6.2.1 A brief overview of image classification methods	163
6.3 Materials and Methods	166
6.3.1 Experimental details.....	166
6.3.2 Acquisition of spectral data	166
6.3.3 Data analysis	166
6.4 Results and Discussion	168
6.5 Conclusions.....	181
CHAPTER 7.....	182
SUMMARY AND GENERAL CONCLUSIONS.....	182
7.1 Summary	182
7.2 Conclusions.....	183

CHAPTER 8	189
CONTRIBUTIONS TO KNOWLEDGE AND SUGGESTIONS FOR FUTURE RESEARCH.....	189
<i>8.1 Contributions to Knowledge</i>	<i>189</i>
<i>8.2 Suggestions for Further Research</i>	<i>190</i>
CHAPTER 9	193
REFERENCES	193
APPENDIX-A	210

LIST OF FIGURES

NUMBER		PAGE
Fig. 2.1	Typical reflectance spectra for vegetation, soil, and water	9
Fig. 2.2	Fully grown sample decision tree	31
Fig. 2.3	Structure of an Artificial Neural Network	34
Fig. 3.1	Mean radiance ($\mu\text{W}/\text{cm}^2/\text{sr}/\text{nm}$) of corn under different weed treatments at different wavebands	51
Fig. 3.2	Mean radiance ($\mu\text{W}/\text{cm}^2/\text{sr}/\text{nm}$) of soybean under different weed treatments at different wavebands	52
Fig. 4.1	Spectral response curve for corn under different nitrogen levels and weed control conditions, during the second flight (tassel stage; August 5, 2000)	87-88
Fig. 4.2	Variation in Leaf Area Index (LAI) among various treatments, during different flights	89
Fig. 4.3	Spectral response curve for corn under normal nitrogen (N_{120}) condition, during different flights	92
Fig. 4.4	Variation in corn grain yield among various treatments	103
Fig. 4.5	Observed and predicted crop condition parameters and crop yield, based on airborne spectral observations at the initial stage (June 30, 2000)	108-109
Fig. 4.6	Observed and predicted crop condition parameters and crop yield, based on airborne spectral observations at the tassel stage (August 5, 2000)	126-127
Fig. 4.7	Observed and predicted crop condition parameters and crop yield, based on airborne spectral observations at the fully-mature stage (August 25, 2000)	133-134

LIST OF FIGURES

NUMBER		PAGE
Fig. 6.1	Color-infrared image of experimental plots during the second flight (August 5, 2000, tassel stage). Bands centered at 747 nm, 558 nm, and 490 nm are displayed as red, green, and blue, respectively	169
Fig. 6.2	Field layout indicating the relative location of various weed and nitrogen treatment plots	170
Fig. 6.3	Classification map for nitrogen categories	174-175
Fig. 6.4	Classification map for weed categories	178-179

LIST OF TABLES

NUMBER		PAGE
Table 3.1	Wavebands used to acquire aerial spectral data	43
Table 3.2	Mean monthly temperature, relative humidity, wind speed, and total precipitation during the year 1999 and for a normal year	45
Table 3.3	Weed count in different weed treatments for corn and soybean crops	48
Table 3.4	Details of various measurements of crop parameters and volumetric soil moisture content	49
Table 3.5	Statistical analysis of radiance in different wavebands for corn	54
Table 3.6	Statistical analysis of radiance in different wavebands for soybean	55
Table 3.7	Statistical analysis of radiance ratios in different wavebands for corn	58
Table 3.8	Statistical analysis on radiance ratios of different wavebands for soybean	59
Table 3.9	Correlation coefficient (r) values relating radiance and crop parameters for corn	61
Table 3.10	Correlation coefficient (r) values relating radiance and crop parameters for soybean	62
Table 3.11	Linear regression analysis of spectral data vs. crop condition parameters	64
Table 4.1	Surface soil properties before corn planting	73
Table 4.2	Details of tillage, sowing, fertilization and other cultural operations	74
Table 4.3	Mean monthly temperature, relative humidity, wind speed, and total precipitation during the year 2000 and for a normal year	75

LIST OF TABLES

NUMBER		PAGE
Table 4.4	Wavebands used to acquire aerial spectral data	76
Table 4.5	CASI specification and data processing	78
Table 4.6	Details of various measurements of crop parameters, soil moisture, biomass and yield at different flight times	80-81
Table 4.7	Details of weed type, number, density, and average ground cover in different weed treatments	82
Table 4.8	Statistical significance calculated from ANOVA for main and subplot treatments, interactions and contrasts, (aerial spectral data)	93-94
Table 4.9	Statistical significance obtained from a pairwise comparison of nitrogen fertilization rate means, for different weed control strategies, for bands in which the interaction between weed and nitrogen fertilization treatments was significant, (aerial spectral data)	96
Table 4.10	Statistical significance obtained from a pairwise comparison of weed treatment means, for different nitrogen fertilization levels, for bands in which the interaction between weed and nitrogen fertilization treatment was significant, (aerial spectral data)	97
Table 4.11	Statistical significance calculated from ANOVA for main and subplot treatments, interactions and contrasts, (field spectroradiometer data)	99
Table 4.12	Useful wavebands and corresponding regression equation parameters for the estimation of various crop-condition indicators and other parameters at early-growth stage, using aerial spectral measurements (first flight; June 30, 2000)	106-107

LIST OF TABLES

NUMBER		PAGE
Table 4.13	Sum of squared error (SSE) and average relative percent error (ARPE) values of the best five-parameter models developed using aerial spectral measurements for the estimation of different crop parameters	110
Table 4.14	Nash-Sutcliffe coefficient values for comparison between observed and predicted values of various crop-condition indicator parameters. Prediction results of the best five-parameter regression models and best NDVI-based model for validation data set, (aerial spectral measurements)	111
Table 4.15	Best three useful NDVI indices and corresponding coefficient of determination (r^2) values for the development of regression models, for the estimation of various crop-condition indicator and other canopy parameters at different crop growth stages, (aerial spectral measurements)	112-113
Table 4.16	Regression equation parameters for the best NDVI-based model for the estimation of various crop-condition indicators and other canopy parameters at different crop growth stages, (aerial spectral measurements)	114
Table 4.17	Sum of squared error (SSE) and average relative percent error (ARPE) values of the best NDVI models, developed for the estimation of different crop parameters, (aerial spectral measurements)	115
Table 4.18	Useful wavebands and corresponding regression equation parameters for the estimation of various crop-condition indicators and other parameters, at the early-growth stage for the data acquired from the field spectroradiometer, (first flight; June 30, 2000)	117-118

LIST OF TABLES

NUMBER		PAGE
Table 4.19	Sum of squared error (SSE) and average relative percent error (ARPE) values of the best five-parameter models, developed for the estimation of different crop parameters using spectral values acquired with the field spectroradiometer	119
Table 4.20	Nash-Sutcliffe coefficient values for the best five-parameter regression models developed, using spectral values acquired with the field spectroradiometer	120
Table 4.21	Useful wavebands and corresponding regression equation parameters for the estimation of various crop-condition indicators and other parameters, prior to the tassel stage for the data acquired from the field spectroradiometer, (July 25, 2000)	122
Table 4.22	Useful wavebands and corresponding regression equation parameters for the estimation of various crop-condition indicators and other parameters at the tassel stage, using aerial spectral measurements (second flight; August 5, 2000)	123-124
Table 4.23	Useful wavebands and corresponding regression equation parameters for the estimation of various crop-condition indicators and other parameters at the tassel stage, for the data acquired from the field spectroradiometer, (second flight; August 5, 2000)	129-130
Table 4.24	Useful wavebands and corresponding regression equation parameters for the estimation of various crop-condition indicators and other parameters at the fully- mature stage, using aerial spectral measurements (third flight; August 25, 2000).	131

LIST OF TABLES

NUMBER		PAGE
Table 5.1	Misclassification matrix (decision tree approach) for the detection of various combinations of weed and nitrogen effects, using the average spectral value of each plot for different flights (crossvalidation method)	145-146
Table 5.2	Misclassification matrix (decision tree approach) for the detection of separate weed and nitrogen effects, using average spectral values of each plot for different flights (crossvalidation method)	147
Table 5.3	Misclassification matrix (decision tree approach) for the detection of various combinations of weed and nitrogen effects, using spectral values at 20 points in each plot for different flights (for the unseen data set)	149-150
Table 5.4	Misclassification matrix (decision tree approach) for the detection of separate weed and nitrogen effects, using spectral values at 20 points in each plot for different flights (for the unseen data set)	151-152
Table 5.5	Risk estimate values indicating the performance of different decision trees developed with spectral values at 20 points in each plot	153
Table 5.6	Misclassification matrix (Artificial Neural Networks models) for the detection of various combinations of weed and nitrogen effects, using spectral values at 20 points in each plot for different flights (for the unseen data set)	156-157
Table 5.7	Misclassification matrix (Artificial Neural Networks models) for the detection of separate weed and nitrogen effects, using spectral values at 20 points in each plot for different flights (for the unseen data set)	158

LIST OF TABLES

NUMBER		PAGE
Table 6.1	Accuracy of different image classification methods for nitrogen treatments	172
Table 6.2	The confusion matrix for nitrogen treatments	173
Table 6.3	Accuracy of different image classification methods for weed detection	176
Table 6.4	The confusion matrix for weed detection	177

LIST OF SYMBOLS

To avoid a long list, only the most commonly used symbols, abbreviations and acronyms are listed below. Symbols specific to a particular equation or section, are described at the place of appearance in the text.

μm = micrometer

μmol = micromole

μW = microwatt

$\Delta\lambda$ = difference between two wavelengths

AISA = airborne imaging spectrometer for applications

ANN = artificial neural network

ANOVA = analysis of variance

ARPE = average relative percent error

ASAE = American society of agricultural engineers

AVIRIS = airborne visible/infrared imaging spectrometer

C&RT = classification and regression trees, also called CART

CASI = compact airborne spectrographic imager

CCD = charged coupled device

C_{eff} = Nash-Sutcliffe coefficient

CIR = color infrared

cm = centimeter

CO_2 = Carbon dioxide

CSWCRTI = central soil and water conservation research and training institute

Cu = Copper

DGPS = differential global positioning systems

DN = digital number

DT = decision tree

DVI = difference vegetation index

EOS = earth observing satellites

ERS = European remote sensing satellite

Fe = Iron
fPAR = fractional interception of photosynthetically active radiation
GEOIDE = geomatics for informed decisions
GLM = general linear model
GIS = geographic information system
GPS = global positioning systems
ha = hectare
ICAR = Indian council of agricultural research
IR = reflectance values in infrared
 κ = Kappa coefficient
kg = kilogram
LAI = leaf area index
LANDSAT = land satellite
lat. = latitude
long. = longitude
LSD = least significant difference
m = meter
MAXR = maximum r^2
MINR = minimum r^2
Mn = Manganese
MSAVI = modified soil-adjusted vegetation index
MSS = multispectral scanner
N = nitrogen
n = number of paired observed-simulated values
NDVI = normalized difference vegetation index
NIR = near-infrared
nm = nanometer
NPCI = normalized pigment chlorophyll ratio index
NSERC = natural science and engineering research council
P = probability
PCM = precision crop management

PE = processing element
PNSI = plant spectral nitrogen stress
PRI = physiological reflectance index
PVI = perpendicular vegetation index
R = reflectance values
r = correlation coefficient
 r^2 = coefficient of determination
ROI = region of interest
RMS = root mean square
RVI = ratio vegetation index
SAM = spectral angle mapper
SAR = synthetic aperture radar
SAVI = soil-adjusted vegetation index
SE = standard error
SI = spectral index
SPAD = specialty products agricultural division (chlorophyll meter)
SR = simple ratio index
sr = steradian
SSE = sum of squared error
SVI = simple ratio vegetation index
TM = thematic mapper
TSAVI = transformed soil-adjusted vegetation index
VI = vegetation index
VRT = variable rate technology
WBI = water band index
YI = yellowness index
Zn = Zinc

CHAPTER 1

INTRODUCTION

Responding to the demand for increased food production, together with an ever-growing concern about the negative impact of agriculture on the environment and also decreasing profit margins, is a challenge for today's researchers, policy planners, and producers. Radical philosophical and technological changes are necessary to meet this challenge. Precision agriculture has demonstrated a step in the right direction, because it offers a means to achieve higher crop production and improve environmental quality (Plant, 2001; Stombaugh and Shearer, 2000; Brisco et al., 1998; Tomer et al., 1997).

Precision agriculture is also known as farming by foot (Reichenberger and Russnogle, 1989) and farming by soil (Carr et al., 1991). It may be defined as the application of technology and basic principles in order to manage the spatial and temporal variability associated with all aspects of agricultural production, with the purpose of improving crop performance and environment quality (Pierce and Nowak, 1999). The basic philosophy behind this developing technology is the management of spatial variability of soil properties and the microenvironment in a field settings (Pierce and Nowak, 1999). The current approach of broadcasting fertilizer or herbicides often results in a less than optimal use of these inputs (i.e. under- or over-dosing), increased risk of environmental contamination, and a lower yield per unit of input. The precision approach allocates inputs according to the needs of subdivisions of the cultivated area, where the subdivisions are determined by analysis of the spatial variations of soil and crop conditions. The timing of inputs is subject to temporal changes in crop requirements and such external factors as weather.

There is little doubt that precision management will be the reality of the future, with such new technologies having a drastic impact on farm management (Schilfgaard, 1999). However, the benefits of precision agriculture are yet to be fully realized because the required technologies have yet to be perfected (Pierce and Nowak, 1999). The implementation of precision agriculture systems is being fueled

by the simultaneous development of more precise Differential Global Positioning Systems (DGPS), as well as more powerful Geographic Information Systems (GISs), Variable Rate Technology (VRT), and sensor technology (Stombaugh and Shearer, 2000). However, the successful implementation of a precision agriculture system concurrently requires a system for the measurement and analysis of variability of soil and crop parameters in the field (Pierce and Nowak, 1999). Once acquired, this information must also be available to decision-making software and to the control mechanisms of VRTs used to apply inputs to the field. In order to make the overall system complete, the inclusion of an evaluation system to measure the application efficiency and efficacy of site-specific inputs is necessary.

Accurate mapping of crop variability across fields is essential to the adoption of precision agriculture (Tomer et al., 1997). Because ground collection of site-specific information may be too expensive and time consuming, (Plant, 2001; Senay et al., 1998) as a result considerable work has been done on evaluating the potential of image-based remote sensing (Moran et al., 1997; Hatfield and Pinter, 1993; Stevens, 1993). With satellites and aircraft used as platforms for spectral sensors (GopalaPillai and Tian, 1999), precision farming is now considered to be the most promising area for the application of remote sensing technology, since the inception of environmental resource monitoring by LANDSAT in the early 1970's (Anderson et al., 1999). Images obtained from aircraft-mounted sensors are currently used for time-specific and time-critical precision crop management, because they provide better spectral and spatial resolution and flexibility in operation (Moran et al., 1997); however, it is anticipated that the resolution of satellite imagery will soon become high enough to provide such advantages as lower operating costs and wider spatial coverage.

Remote sensing has already been successfully used to differentiate crops and estimate yields over relatively extensive areas. The analysis of spectral data is currently under investigation with potential of assessing crop health and crop vigor, and also identifying such specific factors detrimental to crop yield as weed infestation and moisture deficit. Such applications may be easily coupled with precision agriculture technology. Another important advantage of remote sensing imagery is

that point measurements may be converted into spatial information more reliably (Brisco et al., 1998). Images taken from aircraft and satellite remote sensing techniques have been successfully used to determine the cultivated area of various crops by using the visible spectrum (Saha and Jonna, 1994) or radar backscatter (Foody et al., 1994; Brown et al., 1984). Numerous studies have focused on forecasting crop yields from remote sensing data (Senay et al., 1998; Moulin et al., 1998; Moran et al., 1995; Delécolle et al., 1992; Bouman, 1992; Klemm and Fagerlund, 1987; Wiegand et al., 1986; Asrar et al., 1985; Crist, 1984; Holben et al., 1980).

The environmental and economic benefits of precision weed management are recognized widely. However, the factor presently limiting the adoption of site-specific application of chemicals for weed management is the absence of a cost-effective technique for weed maps production (Rew et al., 2001; Hall et al., 2000). Many past studies have indicated, with varying degrees of success, the potential of remote sensing technologies to detect weeds in agricultural fields and rangelands (Medlin et al., 2000; Zwiggelaar, 1998; Lass and Callihan, 1997; Lass et al., 1996; Brown and Steckler, 1995; Hanson et al., 1995; Menges et al., 1985; Everitt et al., (1987, 1994, 1995, 1996)). Greater accuracy in weed detection may be achieved, provided that such spectral differences between weeds, crops and soils exist, and are detectable by instruments with sufficient spectral resolution (Lamb and Brown, 2001). Thus, the requirement is higher resolution instruments.

Management of nitrogenous fertilizers for precision agriculture is most crucial due to the direct environmental benefits and the temporal variation in soil-nitrogen availability and crop demand (Pierce and Nowak, 1999). Currently, the most widely used methods to determine variable fertilizer rates are soil testing and yield mapping (Taylor et al., 1998). However, many studies have indicated the potential of spectral measurements to assess nitrogen status in plants. Plants reflect more light in the red and less in the near-infrared regions when nitrogen is limited due to lower chlorophyll content (Serrano et al., 2000). Various reflectance ratios and indices have been used to detect nitrogen deficiencies in plants (Plant et al., 2000; Lukina et al., 2000; Blackmer and White, 1998; Gopala Pillai et al., 1998; Sui et al., 1998; Taylor et al.,

1998; Martin and Aber, 1997; Bausch and Duke, 1996; Blackmer et al., 1996a; Ma et al., 1996; Buschmann and Nagel, 1993). These studies were conducted at the leaf or canopy scale, and with different sensors (ground based and airborne). Researchers achieved mixed success in differentiating nitrogen stress levels and establishing quantitative relationships.

Accurate estimation of within-field spatial variability of crop parameters such as leaf area index (LAI), biomass, disease incidence and severity, and other factors is essential for precision agriculture (Stafford, 1997). Most of these variables are continuous and a functional relationship is required between these variables and spectral and ancillary data (e.g. topography, sun angle, ground data, etc.). Success in deriving characteristics of vegetation from remotely sensed data will determine the utility of remote sensing technologies in vegetation science (Kimes et al., 1998). Prior conversion of remote sensing data into a vegetation index, LAI, nitrogen deficiency, weed density, and soil organic matter is necessary for the proper application of VRT (Frazier et al., 1997). Researchers are therefore attempting to develop quantitative functional relationships between remotely sensed data and crop parameters. The estimation of various biophysical parameters from remotely sensed data is also important in extending the spatial range of the application of crop growth models. A number of studies have demonstrated that there are significant correlations between spectral measurements, crop biophysical parameters and the concentrations of certain biochemicals in plants (e.g. Patel et al., 2001; Inoue et al., 2000; Thenkabail et al., 2000; Cloutis et al., 1999; Jago et al., 1999; Brown et al., 1997; Curran et al., 1997; Cloutis et al., 1996; Inoue and Morinaga, 1995; Munden et al., 1994).

The potential of remote sensing has been clearly established in the acquisition of spatial information on many parameters of agricultural interest. Most research of this kind has been based on color photography, digital photography or videography, or multi-spectral imaging. These photographs have proved useful in the visual interpretation or qualitative assessment of field conditions; however, there has been limited success in quantifying the various objects or parameters of interest. The major drawbacks of these technologies involve the provision of average reflectance values over a limited number of fairly broad wavebands. This results in the loss of spectral

difference existing in narrow wavelength regions, and perhaps answers why it has been difficult to discriminate between objects having subtle differences in their spectral response. Hyper-spectral imaging systems scan a large number of narrow wavebands, thus providing a greater spectral resolution in a cost-effective manner (Lamb and Brown, 2001; Lamb, 1998). For the efficient integration of remote sensing and precision agriculture, data are required at high spectral resolution i.e. in more narrow wavebands (<25 nm) (Anderson et al., 1999). Furthermore, the digital format of remotely sensed spatial data facilitates automated processing (Frazier et al., 1997) and should provide reliability in extracting quantitative information. Studies using handheld spectroradiometers have demonstrated the potential of hyper-spectral measurements in the detection of weeds and nitrogen levels in crops. Hyper-spectral remote sensing has the greatest potential in providing quantitative estimation of many crop growth parameters, but its current limitation is costs (Lamb, 2000). Extension of hyper-spectral technology to an airborne platform is rather challenging and new for many of the applications in agricultural crop monitoring.

Fast processing algorithms are being developed to deal with the large amount of data generated from remote sensing systems. Data-mining techniques and artificial neural networks (ANNs) are now receiving greater attention from the remote sensing community. In remote sensing image analysis, the usefulness of data-mining techniques in general and decision trees in particular, has been demonstrated by some recent studies (Friedl et al., 1999; Soh and Tsatsoulis, 1999; Friedl and Brodley, 1997; Hansen et al., 1996). There has also been some success in the application of ANNs to deal with remote sensing data (Augusteijn and Warrender, 1998; Augusteijn et al., 1995; Danaher et al., 1997; Hepner et al., 1990; Kanellopoulos et al., 1992).

1.1 Objectives

The present project was conceived after envisaging the growing importance of remote sensing in precision agriculture. The ultimate objective of this research was to contribute to the development of a crop monitoring system for precision crop management (PCM) of corn (*Zea mays* L.) production in central Canada. The specific

objectives of the proposed study were:

1. to study the possibility of using multi-spectral and hyper-spectral images, obtained from an airborne platform, in order to monitor crop growth under different weed management conditions and nitrogen fertilization rates,
2. to identify the wavebands and waveband ratios that best permit the recognition of weed infestations and corn nitrogen status at different growth stages,
3. to develop functional relationships between remotely-sensed data and various biophysical crop canopy parameters,
4. to develop models for the prediction of crop yield, based on hyper-spectral measurements acquired from airborne and ground-based sensors,
5. to develop models for the classification of hyper-spectral data, in order to locate weeds and assess nitrogen levels using artificial neural networks (ANNs) and decision trees, and
6. to assess the potential of aerial hyper-spectral imagery, in order to create weed infestation and nitrogen variability maps using different image classification algorithms.

1.2 Scope

Airborne and ground-based sensors were used to acquire spectral data. In the first year, the study focused upon identifying suitable wavelength regions for the detection of different weeds in corn (*Zea mays* L.) and soybeans (*Glycine max* (L.) Merr.). In the second year of the study, emphasis was placed on the selection of suitable wavelength regions, in order to detect different weeds and different nitrogen fertilization levels in corn. In addition, extensive effort involved the development of functional relationships between spectral data and biophysical indicators of crop condition. Various traditional and innovative approaches to classifying spectral data were used to detect weeds and nitrogen levels in corn.

Because crop growth is influenced by numerous, highly variable factors, application of the models developed in this study is limited to the growth conditions in the field, and to the transmission and illumination conditions of the atmosphere, at the times of spectral data acquisition. The findings of this study are also limited to

airborne platforms and should be validated with satellite-based sensors under varying atmospheric and solar illumination conditions. In general, remote sensing approaches are based on the development of models using small areas of imagery, for which ground information is available, and then extending such models to the whole area. Thus, a similar approach is recommended to extend the scope and application of the results of the study to a larger scale and also over time.

1.3 Thesis Organization

This thesis consists of nine chapters. Chapter 1 introduces the subject, and states the objectives and scope of the study. Chapter 2 refers to the relevant and pertinent literature on the subject. Chapter 3 describes the first year of study, which focused on monitoring corn and soybeans under different weed infestation levels. A multi-spectral sensor was used to acquire spectral data. This chapter focuses on the selection of suitable wavelength regions and wavelength ratios in order to detect weed infestations. Results of efforts to estimate crop biophysical parameters, from remotely sensed data, are also presented in this chapter. In this chapter, the section based on the selection of suitable wavebands has been published in the *Transactions of the ASAE* 45(2): 443-449.

Chapters 4 to 6 describe the work carried out in the second year of the study, involving the investigation of the effects of weeds and nitrogen fertilization on the spectral response of a corn canopy. A highly sophisticated hyper-spectral airborne sensor and a hand-held spectroradiometer were used to acquire spectral data. Chapter 4 focuses on the selection of suitable wavelength regions to detect weeds and crop nitrogen status. Also presented here is a comparison between the airborne sensor and hand-held spectroradiometer. In addition, this chapter deals with the development of functional relationships between spectral data and various crop biophysical parameters and includes efforts to provide pre-harvest yield estimates using spectral data. Two papers are based on this chapter, one accepted for publication in *Computer and Electronics in Agriculture*, and the second submitted and under review for publication in *Transactions of the ASAE*.

Chapter 5 focuses on the use of decision trees, a data-mining technique, and

artificial neural networks (ANNs) for classifying highly complex hyper-spectral data in terms of weed infestation and crop nitrogen status. A paper based on this chapter has been accepted for publication in *Computer and Electronics in Agriculture*.

Chapter 6 summarizes the results of work completed on the development of weed and nitrogen maps, using various widely used traditional image classification algorithms and more sophisticated approaches for hyper-spectral image analysis. A manuscript based on this work has been submitted and is under review for publication in *Transactions of the ASAE*.

Finally, Chapter 7 presents a summary and lists the salient conclusions of this research. Chapter 8 outlines the main contributions to knowledge and suggestions for future research. Chapter 9 outlines a comprehensive list of references.

CHAPTER 2

LITERATURE REVIEW

This chapter reviews the literature relevant to the application of remote sensing for weed detection and the assessment of nitrogen levels in vegetation. The first section covers the spectral properties of vegetation. The next section reviews the remote sensing of weeds and of nitrogen status in plants. This discussion is followed by an overview of studies, which were aimed at estimating crop yield and the biophysical parameters of vegetation using spectral data. The fourth section covers applications of decision trees and artificial neural networks (ANNs) for image analysis. This chapter ends with a brief account of the current status of this area of research.

2.1 Spectral Properties of Vegetation

Light impinging on materials is reflected, absorbed and transmitted. The proportion and quality of energy, falling into each of these categories, depends on the surface properties and internal structure of the material, as well as on the angle of incidence. Remote sensing usually involves the measurement and analysis of the reflected radiation. Typical spectra of healthy green vegetation, dry bare soil, and clear water are shown in Figure 2.1.

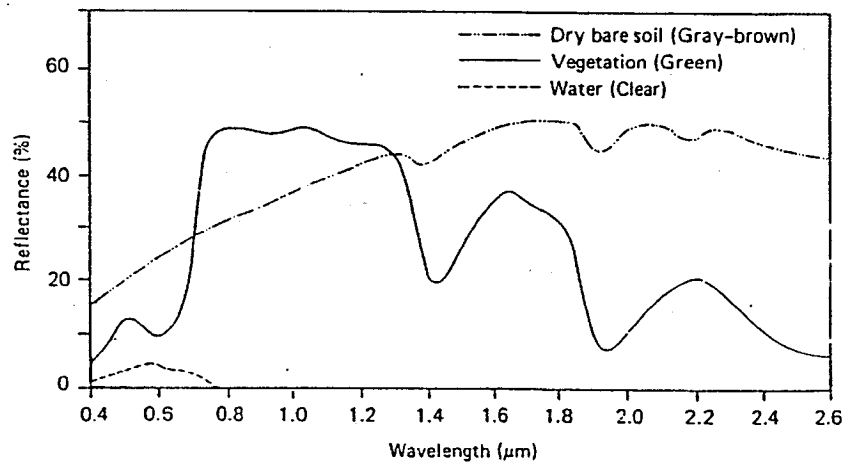


Fig. 2.1 Typical reflectance spectra for vegetation, soil, and water.
(after Swain and Davis, 1978)

Leaves reflect light ranging from the visible to infrared regions (400 to 2500 nm). Reflectance is low in the visible (400 to 700 nm), high in the near-infrared (700-1200 nm), and low in the middle and far infrared (>1200 nm) regions. Important information concerning the structure and physiology of leaves can be related to the spectral responses in the visible and infrared regions, as well as to the differences in spectral response in the red and infrared regions (Peñuelas et al., 1994).

The reflectance spectra are determined in part by the absorbance of important plant pigments and other chemical components. Absorption wavebands of the most relevant components are listed below (after Zwiggelaar, 1998):

chlorophyll a: 435, 670-680, 740 nm;

chlorophyll b: 480, 650 nm;

α -carotenoid: 420, 440, 470 nm;

β -carotenoid: 425, 450, 480 nm;

anthocyanins: 400-550 nm;

lutein: 425, 445, 475 nm;

violaxanthin: 425, 450, 475 nm;

water: 970, 1450, 1944 nm.

It is difficult to obtain plant spectra with sharp absorption peaks, because leaves contain a combination of these chemical components and the wavebands are quite wide. It is now well established that the shape of the reflectance spectra of plants in the visible region are largely determined by green chlorophyll.

The spectral response of plants, and particularly of their leaves, also depends on anatomical features including the physical structure of the plant surface and the cell structure within the leaf (Vogelmann, 1993; Gausman, 1977). The spectral response is also wavelength dependent due to the different refractive indices of cell components (cell wall $n = 1.4$, water $n = 1.3$, and air $n = 1$) and discontinuities in media within leaves (Gausman, 1974; Knipling, 1970). The absorption coefficient, infinite reflectance, and scattering coefficient of the leaves of 30 plant species were determined in a laboratory at seven different wavelengths (Gausman and Allen,

1973). Results indicated that thick, complex, dorsiventral leaves (bifacial mesophyll), such as those found in rubber plants, begonia, sedum and privet, had a lower infinite reflectance and higher absorption coefficient than thinner, less complex, dorsiventral leaves (i.e. soybean, peach, bean, rose). Infinite reflectance was found to be negatively correlated with leaf thickness whereas the absorption coefficient was directly correlated with leaf thickness. However, there was no correlation between the scattering coefficient and leaf thickness.

As earlier mentioned, the chemical components of leaves influence their reflectance spectra. Buschmann and Nagel (1993) determined the reflectance spectra of bean (*Phaseolus vulgaris* L.) leaves with colors varying from yellow to fully-green. In general, the signals were low in the blue (400 to 500 nm) and high in the near-infrared (750 to 800 nm) regions. Higher absorption near 680 nm was associated with higher chlorophyll content. It was also observed that this waveband became broader, and that the point of inflection in the rise from 680 to 750 nm (red edge) shifted to longer wavelengths, with increasing chlorophyll content. Other researchers have also reported a shift of the red edge to longer wavelengths, with an increase in chlorophyll concentration (Vogelmann, 1993; Baret et al., 1992; Horler et al., 1983). Buschmann and Nagel (1993) found that the highest correlation between the reflectance in individual waveband and chlorophyll content was at 550 nm (coefficient of determination, $r^2 = 0.756$). However, much better correlations were obtained with chlorophyll content and functions of the signals at 800 nm and 550 nm ($r^2 = 0.906$ for the difference between the two; $r^2 = 0.942$ for the logarithm of the ratio of the two).

The reflectance spectra of leaves are also affected by water content. Tucker et al. (1980) reported an association between the responses in the near- and middle-infrared regions and the water content of plant tissues. Carlson et al. (1995) found a strong positive correlation between reflectance and water content in corn, soybean, and sorghum (*Sorghum bicolor*) leaves. Buschmann and Nagel (1993) noted that water infiltration in bean leaves resulted in lower reflectance in two wavebands, 500 to 650 nm and 700 to 800 nm. These wavebands are usually characterized by high reflectance.

The interactions of crop or forest canopies with incident radiation are more complex than those of single leaves, because other plant parts also affect the overall response (Guyot, 1990). The canopy architecture and the presence of surfaces, other than those of the crop (soil, crop residue, surface conditions, etc.), complicate the analysis of spectral data obtained over cultivated fields (Jackson and Pinter, 1986). Reflectance in the visible range is generally lower, whereas the same in the near-infrared is higher, when there is more biomass in the crop canopy. Canopy reflectance in the visible range decreases sharply from emergence until the LAI approaches a value of $2 \text{ cm}^2/\text{cm}^2$, and then tapers off asymptotically as ground cover approaches 100%. Hatfield and Pinter (1993) found that canopy reflectance reached a minimum (3 to 5%) in the visible, and a maximum (60 to 70%) in the near-infrared, when the LAI reached 3 to $4 \text{ cm}^2/\text{cm}^2$.

2.2 Remote Sensing for Weed Detection

The detection of weeds by remote sensing depends on the existence of detectable differences between the spectra of weeds and of other objects in the canopy (soil and crop plant), as well as on equipment having sufficient spatial and spectral resolution (Lamb, 1998). Numerous attempts have been made to detect weeds in agricultural fields and rangelands.

2.2.1 Weed detection in agricultural fields

Medlin et al. (2000) noted that the spectra of certain crops are often similar to those of the predominant weeds that invade them. Zwiggelaar (1998) reviewed the work on the potential use of spectral properties of plants for the discrimination of crops and weeds, and concluded that it is nevertheless possible to discriminate between plants with similar spectra if equipment is utilized with a high enough spectral resolution.

There have been many comparisons between the spectra of crops and weeds, focusing on individual leaves, individual plants or canopies of crops or weeds. Spectral observations have been made from a distance of a few centimeters (using handheld devices) to a few hundred meters (airborne sensors), with sensors ranging in

spectral resolution from the capabilities of color or color-infrared cameras to those of scanners providing reflectance at hundreds of wavebands. Some of these studies are summarized and discussed below.

Menges et al. (1985) examined single leaf and canopy reflectance characteristics of different weed species and of agronomic and horticultural crops. Spectral data were collected at seven different wavelengths in the range 450 to 1250 nm. It was concluded that the greatest differences in the spectra of crops and weeds occurred at 850 nm (near-infrared) and 550 nm (visible). The possibility of distinguishing weeds from crops in different weed-crop combinations was demonstrated using conventional color and color infrared photography. Results indicated that it was possible to identify climbing milkweed (*Sarcostemma cyanchoides*) in orange (*Citrus sinensis* Osbeck) trees; ragweed (*Parthenium hysterophorus* L.) in carrots (*Daucus carota* L.); johnsongrass (*Sorghum halepense* (L.) Pers.) in cotton (*Gossypium hirsutum* L.) and in sorghum (*Sorghum bicolor* L.); London rocket (*Sisymbrium irio* L.) in cabbage (*Brassica oleracea* L.); and Palmer amaranth (*Amaranthus palmeri* S. Wats.) in cotton. Their results were attributed to differences in chlorophyll content, color, leaf area and intercellular spaces in the individual leaves. However, these differences were not consistent and depended on the comparative developmental rates of the crops and weeds.

With further advancement in inexpensive and convenient digital imaging systems, researchers explored the potential of still video images and multi-spectral imaging systems. Brown and Steckler (1993) took images from a "cherry-picker" lift (8 m) and from a low-altitude aircraft (600 m) to detect weeds in corn fields. Images were acquired at spatial resolutions of 2.5 cm² and 15 cm² from the lift and aircraft, respectively. The filters used were standard red, blue, green, and infrared. Scanned, digital, aerial images of the corn field were classified into three broad groups (corn, soil, and weeds) using the supervised maximum likelihood algorithms. Weed patches could be classified with an accuracy of over 80% from the aerial images. However, it was not possible to distinguish between weed species with sufficient accuracy. It was suggested that higher spectral resolution was needed for this task. Hatfield and Pinter (1993) mentioned that the use of multi-spectral imagery for weed detection within

crop canopies required further research. The relationships between spectra and the following were mentioned as requiring particular attention: weed infestation levels, weed species, and crop growth stage.

Brown and Steckler (1995) developed herbicide prescription maps from digitized, low-altitude, aerial color and color-infrared photographs with a spatial resolution of 100mm x 100mm per pixel. An overall classification accuracy of 75% was reported between weed maps developed through ground observations and maps derived from aerial imagery (Steckler and Brown, 1993). A decision model was also developed to control the herbicide application rate of a sprayer. It was estimated that about 40% less herbicide would be needed if the proposed approach was used.

Brown et al. (1994) took hyper-spectral measurements over weed-infested corn fields and found that variations in the spectral signatures of different parts of the fields were related to the presence of seven common weeds, as determined by ground-truthing. The weeds were redroot pigweed (*Amaranthus retroflexus* L.), lamb's-quarters (*Chenopodium album* L.), dandelion (*Taraxacum officinale* Weber), milkweed (*Asclepias syriaca* L.), bluegrass (*Poa compressa* L. and *Poa pratensis* L.), quackgrass (*Agropyron repens* (L.) Beauv), and foxtail (*Setaria* sp. Beauv.). The wavebands that best related to the presence of these weeds were those centered at 440, 530, 650, and 730 nm.

In a more recent study, Wang et al. (1998b) evaluated the use of plant reflectance spectra for differentiating between crop plants and weeds. Hyper-spectral data were obtained for various crops, weeds, and soils under artificial light in the laboratory. The spectra of whole plants, leaves and stems were measured separately. Results indicated 100% confidence with distinguishing soil from any of the plant parts. However, success was poor in distinguishing weed plants, leaves or stems, from crop plants, leaves or stems. The researchers suggested that the limited amount of available data was responsible for low classification accuracy.

Mapping weeds in fallow land or against a contrasting background of soil, stubble, or dead vegetation is much easier than in cropped fields, due to the significant difference in spectral signature of classes represented in each pixel of the image. In such cases, the basic objective is usually to discriminate living vegetation

(weeds and volunteer crop) from any other material. This approach was shown to be effective by Lamb and Weedon (1998), who used an airborne multi-spectral video system to map hairy panic (*Panicum effusum* R. Br.) in a fallow field of oilseed rape (*Brassica napus* L.) stubble. Multi-spectral digital imagery was acquired by using 440-, 550-, 650-, and 770-nm filters over the study site. Results demonstrated that it was possible to develop weed maps having an accuracy of about 87%. The success obtained was attributed to the relatively simple criteria used to discriminate weeds (living vegetation) from soil or stubble and to differences in weed phenology.

Deguisse et al. (1999) mapped weed patches in a canola (*Brassica napus* L.) field using hyper-spectral radiance data from an airborne sensor. Automatic and manual end-member selection techniques were applied to unmix the hyper-spectral data, and better results were obtained with manual selection method. Good visual comparisons were found in the weed patches detected in acquired airborne imagery at 587.2 nm wavelength and in the images derived using spectral unmixing. However, further investigation was recommended of end-member selection from the surface reflectance image.

Lamb et al. (1999) evaluated the accuracy of a four-camera, airborne, digital imaging system to map wild oats (*Avena spp* L.) in seedling triticale (X *Triticosecale*). Images were acquired at different spatial resolutions (0.5, 1.0, 2.0, and 2.5 m) in order to assess the effect of resolution of the imaging system on weed detection. The normalized-difference vegetation index (NDVI) and the soil-adjusted vegetation index (SAVI) were derived from the acquired multi-spectral image. Results indicated that the density of wild oats could be correlated to the NDVI or SAVI values. As expected, better results were obtained with images acquired at higher spatial resolutions, i.e. at 0.5 m. The study also indicated that areas with weed populations of over 17 plants per m² could be detected in the field. However, it was found unlikely that treatment maps could be developed from aerial imagery alone. Remote sensing systems could be used in combination with DGPS systems to identify and locate weed patches in the field.

In an effort to evaluate multi-spectral remote sensing for weed detection early in the cropping season, Medlin et al. (2000) acquired images from a four-waveband

Charged Coupled Device (CCD) camera taken over a soybean field, nine weeks after planting. The wavebands were in the green (535 to 545 nm), red (690 to 700 nm and 715 to 725 nm), and near-infrared (835 to 845 nm) regions. There was success in detecting weed-infested and weed-free areas in the field, and the authors reported that *Senna obtusifolia* L., *Ipomea lacunosa* L., and *Solanum carolinense* L. could be detected with an accuracy of 75%. It was recommended that future studies target the early detection of weeds and the detection of specific weeds within a complex mixture of different species in the field.

In a most recently published study, Rew et al. (2001) compared weed maps developed from aerial, multi-spectral imagery and maps generated from a ground weed survey. A kriging method was used to generate weed maps based on weed count in the grid survey. Based on the ground survey, weed density could not be estimated with acceptable accuracy for site-specific weed control; however, it was concluded that multi-spectral imagery could serve to provide accessory data to improve the estimates of weed density and distribution across the field. A cost comparison was also performed and this indicated that multi-spectral imagery was less labor intensive and time consuming, and also more economical. Moreover, weed maps could be produced at much finer resolution by aerial imagery.

2.2.2 Weed detection in rangelands/grasslands

Numerous studies have shown that it is possible to use conventional color and/or color-infrared aerial photography and videography to map weeds in rangeland (Everitt et al., 1984, 1987, 1994, 1995, 1996). Color-infrared photography was used to map broomweed (*Ericameria austrotexana* M. C. Johnston) (Everitt et al., 1984), broom snakeweed (*Gutierrezia sarothrae* (Pursh) Britt & Rusby) and spiny aster (*Aster spinosus* Benth.) (Everitt et al., 1987). The same research group then combined aerial color-videography with GPS and GIS technologies to permit rapid geo-referencing and data processing (Everitt et al., 1994, 1995, 1996). In the 1994 study, attempts were made to detect and map Big Bend loco (*Astragalus mollissimus* Torr.) and Wooton loco (*Astragalus wootonii* Sheldon.), two poisonous rangeland weeds. The 1995 study quantified leafy spurge (*Euphorbia esula* L.), an exotic deep-rooted

perennial rangeland weed, in the study area. Canopy reflectance measurements were made with a ground sensor in the visible red (630 to 690 nm) and near-infrared (760 to 900 nm), followed by the use of aerial photography and videography. The findings indicated that remote sensing observations coupled with GPS and GIS technologies could be successfully used to map rangeland weeds. However, compared to conventional photography, aerial videography had coarser spatial resolution at the same flying altitude. Photographs were taken late in the season when particular weeds had distinct colors due to foliage or flowers.

Lass et al. (1996) were able to detect yellow starthistle (*Centaurea solstitialis* L.) and common St. John's Wort (*Hypericum perforatum* L.) in rangelands from digital images obtained from an airborne Charged Coupled Device (CCD). The images were collected in four wavebands (460 to 570 nm, 575 to 625 nm, 610 to 710 nm and 780 to 1000 nm) and at resolutions of 0.5, 1, and 2 m. Yellow starthistle and St. John's Wort could be detected at densities as low as 30% ground cover. As expected, better results were obtained from the higher resolution images.

Lass and Callihan (1997) also studied the effect of the phenological stage on detection of two perennial rangeland weeds, yellow hawkweed (*Hieracium pratense* Tausch) and oxeye daisy (*Chrysanthemum leucanthemum* L.). They found that the detection of different rangeland weeds was most accurate when they were in full bloom rather than in early or post-bloom. The accuracy of detection was good enough for management of rangelands weeds.

A few studies have gone a step further to realize the potential of remote sensing, for the development and management of pastoral or grazing lands. Hill et al. (1996) used a GIS to create pasture growth maps from satellite imagery, bio-climatic models, topographic and other ancillary data. This approach directly addresses site-specific variations in land productivity and provides a practical tool for managing pastures and rangelands.

Hill et al. (1999) then used satellite data in combination with GRAZPLAN, a pasture simulation model, to estimate production at the farm level. A spatial data layer mapping the growth status was used to determine parameter inputs for the simulation model. It was indicated that future developments, in high spectral and

spatial resolution airborne and space-borne sensors, would provide better qualitative information for the simulation models.

2.3 Remote Sensing of Nitrogen Stress in Plants

Nitrogen is one of the main limiting factors in the growth of plants. Nitrogen is also the most crucial parameter in managing agricultural, non-point source pollution. Various techniques have been developed to determine the timing and nitrogen requirements of crops. However, traditional methods involving soil and plant tissue sampling are very laborious and time consuming. Moreover, there may be considerable time lags between sample collection and the availability of results (Bausch and Duke, 1996).

One alternative that has been widely used to measure nitrogen stress in plants, albeit with varying degrees of success, is the chlorophyll meter, which is based on light reflectance (Blackmer and Schepers, 1995; Schepers et al., 1992; Dwyer et al., 1991). This technology is generally only applicable to a single leaf at a time, which precludes its usefulness for large-scale assessments. However, remote sensing of the reflectance of canopies, in the appropriate wavebands, should be an appropriate basis for mapping the spatial variability of nitrogen status (Blackmer et al., 1996a; Bausch and Duke, 1996) and water stress across a field (Peñuelas et al., 1994).

In general, compared to healthy plant leaves, leaves from stressed plants have higher reflectance in the visible and lower reflectance in the near-infrared spectral region (Gausman, 1977; Peñuelas et al., 1994). Nitrogen-stressed plants have significantly lower levels of plant nitrogen and chlorophyll, higher starch content and greater leaf thickness. They reflect more light in the red region due to lower chlorophyll content, and less light in the near-infrared region (Serrano et al., 2000).

A more detailed review of relationships between nitrogen stress and spectral signature is given in the following sub-sections. One sub-section concerns reflectance measurements at the leaf scale under laboratory or field conditions, and the other regards canopy scale assessments from ground-based or airborne platforms.

2.3.1 Leaf-nitrogen level studies

Various authors have reported significant correlations between reflectance in certain wavebands and nutrient deficiencies. Thomas and Oerther (1972) found that reflectance at 550 nm was a good indicator of the nitrogen content of sweet pepper (*Capsicum annuum* L.) leaves. It was noted that the change in reflectance, at 550 nm, could be detected well before human visual observation of the symptoms of stress. Later, Thomas and Gausman (1977) studied the reflectance of single leaves from eight crops at wavelengths of 450, 550, and 670 nm. These are the absorption bands of chlorophyll and carotenoids, a reflectance peak, and the chlorophyll absorption band, respectively. It was concluded that the reflectance at 550 nm was a better indicator of chlorophyll and carotenoid content than the absorption bands. Takebe et al. (1990) conducted an experiment on rice (*Oryza sativa* L.) leaves and found a significant correlation between leaf chlorophyll content and the ratio of the reflectance at 550 and 800 nm. Chappelle et al. (1992) also obtained best results at 550 nm, in a study to differentiate between nitrogen fertilization levels in corn. Buschmann and Nagel (1993) observed that leaves with higher nitrogen content have stronger reflectance in the blue and near-infrared (NIR) waveband. It was suggested that reflectance in the green (545 nm), red (660 nm), and NIR (800 nm) could also be related to plant nitrogen content.

Blackmer et al. (1994a) found that the best relationships between reflectance and leaf nitrogen content, and between reflectance and chlorophyll meter (Minolta SPAD) readings, occurred at 550 nm. A significant correlation was also reported between relative corn yield and reflectance at 550 nm. These findings could be attributed to a comparatively lower absorption of energy by chlorophyll at 550 nm, resulting in more pronounced differences with varying chlorophyll content.

Peñuelas et al. (1994) demonstrated that narrow waveband indices are more useful than wider wavebands for assessing nitrogen and moisture stress in sunflower (*Helianthus annuus* L.) leaves. This involved the utilization of the normalized difference vegetation index (NDVI), the physiological reflectance index (PRI), the normalized pigment chlorophyll ratio index (NPCl), and the water band index (WBI). These indices were:

$$\text{NDVI} = \left[\frac{R_{850} - R_{680}}{R_{850} + R_{680}} \right], \quad (2.1)$$

$$\text{PRI} = \left[\frac{R_{550} - R_{530}}{R_{550} + R_{530}} \right], \quad (2.2)$$

$$\text{NPCI} = \left[\frac{R_{680} - R_{430}}{R_{680} + R_{430}} \right], \quad (2.3)$$

$$\text{WBI} = \left[\frac{R_{970}}{R_{900}} \right], \quad (2.4)$$

where R_{430} , R_{530} , R_{550} , R_{680} , R_{850} , R_{900} , and R_{970} are the reflectance values at 430, 530, 550, 680, 850, 900, and 970 nm, respectively.

In addition to the above, indices were also used based on the first and second derivative of the reflected spectrum. First derivative minima and maxima in the green region were at 570 nm and 525 nm, respectively. Derivative maxima in the red edge region (700 to 710 nm) and differences between these values were also evaluated. Second derivative minima in the green (530 nm) and red edge (690 nm) were tested as well. It was concluded that nitrogen and water stress caused significant differences between the above listed indices and derivatives. The researchers recommended that the study should be extended to the canopy scale.

2.3.2 Canopy-nitrogen level studies

The canopy level studies may be further classified into two categories: (i) those in which spectral data were acquired from spectral devices kept at a distance of a few meters from the crop canopy; (ii) those in which the imaging systems were airborne to acquire data at the field scale.

2.3.2.1 Studies with ground-based canopy-scale spectral data acquisition systems

Walburg et al. (1982) monitored the spectral signature of a corn canopy over the entire growing season. The range examined was 400 to 2400 nm and images were

taken from a 9 m tower. Results indicated that at higher nitrogen levels, reflectance in the visible (400 to 700 nm) and middle infrared region (1400 to 2500 nm) was lower, while that in the near IR (700 to 1400 nm) was higher. Changes in spectral response could be attributed to changes in canopy factors (LAI, plant biomass, and percent soil cover) and changes in leaf structure and composition (leaf pigment concentration, cell size, and cell wall composition and structure). Reflectance in the red (630 to 690 nm) decreased, while reflectance in the near-infrared increased as LAI, biomass, and soil cover increased through the growing season. Detailed examination of spectral wavebands, corresponding to the LANDSAT multi-spectral scanner (MSS) and thematic mapper (TM), indicated that nitrogen treatments could be more effectively separated using the ratio of near-infrared (NIR) (760 to 900 nm) to red (630 to 690 nm). A highly significant relationship was also obtained between grain yield and the ratio of NIR to red.

Studies at the leaf level were used by Takebe et al. (1990) to design and test a portable green color intensity meter, for estimating nitrogen status in a rice canopy. The meter measured the intensity of incident solar canopy-reflected radiation in the green (550 nm) and near-infrared (800 nm) regions. The results of the field trial of the instrument indicated a good correlation between leaf nitrogen determined with the color-meter and leaf nitrogen determined in the laboratory.

Blackmer et al. (1994b) used a spectroradiometer and aerial photography to study the reflectance spectra of corn under various nitrogen fertilization levels. Wavelengths around 550 nm and 710 nm were the most suitable for detecting nitrogen deficiency in individual leaves. However, reflectance at 550 nm was better correlated to nitrogen deficiency at the canopy scale. Thus, a photometric cell was used to measure reflectance at 550 nm, and aerial black and white photographs were taken with a filter which was sensitive in this range. There was a significant correlation between yield and reflected radiation. Furthermore, the ratio of reflectance of nitrogen-deficient to nitrogen-sufficient corn leaves at each wavelength effectively explained the variation in spectral response due to different nitrogen levels.

In another study, Blackmer et al. (1996a) made spectral observations (350 to 1100-nm range) over irrigated canopies of different corn hybrids, at various nitrogen

fertilization levels. Observations were taken at the R5 (dent) physiological growth stage. Absolute radiation was found to depend on sensor and illumination angle, solar irradiance and canopy architecture. To account for the illumination differences, the researchers referenced all the data to reflected radiation from high nitrogen plots and were thus able to detect differences in spectra that were due to hybrids and nitrogen treatments. It was concluded that the regions near 550 nm and 710 nm were the most useful in detecting nitrogen levels. The ratios of reflectance, from the range 550 to 600 nm to the range 800 to 900 nm, were also found to be useful for this purpose. Correlations between relative corn yield and reflectance in the above wavebands were also high.

In a similar experiment, Ma et al. (1996) measured reflectance in eight broad (50 nm interval) wavebands from 400 to 800 nm, over six different maize hybrids grown under three different nitrogen levels. It was reported that canopy reflectance at 600 nm and 800 nm or a derived NDVI could be used to differentiate nitrogen levels and to estimate crop yield.

Bausch and Duke (1996) compared a ground-based spectral observation system, with a SPAD chlorophyll meter and plant tissue nitrogen, in an irrigated corn canopy. Spectral data were acquired from a radiometer with channels in the blue (450 to 520 nm), green (520 to 600 nm), red (630 to 690 nm), and near-infrared (760 to 900 nm). The researchers reported a nearly 1:1 relationship between the nitrogen sufficiency index (average SPAD value in a general plot to average SPAD value in high nitrogen plots) and the canopy-based normalized reflectance index. The normalized reflectance index used was defined as the reflectance ratio for a particular treatment, divided by the ratio of NIR to green for high nitrogen plots.

Stone et al. (1996) found significant correlations between spectral radiance and both wheat (*Triticum aestivum* L.) forage yield and forage nitrogen uptake. A photodiode detector with filters for red (671 ± 6 nm) and NIR (780 ± 6 nm) was used in the study. The researchers found a slight improvement in correlations, when both red and near-infrared wavebands were combined to calculate plant spectral nitrogen stress (PNSI), the absolute value of the inverse of the NDVI. The PNSI could be defined as:

$$\text{PNSI} = \left| \frac{R_{\text{NIR}} + R_{\text{RED}}}{R_{\text{NIR}} - R_{\text{RED}}} \right|, \quad (2.5)$$

where R_{NIR} and R_{RED} are the reflectance values in the NIR and red wavebands.

Joel et al. (1997) studied the impact of water stress, nitrogen stress, and their combination on sunflower canopy development, and also their effect on the fractional interception of photosynthetically active radiation (fPAR), the NDVI, and the SR (simple ratio index). Strong correlations were reported among fPAR, NDVI, SR, and LAI. However, neither of the stresses (water or nitrogen) had a significant effect on the relationship between fPAR and NDVI or SR. Although spectral observations were acquired with a narrow-waveband field spectroradiometer, reflectance values used were averaged over broad wavebands for calculating NDVI and SR values to mimic AVHRR (Advanced Very High Resolution Radiometer) wavebands.

Sui et al. (1998) used a hand-held spectroradiometer to detect nitrogen deficiency in a cotton canopy. The researchers used a spectral index based on the ratio of observed reflectance in the blue (460 to 490 nm), green (540 to 565 nm), amber (600 to 610 nm), and NIR (740 to 770 nm). A significant correlation was reported between the spectral index and petiole nitrogen. The spectral index (SI) was defined as:

$$\text{SI} = \left[\frac{R_{\text{NIR}} + R_{\text{BLUE}}}{R_{\text{GREEN}} + R_{\text{AMBER}}} \right], \quad (2.6)$$

where R_{NIR} , R_{BLUE} , R_{GREEN} and R_{AMBER} are the reflectance values in the NIR, blue, green, and amber wavebands, respectively.

Adams et al. (2000) related micronutrient deficiencies (Mn, Zn, Fe, and Cu) in soybean to reflectance and fluorescence measurements. In addition to the commonly used vegetation indices, R_{750}/R_{550} , R_{750}/R_{650} , and the NDVI $((R_{750}-R_{650})/(R_{750}+R_{650}))$, they also used a yellowness index (YI), which is a measure of leaf chlorosis. In these

ratios, R_{550} , R_{650} , and R_{750} were the reflectance values at 550, 650, and 750 nm, respectively. The yellowness index could be calculated from the concavity-convexity of the reflected spectrum, at the midpoint between the reflectance maxima at 550 nm and the minima at 670 nm. Mathematically, YI could be defined as the finite difference approximation of the second derivative of the reflectance spectrum between 550 and 670 nm:

$$YI = \frac{d^2 R}{d\lambda^2} = - \left[\frac{R_{\lambda-1} - (R_{\lambda_0}) + R_{\lambda+1}}{\Delta\lambda^2} \right], \quad (2.7)$$

where R_{λ_0} is the reflectance at the central wavelength, $R_{\lambda-1}$ and $R_{\lambda+1}$ are the reflectance values at lower and higher wavelengths, respectively, and $\Delta\lambda$ is the difference between two wavelengths.

2.3.2.2 Studies with airborne field-scale data acquisition systems

Blackmer et al. (1996b) investigated the possibility of using ordinary color aerial photographs to detect variability in corn growth, due to different nitrogen levels. Color photographs were first digitized and digital counts in red, green, and blue were then generated. The results indicated that the red counts provided a better basis for discriminating between nitrogen treatments. A significant relationship existed between the red digital counts and grain yield; however, better correlations ($r^2=0.93$) between yield and digital counts were obtained when black and white aerial photographs were taken, using a filter centered at 536 nm. It was also found non feasible to pool digital data from different years, or even from different crop growth stages, in the same year.

Based on a two-year study, Tomer et al. (1997) also suggested that color scanned photographs could be used to describe spatial variability in yield and nitrogen uptake in corn. It was reported that better predictions could be obtained by this method, rather than using approaches dependent on topographic data or geo-statistical methods.

However, the scanning process results in a considerable loss of spatial and

spectral resolution, and in the signal to noise ratio of color or color-infrared photographs (GopalaPillai et al., 1998). Realizing this, the researchers used high resolution color-infrared (CIR) images (500 to 810 nm) in three channels (infrared, red, and green) to detect in-field, spatial variability of corn. High correlations were obtained between canopy reflectance and applied nitrogen and yield. However, the correlation between reflectance and nitrogen in stalks was poor.

GopalaPillai and Tian (1999) used a digital CCD camera with a filter to acquire a CIR image (500 to 810 nm) in three wavebands: green (500 to 600 nm), red (600 to 710 nm), and NIR (710 to 810 nm). A comparison of standard maps of soil type with maps generated from aerial imagery, according to a supervised classification algorithm, indicated that agreement was 76% (area basis). Nitrogen-stressed areas in the CIR image could be easily detected; however, it was difficult to determine nitrogen levels in nitrogen-sufficient areas. Spatial variations in yield were also found to be highly correlated with CIR reflectance. Better correlations were obtained in the red and green wavebands than in the NIR waveband. Linear models to predict yield were developed from the data and were 76 to 98% accurate for the particular data collection field. When the model was used for other fields, accuracy dropped to 55 to 91%.

2.4 Estimation of Vegetation Biophysical Parameters and Yield

The primary objective of the majority of the current studies in this area, is to establish a quantitative link between spectral data and crop physiological parameters, as an indication of crop growth. Kimes et al. (1998) mentioned that the degree of success in deriving vegetation parameters from remotely sensed data would determine the utility of Earth Observing Satellites (EOS) in vegetation science. The estimation of various biophysical parameters from remotely sensed data is important in order to extend the application of crop growth models to larger areas. These models could be used to assess crop conditions for yield prediction or to facilitate crop management during the growth season. Spectral data could be used to derive variables necessary in crop models, to update indices of canopy status, to re-initialize crop models or to adjust model parameters according to remotely sensed data or ground observations

(Moulin et al., 1998). There have been various attempts to use remote sensing observations to calibrate crop models dynamically (Moran et al., 1995; Bouman, 1992; Delécolle et al., 1992; Wiegand et al., 1986). Inoue and Morinaga (1995) noted that observations, in a number of narrow spectral wavebands, could provide plenty of physiological and ecological information on both at a local and regional scale.

A number of studies are currently underway, exploring the correlation between spectral measurements and the concentrations of certain biochemicals in plants. A strong correlation appears to exist between remotely acquired data and the concentration of many biochemicals within the vegetation canopy (Curran et al., 1997). Chlorophyll is the most important biochemical in the process of conversion of sunlight to chemical energy in plants. Many studies have shown that there is a significant correlation between the concentration of chlorophyll in a crop and spectral measurements (Patel et al., 2001; Jago et al., 1999; Munden et al., 1994; Miller et al., 1990). Numerous research studies have indicated the potential of remote sensing observations, in developing functional relationships between forest canopy chemistry and spectral data (Martin and Aber, 1997; Johnson et al., 1994; Matson et al., 1994; Peterson et al., 1988; Wessman et al., 1988), albeit with varying degrees of success. Martin and Aber (1997) developed a calibration model, for estimating nitrogen and lignin content in a forest canopy, based on Airborne Visible/Infrared Imaging Spectrometer (AVIRIS) data.

Many workers have attempted to develop relationships between spectral measurements and crop growth parameters, such as LAI, plant height, and biomass. Inoue et al. (2000) used a camera mounted on a blimp to collect spectral measurements in four wavebands. They successfully estimated LAI and fresh biomass for soybean and rice crops based on these images. Brown et al. (1997) demonstrated that indicators of canola crop vigor (biomass and leaf area) were significantly related to near-infrared reflectance, as obtained from a Compact Airborne Spectrographic Imager (CASI). In another experiment, Inoue and Morinaga (1995) estimated fresh biomass and greenness using spectral observations taken from a blimp. The researchers found a significant correlation between the remotely and ground-sensed parameters ($r^2=0.971$ for fresh biomass and 0.680 for greenness).

Cloutis et al. (1999, 1996) evaluated high spectral resolution optical and radar imagery for use in the estimation of a number of crop parameters (LAI, plant height, and canopy temperature) for different crops (wheat, canola, beans, peas, and wheat/alfalfa). Several statistically significant correlations were found between the spectral observations and the crop parameters. In a more recent study, Thenkabail et al. (2000) carried out an intensive field campaign to correlate many crop biophysical parameters with spectral values acquired from a hand-held spectroradiometer in the visible to NIR range (350 to 1050 nm). The usefulness of hyper-spectral measurement and narrow waveband indices was clearly indicated in estimating various crop parameters. These spectral observations were acquired over cotton, potato (*Solanum tuberosum* L.), soybean, corn and sunflower.

Numerous studies have shown, with varying degrees of success, that remote sensing technology can be used to estimate crop yield. Different vegetation indices have been used to estimate crop yield for wheat (Asrar et al., 1985), barley (*Hordeum vulgare* L.) (Klemn and Fagerlund, 1987), soybean and corn (Holben et al., 1980; Crist, 1984). Decker (1994) observed that statistical models based on climatological variables could explain only 50% of the variation in yield. However, Hayes and Decker (1998) developed a better yield assessment system for maize, based on satellite and climatic data. Following this approach, the researchers were able to explain about 75% of the observed variability in normalized yield. Moran et al. (1997), reviewing the role of remote sensing in agriculture, indicated that two main approaches are being followed for yield estimation of crops. In the first approach, which is simpler and more straight forward, regression equations based on single or multiple, time-integrated vegetation indices (VI), such as NDVI, could be used for yield estimation. Another approach is to use remote sensing observations or vegetation indices to directly estimate canopy parameters, LAI or fPAR, which could then be used as input parameters for crop growth or agrometeorological models (Clevers, 1997; Clevers et al., 1994). Serrano et al. (2000) reported highly significant correlations between the simple ratio vegetation index ($SVI = R_{900}/R_{680}$) and yield or biomass of wheat. It was also reported that nitrogen fertilization level significantly affected the SVI to LAI relationship. However, under varying nitrogen levels, a better

relationship was developed when total canopy Chlorophyll A (LAI x Chlorophyll A) was considered as a single factor.

2.5 Vegetation Index

Many vegetation indices (VIs), which combine reflectance at two or more wavelengths in different ways, have been shown to be useful in characterizing plant growth and development (Jackson and Huete, 1991). These VIs enhance the spectral contribution from green vegetation and minimize the contribution from soil and atmospheric factors, by taking advantage of typical spectral features of vegetation. These indices are also useful, in reducing multi-spectral remote sensing data into a single value, for assessing vegetation status. The most commonly used vegetation indices are: the ratio vegetation index (RVI), the normalized difference vegetation index (NDVI), the soil-adjusted vegetation index (SAVI), the perpendicular vegetation index (PVI), the difference vegetation index (DVI), the transformed-SAVI (TSAVI), and the modified-SAVI (MSAVI). The basis for most vegetation indices is the contrast between green leaves and soil or dead plant material (Joel et al., 1997). Perry (1984) indicated that, in general, most of these indices are functionally equivalent, i.e. the value of one index may be computed based upon the value of another index. Thus, decisions based on one index are similar to those taken according to another index. However, Joel et al. (1997) mentioned that the performance of most of the vegetation indices depended on the settings. Hatfield and Pinter (1993) reviewed the applications of remote sensing in crop production, and highlighted the limitations of VIs in distinguishing weed populations from field crops. VIs are dependent on changes in plant biomass, leaf area, and the interception of radiation by the green portion of the canopy. Thus, VIs have a limited application for discriminating between different plant species. However, in a recent study, Zwiggelaar (1998) found some ratio vegetation indices (RVIs) and vegetation indices (VIs) to be useful for the discrimination of weeds from crops, particularly in row crops. Similarly, various reflectance ratios and indices have been used to detect nitrogen deficiencies in plants (Lukina et al., 2000; Plant et al., 2000).

2.6 Application of Decision Trees and Artificial Neural Networks (ANNs) in Remote Sensing

There has been an exponential increase in remote sensing data, due to the launching of an increasing number of satellites with improved resolution. In order to make the best use of this large data set, a more fully automated image analysis approach is necessary, with limited human interaction for critical evaluations (Soh and Tsatsoulis, 1999). For the quantitative analysis of remote sensing data, supervised and unsupervised methods are used; however, supervised classification is most frequently used. Moreover, image classification should be capable of tackling noise in the data sets, identifying better features to discriminate between different classes, and minimizing confusion among spectral classes (Friedl et al., 1999). Another important issue related to automated or semi-automated classification algorithms is that they should be capable of handling different situations in the same domain (Soh and Tsatsoulis, 1999). Realizing the need for more efficient remote sensing image classification techniques, many researchers explored the utility of data mining and artificial neural networks. Some of the salient studies are discussed briefly in the following section. With reference to the data-mining category, the decision tree tool is the most suitable for classification problems, and discussion is therefore limited to decision trees.

2.6.1 Decision trees

The decision tree, a frequently-used method of data mining, learns from a given data set and formulates explicit rules to classify, segment, or make predictions about a target variable. This process begins by using the entire training data set. Initially based on one of the attributes, data are split into one or more homogeneous categories. The splitting process is extended into subsets until the split size of the data reaches a level beyond which splitting is either not feasible or desirable. It generates a decision tree, which is basically a step-by-step rule system that splits the data into different categories. The decision tree resembles a simple flow chart of a rule-based expert system, that consists of rules for arriving at a decision. A sample decision tree is presented in Figure 2.2. This classification of the data set, into different categories

or groups, is based on explicit rules that are formulated from the training data. These rules are used to further classify other sets.

Figure 2.2 illustrates the mechanism of the decision tree approach, based on an example classifying a classical Iris data set (Fisher, 1936). The data consists of 150 descriptions of Iris flowers. Each description is a vector whose elements are petal length, petal width, sepal length, sepal width and the target variable (in this case, the species of Iris). There are 50 such descriptions for flowers from each of the following species: *setosa*, *versicolor*, and *virginica*. The objective is to generate a decision tree, on the basis of these 150 records, that will be able to key out (categorize) other such vectors into the correct species.

As indicated in the Figure 2.2, the complete data set is first split into two branches on the basis of the variable that is best correlated with the target variable (species). The rule for segmenting the data at that point is decided by an iterative process that examines all possible partitions into two subsets, and chooses the one that minimizes the combined variability in the two subsets. Based on the petal length, this process defines the split point as 2.450. Thus, all cases for which petal length is ≤ 2.450 are sent to the left node, and the others (petal length > 2.450) are sent to the right node. The improvement values are also given, and these indicate the percentage of correctly identified cases after the split point. An improvement value of 0.3333 at the first node indicates that 33.33% of cases were correctly classified due to the splitting criterion used at the node. In this example, it turns out that all the cases sent to the left node belong to one species, *setosa*.

The process is now repeated only at the right node. At this level, the rule for segmenting at the second node was 'width ≤ 1.750 or > 1.750 '. This rule has classified the remaining 100 cases into *versicolor*, and *virginica*. However, as can be seen, the resulting subsets are not pure, the left node containing 49 *versicolor* and 5 *virginica* and the right node containing 1 *versicolor* and 45 *virginica*. At this node, another 25.98% of cases (improvement value 0.2598) were classified correctly. The tree is fully-grown to two levels at this stage, because none of the other descriptors could reduce the impurity of either node. Overall, this tree correctly classified 59.31%

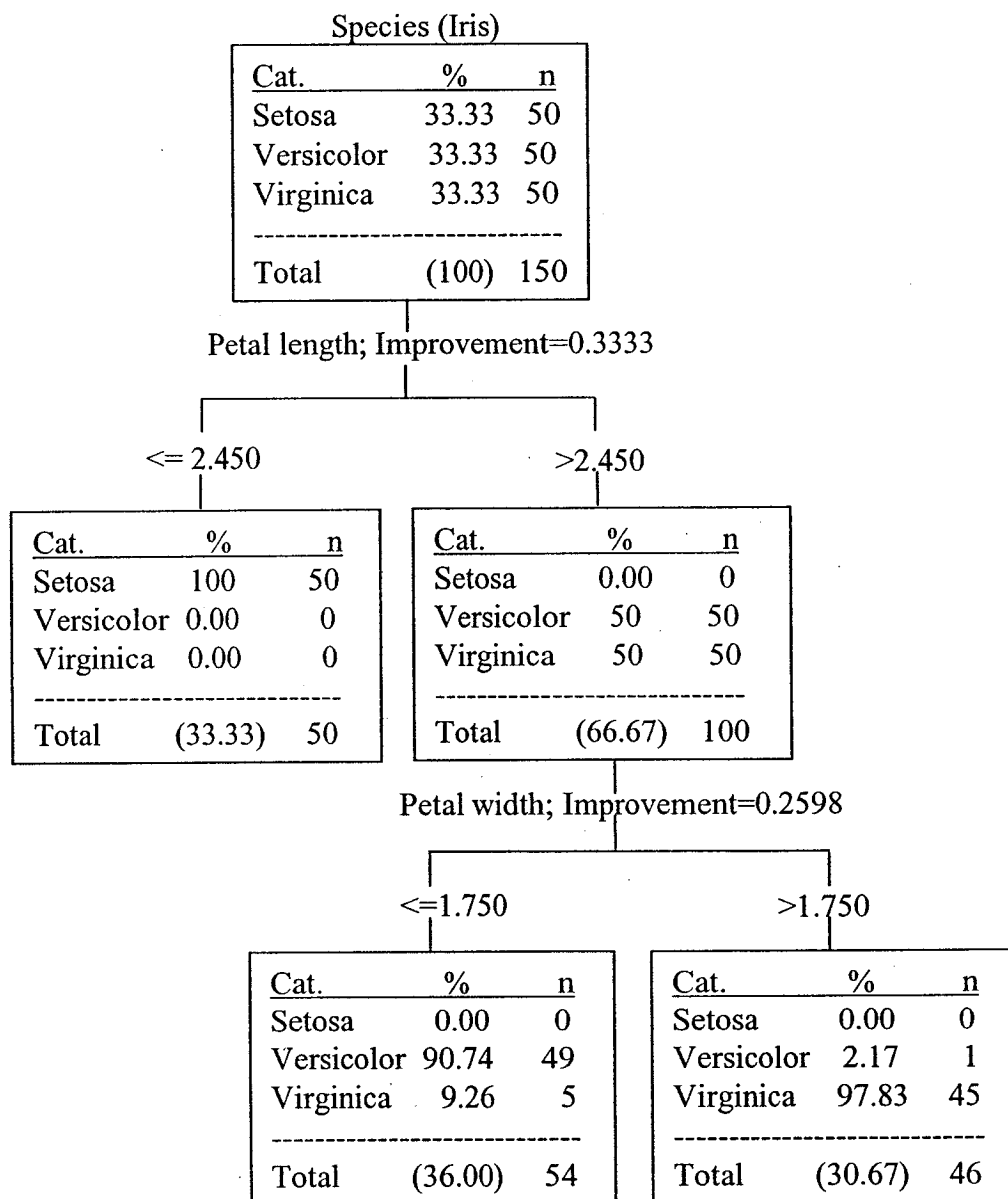


Fig. 2.2 Fully grown sample decision tree
 (Source: AnswerTree 2.0 User's Guide. 1998)

(33.33% + 25.98%) of the cases. Such a tree should then be validated on an unseen data set, in order to better establish the extent of expected correct classification of any other Iris flower, from one of the three possible species. To achieve the highest classification accuracy, the tree is grown to the level at which further node splitting is either impossible or undesirable. This example was taken from AnswerTree, User's Guide (SPSS Inc., Chicago, IL).

A large number of decision tree algorithms have been reported; however, the two most widely used are the C&RT (Classification and Regression Trees, also called CART), developed by statisticians (Breiman et al., 1984), and the C4.5, developed by a computer scientist (Quinlan, 1993). In the C&RT algorithm, decision tree development is based on a desire to minimize impurity measurements. In most cases, impurity-based criteria are used to grow trees by splitting the data at each node. These impurity indices are developed in such a way that after each split, data sets in the child nodes are more homogeneous than the data in the parent node.

In the C&RT algorithm, impurity may be measured in different ways according to the type of target variable involved. The Gini index, twoing, and ordered twoing are used for categorical target variables, while the least squared deviation is applied in the case of a continuous target variable. The most commonly used method is the Gini index, which was proposed by Breiman et al. (1984). At node t , the Gini index, $g(t)$ is given by:

$$g(t) = \sum_{j \neq i} p(j/t)p(i/t), \quad (2.8)$$

where i and j are categories of the target variable and $p(i/t)$ and $p(j/t)$ are the probabilities of a random sample X belonging to class i and j , respectively, given the distribution of data in the set at node t . The adequacy of a split is measured in terms of the decrease in impurity. Thus, split s at node t is chosen so as to maximize the value of the Gini criterion function $\Phi(s,t)$. If p_R and p_L are the proportions of cases in t sent to the right and left hand nodes, respectively, $\Phi(s,t)$ can be defined as:

$$\phi(s, t) = g(t) - p_L g(t_L) - p_R g(t_R), \quad (2.9)$$

where $g(t_L)$ and $g(t_R)$ are the Gini indices for the left and right child nodes, respectively. Based on the algorithm of classification, a tree is developed, which can then be used to classify another data set.

The applicability of data-mining techniques in general and decision trees in particular, to the analysis of remote sensing imagery, has been demonstrated by a few studies at various levels (Friedl et al., 1999; Soh and Tsatsoulis, 1999; Friedl and Brodley, 1997; Hansen et al., 1996).

2.6.2 Artificial neural networks (ANNs)

Artificial neural networks (ANNs) are complex mathematical functions that mimic the brain. They are considered to be capable of converting inputs into desired outputs, with no need for a physical explanation of the input-output relationships. ANN models, through intensive training with known examples, develop a functional relationship between input and output parameters. A typical ANN architecture (Figure 2.3) consists of a number of layers with interconnecting processing elements (PE), each of which is a basic component that receives inputs from many other PEs and generates an output based on a weighted sum of inputs and a transfer function. There are normally three types of layers in ANNs: (i) the input layer, in which the number of PEs is equal to the number of inputs to the model; (ii) the hidden layers, in which the number of hidden layers and processing elements in each hidden layer depends upon the complexity of the problem; and (iii) the output layer, in which the number of PEs is equal to the number of output variables. Many factors should be considered in order to build an effective ANN model. Some of the important parameters are: the number of hidden layers and PEs, the learning rule, and the transfer function. In addition, there should be an appropriate selection of various parameters (such as learning coefficient, epoch, momentum term, etc.) associated with learning algorithms (Lacroix et al., 1997).

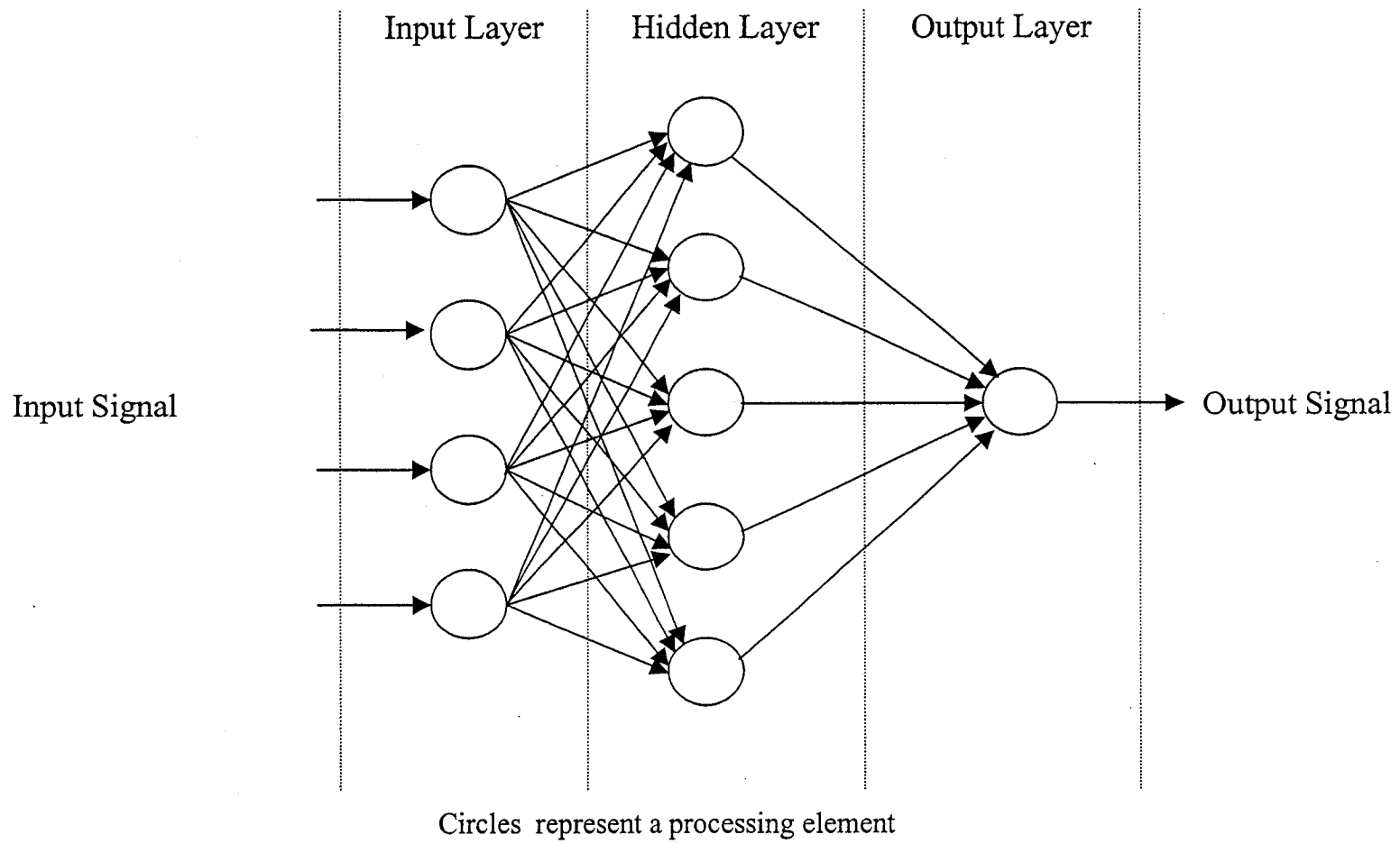


Fig. 2.3 Structure of an Artificial Neural Network.

The output from each PE is a weighted summation of outputs from the PEs in the preceding layer, which is then passed to the next layer PE through a transfer function. Thus the input to any PE, q , can be expressed as:

$$net_q = \sum_{p=1}^b w_{qp} o_p , \quad (2.10)$$

$$o_q = f(net_q) , \quad (2.11)$$

where, w_{qp} is the weight of the link connecting PEs p and q , b is the total number of connected PEs in the layer from which input is being received at PE q . o_p is the input to q from PE p , o_q is the output from PE q , and f is defined as the activation function of the PE output.

$$f(o) = \begin{cases} 1, & o > \theta \\ 0, & \text{otherwise} \end{cases} , \quad (2.12)$$

where θ is the threshold value. Some of the most common activation functions are the sigmoid, hyperbolic, linear threshold and the Gaussian.

Back-propagation is the algorithm that is the most widely used for classification problems (Schalkoff, 1992). This type of ANN model is built by presenting a training data set with both input and output parameters. The response at each PE is passed to the next layer. The final output is then compared with the known output, and the error is back-propagated. The weights of the connections are then adjusted accordingly, and the new responses from PEs are again passed to the next layer. This process, of forward transfer of response and backward propagation of error, is a recursive process which continues until the achievement of a satisfactory output (user-defined limit). The accuracy of the trained network can then be validated on an unseen data set.

Since the early 1980's, ANN-based approaches have been successfully used in pattern recognition problems in diverse fields. From 1988 onwards there has been a

steady growth in their application to the field of remote sensing (Wilkinson, 1997). Today, earth-observing sensors are generating large quantities of data which are being added to huge databases. For the full realization of this activity, fast processing and interpretation of data are necessary (Atkinson and Tatnall, 1997). Reviewing the work of many researchers, Atkinson and Tatnall (1997) commented on many of the qualities of ANNs. Some of the advantages highlighted by the greater accuracy of ANN techniques involves complex feature space classification, faster classification compared to statistical approaches, feasibility of incorporation of prior knowledge, and the possibility of the simultaneous use of data from different sensors or sources.

The use of ANN technology for pattern recognition has drawn considerable attention in recent years. Neural network classifiers have some important advantages over statistical methods. Whereas statistical classification techniques typically require prior information about the pattern distribution, ANN classifiers work well without any knowledge of the distribution (Danaher et al., 1997). Lee et al. (1990) showed that ANNs performed as well as statistical classifiers, but did not require as extensive training data sets. Various studies have demonstrated the usefulness of ANNs in ground cover classification (Augusteijn and Warrender, 1998; Danaher et al., 1997; Augusteijn et al., 1995; Kanellopoulos et al., 1992; Hepner et al., 1990). Singh et al. (1998) also reported better classification results of LANDSAT images with an ANN classifier when compared to statistical classification. In a recent approach, considering the importance and practical utility of fuzzy classification of remotely sensed data, Zhang and Foody (2001) proposed a fully-fuzzy classification approach. Better results were obtained with this approach than with partially-fuzzy or other statistical approaches. ANNs have also been used for identification of clouds patterns (Bankert, 1994; Lee et al., 1990). Depenau (1997) reported a better performance by ANNs over traditional, maximum likelihood classifiers in ice-type classification of Synthetic Aperture Radar (SAR) images from the European Remote Sensing Satellite (ERS-1).

There are numerous studies on the use of ANNs for other applications. Baret et al. (1995) compared ANNs with vegetation index-based approaches, for estimating the canopy gap fraction in sugar beets. Kimes et al. (1996) used ANN models to

estimate forest age. Forest crop growth models were inverted using an ANN approach (Kimes et al., 1997). Pierce et al. (1994) successfully predicted various canopy parameters (trunk density, trunk diameter, height) of Loblolly pine from airborne SAR data. The ANN approach was employed to predict corn yield from airborne images, with much better results than that obtained with traditional statistical techniques (Panda and Panigrahi, 2000). Smith (1993) used a back-propagation ANN method by inverting a multiple scattering model in the visible region (400 to 700 nm), in order to estimate leaf area index (LAI). Jin and Liu (1997) used ANN techniques to estimate wheat and oat (*Avena sativa* L.) canopy parameters from active/passive remote sensing. The estimated parameters were: canopy height, canopy water content, dry matter fraction, and moisture content of the underlying land.

2.7 Current Status and Concluding Remarks

The studies reviewed above demonstrate that it is possible to relate the presence of weeds and nitrogen deficiency in crops to reflectance measurements, made from airborne or ground-based instrumentation systems. Although there is a growing consensus that hyper-spectral sensors (multiple narrow-waveband capability) are the most promising imaging technology for mapping either phenomenon on a large scale, airborne hyper-spectral imaging systems were not used to monitor combined effects of weed infestations and nitrogen stress in any of the studies listed above. There has been no previous attempt to monitor crop growth in conditions of simultaneous weed and nitrogen stress, using such instrumentation, nor have decision trees and ANNs been used to classify hyper-spectral data in classes indicative of combinations of weed and nitrogen stress.

PREFACE TO CHAPTER 3

A review of the research in the application of remote sensing indicated that the use of airborne multi-spectral sensors in weed detection requires further investigation. A pilot field experiment was initiated in the first year (summer 1999) to study the spectral response of corn (*Zea mays* L.) and soybean (*Glycine max* (L.) Merr.), two locally important crops, under different conditions of weed infestation. Different weed treatments were selected to represent the prevailing weed conditions in corn and soybean fields of the region. Spectral observations were acquired from an Airborne Imaging Spectrometer for Applications (AISA) in 24 wavebands (475.12-nm to 910.01-nm spectrum region). The objectives of the study were to determine whether multi-spectral imagery from airborne platforms could be used in monitoring the growth of corn and soybean crops under specific weed conditions or not, and also to develop quantitative relationships between the remotely sensed data and crop physiological parameters related to weed-induced crop stress.

Research papers based on the chapter:

1. Goel, P. K., S. O. Prasher, R. M. Patel, D. L. Smith, and A. DiTommaso. 2002. Use of airborne multi-spectral imagery for weed detection in field crops. *Transactions of the ASAE* 45(2): 443-449.

(Copy of the published paper is given in the attached CD-ROM.)

CHAPTER 3

MULTI-SPECTRAL AIRBORNE REMOTE SENSING FOR WEED DETECTION

3.1 Abstract

An image of an experimental field was obtained with an airborne imaging spectrometer, in order to assess the potential of this technology to provide the data required for precision herbicide application systems, i.e. the location and type of weed present. For this particular application, the objective was to distinguish between three types of weed population, grasses, velvetleaf (*Abutilon theophrasti* Medik.), and mixed weeds, in plots cropped with corn (*Zea mays* L.) or soybean (*Glycine max* (L.) Merr.). The image involved radiance in 24 wavebands in the range 475.12 to 910.01 nm, and was taken over a split-plot experiment with corn and soybean assigned to alternate main plot units (one row of 4) and 4 weed treatments assigned to the sub-plot units. The treatments were: no weed control, removal of all weeds, removal of all weeds except velvetleaf, and removal of all weeds except grasses. The main plots were 3m x 3m and weeding was done by hand. Both crop species and the weeds were in vegetative growth stages at the time the image was acquired.

The comparative spectra indicated that weed-free plots could be distinguished from those containing weeds, based on radiance levels in the red and near infrared (NIR) regions. Statistically significant differences were only found in two wavebands, in the red and a range of wavebands in the NIR. Only one waveband exhibited a significant difference, due to treatments in the case of soybean, and it was in the NIR.

Ratios of wavebands in the red and NIR were examined and it was found that many of them exhibited significant differences due to the weed treatments for both crops. Relationships were also examined between spectral data and direct measurements of LAI, greenness, photosynthetic rate and other indicators of crop status. Certain wavebands exhibited very high correlations with leaf greenness, photosynthetic rate, plant height and LAI in plots cropped with corn. In the case of soybean, the correlations were lower and not always in the same direction.

The results of this study were not very conclusive with respect to the main objective, because it was not possible to determine whether the significant differences in radiance at certain wavebands or in waveband ratio were exclusively associated with the type of weed population or with the weed density, the latter not having been controlled in this study.

3.2 Introduction

The applicability of various kinds of remote sensing images to site-specific weed management has been assessed by various authors. Conventional color or color-infrared films, and videography have been used to detect weeds from aerial platforms (Brown and Steckler, 1995; Hanson et al., 1995; Curran, 1985; Menges et al., 1985; Everitt et al., 1996, 1995, 1987). The more recent work in this field has involved data collection at three or four wavebands with airborne digital imaging systems (Rew et al., 2001; Medlin et al., 2000; Lamb et al., 1999; Lass et al., 1996). The relationships have also been investigated between optical or radar imagery and crop biophysical parameters such as biomass, LAI, plant height, canopy temperature and yield (Cloutis et al., 1999, 1996; Inoue and Morinaga, 1995), and the relationships between spectral data and biochemical indicators of crop status, such as chlorophyll (Jago et al., 1999; Curran et al., 1997; Munden et al., 1994). Success has been limited, basically because the differences in spectral signature between crops and weeds are subtle throughout the vegetative stages of growth, whereas they may be quite marked when crops or weeds approach or are within their blooming or senescent stages. This situation does not leave much leeway in making management decisions for weed control at critical times, except against weeds that approach bloom early in the cropping season. Various authors (Lamb and Brown, 2001; Zwiggelaar 1998) have suggested that sensing systems with higher spectral resolution should be used.

The focus of the present study was to reexamine these issues using reflectance in 24 narrow wavebands (in the range 475.12 to 910.01 nm) acquired from an Airborne Imaging Spectrometer for Applications (AISA). The specific objectives of the study were (i) to identify suitable wavelength regions for the detection of weed infestations in corn and soybean crops, and (ii) to examine the correlation between

such multi-spectral data and the biophysical parameters of crops under stress, due to the presence of different weeds.

3.3 Materials and Methods

3.3.1 Study site and experiment details

A split-plot experiment consisting of six main plots was set up in 1999 on a silty clay loam at the Lods Agronomy Research Center, Macdonald Campus, McGill University, Ste-Anne-de-Bellevue, QC, Canada. The 6 plots were laid out in one row, with corn (pioneer 3921 hybrid) and soybean (Bayfield) sown in alternate plots (3 plots each) in the second week of May 1999. The main plots were divided into four subplots (3m x 3m), to which four weed treatments were randomly assigned within each main plot unit. Thus, each combination of crop type and weed treatment was replicated three times. The first treatment involved full removal of weeds (by hand). The second permitted grass species to proliferate while all other types were removed by hand. The third permitted velvetleaf (*Abutilon theophrasti* Medik.) to proliferate while all other species were removed by hand. All weed species were permitted to proliferate in the plots assigned to the fourth treatment.

Corn was sown at a row spacing of 76-cm and density of 70,000 seeds per ha, and soybean was sown at a row spacing of 18-cm at 500,000 seeds per ha. The fertilizer application rates for corn were 115, 35, and 70 kg/ha (N, P, K, respectively). Soybean received 40 kg/ha P and 40 K kg/ha.

3.3.2 Airborne spectral data acquisition

Images of the study plots were acquired from an AISA imaging spectrometer mounted on a Piper Seneca aircraft (Agrimage Inc., Sherbrooke, Quebec, Canada). On July 12, 1999, the flight took place over the experimental field on a cloudless day. On that day, corn was in its late vegetative growth stages (V15 to V17, depending on the particular plot) and soybean was in the early flowering (R1) stage. Weeds were in mid-vegetative growth. Tassels in corn and pods in soybean started forming a few days later, whereas weeds reached the pre-bloom stage more than two weeks later.

The data were acquired at a spatial resolution of 1 m, in 24 wavebands in the visible to near-infrared range of the spectrum (475.12 nm to 910.01 nm). Bandwidths, central wavelengths and wavelength intervals are given in Table 3.1. The raw data were digital numbers (DN). Radiometric corrections for gain, offset, DN dark current, and integration time were applied to the raw data to obtain radiance images.

The data were also corrected for changes in angle of incidence of the reflected radiation at the sensor, due to aircraft pitch and roll, as recorded by the inertial navigation system. A differential geographical positioning system (DGPS) unit was used to reference the image to earth co-ordinates (geo-referencing). Geo-referencing of the image was facilitated by blue tarpaulin sheets that were fixed to each corner of the experimental field. The data processing was performed by Agrimage Inc. using their in-house software.

It is important to note that radiance is the reflected solar radiation received by the sensor, whereas reflectance is the reflected radiation corrected for downwelling irradiation, which changes depending on sun angle and atmospheric conditions (cloud, haze, etc.). Reflectance is therefore the basis of comparison between images taken under different conditions. The sensor for measuring downwelling irradiance was not installed on the aircraft at the time of the flight; however, only one image was taken over the experimental site. The constraint of the overall study is that the data from 1999 cannot be used for quantitative comparison with the data taken in 2000.

3.3.3 Plant parameters

Crop conditions in the experimental plots were determined the day before and the day of the flight. The measurements included plant height, leaf greenness, leaf area index (LAI), chlorophyll fluorescence, and photosynthetic rate. Plant height, a simple and direct indicator of plant health, was measured to the nearest centimeter. The foliage cover per unit of ground area, as represented by LAI, has a direct influence on radiance. LAI is a dimensionless quantity, but can be expressed as cm^2 foliage area per cm^2 ground area. An LAI-2000 Plant Canopy Analyzer (Li-Cor, Inc., Lincoln, Nebraska, USA) was used to obtain these values. One set of readings

Table 3.1 Wavebands used to acquire aerial spectral data

Waveband number	Wavelength interval (nm)	Waveband center (λ) (nm)	Difference in successive wavebands ($\Delta \lambda$) (nm)	Waveband width (nm)	Spectral region
1	475.12 - 479.86	477.49	-	4.7	Blue
2	500.40 - 508.30	504.35	26.86	7.9	Green
3	541.48 - 549.38	545.43	41.08	7.9	Green
4	552.40 - 560.75	556.58	11.15	8.4	Green
5	572.44 - 580.79	576.62	20.04	8.3	Green
6	587.47 - 595.82	591.65	15.03	8.4	Green
7	632.56 - 639.24	635.90	44.25	6.7	Red
8	672.64 - 679.32	675.98	40.08	6.7	Red
9	682.66 - 687.67	685.17	9.19	5.0	Red
10	687.67 - 692.68	690.18	5.01	5.0	Red
11	697.69 - 702.70	700.20	10.02	5.0	Red
12	702.70 - 707.71	705.21	5.01	5.0	Near-Infrared
13	714.52 - 719.71	717.12	11.91	5.2	Near-Infrared
14	724.90 - 730.09	727.50	10.38	5.2	Near-Infrared
15	733.55 - 738.74	736.15	8.65	5.2	Near-Infrared
16	743.93 - 749.12	746.53	10.38	5.2	Near-Infrared
17	754.31 - 759.50	756.91	10.38	5.2	Near-Infrared
18	775.07 - 778.53	776.80	19.89	3.5	Near-Infrared
19	794.10 - 797.56	795.83	19.03	3.5	Near-Infrared
20	809.67 - 813.13	811.40	15.57	3.5	Near-Infrared
21	826.97 - 830.43	828.70	17.30	3.5	Near-Infrared
22	854.65 - 859.84	857.25	28.55	5.2	Near-Infrared
23	878.87 - 884.06	881.47	24.22	5.2	Near-Infrared
24	904.82 - 910.01	907.42	25.95	5.2	Near-Infrared

consisting of one above-canopy and four below-canopy readings (according to standard procedure) were taken in the center of each plot.

Greenness, or the amount of chlorophyll in a plant, is a visible indicator of stress in plants. Because most of the plant nitrogen is contained in the chlorophyll molecules, this measure is a good indicator of the nitrogen status of plants. Greenness was determined with a SPAD Chlorophyll meter (Minolta Camera Ltd., Osaka, Japan) on the newest fully extended leaf on 10 randomly selected plants in each plot.

Chlorophyll fluorescence has been reported to be a convenient indicator of photosynthetic activity. It has been shown that any change in the overall bioenergetic status of a plant is accompanied by a change in chlorophyll fluorescence (Krause and Weis, 1991). Moreover, the changes that affect the opening of stomata and gas exchange with the atmosphere are reflected by changes in the fluorescence characteristics of a leaf. This measure can be used to indicate the photochemical efficiency of the Photosystem II pathway. Chlorophyll fluorescence was measured with a CF-1000, Chlorophyll Fluorescence Measurement System (Morgan Scientific, Inc., Andover, MA, USA) on the newest fully-extended leaf of five randomly selected plants in each plot.

Photosynthesis is the physico-chemical process that converts radiant energy to the chemical energy used by biological systems, and is also a direct indicator of plant health. The LI-6400, Portable Photosynthesis System (Li-Cor, Inc., Lincoln, Nebraska, USA) instrument was used to measure the photosynthetic rate on two fully extended leaves in each plot.

Soil moisture content was determined gravimetrically. Precipitation was about normal in 1999, being 880.7 mm or slightly below the average of 939.7 mm for the area. Details on the climatic parameters for the entire year are given in Table 3.2.

3.3.4 Observations on weeds

Weed density, composition, and time of emergence are some of the criteria used to assess the impact of weeds on crop development. Weed counts were taken in a 50cm x 50cm quadrant at the center of each plot during the week of the flight. The

Table 3.2 Mean monthly temperature, relative humidity, wind speed, and total precipitation during the year 1999 and for a normal year

Month	Year 1999						Normal year (Average based on the years 1961-1990)					
	Temperature (°C)			Relative humidity (%)	Wind speed (km/h)	Precipitation (mm)	Temperature (°C)			Relative humidity (%)	Wind speed (km/h)	Precipitation (mm)
	Max.	Min.	Avg.				Max.	Min.	Avg.			
January	-5.1	-14.2	-9.7	74.88	14.96	142.2	-5.8	-14.9	-10.3	NA	NA	63.3
February	-0.6	-10.2	-5.6	69.55	11.71	29.4	-4.2	-13.5	-8.8	NA	NA	56.4
March	2.7	-5.4	-1.8	70.21	15.42	76.6	2.0	-6.9	-2.4	NA	NA	67.6
April	12.1	1.5	6.5	58.18	13.24	20.9	10.7	0.6	5.7	NA	NA	74.8
May	22.0	8.8	15.8	59.78	10.94	40.8	18.5	7.3	12.9	NA	NA	68.3
June	26.0	15.6	20.8	68.87	10.56	111.0	23.4	12.5	18.0	NA	NA	82.5
July	27.1	17.1	21.7	75.68	11.01	100.2	26.2	15.4	20.8	NA	NA	85.6
August	24.7	14.1	19.0	74.20	9.40	55.0	24.6	14.1	19.4	NA	NA	100.3
September	23.8	12.6	17.3	78.31	8.41	100.1	19.8	9.3	14.5	NA	NA	86.5
October	12.5	3.2	7.6	74.89	11.31	90.5	13.0	3.6	8.3	NA	NA	75.4
November	9.4	0.9	4.8	73.71	14.22	45.4	5.2	-2.0	1.6	NA	NA	93.4
December	0.5	-6.7	-3.5	78.92	12.95	68.6	-2.9	-11.0	-6.9	NA	NA	85.6

NA: Not available

time of emergence of weeds was not recorded, although it was noted that some weeds had emerged before the crop. At the time of the flight, however, all weeds in the plots were fully established.

3.3.5 Data analysis

Processed radiance images were imported into the IDRISI GIS software (Version 2.00.000, Clark University, MA, USA) using the PCI software (Version 6.2.1 (Demo), PCI Geomatics, ON, Canada). Representative values for each waveband were obtained by extracting the average radiance for the waveband from the central portion of each plot in the image. The central portion of the plot was marked by examining the image visually. The visual interpretation was aided by identifying the soil buffer strips that surrounded each plot.

Scheffe's multiple range test (Steel et al., 1997) was used to determine which wavebands best explained differences between type of weed infestation. SAS software (Version 6.11, North Carolina, USA) was used for the analysis, which was carried out at the 95% significance level ($P < 0.05$). Simple linear regression and correlation analyses were used to relate the spectral data to crop physiological parameters.

3.4 Results and Discussion

The presentation of the results from ground-based observations is of primary importance, because the discussion of the significance of spectral data will necessarily refer to the direct measurements made on the canopies.

3.4.1 Ground-based observations

3.4.1.1 Observations on weeds

Weeds were generally uniformly distributed over the plots. Yellow foxtail (*Setaria glauca*) was the most prominent among the grassy weeds, which also included barnyard grass (*Echinochloa crusgalli*) and yellow nutsedge (*Cyperus esculentus*). Velvetleaf (*Abutilon theophrasti* Medik.), redroot pigweed (*Amaranthus retroflexus*), and lamb's quarters (*Chenopodium album*) were the most prominent

broadleaved weeds. The replicate-averaged weed counts for the four weed treatments are presented in Table 3.3, for each individual crop.

As expected, weed density was higher in the plots without weed control for both crops, and weed density was lower in each treatment class for soybean than for corn. The difference in weed density between corn and soybean is likely due to the latter's ability to compete for light (greater soil coverage due to greater plant density and leaf structure), as exhibited by a much higher LAI for soybean (Table 3.4, section 3.4.1.2) and possibly in part due to poorer growth conditions for weeds in the soybean plots because there was not an application of nitrogenous fertilizer.

3.4.1.2 Crop physiological parameters

The replicate-averaged crop physiological parameters for the four weed treatments are presented in Table 3.4, for each individual crop. The most striking feature of these data involves significant differences in the physiological parameters of corn due to the presence of weeds, whereas there are none apparent in the case of soybean. As suggested in the preceding section, when soybean was seeded at recommended rates and row spacing, this crop holds a greater competitive advantage over the predominant weed species than that exhibited by corn. The sensitivity of corn to the weed populations is evidenced by a definite tendency toward lower photosynthetic rates of corn leaves, where weeds are allowed to proliferate, compared to the rate in weed-free corn canopies. Although the photosynthetic rate is significantly lower only in plots with no weed control (mixed grasses), Table 3.3 indicates that there are more total weeds without weed control in place, compared to the removal of all but one species (velvetleaf) or family (grasses). If the weed density of velvetleaf or grassy weeds was the same as the mixed weeds, it is suggested that the photosynthetic rate of corn would be significantly lower than the weed-free rate. The effect of weeds is manifested by shorter plants and evidence of nitrogen stress in corn (lower greenness).

Table 3.3 Weed count in different weed treatments for corn and soybean crops

Treatment	Grassy weeds (shoots per sq. meter)		Velvetleaf (plants per sq. meter)	Broadleaf weeds* (plants per sq. meter)	Total (shoots/plants per sq. meter)
	Yellow foxtail	Others			
Corn + Velvetleaf	-	-	62	-	62
Corn + Mixed weeds	53	53	-	19	125
Corn + Grasses	48	59	-	-	107
Soybean + Velvetleaf	-	-	21	-	21
Soybean + Mixed weeds	32	22	-	6	60
Soybean + Grasses	23	31	-	-	54

* Broadleaf weeds included velvetleaf plants also

Table 3.4 Details of various measurements of crop parameters and volumetric soil moisture content, (average value \pm SD)

a. Corn

Crop parameter	Corn + Velvetleaf	Corn + Mixed weeds	Corn + Grasses	Corn + No weeds	Variation across various treatments
Leaf area index (cm ² /cm ²)	2.31 \pm 0.24 ^b	3.11 \pm 0.17 ^a	2.11 \pm 0.29 ^b	1.73 \pm 0.13 ^b	1.60 to 3.29
Plant height (cm)	76.5 \pm 6.8 ^b	71.4 \pm 13.3 ^b	99.7 \pm 9.7 ^{ab}	109.3 \pm 10.4 ^a	59.6 to 116.1
Greenness (comparative scale)	20.9 \pm 3.4 ^{cb}	14.0 \pm 4.4 ^c	27.6 \pm 5.4 ^{ab}	36.3 \pm 1.7 ^a	9.5 to 38.2
Chlorophyll fluorescence (ratio, unitless)	0.709 \pm 0.021 ^a	0.672 \pm 0.030 ^a	0.718 \pm 0.034 ^a	0.696 \pm 0.069 ^a	0.619 to 0.754
Photosynthesis rate (μ molCO ₂ m ⁻² s ⁻¹)	21.90 \pm 1.90 ^a	13.38 \pm 4.35 ^b	25.20 \pm 2.65 ^a	27.83 \pm 1.16 ^a	8.45 to 28.90
Soil moisture content (%)	13.20 \pm 1.30 ^a	12.11 \pm 1.95 ^a	12.32 \pm 1.72 ^a	11.85 \pm 1.47 ^a	10.15 to 14.69

b. Soybean

Crop parameter	Soybean + Velvetleaf	Soybean + Mixed weeds	Soybean + Grasses	Soybean + No weeds	Variation across various treatments
Leaf area index (cm ² /cm ²)	7.57 \pm 0.30 ^a	7.40 \pm 0.99 ^a	7.27 \pm 0.98 ^a	6.22 \pm 1.05 ^a	5.01 to 8.33
Plant height (cm)	61.3 \pm 2.8 ^a	62.2 \pm 6.5 ^a	61.8 \pm 7.2 ^a	52.2 \pm 6.1 ^a	45.2 to 69.4
Greenness (comparative scale)	31.4 \pm 1.8 ^a	30.5 \pm 2.1 ^a	32.0 \pm 1.4 ^a	30.4 \pm 1.6 ^a	28.1 to 33.6
Chlorophyll fluorescence (ratio, unitless)	0.628 \pm 0.009 ^a	0.656 \pm 0.012 ^a	0.635 \pm 0.015 ^a	0.661 \pm 0.018 ^a	0.618 to 0.677
Photosynthesis rate (μ molCO ₂ m ⁻² s ⁻¹)	18.93 \pm 1.25 ^a	21.67 \pm 1.07 ^a	20.37 \pm 4.31 ^a	20.33 \pm 3.52 ^a	15.40 to 23.20
Soil moisture content (%)	13.16 \pm 1.73 ^a	13.08 \pm 1.90 ^a	12.35 \pm 2.15 ^a	11.86 \pm 0.73 ^a	10.63 to 15.27

Mean parameter values (\pm SD) with same superscript letters in each row are not significantly different (Scheffe's multiple range test, P<0.05).

3.4.2 Spectral response

The replicate-averaged radiance data obtained at various combinations of weed infestation and crop are presented in Figures 3.1 and 3.2 for corn and soybean, respectively. High absorption in the visible and high reflectance in the near-infrared wavebands are typical of vegetation reflectance curves, according to Guyot (1990) who reported that chlorophyll and other pigments absorb about 85% of the incoming visible radiation and that leaves absorb only about 50% of the incoming NIR. Because chlorophyll a and chlorophyll b in plant leaves exhibit maximum absorption in the blue and red wavebands, leaves show maximum reflectance at 550 nm (yellow-green). Although canopy reflectance spectra can differ somewhat from these general characteristics of leaf spectra, depending on the development stage and extent of the vegetation cover, the spectra of Figures 3.1 and 3.2 do conform to them, because they were obtained at a fairly advanced stage of crop development. The expected peak at 550 nm reflects a plateau from the central wavelengths of wavebands 3 and 4, (545.43 and 556.58 nm).

The clearest distinctions between the four types of vegetation cover (i.e. weed controls) in Figures 3.1 and 3.2 are associated with comparatively higher radiance in the visible red, in weed-free plots, and lower radiance in the NIR in weed-free plots. This is due to the combined effect of a lower proportion of radiance from plants and a higher proportion of radiance from soil under such a condition of sparser leaf coverage. The plots without weed control are associated with comparatively lower radiance in the visible red and comparatively higher radiance in the NIR. In the plots cropped with corn, these effects appear to mimic the trends in LAI, whereas the situation is not so clearly defined in the case of soybean, where there were no significant differences in LAI attributable to the weed treatments. Therefore negative correlations are anticipated between LAI and radiance in the visible red, and positive correlations in the NIR. This expectation is borne out in Tables 3.9 and 3.10.

An interesting comparative feature of Figures 3.1 and 3.2 is that the radiance in the visible spectrum is of the same magnitude for both corn and soybean, although LAI is substantially greater in all soybean plots than in corn plots. However, radiance in the NIR from soybean plots becomes increasingly greater than that of the corn

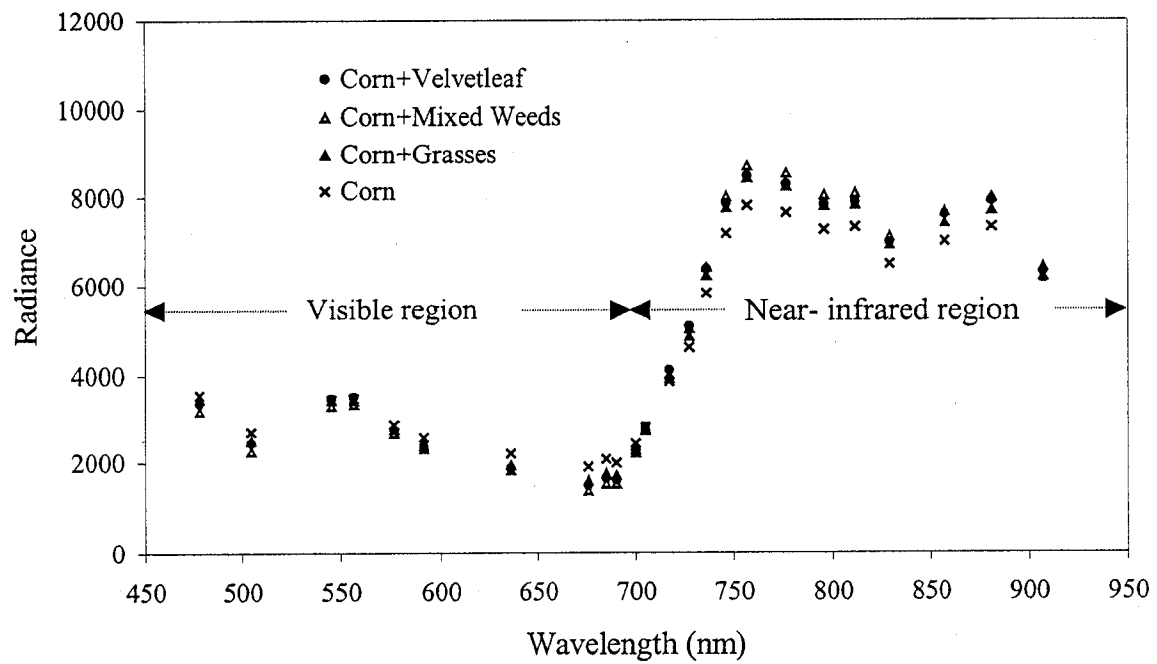


Fig. 3.1 Mean radiance ($\mu\text{W}/\text{cm}^2/\text{sr}/\text{nm}$) of corn under different weed treatments at different wavebands

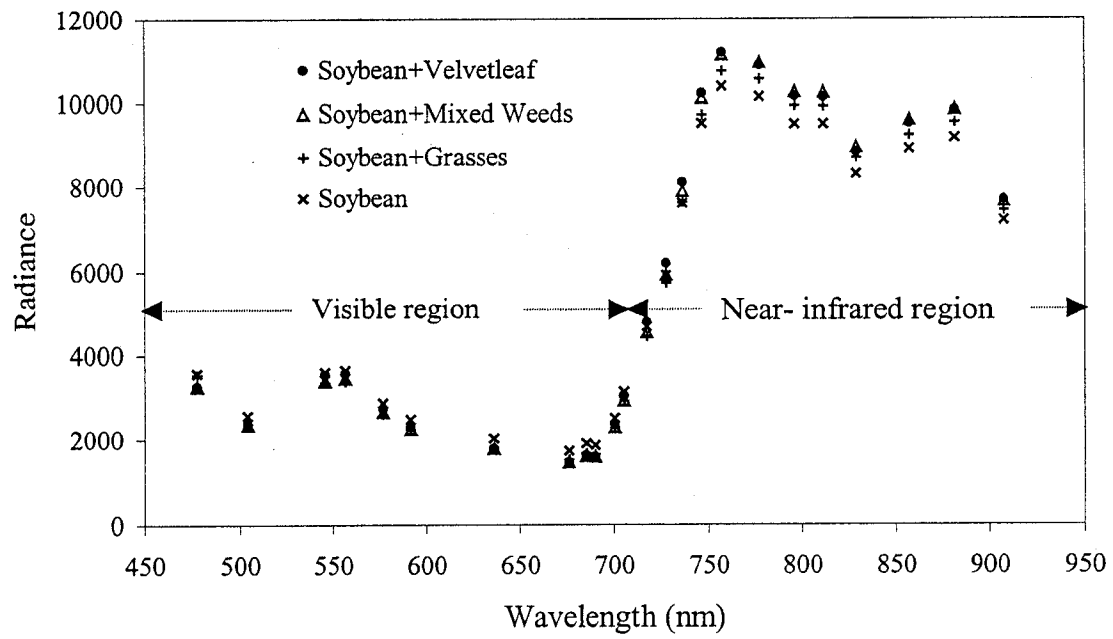


Fig. 3.2 Mean radiance ($\mu\text{W}/\text{cm}^2/\text{sr}/\text{nm}$) of soybean under different weed treatments at different wavebands

plots, as the wavelength increases from about 700 nm to about 750 nm, the difference being maintained on to about 875 nm. The NIR differences appear to reflect the large difference in LAI between plots of the two crops rather than any influence of weeds; however, the question remains as to why the same is not true in the visible spectra. Such different behavior may reflect the combined effects of the denser soybean canopy and the high level of absorption (85%) of visible radiation compared to NIR (50%), as noted by Guyot (1990). Briefly stated, the visible light received by the sensor is mainly a function of the leaf coverage at the upper levels of the canopy, with the light reflected from lower levels being, for the most part, absorbed before reaching leafless regions. In the case of NIR radiation, more energy is transmitted from upper canopy to the lower canopy which can then be reflected back.

3.4.3 Suitable wavebands for detection of weeds

The spectral data were analyzed to determine whether any fine features in the data could be related to the different weed treatments more precisely than the visual analysis of Figures 3.1 and 3.2 as presented above. The results of Scheffé's multiple range test are summarized in Tables 3.5 and 3.6 for corn and soybean, respectively. There were significant differences in radiance in the red part of the spectrum between the plots of weed-free corn and plots of corn with mixed weeds at wavebands 8 and 9 (Table 3.5). However, at the same wavebands, the other weed treatments exhibited no differences in radiance either between themselves or with the weed-free and mixed weed plots.

There were also significant differences in radiance at wavebands 16 to 21 (746.53 to 828.70 nm). The radiance of weed-free corn was significantly lower than that of corn with velvetleaf and corn with mixed weeds in wavebands 16, 17 and 19; however, there was not such a significant difference with that of corn with grasses. In waveband 18 (776.80 nm), the radiance of the weed-free crop was significantly lower ($P < 0.05$) than that of corn infested with any of the weeds.

The above relationships are so similar to the comparisons of LAI, photosynthetic rate and greenness presented in Table 3.4, that it may be concluded

Table 3.5 Statistical analysis of radiance in different wavebands for corn

Waveband Number	Radiance ($\mu\text{W}/\text{cm}^2/\text{sr}/\text{nm}$)			
	Corn + Velvetleaf	Corn + Mixed weeds	Corn + Grasses	Corn + No weeds
1	3379 \pm 140 ^a	3206 \pm 107 ^a	3492 \pm 64 ^a	3566 \pm 131 ^a
2	2454 \pm 97 ^a	2271 \pm 53 ^a	2515 \pm 80 ^a	2705 \pm 162 ^a
3	3473 \pm 18 ^a	3323 \pm 138 ^a	3449 \pm 93 ^a	3459 \pm 148 ^a
4	3513 \pm 11 ^a	3359 \pm 142 ^a	3454 \pm 100 ^a	3485 \pm 159 ^a
5	2773 \pm 9 ^a	2676 \pm 122 ^a	2774 \pm 85 ^a	2891 \pm 158 ^a
6	2382 \pm 21 ^a	2315 \pm 101 ^a	2392 \pm 87 ^a	2576 \pm 167 ^a
7	1871 \pm 48 ^a	1826 \pm 78 ^a	1946 \pm 72 ^a	2205 \pm 150 ^a
8	1484 \pm 57 ^{ab}	1389 \pm 41 ^b	1595 \pm 72 ^{ab}	1898 \pm 170 ^a
9	1637 \pm 70 ^{ab}	1526 \pm 49 ^b	1762 \pm 88 ^{ab}	2073 \pm 184 ^a
10	1604 \pm 73 ^a	1527 \pm 52 ^a	1714 \pm 83 ^a	1988 \pm 165 ^a
11	2273 \pm 62 ^a	2225 \pm 112 ^a	2290 \pm 101 ^a	2437 \pm 150 ^a
12	2824 \pm 81 ^a	2743 \pm 162 ^a	2778 \pm 119 ^a	2823 \pm 150 ^a
13	4104 \pm 84 ^a	4012 \pm 232 ^a	3941 \pm 163 ^a	3863 \pm 143 ^a
14	5062 \pm 60 ^a	5020 \pm 244 ^a	4848 \pm 127 ^a	4608 \pm 105 ^a
15	6392 \pm 28 ^a	6428 \pm 246 ^a	6241 \pm 72 ^a	5831 \pm 82 ^a
16	7858 \pm 43 ^a	8017 \pm 219 ^a	7781 \pm 54 ^{ab}	7198 \pm 85 ^b
17	8484 \pm 61 ^a	8714 \pm 204 ^a	8432 \pm 76 ^{ab}	7824 \pm 101 ^b
18	8295 \pm 72 ^a	8533 \pm 187 ^a	8246 \pm 59 ^a	7662 \pm 77 ^b
19	7846 \pm 110 ^a	8053 \pm 187 ^a	7818 \pm 8 ^{ab}	7282 \pm 58 ^b
20	7899 \pm 135 ^{ab}	8092 \pm 189 ^a	7842 \pm 30 ^{ab}	7339 \pm 37 ^b
21	6994 \pm 159 ^{ab}	7146 \pm 180 ^a	6945 \pm 14 ^{ab}	6498 \pm 36 ^b
22	7621 \pm 178 ^a	7689 \pm 245 ^a	7439 \pm 49 ^a	7022 \pm 75 ^a
23	7916 \pm 227 ^a	8001 \pm 287 ^a	7714 \pm 50 ^a	7344 \pm 137 ^a
24	6334 \pm 230 ^a	6444 \pm 231 ^a	6233 \pm 64 ^a	6038 \pm 180 ^a

Mean radiance values (\pm SE) with same superscript letters in each band are not significantly different (Scheffe's multiple range test, $P < 0.05$).

Table 3.6 Statistical analysis of radiance in different wavebands for soybean

Waveband Number	Radiance ($\mu\text{W}/\text{cm}^2/\text{sr}/\text{nm}$)			
	Soybean + Velvetleaf	Soybean + Mixed weeds	Soybean + Grasses	Soybean + No weeds
1	3266±39 ^a	3277±40 ^a	3534±85 ^a	3576±156 ^a
2	2386±6 ^a	2375±73 ^a	2370±74 ^a	2589±83 ^a
3	3534±114 ^a	3408±121 ^a	3355±79 ^a	3600±52 ^a
4	3566±131 ^a	3458±128 ^a	3384±81 ^a	3648±59 ^a
5	2744±73 ^a	2666±107 ^a	2616±74 ^a	2888±55 ^a
6	2314±44 ^a	2260±100 ^a	2248±83 ^a	2498±58 ^a
7	1800±20 ^a	1786±85 ^a	1801±65 ^a	2041±66 ^a
8	1464±35 ^a	1464±74 ^a	1512±89 ^a	1737±82 ^a
9	1618±33 ^a	1614±81 ^a	1671±94 ^a	1917±92 ^a
10	1595±29 ^a	1596±80 ^a	1646±81 ^a	1861±91 ^a
11	2372±57 ^a	2312±101 ^a	2308±80 ^a	2528±62 ^a
12	3057±94 ^a	2945±108 ^a	2930±96 ^a	3137±62 ^a
13	4778±170 ^a	4542±122 ^a	4443±117 ^a	4679±44 ^a
14	6204±218 ^a	5937±80 ^a	5744±116 ^a	5917±34 ^a
15	8112±237 ^a	7899±41 ^a	7630±150 ^a	7607±46 ^a
16	10229±251 ^a	10113±73 ^a	9722±223 ^a	9528±67 ^a
17	11173±235 ^a	11139±108 ^a	10743±280 ^a	10391±122 ^a
18	10879±187 ^a	10952±151 ^a	10557±263 ^a	10148±119 ^a
19	10168±152 ^a	10262±103 ^a	9934±236 ^a	9512±148 ^a
20	10137±135 ^{ab}	10248±84 ^a	9924±193 ^{ab}	9514±155 ^b
21	8857±135 ^a	8979±118 ^a	8712±173 ^a	8326±117 ^a
22	9517±187 ^a	9617±138 ^a	9248±170 ^a	8929±160 ^a
23	9826±176 ^a	9860±138 ^a	9552±108 ^a	9189±162 ^a
24	7692±132 ^a	7654±125 ^a	7426±69 ^a	7194±163 ^a

Mean radiance ratio values (\pm SE) with same superscript letters in each band are not significantly different (Scheffe's multiple range test, $P < 0.05$).

that the presence of weeds in a corn crop are be detected through analysis of spectral data, if there is a priori knowledge of the contribution to LAI of the corn itself, in respect of its stage of growth, health status and crop density (spacing and plants per row).

The statistical analysis performed on the soybean crop (Table 3.6) indicated that, with the exception of waveband 20 (811.40 nm), the recorded radiance values were not significantly different for the weed-infested and weed-free soybean treatments. At waveband 20 (811.40 nm), however, the only significant difference existed between the two extreme treatments (weed free and mixed weed), as indicated with corn. The scarcity of additional information realized from this analysis of the radiance of the plots with soybeans is not surprising, given that the weed treatments had no significant effect on the soybean physiological parameters, which is in all likelihood due to the comparatively low weed densities.

Multi-spectral imaging systems were used in previous studies aimed at detecting weeds or distinguishing them from other vegetation. These systems usually had broad waveband sensors, with wavebands centered or sensitive in the blue (400 to 500 nm), green (500 to 600 nm), red (600 to 700 nm), and near-infrared (700 to 1000 nm) ranges (Bajwa and Tian, 2001; Lamb et al., 1999; Lass and Callihan, 1997; Lass et al. 1996; Everitt et al., (1996, 1995, 1994)). Brown et al. (1994) found that wavebands centered at 440, 530, 650, and above 730 nm were useful in distinguishing between weed species. Brown et al. (1994) selected these wavebands based on field-spectroradiometer measurements acquired over weed canopies rather than over weed-infested crop canopies, yet had limited success in separating different weeds. Results were even poorer when the images were acquired from a still-video camera, with four filters from a height of 10m. Very high within-class variability was cited as the reason for poor discrimination. However, in another study of the same field, slightly better results were reported, when images were acquired from an airborne platform (Brown and Steckler, 1993). Good weed classification results were reported when all weeds were grouped into one class and separated from corn or from the soil. Similarly, using a field-spectroradiometer, Everitt et al. (1987) reported significant differences in the spectral response of various rangeland weeds and other vegetation at 550, 650, and

850 nm. The differences in the spectral response of weeds were attributed to differences in foliage color and biomass.

3.4.4 Ratios of wavebands in the red and NIR

Many vegetation indices (VIs), that combine reflectance at two or more wavelengths in different ways, have been found useful in characterizing plant growth and development (Jackson and Huete, 1991). In a recent study, Zwiggelaar (1998) found some ratio vegetation indices (RVIs) useful in the discrimination of weeds from crops, and in particular from row crops. As a result, this study has attempted to evaluate different waveband ratios for discriminating between the different weed treatments.

Wavebands 8, 9, and 10 and wavebands 16 to 24 in the near-infrared plateau region were combined in all possible ratios of red to near-infrared on a one-to-one basis. Scheffe's multiple range test was used to detect significant differences in the ratios due to the weed treatments, as was the case for the analysis of individual wavebands.

The results of this analysis are presented in Tables 3.7 and 3.8. The results for corn clearly establish that the values of these waveband ratios for pure corn were significantly different ($P < 0.05$) from those of corn infested with velvetleaf and mixed weeds. Thus, the waveband ratios, given in Table 3.7, and waveband 18 (776.80 nm) may be used to determine the presence of weeds in corn fields.

In the case of soybean (Table 3.8), it is evident that waveband ratios are more effective at discriminating between weed treatments than are radiance values. However, there was a similar difficulty in distinguishing the velvetleaf only and grasses only treatments. Although the weed-free soybean crop and soybeans with mixed weeds were distinguishable at several waveband ratios, it was not possible to differentiate the other weed treatments. It was difficult to make a distinction between the different weed treatments visually, because the dominant canopy coverage of the soybean crop suppressed weed growth in the velvetleaf and grass weed treatments.

Table 3.7 Statistical analysis of radiance ratios in different wavebands for corn

Waveband ratio	Radiance ratio ($\times 10^{-3}$) (unitless)			
	Corn + Velvetleaf	Corn + Mixed weeds	Corn + Grasses	Corn + No weeds
8/16	189 \pm 7 ^b	173 \pm 4 ^b	205 \pm 9 ^{ab}	264 \pm 25 ^a
8/17	175 \pm 7 ^b	159 \pm 3 ^b	189 \pm 9 ^{ab}	243 \pm 23 ^a
8/18	179 \pm 6 ^b	163 \pm 4 ^b	194 \pm 9 ^{ab}	248 \pm 24 ^a
8/19	189 \pm 5 ^b	173 \pm 5 ^b	204 \pm 9 ^{ab}	261 \pm 25 ^a
8/20	188 \pm 4 ^b	172 \pm 5 ^b	203 \pm 9 ^{ab}	259 \pm 24 ^a
8/21	212 \pm 3 ^b	195 \pm 6 ^b	230 \pm 11 ^{ab}	292 \pm 28 ^a
8/22	195 \pm 3 ^b	181 \pm 6 ^b	214 \pm 10 ^{ab}	270 \pm 25 ^a
8/23	187 \pm 2 ^b	174 \pm 5 ^b	207 \pm 9 ^{ab}	259 \pm 26 ^a
8/24	234 \pm 1 ^{ab}	216 \pm 7 ^b	256 \pm 11 ^{ab}	316 \pm 34 ^a
9/16	208 \pm 9 ^b	190 \pm 4 ^b	227 \pm 11 ^{ab}	289 \pm 27 ^a
9/17	193 \pm 8 ^b	175 \pm 4 ^b	209 \pm 10 ^{ab}	265 \pm 25 ^a
9/18	197 \pm 7 ^b	179 \pm 5 ^b	214 \pm 11 ^{ab}	271 \pm 26 ^a
9/19	209 \pm 6 ^b	190 \pm 6 ^b	225 \pm 11 ^{ab}	285 \pm 27 ^a
9/20	207 \pm 5 ^b	189 \pm 6 ^b	225 \pm 11 ^{ab}	283 \pm 26 ^a
9/21	234 \pm 5 ^b	214 \pm 6 ^b	254 \pm 13 ^{ab}	319 \pm 30 ^a
9/22	215 \pm 4 ^b	199 \pm 7 ^b	237 \pm 12 ^{ab}	295 \pm 27 ^a
9/23	207 \pm 3 ^b	191 \pm 6 ^b	228 \pm 11 ^{ab}	283 \pm 28 ^a
9/24	258 \pm 2 ^{ab}	237 \pm 7 ^b	283 \pm 13 ^{ab}	345 \pm 37 ^a
10/16	204 \pm 9 ^b	190 \pm 2 ^b	220 \pm 10 ^{ab}	276 \pm 24 ^a
10/17	189 \pm 9 ^b	175 \pm 3 ^b	203 \pm 10 ^{ab}	254 \pm 22 ^a
10/18	193 \pm 8 ^b	179 \pm 4 ^b	208 \pm 10 ^{ab}	260 \pm 23 ^a
10/19	204 \pm 7 ^b	190 \pm 4 ^b	219 \pm 10 ^{ab}	273 \pm 24 ^a
10/20	203 \pm 6 ^b	189 \pm 4 ^b	219 \pm 11 ^{ab}	271 \pm 23 ^a
10/21	229 \pm 6 ^b	214 \pm 5 ^b	247 \pm 12 ^{ab}	306 \pm 27 ^a
10/22	210 \pm 5 ^b	199 \pm 5 ^b	230 \pm 12 ^{ab}	283 \pm 25 ^a
10/23	202 \pm 4 ^{ab}	191 \pm 4 ^b	222 \pm 11 ^{ab}	271 \pm 25 ^a
10/24	253 \pm 3 ^{ab}	237 \pm 5 ^b	275 \pm 13 ^{ab}	331 \pm 34 ^a

Mean radiance ratio (\pm SE) with same superscript letters in each waveband ratio are not significantly different (Scheffe's multiple range test, $P < 0.05$).

Table 3.8 Statistical analysis on radiance ratios of different wavebands for soybean

Waveband Ratio	Radiance ratio (x 10 ³) (unitless)			
	Soybean + Velvetleaf	Soybean + Mixed weeds	Soybean + Grasses	Soybean + No weeds
8/16	143±7 ^a	145±8 ^a	155±8 ^a	182±8 ^a
8/17	131±6 ^b	132±8 ^{ab}	141±8 ^{ab}	167±7 ^a
8/18	135±6 ^{ab}	134±9 ^b	143±8 ^{ab}	171±7 ^a
8/19	144±6 ^b	143±9 ^b	152±8 ^{ab}	183±7 ^a
8/20	145±5 ^b	143±8 ^b	152±8 ^{ab}	182±7 ^a
8/21	165±7 ^{ab}	163±10 ^b	173±9 ^{ab}	209±8 ^a
8/22	154±6 ^a	153±10 ^a	164±10 ^a	194±7 ^a
8/23	149±6 ^a	149±10 ^a	158±9 ^a	189±8 ^a
8/24	190±7 ^b	192±13 ^{ab}	203±11 ^{ab}	241±8 ^a
9/16	158±7 ^a	160±9 ^a	172±9 ^a	201±9 ^a
9/17	145±6 ^b	145±9 ^b	156±9 ^{ab}	184±8 ^a
9/18	149±6 ^b	148±9 ^b	158±9 ^{ab}	189±8 ^a
9/19	159±6 ^b	157±10 ^b	168±9 ^{ab}	201±8 ^a
9/20	160±5 ^b	158±9 ^b	168±9 ^{ab}	201±8 ^a
9/21	183±7 ^b	180±11 ^b	192±10 ^{ab}	230±9 ^a
9/22	170±7 ^{ab}	168±11 ^b	181±11 ^{ab}	215±8 ^a
9/23	165±6 ^{ab}	164±10 ^b	175±10 ^{ab}	209±9 ^a
9/24	211±7 ^b	211±14 ^b	225±12 ^{ab}	266±9 ^a
10/16	156±6 ^a	158±9 ^a	169±8 ^a	195±9 ^a
10/17	143±5 ^a	143±9 ^a	153±7 ^a	179±8 ^a
10/18	147±5 ^a	146±9 ^a	156±8 ^a	183±8 ^a
10/19	157±5 ^{ab}	156±5 ^b	166±8 ^{ab}	196±8 ^a
10/20	157±5 ^b	156±9 ^b	166±8 ^{ab}	195±8 ^a
10/21	180±6 ^{ab}	178±11 ^b	189±9 ^{ab}	223±9 ^a
10/22	168±6 ^a	166±11 ^a	178±9 ^a	208±9 ^a
10/23	163±6 ^a	162±10 ^a	172±8 ^a	203±9 ^a
10/24	208±7 ^a	209±14 ^a	222±10 ^a	259±10 ^a

Mean radiance ratio (±SE) with same superscript letters in each waveband ratio are not significantly different (Scheffe's multiple range test, P<0.05).

3.4.5 Relationship between crop physiological parameters and spectral data

This section discusses the results of the analysis linking ground observations of crop physiological parameters (Table 3.4 above) and the corresponding spectral measurements.

The simple correlation coefficients (r) between the crop physiological parameters and the spectral measurements are given in Tables 3.9 and 3.10 for corn and soybean, respectively. Good correlation was observed between radiance and the various crop parameters. The maximum correlation between radiance and the crop parameters for corn were: -0.809 for LAI, -0.812 for plant height, -0.858 for greenness, -0.814 for photosynthesis rate, 0.389 for chlorophyll fluorescence and -0.263 for soil moisture, in wavebands 9, 14, 19, 18, 9 and 24, respectively. Similarly, the maximum correlation coefficients between the radiance and the crop parameters for soybean were: 0.786 for LAI; -0.733 for plant height; -0.549 for greenness; 0.455 for photosynthesis rate; -0.605 for chlorophyll fluorescence; and 0.736 for soil moisture, in wavebands 24, 21, 4, 19, 24, and 22, respectively. This analysis indicated that the highest correlation between radiance and a given parameter was not always found in the same waveband for both crops.

In general, it was observed that the correlations between crop physiological parameters and radiance were higher for corn, corresponding to the greater influence of weeds on corn than on soybean, as discussed in section 3.4.1.2. It is also interesting to note that higher correlation values were obtained for wavebands in the near-infrared region, with the exception of three cases within the visible region: soybean greenness in waveband 4 (556.58 nm) and corn LAI and chlorophyll fluorescence in waveband 9 (585.17 nm).

The observed spectral responses of the canopies were the result of complex interactions between crops, weeds and soil factors. In the present study, complications arose due to the presence of weeds, differences in individual leaf properties, and canopy structures. For example, in the case of soybean, the highest negative correlation was obtained between greenness and radiance values in waveband 4 (556.58 nm). However, higher radiance in this region usually indicates better growth and more biomass. Thus, it is difficult to extrapolate results obtained at leaf scale or

Table 3.9 Correlation coefficient (r) values relating radiance and crop parameters for corn

Waveband	Leaf area index	Plant height	Greenness	Photosynthesis rate	Chlorophyll fluorescence	Soil moisture
1	-0.716	0.441	0.507	0.445	0.057	-0.013
2	-0.790	0.339	0.569	0.561	0.376	-0.005
3	-0.493	-0.162	0.096	0.127	0.220	-0.105
4	-0.457	-0.210	0.064	0.073	0.199	-0.108
5	-0.583	0.017	0.306	0.231	0.252	-0.155
6	-0.618	0.089	0.387	0.267	0.287	-0.138
7	-0.728	0.339	0.590	0.446	0.288	-0.210
8	-0.798	0.471	0.710	0.564	0.373	-0.135
9	-0.809	0.462	0.701	0.558	0.389	-0.158
10	-0.792	0.415	0.656	0.495	0.362	-0.165
11	-0.589	-0.007	0.263	0.170	0.229	-0.210
12	-0.394	-0.313	-0.066	-0.100	0.166	-0.218
13	-0.053	-0.633	-0.452	-0.416	0.011	-0.194
14	0.275	-0.812	-0.715	-0.651	-0.104	-0.119
15	0.460	-0.802	-0.795	-0.744	-0.195	-0.068
16	0.622	-0.737	-0.822	-0.777	-0.283	-0.043
17	0.654	-0.724	-0.813	-0.797	-0.287	-0.048
18	0.679	-0.730	-0.838	-0.814	-0.274	-0.011
19	0.633	-0.742	-0.858	-0.786	-0.267	-0.016
20	0.613	-0.746	-0.840	-0.801	-0.221	-0.024
21	0.565	-0.731	-0.831	-0.755	-0.193	-0.048
22	0.507	-0.756	-0.816	-0.717	-0.161	0.010
23	0.442	-0.704	-0.770	-0.685	-0.190	-0.121
24	0.312	-0.558	-0.650	-0.569	-0.198	-0.263

Table 3.10 Correlation coefficient (r) values relating radiance and crop parameters for soybean

Waveband	Leaf area index	Plant height	Greenness	Photosynthesis rate	Chlorophyll fluorescence	Soil moisture
1	-0.177	-0.001	0.099	0.394	0.050	-0.061
2	-0.220	-0.207	-0.222	0.196	0.224	-0.524
3	-0.308	-0.287	-0.522	-0.204	0.218	-0.498
4	-0.313	-0.288	-0.549	-0.177	0.245	-0.480
5	-0.344	-0.322	-0.471	-0.084	0.296	-0.541
6	-0.340	-0.316	-0.376	0.018	0.310	-0.591
7	-0.356	-0.319	-0.288	0.179	0.332	-0.559
8	-0.216	-0.179	-0.099	0.310	0.234	-0.540
9	-0.240	-0.200	-0.123	0.289	0.244	-0.538
10	-0.253	-0.215	-0.166	0.290	0.237	-0.525
11	-0.311	-0.271	-0.395	0.093	0.268	-0.541
12	-0.210	-0.168	-0.412	0.034	0.136	-0.464
13	-0.092	-0.066	-0.427	-0.084	-0.005	-0.232
14	0.104	0.128	-0.357	-0.053	-0.182	0.053
15	0.362	0.385	-0.181	0.100	-0.354	0.313
16	0.541	0.563	0.008	0.209	-0.448	0.502
17	0.629	0.647	0.119	0.340	-0.524	0.608
18	0.679	0.692	0.197	0.383	-0.518	0.638
19	0.724	0.724	0.265	0.455	-0.546	0.634
20	0.737	0.723	0.260	0.450	-0.544	0.616
21	0.743	0.733	0.315	0.439	-0.539	0.644
22	0.706	0.663	0.328	0.408	-0.532	0.736
23	0.761	0.691	0.449	0.342	-0.558	0.669
24	0.786	0.701	0.489	0.374	-0.605	0.704

from canopies having only one species of plant, to complex canopies involving crops and weeds.

These results were nevertheless comparable to those of other relationship estimates between crop parameters and remotely sensed spectral data. Ma et al. (1996) reported significant negative correlations (r ranged from -0.52 to -0.95) between data acquired with a hand-held multi-spectral radiometer and greenness (SPAD readings) at 600 nm, and LAI ($r = -0.49$ to -0.87) of corn plants at different stages of growth. In the above experiment, spectral measurements were acquired in eight wavebands (450 to 800 nm) over corn plots with different nitrogen application rates. The wavebands centered at 600 and 800 nm were found useful in deriving such relationships. Cloutis et al. (1996) reported correlation coefficients of 0.75 and greater between aerial spectral data and parameters describing crop condition (LAI, plant height, and difference in the canopy and ambient temperature) for various crops. The highest correlations were obtained at different wavebands for different crops and at different growth stages. Leaf chlorophyll was negatively correlated to spectral data near 600 nm for soybean (Adcock et al., 1990), and at 550 nm for corn (Blackmer et al., 1994a). Similarly, Thenkabail et al. (2000) reported correlations of 0.88 and 0.81 between ground spectral data and LAI, and ground spectral data and plant height, respectively. However, these studies did not report the effect of weeds on these relationships, which makes it difficult to compare such results with those of the present study. Moreover, differences in type of sensor (multi- or hyper-spectral), type of platforms (ground- or air-based) of the study, and the scale of study (leaf or canopy) make it all the more difficult to draw comparisons or make inferences from previous work.

Simple linear regressions were also executed in an attempt to develop relationships between crop parameters and spectral measurements. These relationships could then be used to estimate various crop parameters, based on the recorded radiance data. The regressions were based on the waveband with the highest correlation within the given crop parameter. Table 3.11 shows the crop, wavebands, crop parameters, linear regression parameters and the level of significance of the regression. The F-test was used to determine the statistical significance of the

Table 3.11 Linear regression analysis of spectral data vs. crop condition parameters

Crop	Crop parameter	Waveband	Regression equation coefficients		F value
			a	b	
Corn	Chlorophyll fluorescence (ratio, unitless)	9	0.596	5.89E-05	1.78
	Greenness (comparative scale, unitless)	19	205.47	-0.0233	27.89**
	LAI (cm ² /cm ²)	9	5.25	-0.0017	18.89**
	Photosynthesis rate (μmolCO ₂ m ⁻² s ⁻¹)	18	132.86	-0.0135	19.64**
	Soil moisture (%)	24	20.00	-0.0012	0.74
	Plant height (cm)	14	488.94	-0.0767	19.39**
	Soybean	Chlorophyll fluorescence (ratio, unitless)	24	0.947	-4E-05
Greenness (comparative scale, unitless)		4	48.08	-0.0048	4.32*
LAI (cm ² /cm ²)		24	-12.53	0.0026	16.17**
Photosynthesis rate (μmolCO ₂ m ⁻² s ⁻¹)		19	-10.73	0.0031	2.61
Soil moisture (%)		22	-16.42	0.0031	11.81**
Plant height (cm)		21	-67.48	0.0160	11.62**

Note: a and b are the intercept and the slope of the regression equation ($y = a + bx$), where y is the crop parameter and x the radiance at a given waveband.

* P < 0.05 and ** P < 0.01

regression equations. Highly significant ($P < 0.01$) linear relationships between spectral data and greenness, LAI, photosynthesis rate and plant height were obtained for corn.

A similar analysis for soybean indicated that linear relationships ($P < 0.01$) existed between the spectral data and LAI, plant height and soil moisture content; the relationships between spectral data and chlorophyll fluorescence and greenness were also approximately linear ($P < 0.05$). However, photosynthetic rate did not have a relationship with spectral data in the case of soybean. In general, this analysis indicated that many crop physiological parameters could be estimated from remotely sensed data.

3.5 Conclusions

Researchers have reported that weed detection is easier at the flowering stage (Lass and Callihan, 1997). However, if detection is carried out early in the growing season, weeds may be eliminated quickly and effectively without causing any serious damage to the main crop. Even though the image in the present study was taken when the weeds were at the vegetative growth stage, and therefore difficult to distinguish from crops on the basis of radiance in the wavebands used, it is suggested that the presence of weeds in a corn crop or soybean crop can nevertheless be deduced with adequate reference data obtained by ground-truthing.

On the other hand, it has been suggested that weed aggregations (mainly grassy weeds) at a specific location tend to be stable over time (Johnson et al., 1997; Cardina et al., 1995). In such situations, weed mapping at the flowering stage could permit the application of measures that prevent seed formation and propagation in time and space.

The relationships between incident light and recorded vegetation response are highly complex in themselves (Goel, 1988). A lot more research needs to be accomplished, if radiance or reflectance measurements are to be used for weed identification and mapping, in which the latter would be extremely useful in applications such as precision spraying. The results of the present study provide some indication that spectral data may be useful in distinguishing between fields with very

high or very low weed densities, if the field over which the image has been taken is known to have a specific crop at a given density.

Various relationships between spectral data and many other factors involved in crop-weed interactions and in the interactions of plants and incident radiation have yet to be elucidated before one can consider the direct application of spectral data to weed management. Interpretation of spectral data at this time is difficult without fairly extensive ground-truthing. The results presented here do not indicate the plausible use of spectral data in providing more elaborate information on the weed status of cropped areas, when both crop and weed are in vegetative growth stages. At low weed densities, much higher spatial resolution combined with higher spectral resolution might help in locating weeds and distinguishing them from each other and from crop plants. The results presented here do not give a clear indication that the differences in spectra are attributable to anything other than weed density; however, similar investigations at higher spectral and/or spatial resolution may reveal that the technology may, in fact, satisfy the original objective of discriminating between types of weed infestation.

PREFACE TO CHAPTER 4

Despite not very conclusive 1999 results, many lessons were learned throughout the field season, especially during data evaluation over the winter. Given the spatial resolution available from the airborne platform, it became evident that plot sizes were far too small. Also, the choice of soybean as a second crop was ill-advised in the study of weed control strategies, because soybean was so densely seeded compared to corn, that weeds of any of the locally predominant species did not provide it with much competition. Moreover, because soybean did not receive any nitrogen fertilizer, the weed populations in the corn and the soybean crops were not directly comparable.

The first major change made in the planning of the second study year involved focusing on only one crop: corn (*Zea mays* L.). The second change involved enlarging the dimensions of the square plots, from 9 m² to 400 m², in order to obtain more data records per plot and thereby enhance the relative resolution. Given the impracticality of managing a single specific broadleaf weed, i.e. velvetleaf in plots of a larger dimension, a decision was made to use herbicides against grasses and to permit the proliferation of all broadleaved weeds in the designated plots.

The results of the 1999 study appeared to corroborate the suggestion by several other researchers, that higher spectral resolution was needed to discriminate between weeds and crops, particularly at stages of development where there are such subtle differences in spectral signature. A 72-waveband imager was therefore chosen for the aerial measurements, and a 512-waveband spectroradiometer was obtained for ground-truthing. In order to continue in this vein, a decision was made to induce differences in spectral response in both the crop and the weeds by creating controlled nitrogen stress. This was effected by combining the weed control strategies with various nitrogen application rates in a factorial experiment.

Research papers based on the chapter:

1. Goel, P. K., S. O. Prasher, J.-A. Landry, R. M. Patel, R. B. Bonnell, A. A. Viau, and J. R. Miller. 2003. Potential of airborne hyperspectral remote sensing to detect nitrogen deficiency and weed infestation in corn. *Computers and Electronics in Agriculture* 38(2): 99-124.

2. Goel, P. K., S. O. Prasher, J.-A. Landry, R. M. Patel, and A. A. Viau. 2003. Estimation of crop biophysical parameters through airborne hyper-spectral remote sensing. *Transactions of the ASAE* (In press).
3. Goel, P. K., S. O. Prasher, J.-A. Landry, R. M. Patel, and A. A. Viau. 2003. Assessment of corn growth parameters through hyperspectral field measurements. (Under preparation).

(Copies of the published papers are given in the attached CD-ROM.)

CHAPTER 4

HYPER-SPECTRAL REMOTE SENSING TO DETECT NITROGEN AND WEED STRESSES

4.1 Abstract

Hyper-spectral images of a field experiment, aimed at studying the combined effects of weed and nitrogen stresses on corn, were acquired from ground-based and airborne sensors. The main objective of the study was to determine whether the effects of these stresses on crop physiological parameters, measured in the canopies, could be deduced from the hyper-spectral data. Four weed control strategies (no weed control, grass weed control, broadleaf weed control, and full weed control) were replicated four times and assigned to the main plots; also three nitrogen fertilization rates (60, 120, 250 N kg ha⁻¹) were randomized to the subplots within each weed control strategy. Using a Compact Airborne Spectrographic Imager (CASI) sensor, hyper-spectral data in 72 narrow wavebands (407 to 949 nm) were collected 30 days after planting, at tassel stage, and at the fully-mature stage when most kernels were filled. Over the same time frame, a 512-waveband field spectroradiometer, with a range of 270 to 1072 nm, was used to acquire spectral data at ground level. Leaf greenness (SPAD readings), leaf area index (LAI), plant height, leaf nitrogen content, leaf chlorophyll content, and ancillary data were also determined on these days.

The data analysis indicated that there were significant ($\alpha=0.05$) differences in reflectance at certain wavebands, due to weed control strategies and nitrogen application rates. The influence of weeds was most readily observed, in the aerial and field spectroradiometer data, when the corn had tassel about nine weeks after planting. A study of the aerial data acquired at all three growth stages revealed that the nitrogen effect was most closely related to reflectance at 498-nm and 671-nm wavebands. In these wavebands, no interaction was shown between nitrogen levels and weed controls. Differences in other regions of the spectrum, whether related to nitrogen or weeds, appeared to be dependent on the growth stage.

Regression models were generated to represent crop biophysical parameters and yield, in terms of reflectance at one or more wavebands, using the maximum r^2 improvement criterion. The models that best represented the data had five wavebands as independent variables. Coefficients of determination (r^2) for the regressions were generally greater than 0.9, when based on spectral data taken at the tassel stage. Models based on normalized difference vegetation indices (NDVI) were more reliable at estimating the validation data sets than were the reflectance models. For most of the parameters, the best results were obtained using data acquired at the tassel stage; in general, the wavebands at 701 nm and 839 nm were the most prevalent in the NDVI-based models.

This study confirmed previous suggestions that greater spectral resolution should lead to more reliable relationships between the spectral data and the various indicators of crop status. The comparison between results obtained from airborne sensors and those acquired on the ground, indicated that unless there is willingness to provide the same coverage of a canopy with ground-based instruments, as is possible from airborne systems, the higher resolution of the ground-based sensors does not compensate for the full coverage at lower resolution from high altitude.

4.2 Introduction

Attempts to relate remote sensing data from aircraft or satellites to nitrogen stress of crops, or to the characteristics of weed populations in agricultural fields, have been based on film or digital photography, videography, or multi-spectral digital imaging systems, utilizing three or four broad wavebands. Although, these photographs or images provided invaluable assistance in the visual interpretation or qualitative assessment of field conditions, these images were only partly successful in quantifying the various objects or parameters of interest. The major drawback is that these technologies provide average reflectance over a limited number of fairly broad wavebands. This results in a considerable loss of spectral information, and is suggested as the reason for the difficulties associated with discriminating species or objects showing subtle differences in very narrow spectral ranges. Hyper-spectral imaging systems scan a large number of narrow wavebands, and are thus capable of

acquiring information at much higher spectral resolution (Lamb and Brown, 2001; Lamb, 1998). Moreover, the digital format of remotely sensed spatial data facilitates automated processing (Frazier et al., 1997).

Studies using handheld spectroradiometers have demonstrated the potential of hyper-spectral measurements in the detection of weeds (Wang et al., 1998b; Brown et al., 1994) and nitrogen level in crops (Sui et al., 1998; Blackmer et al., 1996a; Blackmer et al., 1994a; Walburg et al., 1982). In a recent review of weed detection in crops using remote sensing, Lamb and Brown (2001) also emphasized the need for remote sensing instruments with a higher spectral resolution. It is expected that high resolution, hyper-spectral satellite imagery will eventually be available, to provide a basis for monitoring crop health and the variability of several factors affecting growth, at a scale suitable for precision farming (Brisco et al., 1998; Moran et al., 1997). In the future this would provide a basis for multi-dimensional mapping (Ponzoni and Goncalves, 1999). Thus, the extension of hyper-spectral technology from a ground-based system to an airborne platform is rather challenging and new for many applications in agricultural crop monitoring. Research is not yet available on the change in the reflectance spectrum of a crop canopy under the simultaneous influences of nitrogen stress and competition from weeds, specifically utilizing ground-based, aerial or satellite platforms in a controlled experimental field setting.

The aim of the present study was therefore to study the spectral response of corn to controlled combinations of weed and nitrogen stresses, using hyper-spectral imaging technology simultaneously from ground-based and airborne platforms.

The specific objectives of the study were: (1) to identify specific wavebands or spectral regions in which variations in crop reflectance can be directly associated with: (a) the type and/or extent of the weed population in a corn canopy, and/or (b) the nitrogen status of the crop, and (2) to develop functional relationships between hyper-spectral data and: (a) crop biophysical parameters; (b) crop yield.

4.3 Materials and Methods

4.3.1 Experimental design and layout

The study was conducted in the summer of the year 2000 at the Lods

Agronomy Research Center of Macdonald Campus, McGill University, Ste. Anne-de-Bellevue, Québec, Canada (45°25'45" N lat., 73°56'00" W long.). The soils at the study site are classified as Bearbrook clay and Ste. Rosalie clay. Both soils belong to the Dark Gray Gleysolic group. Corn was grown under different levels of nitrogen and weed infestation in order to simulate a wide range of growth scenarios. The experiment was a two-factor, split-plot, completely randomized design. Four weed control strategies were assigned to the main plots (80m x 20m) and three nitrogen application rates were assigned to the sub-plots (20m x 20m). Each sub-plot had 26 rows of corn. The weed treatments were: no weed control (W1), control of grasses (W2), control of broadleaf (W3), and full weed control (W4). Nitrogen treatments were: low nitrogen (N₆₀, 60 kg N/ha), normal nitrogen (N₁₂₀, 120 kg N/ha), and high nitrogen (N₂₅₀, 250 kg N/ha). Potassium, phosphorous and micronutrients were applied at the locally recommended rates. The initial surface soil test report is given in Table 4.1. Corn was sown on May 30, 2000, at a rate of 76000 seeds per ha and a row spacing of 75 cm. Herbicides were applied on June 26, 2000, and nitrogen fertilizer, above the minimal rate of 60 kg/ha (which had been banded with the seeds) was broadcast in the second week of July. Details of the cultural operations and other relevant information are summarized in Table 4.2. The total precipitation for the year was 1005.2 mm, which was almost equal to the average (939.7 mm) for the region. However, precipitation from April to September was 613.6 mm, about 23% above the average for that period. Details on other weather conditions during the year are given in Table 4.3.

4.3.2 Spectral measurements

Hyper-spectral data were acquired from a Compact Airborne Spectrographic Imager (CASI), and at ground level using a 512-waveband field spectroradiometer (FieldSpec HH model, Analytical Spectral Device, Boulder, CO, USA).

The CASI provided reflectance in 72-narrow wavebands in the visible and near-infrared regions (407 to 949 nm) at 2-m spatial resolution. Various details about the selected CASI wavebands are given in Table 4.4. Images were taken at three critical growth stages of the crop: (1) early growth - 30 days after planting

Table 4.1 Surface soil properties before corn planting

Properties	pH	Organic matter %	Phosphorous (P) mg/kg	Potash (K) mg/kg	Calcium (Ca) mg/kg	Magnesium (Mg) mg/kg	Nitrogen (N) (mg/kg)			
							Dry soil		Moist soil	
							NH ₄ -N*	NO ₃ -N†	NH ₄ -N*	NO ₃ -N†
Average	6.7	5.1	26.9	238.9	3286.2	828.8	6.0	4.8	2.2	5.9
Min.	6.5	4.5	8.2	195.5	2165.4	100.9	4.0	2.7	0.3	1.3
Max.	7.1	6.0	67.2	328.7	4183.3	1155.4	8.7	7.6	10.9	15.1

* Ammonium nitrogen (NH₄-N)

† Nitrate nitrogen (NO₃-N)

Table 4.2 Details of tillage, sowing, fertilization and other cultural operations

Operation	Date	Specific details
Tillage	May first week	
Sowing	May 30, 2000	76000 seeds/ha, 75 cm row spacing
Fertilization	a. May 30, 2000 b. June 01, 2000 c. July 12, 2000	10-120-50, in all plots (N-P ₂ O ₅ -K ₂ O) (kg/ha) 0 in N ₆₀ ; 10 in N ₁₂₀ ; 90 in N ₂₅₀ (N kg/ha) 50 in N ₆₀ ; 100 in N ₁₂₀ ; 150 in N ₂₅₀ (N kg/ha)
Herbicide application	June 26, 2000	a. Grass control (W2): Ultim & Agral 90 b. Broadleaf control (W3): Banvel II c. Full weed control (W4): Ultim, Agral 90, and Banvel II Ultim: 18.7% Rimsulfuron and 18.7% Nicosulfuron; applied at a rate of 67g/ha. Banvel II: Dicamba; applied at a rate of 288 g/ha when applied with Ultim, and 576 g/ha when applied alone. Agral 90: surfactant; 0.2% of herbicide amount except in plots where only Banvel II was applied
CASI hyper-spectral observations	a. First flight on June 30, 2000 b. Second flight on August 05, 2000 c. Third flight on August 25, 2000	a. 30 Days after planting b. 66 Days after planting c. 86 Days after planting

Table 4.3 Mean monthly temperature, relative humidity, wind speed, and total precipitation during the year 2000 and for a normal year

Month	Year 2000						Normal year (Average based on the years 1961-1990)					
	Temperature (°C)			Relative humidity (%)	Wind speed (km/h)	Precipitation (mm)	Temperature (°C)			Relative humidity (%)	Wind speed (km/h)	Precipitation (mm)
	Max.	Min.	Avg.				Max.	Min.	Avg.			
January	-5.1	-14.1	-10.2	72.01	14.57	90.6	-5.8	-14.9	-10.3	NA	NA	63.3
February	-1.9	-12.1	-6.9	72.11	13.47	39.0	-4.2	-13.5	-8.8	NA	NA	56.4
March	6.3	-2.5	1.4	69.68	13.25	58.0	2.0	-6.9	-2.4	NA	NA	67.6
April	10.4	1.3	5.1	68.79	14.11	100.0	10.7	0.6	5.7	NA	NA	74.8
May	18.6	8.1	12.8	71.35	12.30	133.2	18.5	7.3	12.9	NA	NA	68.3
June	22.3	12.0	16.6	72.99	11.27	89.9	23.4	12.5	18.0	NA	NA	82.5
July	24.7	14.6	19.2	74.83	10.57	81.0	26.2	15.4	20.8	NA	NA	85.6
August	24.0	14.6	18.8	80.25	10.42	125.5	24.6	14.1	19.4	NA	NA	100.3
September	19.1	8.9	13.7	79.14	10.35	84.0	19.8	9.3	14.5	NA	NA	86.5
October	13.6	4.4	8.6	76.83	10.82	28.9	13.0	3.6	8.3	NA	NA	75.4
November	5.4	-0.5	2.4	82.90	9.92	72.6	5.2	-2.0	1.6	NA	NA	93.4
December	-5.1	-12.7	-9.2	78.29	14.85	102.5	-2.9	-11.0	-6.9	NA	NA	85.6

NA: Not available

Table 4.4 Wavebands used to acquire aerial spectral data

Waveband				Spectral region	Waveband				Spectral region	Waveband				Spectral region
Number	Center (λ) (nm)	Width (nm)	$\Delta \lambda^*$ (nm)		Number	Center (λ) (nm)	Width (nm)	$\Delta \lambda^*$ (nm)		Number	Center (λ) (nm)	Width (nm)	$\Delta \lambda^*$ (nm)	
1	408.73	4.27	-	Blue	25	587.86	4.32	7.52	Green	49	770.00	4.37	7.65	NIR
2	416.13	4.28	7.40	Blue	26	595.39	4.33	7.53	Green	50	777.65	4.37	7.65	NIR
3	423.53	4.28	7.40	Blue	27	602.93	4.33	7.54	Red	51	785.30	4.37	7.65	NIR
4	430.95	4.28	7.42	Blue	28	610.47	4.33	7.54	Red	52	792.96	4.37	7.66	NIR
5	438.36	4.28	7.41	Blue	29	618.02	4.33	7.55	Red	53	800.62	4.37	7.66	NIR
6	445.79	4.28	7.43	Blue	30	625.57	4.33	7.55	Red	54	808.29	4.38	7.67	NIR
7	453.21	4.29	7.42	Blue	31	633.13	4.33	7.56	Red	55	815.96	4.38	7.67	NIR
8	460.65	4.29	7.44	Blue	32	640.69	4.34	7.56	Red	56	823.64	4.38	7.68	NIR
9	468.09	4.29	7.44	Blue	33	648.26	4.34	7.57	Red	57	831.32	4.38	7.68	NIR
10	475.53	4.29	7.44	Blue	34	655.83	4.34	7.57	Red	58	839.01	4.38	7.69	NIR
11	482.98	4.30	7.45	Blue	35	663.41	4.34	7.58	Red	59	846.70	4.38	7.69	NIR
12	490.44	4.30	7.46	Blue	36	670.99	4.34	7.58	Red	60	854.39	4.39	7.69	NIR
13	497.90	4.30	7.46	Blue	37	678.57	4.34	7.58	Red	61	862.09	4.39	7.70	NIR
14	505.37	4.30	7.47	Green	38	686.17	4.35	7.60	Red	62	869.80	4.39	7.71	NIR
15	512.84	4.30	7.47	Green	39	693.76	4.35	7.59	Red	63	877.51	4.39	7.71	NIR
16	520.32	4.31	7.48	Green	40	701.36	4.35	7.60	NIR	64	885.22	4.39	7.71	NIR
17	527.80	4.31	7.48	Green	41	708.97	4.35	7.61	NIR	65	892.93	4.39	7.71	NIR
18	535.29	4.31	7.49	Green	42	716.58	4.36	7.61	NIR	66	900.66	4.40	7.73	NIR
19	542.79	4.31	7.50	Green	43	724.20	4.36	7.62	NIR	67	908.38	4.40	7.72	NIR
20	550.29	4.31	7.50	Green	44	731.82	4.36	7.62	NIR	68	916.11	4.40	7.73	NIR
21	557.79	4.32	7.50	Green	45	739.45	4.36	7.63	NIR	69	923.84	4.40	7.73	NIR
22	565.30	4.32	7.51	Green	46	747.08	4.36	7.63	NIR	70	931.58	4.40	7.74	NIR
23	572.82	4.32	7.52	Green	47	754.71	4.36	7.63	NIR	71	939.33	4.40	7.75	NIR
24	580.34	4.32	7.52	Green	48	762.35	4.37	7.64	NIR	72	947.07	4.41	7.74	NIR

Note: NIR: Near-infrared

* $\Delta \lambda$ is the difference in the center of two successive wavebands

(June 30, 2000); (2) tassel stage - 66 days after planting (August 5, 2000); and, (3) fully-mature stage - 86 days after planting (August 25, 2000). Radiometric, geometric, and atmospheric corrections were applied to the reflectance data. Specifications for the CASI sensor and the various radiometric, atmospheric, and geometric correction procedures used to correct the images are summarized in the Table 4.5. The corrected images were imported into ENVI software (ENVI 3.3, Research System, Inc., Boulder, Colorado, USA), and average reflectance values were extracted for each plot. Waveband 72 (centered at 947 nm) could not be used in the analyses due to excessive noise in the signal.

The FieldSpec had a range of 270 to 1072 nm. Observations were made concurrently on the day of the first and second flights i.e., on 30th June and 5th August, respectively. Due to some instrument technical problems, ground measurements could not be made with this instrument on the day of the third flight. Spectral observations were acquired with a 15° field of view. Six scans were made in each plot. The first three were made with the spectroradiometer placed directly over corn plants, whereas the other three were made with the instrument placed between corn rows. A four-band moving average filter was used to smooth the spectra. The smoothed spectra were then averaged. The data from 346 wavebands (with centers from 378.8 to 920.5 nm) were used for the analysis, due to excessive noise at the two ends of the nominal range of the instrument.

4.3.3 Plant parameters

Measurements on the various crop canopy and other parameters were taken on the day of the flight and on the following day. These measurements included: plant height, leaf greenness, leaf area index (LAI), leaf chlorophyll content, leaf nitrogen content and soil moisture. Crop yield and biomass were also recorded at the end of crop season. Plant height, a simple and direct indicator of plant health, was measured for ten plants in each plot, and then averaged. A LAI-2000 Plant Canopy Analyzer (Li-Cor, Inc., Lincoln, Nebraska, USA) was used to measure LAI values. LAI is a dimensionless quantity, but can be expressed as cm² foliage area per cm² ground area. Greenness or the amount of chlorophyll in a plant is another visible indicator of stress

Table 4.5 CASI specification and data processing

Type of sensor	Pushbroom imager
Field of view	37.8°
Wavelength range	407 to 949 nm
Number of wavebands	72
Sampling rate	405 (spatial direction)
Spectral resolution	7.5 nm
Spatial resolution	2 m x 2 m
Noise floor	1.4 DN
S/N ratio	420:1 peak
a. June 30th, 2000 b. August 5th, 2000 c. August 25th, 2000	a. Heading: 150.732 North, Altitude above sea level: 1148 m, Time: 18:22, Cloud free; b. Heading: 150.859 North, Altitude above sea level: 1130 m, Time: 15:30, Cloud free; c. Heading: 331.225 North, Altitude above sea level: 1152 m, Time: 14:58, Cloud free.
Data processing	
a. Radiometric and atmospheric corrections	Data collected from CASI were processed to at-sensor radiance using calibration coefficients determined in the laboratory by CRESTech (Center for Research in Earth and Space Technology). The CAM5S atmospheric correction model (O'Neill et al., 1997) was used to transform at-sensor radiance to ground-reflectance. Further, spectrally-flat uniform areas in each image (asphalt, bare soil and concrete surfaces) were used to do flat field adjustments in the spectral regions affected, residually by atmospheric absorption features for improved reflectance image data cubes.
b. Geometric corrections, geo-referencing, and image co-registration	Images were corrected for the aircraft movements (yaw, pitch, and roll) using GPS data onboard the aircraft, then rectified to UTM geographic coordinates. Further, white targets at the corners of the field were used for precise correction and error assessment. The estimated RMSE (root mean square error) was about 0.5 pixel.

in plants and was measured with a SPAD Chlorophyll meter (Minolta Camera Ltd., Osaka, Japan). This measure reveals the N status of the plant, because most leaf nitrogen (N) is contained in the chlorophyll molecules. Chlorophyll content was determined in the laboratory on twelve leaves from representative plants in each plot, following the procedure described by Arnon (1949). The total Kjeldahl nitrogen in the leaves was also determined. Biomass was estimated on the basis of ten plants harvested and weighed from each plot. Finally, crop yield was calculated by harvesting ten representative plants, from each of four randomly chosen locations in each plot. Variations in crop growth indicators due to the various treatments are summarized in Table 4.6, for each aerial data acquisition campaign.

4.3.4 Observations on weeds

Two survey sets of observations were collected with reference to the weeds in the experimental plots. The first set was collected on July 14, and included details of weed species, density, plant height, and percentage cover. The second set was collected on August 15. Because weeds were fully established at the time of the first observation (July 14), and no change in weed density was observed thereafter, the second set focused on percentage cover of broadleaf, grassy, and total weeds in each plot. For the weed survey, 50cm x 50cm quadrates were used. Data were collected by placing the quadrate at three (first survey) and four (second survey) randomly selected areas within each plot. During the weed count, grass species were counted as the number of shoots per m², while broadleaf weeds were counted as the number of plants per m².

Results of the weed surveys are summarized in Table 4.7. The most common grassy weeds were barnyard grass, yellow nutsedge, and crab grass. The predominant broadleaved weeds were Canada thistle, sow thistle, lamb's quarter, and redroot pigweed. The grassy weed population exhibited less variability across the various treatments than did the broadleaved weeds. No specific conclusions could be drawn about the effect of nitrogen application rate on individual weed species. As expected under field conditions, there were differences in the species of grassy weed present across different treatments. However, measurements on percentage weed cover

Table 4.6 Details of various measurements of crop parameters, soil moisture, biomass and yield at different flight times

Crop parameter	Treatments*									Variation across various plots
	N ₆₀ W1	N ₆₀ W3	N ₆₀ W4	N ₁₂₀ W1	N ₁₂₀ W3	N ₁₂₀ W4	N ₂₅₀ W1	N ₂₅₀ W3	N ₂₅₀ W4	
First flight (June 30, 2000)[#]										
Leaf area index (cm ² /cm ²)	1.14 ±0.54	0.59 ±0.22	0.77 ±0.16	1.24 ±0.18	0.86 ±0.45	0.72 ±0.21	1.50 ±0.32	1.13 ±0.44	1.06 ±0.29	0.30 to 2.18
Plant height (cm)	18.8 ±1.7	18.7 ±1.9	18.3 ±1.2	20.1 ±2.5	19.5 ±1.1	19.3 ±2.1	21.3 ±1.5	21.2 ±1.3	20.6 ±1.1	14.8 to 23.7
Greenness (unitless)	34.9 ±3.6	32.6 ±4.8	33.3 ±3.8	35.7 ±3.0	36.2 ±3.2	34.7 ±2.1	41.7 ±1.6	41.7 ±2.3	39.3 ±1.6	26.1 to 43.67
Leaf nitrogen (g/kg)	41.65 ±12.59	38.75 ±4.39	42.95 ±4.41	40.18 ±4.75	48.41 ±5.58	44.53 ±10.10	56.66 ±8.04	57.57 ±6.76	55.84 ±4.46	28.16 to 68.35
Chlorophyll (mg/cm ²)	0.0104 ±0.0024	0.0096 ±0.0026	0.0106 ±0.0025	0.0096 ±0.0040	0.0099 ±0.0028	0.0107 ±0.0013	0.0108 ±0.0017	0.0139 ±0.0019	0.0134 ±0.0007	0.0051 to 0.016
Soil moisture content (%)	34.2 ±2.9	33.9 ±2.4	33.9 ±3.6	34.8 ±4.8	33.5 ±2.1	34.0 ±2.1	33.7 ±3.7	34.0 ±1.9	32.7 ±3.9	27.3 to 39.5
Second flight (Aug. 05, 2000)										
Leaf area index (cm ² /cm ²)	3.98 ±1.36	3.89 ±0.85	2.84 ±0.91	4.45 ±0.94	4.63 ±0.62	3.45 ±0.24	5.17 ±1.18	4.46 ±1.11	3.70 ±0.34	2.04 to 6.19
Plant height (cm)	151.6 ±17.9	152.6 ±32.4	159.0 ±26.3	173.8 ±22.7	183.1 ±21.2	182.7 ±19.4	204.5 ±21.4	206.0 ±17.5	199.7 ±13.3	113.7 to 230.5
Greenness (unitless)	32.8 ±0.6	38.3 ±5.3	40.0 ±2.7	40.6 ±4.3	44.8 ±2.3	46.2 ±4.4	46.8 ±4.8	47.5 ±3.1	47.9 ±2.7	31.0 to 54.0

Note- For each parameter average value ±SD for a treatment is given;

* Treatments: W1- no weed control; W3-broadleaf weed control; W4-full weed control; N₆₀-60 kg N/ha; N₁₂₀-120 kg N/ha; N₂₅₀-250 kg N/ha.

At the time of first flight, nitrogen rates in N₆₀, N₁₂₀, and N₂₅₀ treatments were 10, 20, and 100 kg N/ha, respectively.

Table 4.6 (cont'd) Details of various measurements of crop parameters, soil moisture, biomass and yield at different flight times

Crop parameter	Treatments*									Variation across various plots
	N ₆₀ W1	N ₆₀ W3	N ₆₀ W4	N ₁₂₀ W1	N ₁₂₀ W3	N ₁₂₀ W4	N ₂₅₀ W1	N ₂₅₀ W3	N ₂₅₀ W4	
Second flight (Aug. 05, 2000)										
Leaf nitrogen (g/kg)	49.07 ±11.14	57.09 ±6.96	63.39 ±4.88	57.42 ±7.91	66.98 ±7.09	71.56 ±1.23	69.08 ±5.71	73.60 ±3.31	77.58 ±1.35	33.34 to 78.72
Chlorophyll (mg/cm ²)	0.0112 ±0.0020	0.0128 ±0.0020	0.0136 ±0.0014	0.0150 ±0.0030	0.0145 ±0.0014	0.0151 ±0.0022	0.0159 ±0.0020	0.0165 ±0.0011	0.0174 ±0.0008	0.0093 to 0.0191
Soil moisture content (%)	32.1 ±2.7	32.9 ±2.3	33.8 ±3.2	34.6 ±3.3	32.1 ±1.2	31.7 ±1.7	30.9 ±1.7	30.6 ±0.2	30.9 ±2.4	27.5 to 38.3
Third flight (Aug. 25, 2000)										
Leaf area index (cm ² /cm ²)	4.04 ±0.52	3.68 ±0.56	2.90 ±0.57	4.26 ±0.48	4.22 ±0.52	3.31 ±0.58	4.58 ±0.25	4.27 ±0.26	3.65 ±0.37	2.27 to 4.87
Plant height (cm)	151.6 ±17.9	152.6 ±32.4	159.0 ±26.3	173.7 ±22.7	183.0 ±21.2	182.7 ±19.4	204.4 ±21.4	206.0 ±17.5	199.6 ±13.2	113.7 to 230.5
Greenness (unitless)	32.1 ±4.5	34.8 ±6.6	38.8 ±3.4	43.6 ±4.6	46.4 ±3.8	46.6 ±2.6	52.1 ±4.3	52.0 ±2.4	51.5 ±1.3	28.3 to 56.2
Soil moisture content (%)	34.00 ±4.38	34.37 ±2.11	34.26 ±4.05	32.49 ±2.70	33.80 ±1.37	33.05 ±2.27	33.75 ±5.03	32.71 ±3.46	32.60 ±2.63	27.1 to 40.2
Harvesting										
Biomass (kg/m ²)	1.0554 ±0.1629	0.9853 ±0.2502	1.1464 ±0.1583	1.0723 ±0.2392	1.1627 ±0.3591	1.2636 ±0.1447	1.3469 ±0.3254	1.3733 ±0.1871	1.4564 ±0.184	0.765 to 1.723
Yield (t/ha)	4.072 ±1.199	3.605 ±1.521	4.803 ±1.000	5.015 ±1.147	6.135 ±0.823	6.114 ±0.591	6.551 ±1.112	6.859 ±0.500	6.754 ±0.658	2.291 to 7.820

Note- For each parameter average value ±SD for a treatment is given;

* Treatments: W1- no weed control; W3-broadleaf weed control; W4-full weed control; N₆₀-60 kg N/ha; N₁₂₀-120 kg N/ha; N₂₅₀-250 kg N/ha.

Table 4.7 Details of weed type, number, density, and average ground cover in different weed treatments

a. Weeds count (plants/shoots per sq. meter) and average height (cm) of weeds on July 14, 2000

Treatment*	Grassy weeds								Broadleaf weeds									
	Barnyard		Yellow nutsedge		Crab		Quack		Canada thistle		Sow thistle		Lamb's-Quarter		Redroot pigweed		Others	
	No.	Ht.	No.	Ht.	No.	Ht.	No.	Ht.	No.	Ht.	No.	Ht.	No.	Ht.	No.	Ht.	No.	Ht.
N ₆₀ W ₁	57	12.3	57	11.1	70	3.0	0	0.0	2	3.7	1	0.3	9	5.3	10	4.8	13	5.1
N ₆₀ W ₃	33	12.3	24	8.1	18	1.8	0	0.0	0	0.0	0	0.0	0	0.0	0	0.0	0	0.0
N ₁₂₀ W ₁	72	19.6	66	14.1	46	2.3	68	5.0	1	0.6	2	1.1	17	5.5	12	3.3	16	4.7
N ₁₂₀ W ₃	51	18.1	8	7.4	44	3.4	0	0.0	0	0.0	0	0.0	0	0.0	0	0.0	0	0.0
N ₂₅₀ W ₁	67	17.3	107	13.8	119	5.4	0	0.0	1	3.4	2	1.4	11	7.5	9	5.9	10	5.1
N ₂₅₀ W ₃	43	19.4	13	7.6	29	3.3	0	0.0	0	0.0	0	0.0	0	0.0	0	0.0	0	0.0

b. Weed cover

Treatment*	Weed cover on July 14, 2000 (%)			Weed cover on August 15, 2000 (%)		
	Grassy	Broadleaf	Total	Grassy	Broadleaf	Total
N ₆₀ W ₁	31.3 ±3.8	6.0 ±0.1	37.3 ±3.7	77.5 ±5.2	10.68 ±1.2	88.1 ±5.4
N ₆₀ W ₃	8.8 ±2.2	0.0	8.8 ±2.2	38.3 ±11.8	0.0	38.3 ±11.8
N ₁₂₀ W ₁	29.1 ±3.3	5.6 ±1.2	34.7 ±4.4	78.3 ±2.7	10.4 ±2.5	88.7 ±4.2)
N ₁₂₀ W ₃	19.9 ±5.9	0.0	19.9 ±5.9	47.9 ±18.1	0.0	47.9 ±18.1
N ₂₅₀ W ₁	36.1 ±6.9	5.8 ±0.8	41.9 ±7.4	78.7 ±10.7	11.4 ±1.3	90.00 ±10.0
N ₂₅₀ W ₃	15.7 ±7.4	0.0	15.7 ±7.4	55.4 ±10.1	0.0	55.4 ±10.1

Note- Average value ±SD for a treatment is given;

* Treatments: W1- no weed control; W3-broadleaf weed control; N₆₀-60 kg N/ha; N₁₂₀-120 kg N/ha; N₂₅₀-250 kg N/ha.

suggested little variation across weed categories. At the time of the first survey, weed cover in plots with no weed control (W1) ranged from 34.7 (\pm 4.4) to 41.9 (\pm 7.4) percent across nitrogen application rates. Where broadleaved weeds were controlled (W3), the coverage ranged from 8.8 (\pm 2.20) to 19.9 (\pm 5.9) percent. However, on August 15th, weed coverage ranged from 88.1 (\pm 5.4) to 90.00 (\pm 10.0), and from 38.3 (\pm 11.8) to 55.4 (\pm 10.1), for W1 and W3 plots, respectively. In plots with no weed control, grassy weeds accounted for 94.0 and 90.0 percent of the weed populations within the first and second surveys, respectively. The predominance of grassy weeds was not related to any residual effect of herbicide applications in previous years.

4.3.5 Data analysis

4.3.5.1 Selection of suitable wavebands

Reflectance in different wavebands was analyzed using the General Linear Model (GLM) procedure of SAS (SAS Institute, Inc., Cary, NC, USA). Analyses of variance (ANOVA) were conducted, including single degree of freedom contrasts, for each of the 71 wavebands from the airborne sensor and each of the 346 wavebands from the field spectroradiometer. The ANOVA model was adjusted to involve only three weed treatments because very few broadleaved weeds were found in the plots where the herbicide application was only a control for grassy weeds. With reference to the natural variability in weed germination, the results of treatment W2 were considered to be normal. Thus, data associated with treatment W2 were excluded from the analyses.

4.3.5.2 Estimation of crop biophysical parameters

The spectral data were analyzed separately for the three flights. Multiple regression models were generated with reflectance values at the different wavebands as the independent variables, and crop biophysical parameters as the dependent variables. The maximum r^2 criterion (MAXR) was used with PROC REG (SAS, Version 6.12) to choose the best one, two, three, four and five parameter models for each biophysical parameter, based on half the available data from a given flight. The

remaining data were used to test the performances of these models in order to select the best model for each dependent variable.

This method had been used previously by Thenkabail et al. (2000), whereas Ingleby and Crowe (2000) used the closely related minimum r^2 (MINR) improvement in a similar analyses of spectral data. Derived regression models with a maximum of five independent parameters were,

$$P = b_0 + b_1S_1 + b_2S_2 + b_3S_3 + b_4S_4 + b_5S_5, \quad (4.1)$$

where: P = parameter to be estimated,

$b_0, b_1, b_2, b_3, b_4, b_5$ = regression coefficients, and

$S_0, S_1, S_2, S_3, S_4, S_5$ = the percentage reflectance values recorded at 1, 2, 3, 4, and 5 wavelengths, respectively.

The plots of MAXR vs. the number of wavebands in the model indicated that inclusion of more than five parameters in the model had little effect on the performance of model. Furthermore, the criterion ratio of the number of wavebands in the model to the total number of field samples (5/24), being between 0.15 and 0.20 (Thenkabail et al., 2000; Hruschka, 1987), led to the use of a maximum of five wavebands in the regression model.

Performance of the developed models was then evaluated by comparing the observed and model predicted values. The sum of squared error (SSE) and the average relative percent error (ARPE) values were calculated for both the calibration and validation data sets, while the more stringent coefficient of efficiency (or Nash-Sutcliffe coefficient), C_{eff} , (James and Burges, 1982) was calculated for the validation data only:

$$SSE = \frac{\sum_{i=1}^{i=n} (S_i - O_i)^2}{n}, \quad (4.2)$$

$$ARPE = \frac{\sum_{i=1}^{i=n} (S_i - O_i)}{\sum_{i=1}^{i=n} O_i}, \quad (4.3)$$

$$C_{\text{eff}} = \frac{\sum_{i=1}^{i=n} (O_i - \bar{O})^2 - \sum_{i=1}^{i=n} (S_i - O_i)^2}{\sum_{i=1}^{i=n} (O_i - \bar{O})^2}, \quad (4.4)$$

where: O_i = individual observed value,

S_i = individual simulated value,

\bar{O} = mean observed value, and

n = the number of paired observed-simulated values.

The SSE is an indicator of quantitative dispersion between the observed and estimated values, while the ARPE expresses the error and sign of the error (i.e., over- or under-estimation) on a percentage basis. The C_{eff} evaluates the error relative to the natural variation in the observed values. A C_{eff} of 1.0 represents a perfect prediction, while a value of 0 (zero) represents a prediction no better than simply using the observed mean as a prediction; increasingly negative values indicate increasingly poorer predictions.

Efforts were also made to develop simple linear regression models to predict crop biophysical parameters, based on a Normalized Difference Vegetation Index (NDVI).

$$NDVI = \frac{NIR - R}{NIR + R}, \quad (4.5)$$

where NIR and R are the reflectance values in the near-infrared and red spectrum regions, respectively.

The NDVI is the most widely used vegetation index used to highlight the vegetation component in a soil background, and to minimize the effects of illumination and other measurement conditions. Based on the results of the MAXR procedure, ten red wavebands (633 to 701 nm) and eleven near-infrared wavebands (778 to 854 nm) were found to be the most descriptive of crop biophysical parameters, for all crop stages. These wavebands were selected to carry out further analysis. NDVI values, resulting from all possible combinations of the selected red and near-infrared wavebands, were used to develop prediction models.

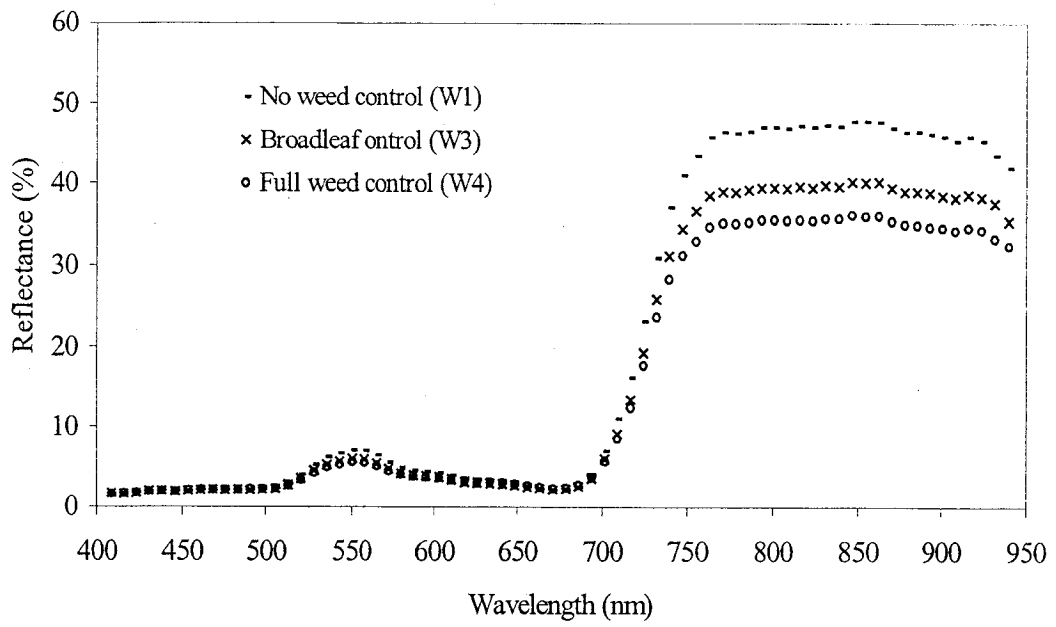
4.4 Results and Discussion

The results of the analysis, aimed at selecting suitable wavebands for the detection of weeds and nitrogen fertilization levels, are presented and discussed first (section 4.4.1). A discussion of the models relating crop biophysical parameters to reflectance measurements follows in section 4.4.2. In both sections, the results of spectral observations are presented in order of crop growth stage (early growth, tassel, and fully mature). Furthermore, the results from the aerial and field spectral measurements are discussed under separate subheadings for each growth stage.

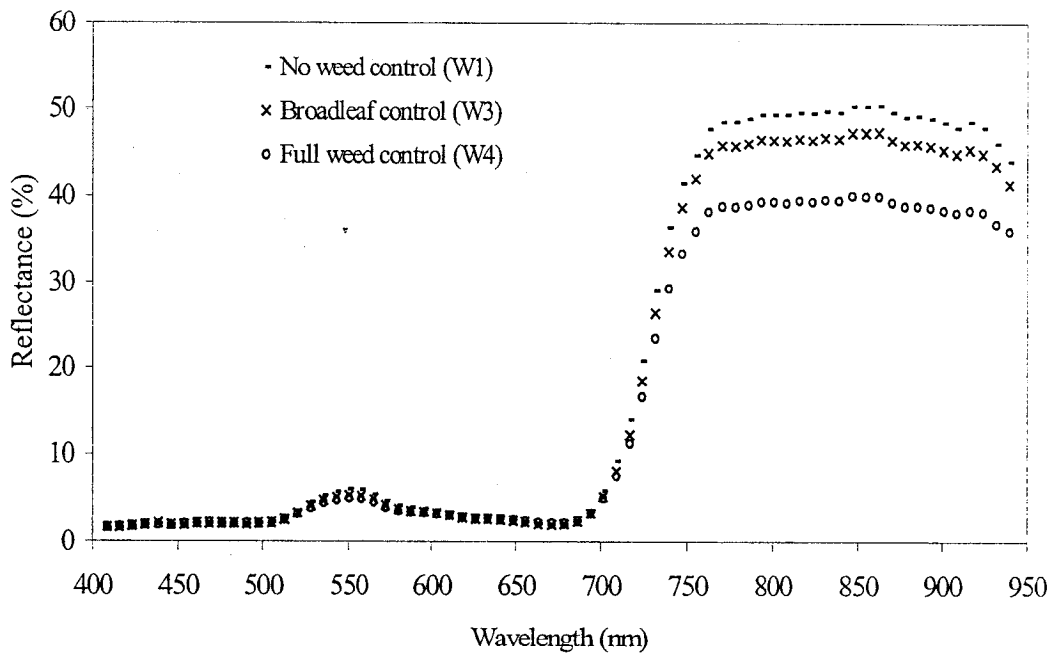
4.4.1 Selection of wavebands

The average reflectance values obtained from aerial imagery at the tassel stage are shown in Figures 4.1a-c, for each nitrogen application rate. At this stage, the effect of nitrogen and weed treatments was quite evident in the different plots. Each of these figures exhibits a broad low intensity peak, centered in the green region at 550 nm, and a sharp rise starting at about 675 nm, to a plateau in the vicinity of 762 nm. The near-infrared reflectance associated with the weed controls is similar in shape but differs clearly in intensity at all three nitrogen application rates.

The highest intensity in the near-infrared was always associated with no weed control, whereas the lowest was associated with full weed control. This is probably related to a greater standing biomass, as indicated by the higher LAI values (Figure 4.2 and Table 4.6) in the plots with no weed control. The near-infrared intensities associated with control of broadleaved weeds were close to those of the full control

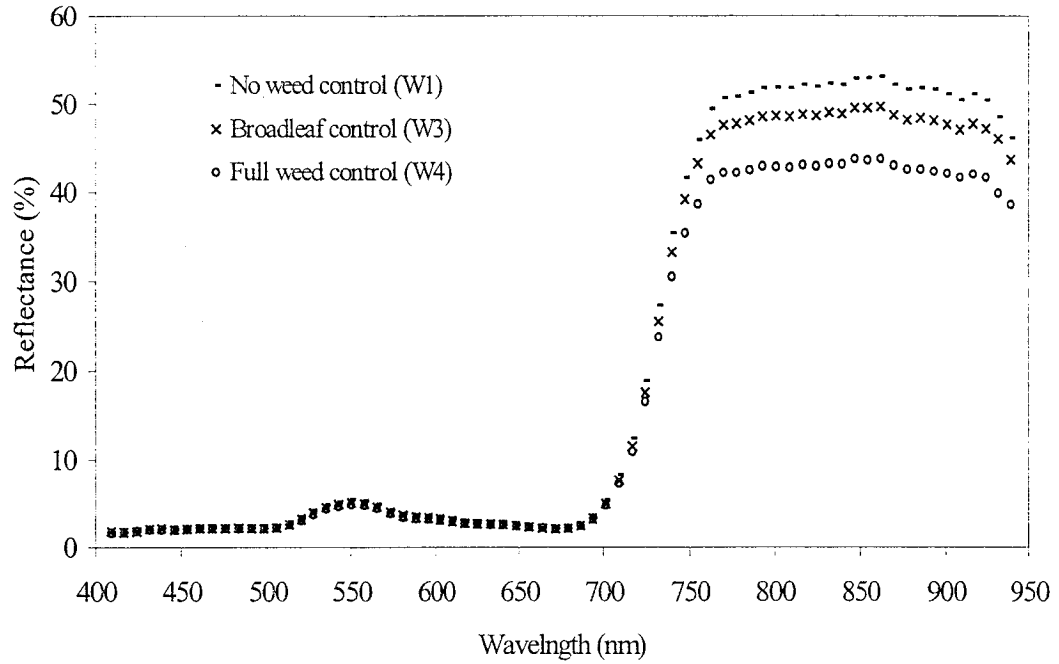


a. Low nitrogen, (N_{60})



b. Normal nitrogen, (N_{120})

Fig. 4.1 Spectral response curve for corn under different nitrogen levels and weed control conditions, during the second flight (tassel stage; August 5, 2000)



c. High nitrogen, (N_{250})

Fig. 4.1 (cont'd) Spectral response curve for corn under different nitrogen levels and weed control conditions, during second flight (tassel stage; August 5, 2000)

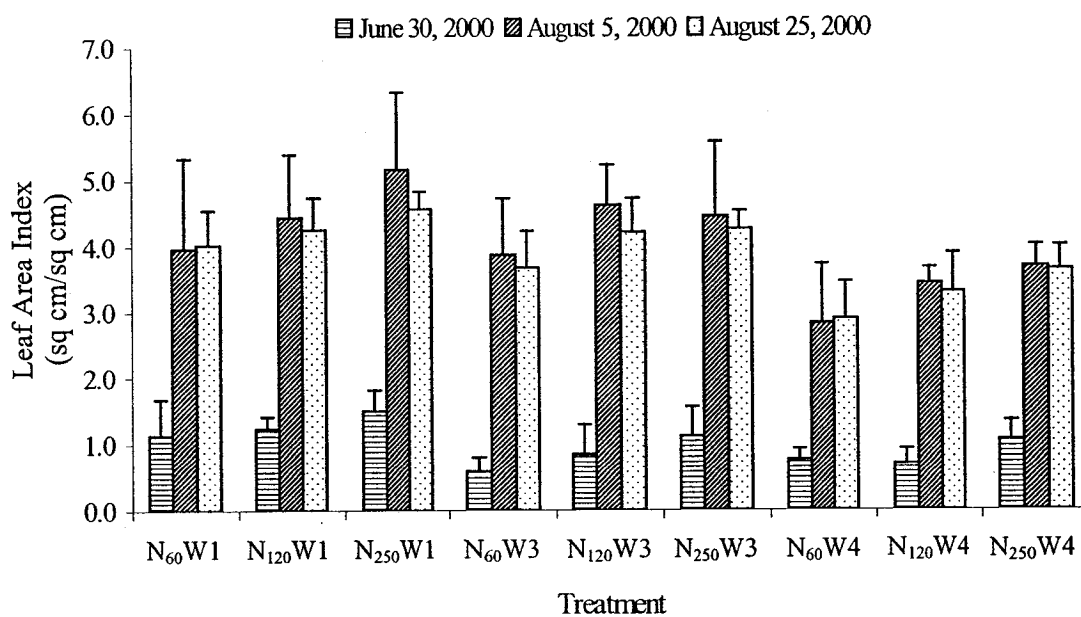


Fig. 4.2 Variation in Leaf Area Index (LAI) among various treatments, during different flights
(Error bar represents one standard deviation)

Note: At the time of first flight, nitrogen rates in N₆₀, N₁₂₀, and N₂₅₀ treatments were 10, 20, and 100 kg N/ha, respectively.

situation in Figure 4.1a; however, they were even closer to the no weed control treatment (Figures 4.1b and 4.1c). Although for a given weed control, it is difficult to see the differences in intensity from one figure to the next, a careful inspection shows that the near-infrared plateaus are at greater reflectance intensities in Figure 4.1c (highest nitrogen rate), and lowest in Figure 4.1a (lowest nitrogen rate). This also implies a correspondence between total reflected energy in the near-infrared and standing biomass. With reference to the weed treatments, a higher biomass was observed in the high nitrogen treatments, as compared to the low nitrogen treatments; for example, average LAI values were 5.17 and 3.98 cm^2/cm^2 in N_{250} and N_{60} treatments, respectively, under a no weed control (W1) condition. The average LAI values across various treatments, at the time of tasseling, ranged from 2.84 to 5.17 cm^2/cm^2 in $N_{60}W4$ (low nitrogen and full weed control) and $N_{250}W1$ (high nitrogen and no weed control) plots, respectively. Healthier plants in the higher nitrogen treatment plots, as supported by the higher greenness and plant height values, also caused higher reflectance in the near- infrared region (Table 4.6). In general, higher nitrogen levels resulted in more biomass, due to more vigorous growth of both crop and weeds.

There was a general tendency for LAI values to decrease from tassel to fully-mature stage, which was due to a waning weed population (due to inability to compete with the corn), and also due to the start of corn senescence. A decrease in LAI values, from tassel stage to fully-mature stage, is evident in Figure 4.2. In general, at tassel stage, the crop biophysical parameters ranged in magnitude across different treatments: LAI from 2.04 to 6.19 cm^2/cm^2 ; plant height from 113.7 to 230.5 cm; greenness from 31.0 to 54.0 on a comparative scale; leaf nitrogen from 33.34 to 78.72 g/kg; leaf chlorophyll content from 0.0093 to 0.0191 mg/cm^2 (Table 4.6). These large variations in various plant parameters demonstrated the combined effect of weeds and nitrogen on crop growth. Better crop growth in higher nitrogen plots was also supported by the measurements on other plant parameters (Table 4.6).

It is interesting to note that peaks in the green region of the visible spectrum are not the only areas where it is possible to make some distinction associated with weed controls. The intensities are also ordered, being greatest in Figure 4.1a, and

lowest in Figure 4.1c. When there is insufficient nitrogen tasseling is incomplete or delayed, resulting in decreased color change from green compared to a plot of tasseled plants.

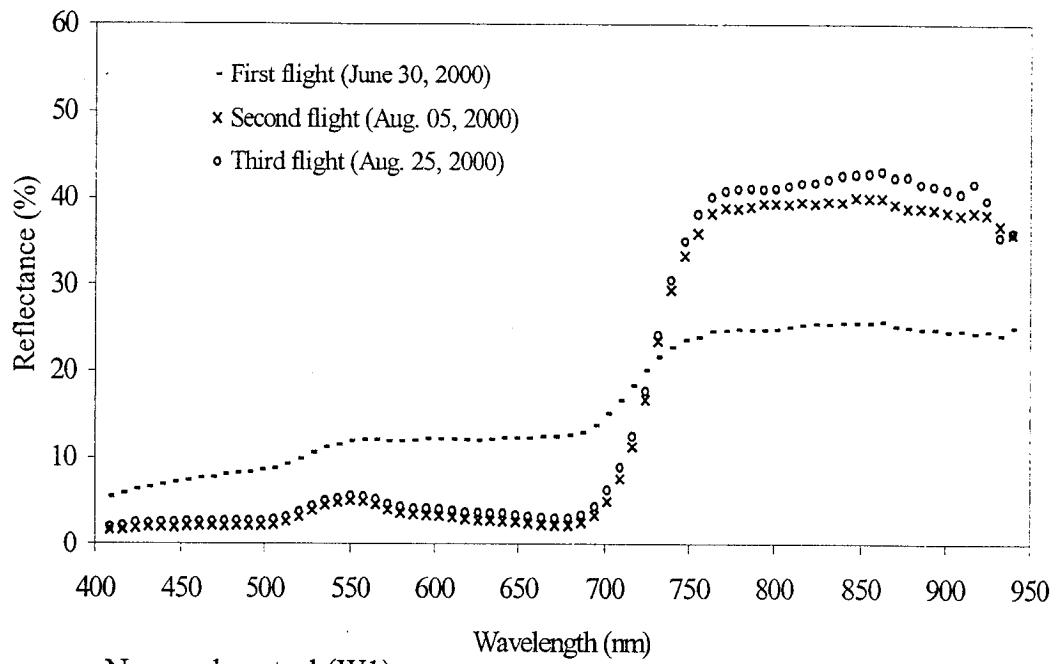
Figures 4.3a and 4.3b permit a comparison of the spectral response between no weed control and full weed control, at 120 kg/ha N, at the three growth stages. The reflectance in the near-infrared region was higher at the tassel stage when there was no weed control. However, at the fully-mature stage, the near-infrared reflectance was greater with full weed control. This is attributed to the fact that at the fully-mature stage, the crop and weeds were beginning to die back without weed control, whereas the corn did not start to die back until after the fully-mature stage had been reached when there was full weed control.

To enable the separation of different weed and nitrogen effects on the basis of reflectance, a statistical analysis was performed for the different growth stages and the results are given in Tables 4.8 to 4.10 for aerial observations, and in Table 4.11 for ground-based spectral data. A note of explanation is in order here. Although the analyses were done for each waveband separately, the total number of wavebands (71 for the aerial and 346 for the field spectroradiometer) were recombined into regions of identical significance, in order to reduce the size of the tables. For example, wavebands 45 to 69, inclusively, were the same with respect to the significance of effects and contrasts, and are presented as one large region.

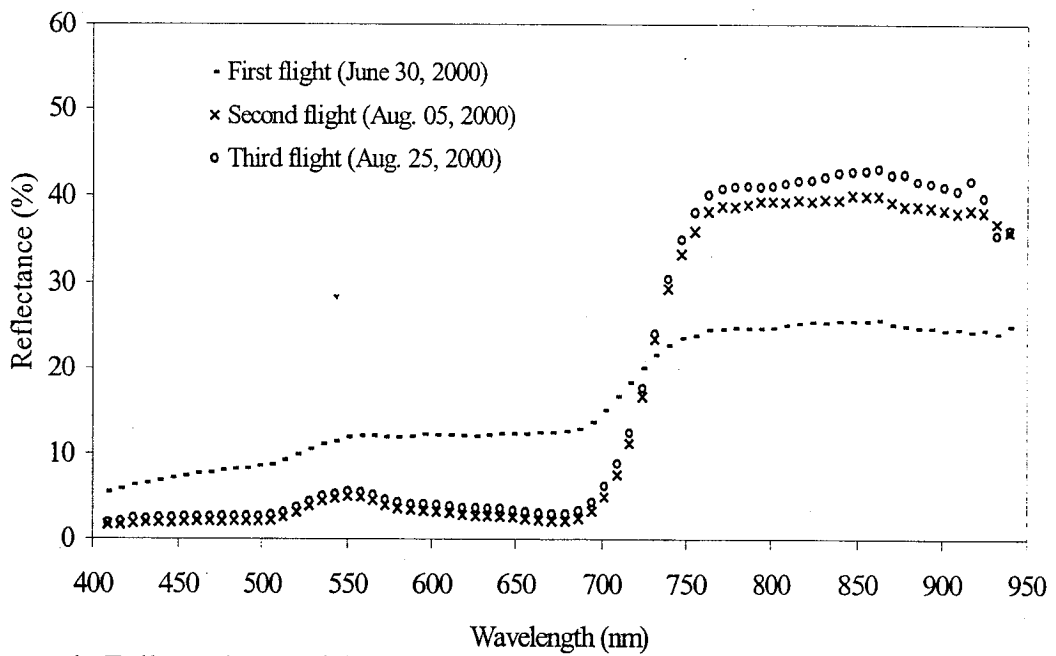
4.4.1.1 Early-growth stage

4.4.1.1.1 Aerial measurements

Although the crop was only four weeks old at the time of the first flight (June 30, 2000), there were significant differences ($\alpha=0.05$) in reflectance, attributable to the nitrogen application rate at all wavebands, except at 717 nm and 724 nm (Table 4.8). The contrasts between pairs of nitrogen application rates (N-rate) indicated that the differences were detectable only between the highest N-rate and the two others, but not between the two lowest, except in the waveband region of 739 to 924 nm. It should be noted at this stage, that there was no significant difference (difference of 10 kg N/ha) between the N₆₀ and N₁₂₀ treatments because the additional dose of nitrogen



a. No weed control (W1)



b. Full weed control (W4)

Fig. 4.3 Spectral response curve for corn under normal nitrogen (N_{120}) condition, during different flights

Table 4.8 Statistical significance calculated from ANOVA for main and subplot treatments, interactions and contrasts, (aerial spectral data)

Waveband		Weed	Nitrogen	Interaction	Contrast					
Number	Center or Range (nm)	(W)	(N)	W*N	W1	W1	W3	N ₆₀	N ₆₀	N ₁₂₀
					vs. W3	vs. W4	vs. W4	vs. N ₁₂₀	vs. N ₂₅₀	vs. N ₂₅₀
First flight (June 30, 2000)[#]										
1 to 13	409 to 498	NS	*	NS	NS	NS	NS	NS	*	*
14 to 27	505 to 603	NS	*	*	NS	NS	NS	NS	*	*
28 to 35	610 to 663	NS	*	*	NS	*	NS	NS	*	*
36	671	NS	*	NS	NS	*	NS	NS	*	*
37 to 40	679 to 701	NS	*	*	NS	*	NS	NS	*	*
41	709	NS	*	*	NS	NS	NS	NS	*	*
42	717	NS	NS	NS	NS	NS	NS	NS	NS	NS
43	724	NS	NS	NS	NS	NS	NS	NS	*	NS
44	732	NS	*	NS	NS	NS	NS	NS	*	NS
45	739	NS	*	NS	NS	NS	NS	*	*	NS
46 to 69	747 to 924	NS	*	NS	NS	NS	NS	*	*	*
70 to 71	932 to 939	NS	*	NS	NS	NS	NS	NS	*	*
Second flight (Aug. 05, 2000)										
1 to 3	409 to 424	NS	NS	NS	NS	NS	NS	NS	NS	NS
4	431	NS	NS	NS	NS	NS	NS	NS	NS	*
5 to 8	438 to 461	NS	NS	NS	NS	NS	NS	NS	NS	NS
9	468	NS	NS	NS	NS	NS	NS	NS	NS	*
10 to 11	476 to 483	NS	*	NS	NS	NS	NS	NS	NS	*
12	490	NS	*	NS	NS	NS	NS	*	NS	*
13 to 14	498 to 505	NS	*	NS	NS	NS	NS	*	NS	NS
15	513	NS	*	NS	NS	NS	NS	*	*	NS
16	520	*	*	NS	*	*	NS	*	*	NS
17 to 22	528 to 565	*	*	*	*	*	NS	*	*	*
23	573	*	*	NS	*	*	NS	*	*	NS
24	580	*	*	NS	*	*	NS	*	*	*
25 to 27	588 to 603	*	*	NS	*	*	NS	*	*	NS
28	610	NS	*	NS	*	*	NS	*	*	NS
29	618	NS	*	NS	*	NS	NS	*	*	NS
30 to 39	626 to 694	NS	*	NS	NS	NS	NS	*	*	NS
40	701	*	*	NS	*	*	NS	*	*	*

*Significant at < 0.05 probability level; NS-Non significant at < 0.05 probability level; W1- no weed control; W3-broadleaf weed control; W4-full weed control; N₆₀-60 kg N/ha; N₁₂₀-120 kg N/ha; N₂₅₀-250 kg N/ha.

At the time of first flight, nitrogen rates in N₆₀, N₁₂₀, and N₂₅₀ treatments were 10, 20, and 100 kg N/ha, respectively.

Table 4.8 (cont'd) Statistical significance calculated from ANOVA for main and subplot treatments, interactions and contrasts, (aerial spectral data)

Waveband		Weed	Nitrogen	Interaction	Contrast					
Number	Center or range (nm)	(W)	(N)	W*N	W1 vs. W3	W1 vs. W4	W3 vs. W4	N ₆₀ vs. N ₁₂₀	N ₆₀ vs. N ₂₅₀	N ₁₂₀ vs. N ₂₅₀
Second flight (Aug. 05, 2000)										
41 to 42	709 to 717	*	*	*	*	*	NS	*	*	*
43	724	*	*	*	*	*	*	*	*	*
44	732	*	*	*	*	*	*	NS	*	*
45	739	*	NS	*	*	*	*	NS	NS	NS
46	747	*	*	NS	*	*	*	*	*	NS
47 to 71	755 to 939	*	*	NS	*	*	*	*	*	*
Third flight (Aug. 25, 2000)										
1 to 10	409 to 476	NS	NS	NS	NS	NS	NS	NS	NS	NS
11	483	NS	NS	NS	NS	NS	NS	NS	*	NS
12	490	NS	NS	*	NS	NS	NS	NS	NS	NS
13 to 14	498 to 505	NS	*	NS	NS	NS	NS	*	*	NS
15 to 28	513 to 595	NS	*	NS	NS	NS	NS	*	*	*
29 to 39	618 to 694	NS	*	NS	NS	NS	NS	*	*	NS
40 to 44	701 to 732	NS	*	NS	NS	NS	NS	*	*	*
45	739	NS	*	*	NS	NS	NS	*	*	*
46 to 52	747 to 785	NS	NS	*	NS	NS	NS	NS	NS	NS
53 to 57	801 to 831	NS	NS	*	NS	NS	NS	NS	*	NS
58 to 61	839 to 862	NS	NS	*	NS	NS	NS	*	*	NS
62	870	NS	*	*	NS	NS	NS	*	*	NS
63	877	NS	NS	*	NS	NS	NS	*	*	NS
64 to 69	885 to 924	NS	*	*	NS	NS	NS	*	*	NS
70	932	NS	NS	NS	NS	NS	NS	NS	NS	NS
71	939	NS	*	NS	NS	NS	NS	NS	NS	NS

*Significant at < 0.05 probability level; NS-Non significant at < 0.05 probability level; W1- no weed control; W3- broadleaf weed control; W4-full weed control; N₆₀-60 kg N/ha; N₁₂₀-120 kg N/ha; N₂₅₀-250 kg N/ha.

was applied as topdressing after the first flight. The difference in plant growth due to nitrogen, especially that between the highest (N_{250}) and lowest level (N_{60}), is also evident from the observations of various plant parameters (Table 4.6). The maximum average values of LAI, plant height, greenness, chlorophyll, and nitrogen content were recorded in the high nitrogen (N_{250}) plots as $1.50 \text{ cm}^2/\text{cm}^2$, 21.3 cm, 41.7 on a comparative scale, 57.57 g/kg, and $0.0139 \text{ mg}/\text{cm}^2$, respectively. The corresponding minimum values were recorded in plots with the lowest nitrogen fertilization (N_{60}) as $0.59 \text{ cm}^2/\text{cm}^2$, 18.3 cm, 32.6 on a comparative scale, 38.75 g/kg, and $0.0096 \text{ mg}/\text{cm}^2$, respectively.

Response to weed control, so early in the season, could not be associated with the changes in reflectance at any waveband. Visual observations supported that this was due to the fact that herbicide had been applied only five days earlier and had not taken full effect. In general, there is a time lag of a few days between the time of application of a herbicide and the die-back of weeds. Even at this stage, observations of various plant parameters did not show a clear trend in the crop growth difference among various weed treatments for a particular nitrogen fertilization level (Table 4.6).

There was an interaction between weed and nitrogen in four waveband regions. As shown in Table 4.9, the contrasts between nitrogen-rates depended on the type of weed control. With no weed control, all contrasts between pairs of nitrogen-rates are significant at this early-growth stage of growth. It is interesting to note that the interaction was mainly associated with the reflectance values in the green and red regions of the visible spectrum. Where there was no weed control, the differences in reflectance between various pairings of nitrogen-rate were all significant at the waveband regions indicated by the table. The situation is not as clear in plots with broadleaf and full weed controls.

When the differences between the various weed controls were examined at separate nitrogen-rates (Table 4.10), it was apparent that differences between no weed control (W1) and broadleaf control (W3) at the lowest nitrogen-rate (N_{60}) were not significant except at waveband 41. At the normal (N_{120} , 120 kg N/ha) and higher (N_{250} , 250 kg N/ha) nitrogen-rates, there were no significant differences in reflectance

Table 4.9 Statistical significance obtained from a pairwise comparison of nitrogen fertilization rate means, for different weed control strategies, for bands in which the interaction between weed and nitrogen fertilization treatments was significant, (aerial spectral data)

Waveband		W1			W3			W4		
Number	Center or range (nm)	N ₆₀	N ₆₀	N ₁₂₀	N ₆₀	N ₆₀	N ₁₂₀	N ₆₀	N ₆₀	N ₁₂₀
		vs. N ₁₂₀	vs. N ₂₅₀	vs. N ₂₅₀	vs. N ₁₂₀	vs. N ₂₅₀	vs. N ₂₅₀	vs. N ₁₂₀	vs. N ₂₅₀	vs. N ₂₅₀
First flight (June 30, 2000)[#]										
14	505	*	*	*	NS	NS	NS	NS	*	*
15 to 17	513 to 528	*	*	*	NS	NS	*	NS	*	*
18	535	*	*	*	*	NS	*	NS	*	NS
19	543	*	*	*	NS	NS	*	NS	NS	NS
20	550	*	*	*	*	NS	*	NS	NS	NS
21	558	*	*	*	NS	NS	*	NS	*	NS
22 to 34	565 to 656	*	*	*	NS	NS	*	NS	*	*
35	663	*	*	*	NS	NS	NS	NS	*	*
37 to 38	679 to 686	*	*	*	NS	NS	NS	NS	*	*
39	694	*	*	*	NS	NS	*	NS	*	*
40	701	*	*	*	NS	NS	*	NS	*	NS
41	709	*	*	*	*	NS	*	NS	NS	NS
Second flight (Aug. 05, 2000)										
17 to 22	528 to 565	*	*	*	*	*	NS	*	*	NS
41	709	*	*	*	*	*	NS	*	*	NS
42	717	*	*	*	*	*	*	*	*	NS
43	724	*	*	*	NS	*	*	NS	*	NS
44	732	*	*	*	NS	NS	NS	NS	NS	NS
45	739	NS	NS	NS	*	*	NS	NS	*	NS
Third flight (Aug. 25, 2000)										
12	490	*	*	NS						
45	739	*	*	*	NS	NS	NS	NS	NS	NS
46	747	*	*	NS						
47	755	NS	*	NS	*	NS	NS	NS	NS	NS
48 to 69	762 to 924	NS	NS	NS	*	*	NS	NS	NS	NS

*Significant at < 0.05 probability level; NS-Non significant at < 0.05 probability level; W1- no weed control; W3- broadleaf weed control; W4-full weed control; N₆₀-60 kg N/ha; N₁₂₀-120 kg N/ha; N₂₅₀-250 kg N/ha.

At the time of first flight, nitrogen rates in N₆₀, N₁₂₀, and N₂₅₀ treatments were 10, 20, and 100 kg N/ha, respectively.

Table 4.10 Statistical significance obtained from a pairwise comparison of weed treatment means, for different nitrogen fertilization levels, for bands in which the interaction between weed and nitrogen fertilization treatment was significant, (aerial spectral data)

Waveband		N ₆₀			N ₁₂₀			N ₂₅₀		
Number	Center or range (nm)	W1 vs. W3	W1 vs. W4	W3 vs. W4	W1 vs. W3	W1 vs. W4	W3 vs. W4	W1 vs. W3	W1 vs. W4	W3 vs. W4
First flight (June 30, 2000)[#]										
14	505	NS	*	NS	*	*	NS	*	*	NS
15 to 16	513 to 520	NS	*	*	*	*	NS	*	*	NS
17 to 22	528 to 565	NS	NS	*	*	*	NS	*	*	NS
23 to 31	573 to 633	NS	*	*	*	*	NS	*	*	NS
32 to 35	641 to 663	NS	*	NS	*	*	NS	*	*	NS
37 to 38	679 to 686	NS	*	NS	*	*	NS	*	*	NS
39	694	NS	*	*	*	*	NS	*	*	NS
40	701	NS	*	*	*	*	NS	*	*	*
41	709	*	NS	*	*	*	NS	NS	*	*
Second flight (Aug. 05, 2000)										
17 to 22	528 to 565	*	*	NS	*	*	NS	*	*	NS
41	709	*	*	NS	*	*	NS	*	*	NS
42 to 43	717 to 724	*	*	*	*	*	*	*	*	NS
44 to 45	732 to 739	*	*	*	*	*	*	*	*	*
Third flight (Aug. 25, 2000)										
12	490	*	NS	*	NS	NS	NS	NS	NS	NS
45	739	*	*	NS	NS	*	NS	NS	NS	NS
46 to 69	747 to 924	*	*	NS	NS	NS	*	NS	NS	NS

*Significant at < 0.05 probability level; NS-Non significant at < 0.05 probability level; W1- no weed control; W3- broadleaf weed control; W4-full weed control; N₆₀-60 kg N/ha; N₁₂₀-120 kg N/ha; N₂₅₀-250 kg N/ha.

At the time of first flight, nitrogen rates in N₆₀, N₁₂₀, and N₂₅₀ treatments were 10, 20, and 100 kg N/ha, respectively.

between the broadleaved weed and full weed controls, whereas there were significant differences between no control and the other controls at all waveband regions except one (41 under high nitrogen-rate).

4.4.1.1.2 Field spectroradiometer measurements

Results of the analysis and the single-degree of freedom contrast for the data obtained with the field spectroradiometer are reported in Table 4.11. Results indicated that at this early stage, recorded reflectance values over different treatments were not significantly different in most of the wavelength regions. A significant difference in the overall nitrogen treatments was observed in the near-infrared wavelength region, from 744.6 to 920.5 nm. Only low (N₆₀) and high (N₂₅₀) nitrogen treatments plots could be separated in this region. However, from the airborne platform, in the corresponding wavelength region (747 to 924 nm), all three nitrogen levels were separable (Table 4.8). As expected, and also discussed in the previous section, the reflectance values in the weed treatments did not differ significantly, thus indicating that it was not possible to discriminate between weed control strategies on the basis of the field spectroradiometer data.

In general, better results were obtained from aerial observations. This could be attributed to higher variability from the ground-based spectral data, because of too high a spatial resolution relative to the proportion of the plot included in the images. Brown et al. (1994) also reported better results with data acquired at low resolution (high altitude), with less within-class variability.

4.4.1.2 Tassel stage

4.4.1.2.1 Aerial measurements

At the time of tasseling (second flight), the crop was about nine weeks old. At this stage, the effect of weeds and nitrogen fertilization levels was more evident in the field. A wide range of variation in the values of the various plant parameters, across various weed and nitrogen treatments (Table 4.6), indicated better separability of the various treatments at this stage. The results of the statistical analysis (Table 4.8) indicated significant differences associated with nitrogen-rate across most of the

Table 4.11 Statistical significance calculated from ANOVA for main and subplot treatments, interactions and contrasts, (field spectroradiometer data)

Waveband		Weed	Nitrogen	Interaction	Contrast					
Number	Center or range (nm)	(W)	(N)	W*N	W1 vs. W3	W1 vs. W4	W3 vs. W4	N ₆₀ vs. N ₁₂₀	N ₆₀ vs. N ₂₅₀	N ₁₂₀ vs. N ₂₅₀
During first flight (June 30, 2000)[#]										
1 to 226	378.8 to 732.1	NS	NS	NS	NS	NS	NS	NS	NS	NS
227 to 233	733.6 to 743.1	NS	NS	NS	NS	NS	NS	NS	*	NS
234 to 346	744.6 to 920.5	NS	*	NS	NS	NS	NS	NS	*	NS
During second flight (Aug. 05, 2000)										
1 to 89	378.8 to 517.0	NS	NS	NS	NS	NS	NS	NS	NS	NS
90 to 91	518.6 to 520.1	NS	NS	NS	NS	NS	NS	NS	*	NS
92 to 94	521.7 to 524.8	NS	*	NS	NS	NS	NS	NS	*	NS
95 to 96	526.4 to 528.0	NS	*	NS	NS	NS	NS	*	*	NS
97 to 106	529.5 to 543.7	NS	*	NS	NS	*	NS	*	*	NS
107 to 109	545.2 to 548.4	*	*	NS	NS	*	NS	*	*	NS
110	550.0	NS	*	NS	NS	*	NS	*	*	NS
111 to 116	551.5 to 559.4	*	*	NS	NS	*	NS	*	*	NS
117 to 127	561.0 to 576.6	NS	*	NS	NS	*	NS	*	*	NS
128 to 165	578.2 to 636.3	NS	*	NS	NS	NS	NS	*	*	NS
166	637.9	NS	NS	NS	NS	NS	NS	NS	NS	NS
167 to 174	639.4 to 650.4	NS	NS	NS	NS	NS	NS	NS	*	NS
175 to 200	652.0 to 691.3	NS	NS	NS	NS	NS	NS	NS	NS	NS
201 to 203	692.8 to 696.0	NS	*	NS	NS	NS	NS	NS	*	NS
204 to 205	697.5 to 699.1	NS	*	NS	NS	NS	NS	*	*	NS
206 to 207	700.7 to 702.2	NS	*	NS	NS	*	NS	*	*	NS
208 to 212	703.8 to 710.1	*	*	NS	NS	*	NS	*	*	NS
213 to 214	711.7 to 713.2	*	*	NS	NS	*	NS	*	*	*
215 to 219	714.8 to 721.1	*	*	NS	*	*	*	*	*	*
220 to 226	722.7 to 732.1	*	*	NS	*	*	*	NS	*	*
227	733.6	*	NS	NS	*	*	*	NS	*	NS
228 to 230	735.2 to 738.4	*	NS	*	*	*	*	NS	NS	NS
231 to 238	739.9 to 750.9	*	NS	NS	*	*	*	NS	NS	NS
239 to 240	752.5 to 754.1	*	NS	NS	*	*	*	NS	*	NS
241	755.6	*	*	NS	*	*	*	NS	*	NS
242 to 346	757.2 to 920.5	*	*	NS	*	*	*	*	*	NS

*Significant at < 0.05 probability level; NS-Non significant at < 0.05 probability level; W1- no weed control; W3- broadleaf weed control; W4-full weed control; N₆₀-60 kg N/ha; N₁₂₀-120 kg N/ha; N₂₅₀-250 kg N/ha.

At the time of first flight, nitrogen rates in N₆₀, N₁₂₀, and N₂₅₀ treatments were 10, 20, and 100 kg N/ha, respectively.

spectral regions investigated. Significant differences were associated with weed controls in 44 of the wavebands, and significant interactions only in 11 wavebands (17 to 22, and 41 to 45). The regions in which the nitrogen-rate effects were significant, included the wavebands noted, as relevant to plant nitrogen content by Buschmann and Nagel (1993) – 545 nm (green), 660 nm (red) and 800 nm (near-infrared) – and by Blacker et al. (1996a) – 550 nm. By combining the information from the additional wavebands, available through hyper-spectral imagery, it may be possible to detect more subtle differences in crop condition than has been possible before.

Within the different weed treatments, significant differences in reflectance values occurred over much fewer wavebands. Wavelength regions, from 520 to 603 nm and 701 to 939 nm, were found to be useful in the detection of different weed infestations. These included two of the four wavebands (centered at 440, 530, 650, and above 730 nm wavelengths) found useful in discriminating between weed species by Brown et al. (1994). Ten days after the flight, on August 15th, the weed cover observations also indicated a significant difference in weed cover between the various weed treatments. The average total weed cover in no weed control (W1) and broad leaf weed control (W3) plots were about 89 and 47 percent, respectively (Table 4.7). The LAI values were also quite high, ranging from 2.04 to 6.19 cm²/cm² across the various treatments (Table 4.6). Thus, it seems that differentiating between weed species in a cropping context, where the vegetation cover provided by the crop is substantially greater than that provided by weeds, would probably require a spatial resolution of the order of the row spacing at early stages of growth, and much better resolution as the crop reaches the fully-mature stage.

The contrasts, presented in Table 4.8, indicate that the significant differences between W3 (broadleaf control) and W4 (full weed control) only occurred in the near-infrared region. In the case of nitrogen, the contrasts indicated that differences occurred between N₆₀ (low nitrogen level) and the other two nitrogen treatments over most of the investigated spectral range. Significant differences between N₁₂₀ and N₂₅₀ were present in only a few wavelength regions. In general, it was concluded that the differences in spectral response, associated with nitrogen-rate, weed control, and their

interaction, cannot be attributed to a specific waveband. The difference in spectral response in weed treatments could be attributed to the level of weeds and their contribution to canopy formation. As shown by Brown et al. (1994) and various other researchers, reflectance can be significantly different at specific wavebands from one species to the next.

In general, no interaction was found between weed and nitrogen treatments, except in the wavelength regions from 528 to 565 nm and in 709 to 739 nm range. The results of the analysis for wavebands, where interaction had taken place (Tables 4.9 and 4.10), also indicate that at this stage, the differences in reflectance are quite significant for most of the weed and nitrogen treatment conditions. However, under full weed control, it is difficult to separate out N₁₂₀ and N₂₅₀ nitrogen levels (Table 4.9). With respect to the different nitrogen levels, the reflectance value under different weed treatments was significantly different in most of the cases. With the presence of excess nitrogen, it was difficult to separate W3 and W4 treatments (Table 4.10).

4.4.1.2.2 Field spectroradiometer measurements

At the time of the second flight, the crop canopy was almost fully developed with evidence of more pronounced effects of weeds and nitrogen treatments. Analysis of variance of the spectral data showed significant differences due to both weed and nitrogen treatments in many wavelength regions (Table 4.11). Compared to weeds, the effect of nitrogen treatment was evident over a much wider range of the spectrum. The nitrogen effect was evident from 522 to 636 nm in the visible spectrum, and also in the entire near-infrared region, except for the region from 734 to 754 nm region. However, the presence of weeds significantly influenced the spectral response in the entire near-infrared. Weeds were only detectable in a small part of the visible, from 545 to 548 nm, and from 551 to 559 nm. The most useful region was found to be in the NIR from 715 to 721 nm, wherein all weed and nitrogen treatments were separable. Weed treatments W1 (no weed control) and W4 (full weed control) were separable in the rest of the NIR. Significant differences between N₁₂₀ (normal) and N₂₅₀ (high) nitrogen plots occurred in only a few regions, whereas there were several

regions in which N_{60} could be differentiated from both N_{120} and N_{250} . A comparison with aerial observations suggested that better results could be obtained from aerial platforms due to the same reasons given in the previous section.

4.4.1.3 Fully-mature stage

4.4.1.3.1 Aerial measurements

Most of the crop had reached full maturity by the time of third flight (August 25). By this time, there were no significant differences in spectral response due to weed control. This is likely due to the fact that the corn canopy completely masked any weeds that may have survived the season. There were significant differences associated with the nitrogen-rate in many waveband regions, especially in the green to near-infrared region (498 to 732 nm) (Table 4.8). There was no interaction between weed control and nitrogen-rate in this region. The contrasts indicated that the reflectance values at different nitrogen levels were statistically different. All contrasts between nitrogen rates were significant in the green region (513 to 595 nm). The nitrogen effect on total biomass (represented by LAI) was quite evident, given a specific weed treatment. Higher nitrogen resulted in higher total biomass due to better crop and weed growth (Figure 4.2). However, there was more biomass within nitrogen levels when there was no weed control. Thus, the green range (513 to 595 nm) was proficient in detecting differences due to nitrogen availability.

The results of analyses of cases, where the weed/nitrogen interaction was significant, are summarized in Tables 4.9 and 4.10. The contrasts in Table 4.9 indicate that it was not easy to discriminate between nitrogen-rates under fixed weed control. It is interesting to note that there were no significant differences in spectral response, due to nitrogen-rates, where there was full weed control. This could not be explained by the yield data (Figure 4.4). Although grain yields and total corn biomass were higher, when more nitrogen was applied, there was no evidence of the effect of weeds on crop yield. With no weed control and control of broadleaved weeds only, the observed differences between nitrogen-rates did not occur within the same waveband regions. Thus, it was difficult to draw further conclusions regarding the discrimination of nitrogen-rates.

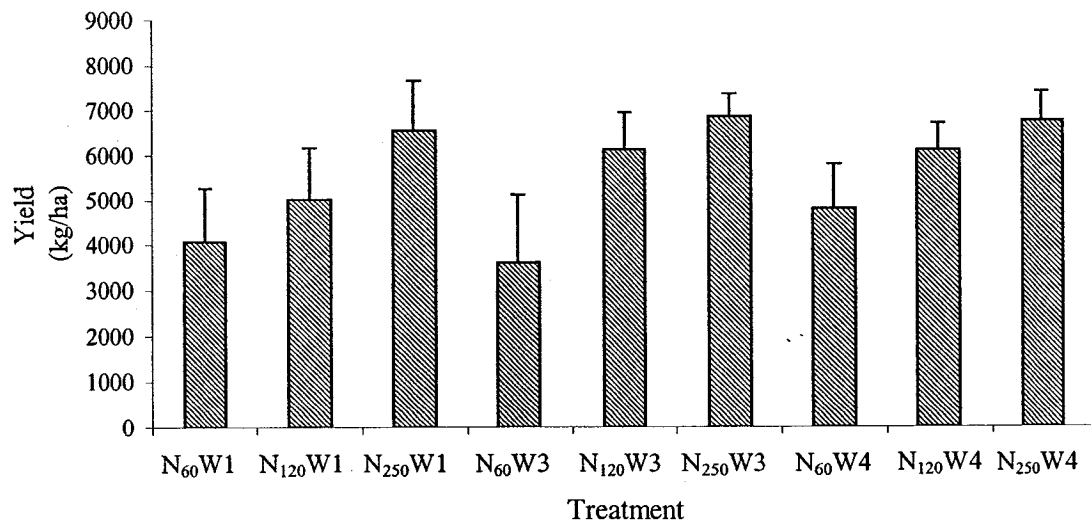


Fig. 4.4 Variation in corn grain yield among various treatments
(Error bar represents one standard deviation)

The contrasts between weed controls at fixed nitrogen-rates are given in Table 4.10. There were significant differences at most wavebands between no weed control (W1) and the others (W3 and W4) at the lowest nitrogen-rate (N_{60}). There were no significant differences between weed controls at the highest nitrogen-rate. There was an indication of some potential of discriminating different weeds at the normal nitrogen-rate, particularly in the near-infrared region.

In summary, the statistical analysis of spectral response of corn under different weed control strategies and nitrogen levels clearly indicated that various spectral regions in the visible and near-infrared regions of the spectrum could be used to detect weeds and plant stress due to nitrogen level. The spectral measurements, acquired near 498 nm and 671 nm with the airborne sensor, were found to be the most indicative of nitrogen stress; this was irrespective of the time of flight and without the interaction with weed treatments. The significant impact of weeds was found only during the second flight. Thus, from the aforementioned analysis it may be concluded that the impact of weeds and nitrogen could be detected by spectral measurements. The selection of specific spectral regions to detect a particular category of stress, weed or nitrogen, therefore appears to depend upon the growth stage of corn at which spectral data are acquired.

4.4.2 Estimation of crop biophysical parameters

The models which express crop biophysical parameters and other canopy descriptors, in terms of reflectance in up to five wavebands as measured by the airborne sensor, are summarized in Tables 4.12, 4.22, and 4.24 for each of the three flights. Corresponding models based on data acquired with the field spectroradiometer are given in Tables 4.18, 4.21, and 4.23.

4.4.2.1 Early-growth stage

4.4.2.1.1 Aerial measurements

The average values of the biophysical crop parameters at the nine retained combinations of weed control and nitrogen-rate are given in Table 4.6. The crop

canopy was small and the soil was visible in most plots at the time of the first flight, 30 days after sowing. The regression models with the highest r^2 were those involving five wavebands as predictors of biophysical parameters (Table 4.12). In general, wavebands in the blue and near-infrared regions were the most prevalent in these models (recall that all possible combinations of up to five wavebands were assessed by the MAXR criterion during the stepwise multiple regression procedure). Table 4.12 also reveals that the models of a given biophysical parameter, involving 3, 4 or 5 wavebands, often share common wavelengths.

The performance of the five-waveband models was evaluated using the validation data sets. The relationships between the observed and predicted values of the various parameters are shown in Figure 4.5. The values of SSE, ARPE and C_{eff} are presented in Tables 4.13 and 4.14. The SSE values for all parameters were comparatively higher for the validation data set than for the calibration data set. While this is expected, it certainly suggests caution in applying the equations. The ARPE values show an underestimation by as much as 18% (LAI), and an overestimation of 34% for grain yield. Figure 4.5 shows that, although good agreements between the observed and predicted values were obtained for most of the parameters, the values of C_{eff} , ranging from -1.444 to -0.193, suggest that the models can be improved.

The three most significant NDVI ratios for each crop parameter are presented in Table 4.15. Regression coefficients of the best NDVI-based models are given in Table 4.16. Although the coefficients of determination are very low, the values of SSE and ARPE for the calibration and validation data sets (Table 4.17) indicate that the NDVI models predict the validation data adequately. The ARPE values indicate a 3.3% over-prediction of yield, and a 6.9% under-prediction of leaf nitrogen. The positive Nash-Sutcliffe (C_{eff}) values, presented in Table 4.14, also supported the observation that better prediction results from the NDVI-based models. Thus, although r^2 values were higher for the models, based on the direct reflectance values compared to NDVI-based models, a further validation analysis indicated that the latter performed better. The C_{eff} values clearly indicated that better models could be developed with NDVI for LAI, plant height, and greenness estimation. The NDVI

Table 4.12 Useful wavebands and corresponding regression equation parameters for the estimation of various crop-condition indicators and other parameters at early-growth stage, using aerial spectral measurements (first flight; June 30, 2000)

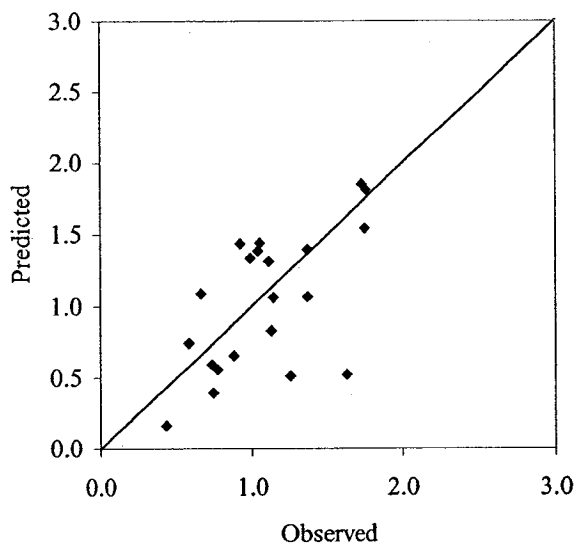
Crop parameter	r ²	Wavelength (nm)	Regression equation coefficient*						
			b ₀	b ₁	b ₂	b ₃	b ₄	b ₅	
Leaf area index	0.23	939	-1.724	0.105					
	0.37	724 939	-0.886	-0.177	0.210				
	0.63	709 724 732	-1.354	1.504	-4.399	3.026			
	0.79	701 724 732 893	0.381	0.823	-4.530	4.939	-1.123		
	0.82	709 724 732 831 893	-0.241	1.435	-4.884	4.151	0.805	-1.413	
Plant height	0.43	701	33.221	-0.935					
	0.63	416 461	28.855	5.024	-5.013				
	0.68	453 461 505	27.343	16.108	-6.801	-8.423			
	0.73	438 453 461 505	27.113	4.530	13.571	-8.603	-8.252		
	0.84	424 438 453 513 932	15.455	-4.927	4.724	13.552	-12.02	0.621	
Greenness	0.51	694	60.840	-1.933					
	0.70	717 932	40.647	-2.829	1.879				
	0.93	490 558 724	59.787	20.134	-26.638	6.448			
	0.95	453 490 558 724	67.590	-9.467	30.031	-28.893	6.771		
	0.97	453 490 528 558 724	68.310	-15.204	40.740	-16.960	-18.494	7.092	
Leaf chlorophyll content	0.21	461	0.0198	-0.0012					
	0.28	453 461	0.0183	0.0080	-0.0086				
	0.53	573 595 901	0.0033	-0.0235	0.0203	0.0016			
	0.66	580 633 901 916	-0.0043	-0.0187	0.0163	0.0098	-0.0082		
	0.74	686 694 732 901 916	-0.0161	-0.0082	0.0115	-0.0108	0.0182	-0.0097	
Total leaf nitrogen	0.26	694	85.341	-3.110					
	0.37	431 618	77.784	20.180	-13.679				
	0.42	431 461 618	65.854	45.312	-25.952	-9.564			
	0.48	431 476 618 618	79.900	37.941	46.191	-51.386	-19.104		
	0.74	476 573 610 618 717	62.318	49.206	-97.279	259.67	-219.66	13.460	
Total soil moisture	0.53	717	70.652	-2.032					
	0.70	438 528	63.551	8.097	-8.056				
	0.82	431 453 513	54.783	-24.091	38.455	-15.830			
	0.88	431 453 498 543	62.918	-19.845	35.578	-12.565	-4.713		
	0.91	431 453 490 535 543	54.611	-16.867	35.288	-18.556	30.622	-31.168	

* Regression equation coefficients of one-, two-, three-, four- and five-variable models
 Note-General form of the equation: crop parameter = b₀ + b₁S₁ + b₂S₂ + b₃S₃ + b₄S₄ + b₅S₅, where S₁, S₂, S₃, S₄, and S₅ are the reflectance values at the respective wavelengths listed above.

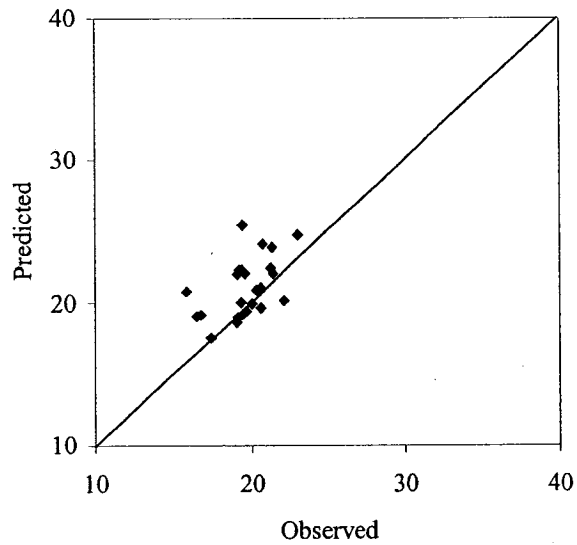
Table 4.12 (cont'd) Useful wavebands and corresponding regression equation parameters for the estimation of various crop-condition indicators and other parameters at early-growth stage, using aerial spectral measurements (first flight; June 30, 2000)

Crop parameter	r ²	Wavelength (nm)	Regression equation coefficient*					
			b ₀	b ₁	b ₂	b ₃	b ₄	b ₅
Grain yield	0.31	528	14.057	-0.821				
	0.43	717 939	6.132	-0.725	0.489			
	0.85	476 550 724	12.333	6.724	-9.027	2.326		
	0.89	476 490 550 724	13.078	3.777	4.213	-10.597	2.660	
	0.92	446 476 490 550 724	14.170	-3.360	4.205	7.529	-11.781	2.957
Biomass	0.22	717	2.992	-0.096				
	0.31	724 939	2.125	-0.157	0.088			
	0.55	709 724 801	0.929	0.716	-1.265	0.554		
	0.75	686 709 724 801	0.734	-0.547	2.398	-2.962	1.092	
	0.80	618 709 724 801 885	0.895	-0.721	2.402	-2.832	1.678	-0.634

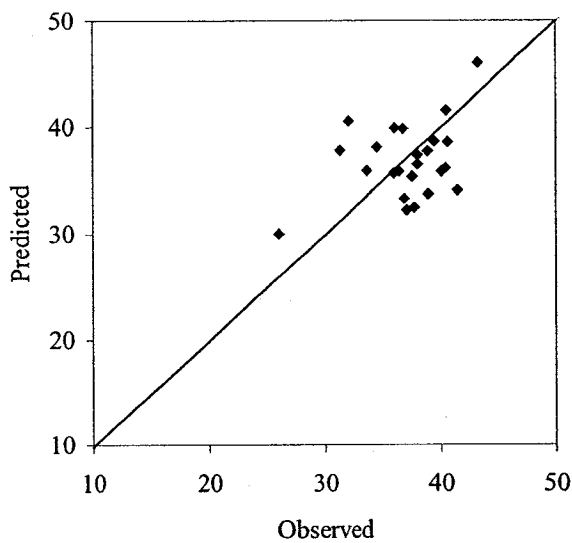
* Regression equation coefficients of one-, two-, three-, four- and five-variable models
 Note-General form of the equation: crop parameter = b₀ + b₁S₁ + b₂S₂ + b₃S₃ + b₄S₄ + b₅S₅, where S₁, S₂, S₃, S₄, and S₅ are the reflectance values at the respective wavelengths listed above.



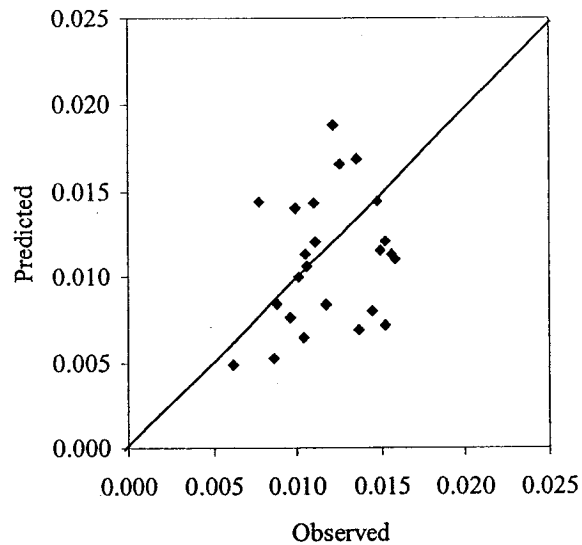
a. Leaf area index (cm^2/cm^2)



b. Plant height (cm)

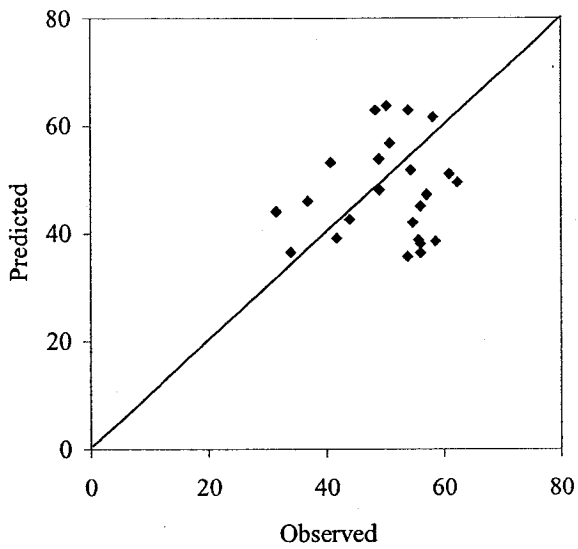


c. Greenness (SPAD reading, unitless)

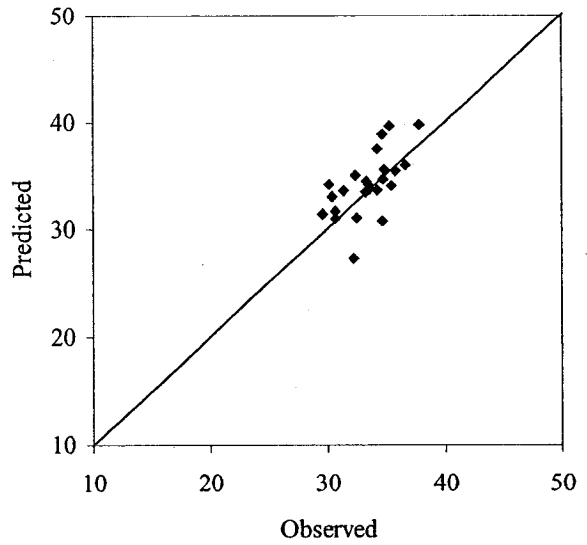


d. Leaf total chlorophyll content (mg/cm^2)

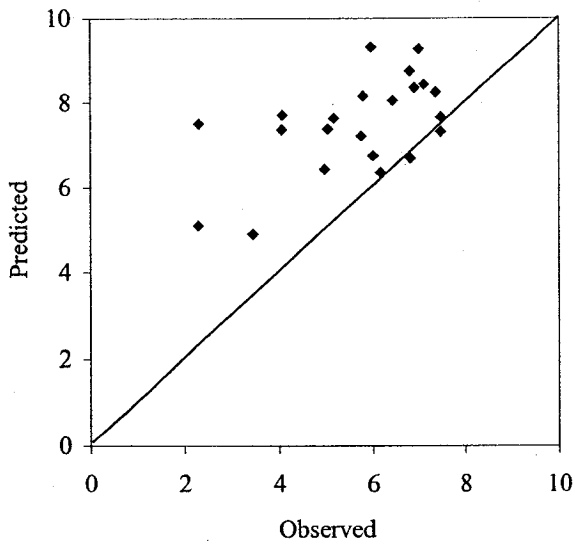
Fig. 4.5 Observed and predicted crop condition parameters and crop yield, based on airborne spectral observations at the initial stage (June 30, 2000)



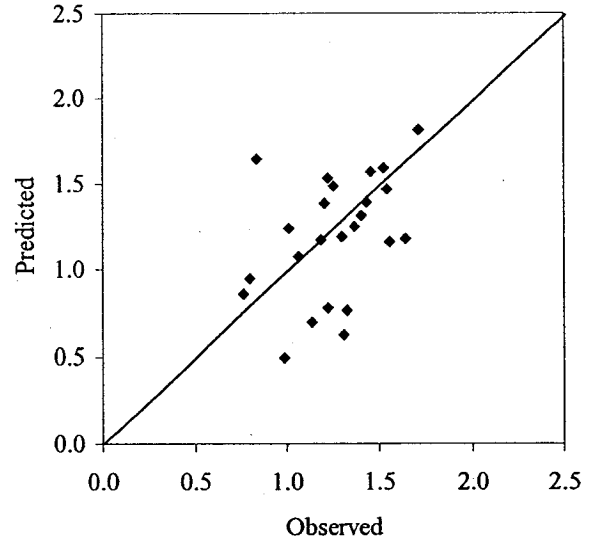
e. Leaf total nitrogen content (g/kg)



f. Total soil moisture content (%)



g. Corn grain yield (t/ha)



h. Dry biomass (kg/m²)

Fig. 4.5 (cont'd) Observed and predicted crop condition parameters and crop yield, based on airborne spectral observations at the initial stage (June 30, 2000)

Table 4.13 Sum of squared error (SSE) and average relative percent error (ARPE) values of the best five-parameter models developed using aerial spectral measurements for the estimation of different crop parameters

Crop parameters	First flight (Early-growth stage)				Second flight (Tassel stage)				Third flight (Fully-mature stage)			
	Sum of squared error (SSE)		Average relative percent error (ARPE)		Sum of squared error (SSE)		Average relative percent error (ARPE)		Sum of squared error (SSE)		Average relative percent error (ARPE)	
	Cali.*	Vali.#	Cali.*	Vali.#	Cali.*	Vali.#	Cali.*	Vali.#	Cali.*	Vali.#	Cali.*	Vali.#
Leaf area index, (cm ² /cm ²)	0.034	0.298	0.007	-0.182	0.161	1.110	0.001	0.041	0.035	0.301	0.0	0.034
Plant height, (cm)	0.653	5.581	-0.001	0.074	39.140	220.405	0.0	-0.007	24.260	442.703	0.0	0.017
Greenness (unitless)	0.560	15.708	0.000	-0.009	2.405	17.628	0.0	0.031	1.250	17.248	0.0	0.010
Leaf chlorophyll content, (mg/cm ²)	0.000	0.000	-0.002	-0.072	0.000	0.000	0.004	-0.040	-	-	-	-
Total leaf nitrogen, (g/kg)	25.529	138.704	0.007	-0.054	13.590	51.985	-0.001	0.051	-	-	-	-
Total soil moisture, (%)	1.125	5.837	0.001	0.023	1.789	11.155	0.002	0.045	2.946	14.766	0.0	-0.052
Grain yield, (t/ha)	3.726	5.590	0.318	0.342	0.118	3.268	0.0	0.012	0.128	1.796	0.001	-0.003
Biomass (kg/m ²)	0.013	0.115	0.005	-0.051	0.120	0.109	-0.249	-0.201	0.013	0.167	0.001	0.013

Cali.* : Calibration data

Vali.#: Validation data

Table 4.14 Nash-Sutcliffe coefficient values for comparison between observed and predicted values of various crop-condition indicator parameters. Prediction results of the best five-parameter regression models and best NDVI-based model for validation data set, (**aerial spectral measurements**)

Crop parameter	Nash-Sutcliffe Coefficient					
	Best five parameter regression model			Best NDVI based model		
	First flight (Early-growth stage)	Second flight (Tassel stage)	Third flight (Fully-mature stage)	First flight (Early-growth stage)	Second flight (Tassel stage)	Third flight (Fully-mature stage)
Leaf area index	-0.993	-0.035	0.189	0.427	0.384	0.036
Plant height	-0.962	0.778	0.382	0.124	0.834	0.514
Greenness	-0.193	0.519	0.680	0.224	0.587	0.828
Leaf chlorophyll content	-1.351	0.125	-	-0.071	0.514	-
Total leaf nitrogen	-1.039	0.539	-	-0.383	0.414	-
Total soil moisture	-0.273	-1.673	-0.714	-0.182	-0.289	-0.530
Grain yield	-1.444	-0.217	0.350	0.091	0.782	0.673
Biomass	-0.798	-0.297	-0.990	0.060	0.349	-0.427

Table 4.15 Best three useful NDVI indices and corresponding coefficient of determination (r^2) values for the development of regression models, for the estimation of various crop-condition indicators and other canopy parameters at different crop growth stages, (aerial spectral measurements)

Crop parameter	Model-1		Model-2		Model-3	
	NDVI-1	r^2	NDVI-2	r^2	NDVI-3	r^2
Early-growth stage (First flight, June 30, 2000)						
Leaf area index	$(\text{NIR}_{831} - \text{R}_{701}) / (\text{NIR}_{831} + \text{R}_{701})$	0.283	$(\text{NIR}_{785} - \text{R}_{701}) / (\text{NIR}_{785} + \text{R}_{701})$	0.282	$(\text{NIR}_{778} - \text{R}_{701}) / (\text{NIR}_{778} + \text{R}_{701})$	0.281
Plant height	$(\text{NIR}_{793} - \text{R}_{701}) / (\text{NIR}_{793} + \text{R}_{701})$	0.388	$(\text{NIR}_{785} - \text{R}_{701}) / (\text{NIR}_{785} + \text{R}_{701})$	0.386	$(\text{NIR}_{801} - \text{R}_{701}) / (\text{NIR}_{801} + \text{R}_{701})$	0.384
Greenness	$(\text{NIR}_{801} - \text{R}_{701}) / (\text{NIR}_{801} + \text{R}_{701})$	0.569	$(\text{NIR}_{847} - \text{R}_{701}) / (\text{NIR}_{847} + \text{R}_{701})$	0.566	$(\text{NIR}_{831} - \text{R}_{701}) / (\text{NIR}_{831} + \text{R}_{701})$	0.565
Leaf chlorophyll	$(\text{NIR}_{847} - \text{R}_{701}) / (\text{NIR}_{847} + \text{R}_{701})$	0.223	$(\text{NIR}_{785} - \text{R}_{701}) / (\text{NIR}_{785} + \text{R}_{701})$	0.217	$(\text{NIR}_{793} - \text{R}_{701}) / (\text{NIR}_{793} + \text{R}_{701})$	0.217
Total leaf nitrogen	$(\text{NIR}_{778} - \text{R}_{701}) / (\text{NIR}_{778} + \text{R}_{701})$	0.352	$(\text{NIR}_{801} - \text{R}_{701}) / (\text{NIR}_{801} + \text{R}_{701})$	0.351	$(\text{NIR}_{785} - \text{R}_{701}) / (\text{NIR}_{785} + \text{R}_{701})$	0.345
Total soil moisture	$(\text{NIR}_{839} - \text{R}_{679}) / (\text{NIR}_{839} + \text{R}_{679})$	0.024	$(\text{NIR}_{839} - \text{R}_{671}) / (\text{NIR}_{839} + \text{R}_{671})$	0.023	$(\text{NIR}_{816} - \text{R}_{679}) / (\text{NIR}_{816} + \text{R}_{679})$	0.023
Grain yield	$(\text{NIR}_{801} - \text{R}_{701}) / (\text{NIR}_{801} + \text{R}_{701})$	0.327	$(\text{NIR}_{793} - \text{R}_{701}) / (\text{NIR}_{793} + \text{R}_{701})$	0.326	$(\text{NIR}_{785} - \text{R}_{701}) / (\text{NIR}_{785} + \text{R}_{701})$	0.326
Biomass	$(\text{NIR}_{801} - \text{R}_{701}) / (\text{NIR}_{801} + \text{R}_{701})$	0.024	$(\text{NIR}_{847} - \text{R}_{701}) / (\text{NIR}_{847} + \text{R}_{701})$	0.023	$(\text{NIR}_{785} - \text{R}_{701}) / (\text{NIR}_{785} + \text{R}_{701})$	0.022
Tassel stage (Second flight, August 5, 2000)						
Leaf area index	$(\text{NIR}_{847} - \text{R}_{671}) / (\text{NIR}_{847} + \text{R}_{671})$	0.464	$(\text{NIR}_{839} - \text{R}_{671}) / (\text{NIR}_{839} + \text{R}_{671})$	0.462	$(\text{NIR}_{854} - \text{R}_{671}) / (\text{NIR}_{854} + \text{R}_{671})$	0.462
Plant height	$(\text{NIR}_{839} - \text{R}_{701}) / (\text{NIR}_{839} + \text{R}_{701})$	0.708	$(\text{NIR}_{831} - \text{R}_{701}) / (\text{NIR}_{831} + \text{R}_{701})$	0.706	$(\text{NIR}_{824} - \text{R}_{701}) / (\text{NIR}_{824} + \text{R}_{701})$	0.704
Greenness	$(\text{NIR}_{839} - \text{R}_{701}) / (\text{NIR}_{839} + \text{R}_{701})$	0.293	$(\text{NIR}_{778} - \text{R}_{701}) / (\text{NIR}_{778} + \text{R}_{701})$	0.293	$(\text{NIR}_{801} - \text{R}_{701}) / (\text{NIR}_{801} + \text{R}_{701})$	0.292
Leaf chlorophyll	$(\text{NIR}_{847} - \text{R}_{701}) / (\text{NIR}_{847} + \text{R}_{701})$	0.177	$(\text{NIR}_{816} - \text{R}_{701}) / (\text{NIR}_{816} + \text{R}_{701})$	0.175	$(\text{NIR}_{824} - \text{R}_{701}) / (\text{NIR}_{824} + \text{R}_{701})$	0.174
Total leaf nitrogen	$(\text{NIR}_{839} - \text{R}_{701}) / (\text{NIR}_{839} + \text{R}_{701})$	0.197	$(\text{NIR}_{831} - \text{R}_{701}) / (\text{NIR}_{831} + \text{R}_{701})$	0.194	$(\text{NIR}_{778} - \text{R}_{701}) / (\text{NIR}_{778} + \text{R}_{701})$	0.192
Total soil moisture	$(\text{NIR}_{831} - \text{R}_{701}) / (\text{NIR}_{831} + \text{R}_{701})$	0.011	$(\text{NIR}_{854} - \text{R}_{701}) / (\text{NIR}_{854} + \text{R}_{701})$	0.011	$(\text{NIR}_{847} - \text{R}_{701}) / (\text{NIR}_{847} + \text{R}_{701})$	0.010
Grain yield	$(\text{NIR}_{839} - \text{R}_{701}) / (\text{NIR}_{839} + \text{R}_{701})$	0.567	$(\text{NIR}_{831} - \text{R}_{701}) / (\text{NIR}_{831} + \text{R}_{701})$	0.565	$(\text{NIR}_{824} - \text{R}_{701}) / (\text{NIR}_{824} + \text{R}_{701})$	0.563
Biomass	$(\text{NIR}_{839} - \text{R}_{701}) / (\text{NIR}_{839} + \text{R}_{701})$	0.274	$(\text{NIR}_{778} - \text{R}_{701}) / (\text{NIR}_{778} + \text{R}_{701})$	0.273	$(\text{NIR}_{824} - \text{R}_{701}) / (\text{NIR}_{824} + \text{R}_{701})$	0.271

Note: Subscripts represent wavelength for near-infrared (NIR) and red (R) reflectance

Table 4.15 (cont'd) Best three useful NDVI indices and corresponding coefficient of determination (r^2) values for the development of regression models, for the estimation of various crop-condition indicators and other canopy parameters at different crop growth stages, (aerial spectral measurements)

Crop parameter	Model-1		Model-2		Model-3	
	NDVI-1	r^2	NDVI-2	r^2	NDVI-3	r^2
Fully-mature stage (Third flight, August 25, 2000)						
Leaf area index	$(\text{NIR}_{831}-\text{R}_{663})/(\text{NIR}_{831}+\text{R}_{663})$	0.590	$(\text{NIR}_{839}-\text{R}_{663})/(\text{NIR}_{839}+\text{R}_{663})$	0.590	$(\text{NIR}_{847}-\text{R}_{679})/(\text{NIR}_{847}+\text{R}_{679})$	0.589
Plant height	$(\text{NIR}_{854}-\text{R}_{648})/(\text{NIR}_{854}+\text{R}_{648})$	0.866	$(\text{NIR}_{801}-\text{R}_{648})/(\text{NIR}_{801}+\text{R}_{648})$	0.866	$(\text{NIR}_{839}-\text{R}_{633})/(\text{NIR}_{839}+\text{R}_{633})$	0.865
Greenness	$(\text{NIR}_{839}-\text{R}_{701})/(\text{NIR}_{839}+\text{R}_{701})$	0.934	$(\text{NIR}_{831}-\text{R}_{701})/(\text{NIR}_{831}+\text{R}_{701})$	0.932	$(\text{NIR}_{839}-\text{R}_{694})/(\text{NIR}_{839}+\text{R}_{694})$	0.932
Total soil moisture	$(\text{NIR}_{854}-\text{R}_{679})/(\text{NIR}_{854}+\text{R}_{679})$	0.003	$(\text{NIR}_{816}-\text{R}_{679})/(\text{NIR}_{816}+\text{R}_{679})$	0.003	$(\text{NIR}_{839}-\text{R}_{663})/(\text{NIR}_{839}+\text{R}_{663})$	0.003
Grain yield	$(\text{NIR}_{831}-\text{R}_{701})/(\text{NIR}_{831}+\text{R}_{701})$	0.897	$(\text{NIR}_{839}-\text{R}_{701})/(\text{NIR}_{839}+\text{R}_{701})$	0.894	$(\text{NIR}_{831}-\text{R}_{694})/(\text{NIR}_{831}+\text{R}_{694})$	0.889
Biomass	$(\text{NIR}_{778}-\text{R}_{701})/(\text{NIR}_{778}+\text{R}_{701})$	0.400	$(\text{NIR}_{785}-\text{R}_{701})/(\text{NIR}_{785}+\text{R}_{701})$	0.395	$(\text{NIR}_{793}-\text{R}_{701})/(\text{NIR}_{793}+\text{R}_{701})$	0.395

Note: Subscripts represent wavelength for near-infrared (NIR) and red (R) reflectance.

Table 4.16 Regression equation parameters for the best NDVI-based model for the estimation of various crop-condition indicators and other canopy parameters at different crop growth stages, (aerial spectral measurements)

Crop parameter	NDVI	r ²	Intercept (b ₀)	Coefficient (b ₁)
Early-growth stage (First flight, June 30, 2000)				
Leaf area index	(NIR ₈₃₁ -R ₇₀₁)/ (NIR ₈₃₁ +R ₇₀₁)	0.283	0.0128	3.3407
Plant height	(NIR ₇₉₃ -R ₇₀₁)/ (NIR ₇₉₃ +R ₇₀₁)	0.388	14.70	17.96
Greenness	(NIR ₈₀₁ -R ₇₀₁)/ (NIR ₈₀₁ +R ₇₀₁)	0.569	22.66	47.01
Leaf chlorophyll content	(NIR ₈₄₇ -R ₇₀₁)/ (NIR ₈₄₇ +R ₇₀₁)	0.223	0.0059	0.0174
Total leaf nitrogen	(NIR ₇₇₈ -R ₇₀₁)/ (NIR ₇₇₈ +R ₇₀₁)	0.352	21.88	82.76
Total soil moisture	(NIR ₈₃₉ -R ₆₇₉)/ (NIR ₈₃₉ +R ₆₇₉)	0.024	36.1	-5.845
Grain yield	(NIR ₈₀₁ -R ₇₀₁)/ (NIR ₈₀₁ +R ₇₀₁)	0.327	2.31	11.97
Biomass	(NIR ₈₀₁ -R ₇₀₁)/ (NIR ₈₀₁ +R ₇₀₁)	0.024	1.090	0.565
Tassel stage (Second flight, August 5, 2000)				
Leaf area index	(NIR ₈₄₇ -R ₆₇₁)/ (NIR ₈₄₇ +R ₆₇₁)	0.464	-28.17	35.30
Plant height	(NIR ₈₃₉ -R ₇₀₁)/ (NIR ₈₃₉ +R ₇₀₁)	0.708	-296.29	614.90
Greenness	(NIR ₈₃₉ -R ₇₀₁)/ (NIR ₈₃₉ +R ₇₀₁)	0.293	-29.83	94.49
Leaf chlorophyll content	(NIR ₈₄₇ -R ₇₀₁)/ (NIR ₈₄₇ +R ₇₀₁)	0.177	-0.0061	0.0269
Total leaf nitrogen	(NIR ₈₃₉ -R ₇₀₁)/ (NIR ₈₃₉ +R ₇₀₁)	0.197	-25.80	118.62
Total soil moisture	(NIR ₈₃₁ -R ₇₀₁)/ (NIR ₈₃₁ +R ₇₀₁)	0.011	38.63	-7.75
Grain yield	(NIR ₈₃₉ -R ₇₀₁)/ (NIR ₈₃₉ +R ₇₀₁)	0.567	-17.05	29.34
Biomass	(NIR ₈₃₉ -R ₇₀₁)/ (NIR ₈₃₉ +R ₇₀₁)	0.274	-1.313	3.321
Fully-mature stage (Third flight, August 25, 2000)				
Leaf area index	(NIR ₈₃₁ -R ₆₆₃)/ (NIR ₈₃₁ +R ₆₆₃)	0.590	-41.33	51.65
Plant height	(NIR ₈₅₄ -R ₆₄₈)/ (NIR ₈₅₄ +R ₆₄₈)	0.866	-1521.84	1999.07
Greenness	(NIR ₈₃₉ -R ₇₀₁)/ (NIR ₈₃₉ +R ₇₀₁)	0.934	-32.24	145.36
Total soil moisture	(NIR ₈₅₄ -R ₆₇₉)/ (NIR ₈₅₄ +R ₆₇₉)	0.003	46.239	-16.297
Grain yield	(NIR ₈₃₁ -R ₇₀₁)/ (NIR ₈₃₁ +R ₇₀₁)	0.897	-9.51	28.58
Biomass	(NIR ₇₇₈ -R ₇₀₁)/ (NIR ₇₇₈ +R ₇₀₁)	0.400	-1.967	4.435

Note-General form of the regression equation: crop parameter = b₀ + b₁(NDVI), where NDVI is the normalized difference vegetation index.

Subscripts represent wavelength for near-infrared (NIR) and red (R) reflectance.

Table 4.17 Sum of squared error (SSE) and average relative percent error (ARPE) values of the best NDVI models, developed for the estimation of different crop parameters, (aerial spectral measurements)

Crop parameter	First flight (Early-growth stage)				Second flight (Tassel stage)				Third flight (Fully-mature stage)			
	Sum of squared error (SSE)		Average relative percent error (ARPE)		Sum of squared error (SSE)		Average relative percent error (ARPE)		Sum of squared error (SSE)		Average relative percent error (ARPE)	
	Cali.*	Vali.#	Cali.*	Vali.#	Cali.*	Vali.#	Cali.*	Vali.#	Cali.*	Vali.#	Cali.*	Vali.#
Leaf area index, (cm ² /cm ²)	0.136	0.086	0.0	0.005	0.409	0.730	0.0	-0.02	0.155	0.358	0.0	-0.05
Plant height, (cm)	2.522	2.490	0.0	0.025	180.088	165.693	0.0	-0.02	115.532	348.461	0.0	0.05
Greenness, (unitless)	8.238	10.219	0.0	-0.008	24.858	11.444	0.0	-0.01	4.316	9.300	0.0	0.01
Leaf chlorophyll content, (mg/cm ²)	0.000	0.000	0.0	-0.040	0.000	0.000	0.0	0.01	-	-	-	-
Total leaf nitrogen, (g/kg)	62.950	94.135	0.0	-0.069	66.360	66.113	0.0	0.02	-	-	-	-
Total soil moisture, (%)	11.760	5.420	0.0	0.007	7.440	5.378	0.0	0.03	6.901	13.183	0.0	-0.06
Grain yield, (t/ha)	1.450	2.078	0.0	0.033	0.759	0.586	0.0	0.00	0.273	0.587	0.0	-0.03
Biomass, (kg/m ²)	0.065	0.060	0.0	0.001	0.034	0.055	0.0	0.02	1.273	0.120	0.0	0.01

Cali.* : Calibration data

Vali.#: Validation data

ratio of reflectance at 701 nm (red) and at 801 nm (NIR), was found to be most successful predicting greenness, yield and biomass estimation. However, no single ratio was found to be useful for all the given parameters. The reflectance at 701 nm was involved in the NDVI models of all crop physiological parameters.

4.4.2.1.2 *Field spectroradiometer measurements*

Following the MAXR procedures, regression models were also developed using the spectral data acquired from the field spectroradiometer. Best models (highest r^2 value), with a minimum of one to a maximum of five independent parameters for the estimation of the various biophysical parameters, are summarized in the Table 4.18. Higher coefficient of determination ($r^2 > 0.8$) values for the five-waveband model were obtained for most of the biophysical variables, except for the biomass ($r^2 = 0.71$). The results suggest that significant models can be developed for the estimation of the various biophysical variables, using spectral data acquired from a field spectroradiometer. As observed in the case of aerial measurements, no single wavelength region was found to be useful for the estimation of all of the parameters. However, maximally useful wavebands for the development of prediction models were found in the near-infrared regions, followed by the wavebands in the blue region.

The next procedure involved the best five-parameter models for each variable and their validation with the unseen data set. The SSE and ARPE values, indicating the usefulness of the models for both calibration and validation data sets, are presented in Table 4.19. The ARPE values indicated that the model under-estimated LAI by 3.8 % and over-estimated leaf chlorophyll by 12.3%. However, when models were examined, based on much stiffer C_{eff} values, the results were not very encouraging, with the C_{eff} values ranging from 0.202 to -2.158 (Table 4.20).

A comparative evaluation (based on r^2 values) between the different models, developed using the field spectroradiometer and aerial observations, indicated that slightly better estimates for LAI, leaf chlorophyll, and leaf nitrogen could be made from the former.

Table 4.18 Useful wavebands and corresponding regression equation parameters for the estimation of various crop-condition indicators and other parameters, at the early-growth stage for the data acquired from the field spectroradiometer, (first flight; June 30, 2000)

Crop parameter	r ²	Wavelength (nm)	Regression equation coefficient*					
			b ₀	b ₁	b ₂	b ₃	b ₄	b ₅
Leaf area index	0.30	903	-0.171	0.044				
	0.46	906 909	-0.189	0.535	-0.489			
	0.54	911 913 914	0.013	-0.605	1.237	-0.593		
	0.83	873 875 886 917	-0.092	-1.966	1.314	1.010	-0.321	
	0.88	815 873 875 886 917	-0.238	0.423	-2.213	1.155	1.005	-0.322
Plant height	0.50	404	29.042	-2.276				
	0.54	379 404	28.417	0.676	-2.716			
	0.56	379 404 410	28.311	0.685	-4.938	2.122		
	0.76	603 705 903 905	20.198	2.595	-3.061	2.868	-2.287	
	0.80	379 603 705 903 905	18.947	0.713	2.645	-3.272	3.189	-2.570
Greenness	0.54	406	56.721	-4.959				
	0.61	406 421	55.262	-11.455	5.992			
	0.87	622 668 884	32.580	-14.671	13.155	1.016		
	0.93	627 669 867 883	32.474	-19.458	17.413	-6.605	7.794	
	0.96	399 627 669 867 883	36.334	-4.094	-19.325	18.809	-7.721	8.867
Leaf chlorophyll content	0.31	886	0.0049	0.0002				
	0.71	760 815	0.0027	-0.0033	0.0035			
	0.78	382 765 815	0.0057	-0.0012	-0.0096	0.0097		
	0.89	384 765 815 888	0.0067	-0.0016	-0.0118	0.0090	0.0028	
	0.94	384 763 765 815 888	0.0091	-0.0020	0.0060	-0.0175	0.0085	0.0030
Total leaf nitrogen	0.21	385	69.516	-5.938				
	0.63	765 803	9.822	-34.250	34.709			
	0.73	765 803 844	15.157	-27.514	45.212	-17.058		
	0.81	767 803 855 855	14.640	-34.264	52.565	-37.211	19.416	
	0.84	385 767 803 844 855	29.663	-3.126	-36.329	50.026	-34.586	21.149
Total soil moisture	0.19	704	43.939	-0.768				
	0.31	567 704	42.119	4.822	-4.513			
	0.45	526 570 704	45.080	-8.561	11.807	-4.401		
	0.79	388 566 567 698	45.155	-2.841	-80.384	85.835	-4.669	
	0.86	415 537 566 567 702	44.344	-5.150	9.212	-83.273	82.500	-5.159

* Regression equation coefficients of one-, two-, three-, four- and five-variable models
 Note-General form of the equation: crop parameter = $b_0 + b_1S_1 + b_2S_2 + b_3S_3 + b_4S_4 + b_5S_5$, where $S_1, S_2, S_3, S_4,$ and S_5 are the reflectance values at the respective wavelengths listed above.

Table 4.18 (cont'd) Useful wavebands and corresponding regression equation parameters for the estimation of various crop-condition indicators and other parameters, at the early-growth stage for the data acquired from the field spectroradiometer, (first flight; June 30, 2000)

Crop parameter	r ²	Wavelength (nm)	Regression equation coefficient*						
			b ₀	b ₁	b ₂	b ₃	b ₄	b ₅	
Grain yield	0.49	401	12.404	-1.666					
	0.59	401 696	11.308	-3.385	0.745				
	0.70	401 611 696	10.590	-2.599	-2.874	3.054			
	0.78	401 493 624 696	7.736	-4.157	4.447	-5.308	3.468		
	0.91	401 493 504 624 696	8.359	-4.130	12.887	-8.994	-5.214	3.984	
Biomass	0.20	398	1.976	-0.174					
	0.36	390 398	1.885	0.458	-0.581				
	0.53	398 424 434	1.872	-0.566	1.437	-1.044			
	0.62	398 424 449 665	2.409	-0.709	1.457	-1.632	0.411		
	0.71	398 424 454 665 671	2.317	-0.599	1.587	-1.893	2.178	-1.701	

* Regression equation coefficients of one-, two-, three-, four- and five-variable models
 Note-General form of the equation: crop parameter = b₀ + b₁S₁ + b₂S₂ + b₃S₃ + b₄S₄ + b₅S₅, where S₁, S₂, S₃, S₄, and S₅ are the reflectance values at the respective wavelengths listed above.

Table 4.19 Sum of squared error (SSE) and average relative percent error (ARPE) values of the best five-parameter models, developed for the estimation of different crop parameters using spectral values acquired with the field spectroradiometer

Crop parameter	First flight, 30 th June (Early-growth stage)				25 th July (Before tassal stage)				Second flight, 5 th August (Tassel stage)			
	Sum of squared error (SSE)		Average relative percent error (ARPE)		Sum of squared error (SSE)		Average relative percent error (ARPE)		Sum of squared error (SSE)		Average relative percent error (ARPE)	
	Cali.*	Vali.#	Cali.*	Vali.#	Cali.*	Vali.#	Cali.*	Vali.#	Cali.*	Vali.#	Cali.*	Vali.#
Leaf area index, (cm ² /cm ²)	0.024	0.358	0.000	-0.038	0.055	0.588	0.0	0.215	0.147	1.841	0.0	-0.037
Plant height, (cm)	0.839	2.903	0.000	-0.011	16.934	116.944	0.0	-0.038	81.593	603.904	0.0	-0.033
Greenness, (unitless)	0.837	23.479	0.000	0.019	2.206	10.151	0.0	-0.028	2.006	56.818	0.0	0.090
Leaf chlorophyll content, (mg/cm ²)	0.000	0.000	-0.002	0.123	-	-	-	-	0.000	0.000	0.0	-0.103
Total leaf nitrogen, (g/kg)	11.333	81.962	0.000	0.017	-	-	-	-	21.200	216.853	0.0	0.020
Total soil moisture, (%)	1.115	16.249	0.000	0.013	2.607	36.845	0.0	0.120	1.033	14.667	0.0	0.058
Grain yield, (t/ha)	0.212	6.433	0.000	0.121	0.148	1.261	0.0	-0.105	0.298	2.348	0.0	0.029
Biomass, (kg/m ²)	0.020	0.149	0.000	0.080	0.053	0.069	0.0	-0.056	0.015	0.080	0.0	-0.045

Cali.* : Calibration data

Vali.# : Validation data

Table 4.20 Nash-Sutcliffe coefficient values for the best five-parameter regression models developed, using spectral values acquired with the field spectroradiometer

Crop parameter	First flight (Early-growth stage)	25 th July (Before tassel stage)	Second flight (Tassel stage)
Leaf area index	-1.898	0.001	-0.874
Plant height	-0.148	0.658	-0.146
Greenness	-0.770	0.702	-0.947
Leaf chlorophyll content	-0.791	-	-2.860
Total leaf nitrogen	0.202	-	-2.860
Total soil moisture	-0.945	-6.041	-2.758
Grain yield	-2.158	0.418	-0.893
Biomass	-1.661	0.100	-0.631

4.4.2.2 Before tassel stage

4.4.2.2.1 Field spectroradiometer measurements

An additional set of ground-based reflectance measurements was made on July 25th, ten days before the second flight. Corn plants began developing tassels a few days after this measurement. The results of the MAXR analysis of these spectral data are presented in Table 4.21. A much higher percentage of the overall variability of crop physiological parameters just prior to tasseling could be explained by models than was the case at the early-growth stage. This is evidenced by the high r^2 values (>0.90) of the models based on reflectance at five wavebands. Again, however, no particular wavelength region could be pronounced as a best estimator for physiological parameters. The SSE and APRE values for the calibration and validation data sets are presented in Table 4.19. The five-waveband models resulted in a maximum overestimation of 21.5% of the LAI, and a maximum underestimation of grain yield of 10.5%. Overall, the prediction errors could be considered well within the acceptable range. The higher C_{eff} values for most of the parameters, except for soil moisture, also suggest that better prediction models were developed at this stage (Table 4.20)

4.4.2.3 Tassel stage

4.4.2.3.1 Aerial measurements

Table 4.22 summarizes the results of the MAXR multiple regression analysis. The second spectral data acquisition was carried out 66 days after planting, when most of the corn had tassels and the canopy coverage was greater (the highest LAI value was about $6 \text{ cm}^2/\text{cm}^2$). Consequently, the characteristic vegetation reflectance was proportionally greater than at the previous acquisition date. Thus, better relationships were expected between spectral values and crop biophysical parameters. Models with five independent parameters explained over 90% of the variability in plant height, greenness and yield, and over 74% of the variability of the other parameters (Table 4.22). No single waveband was found to be representative of changes in all the parameters, as was the case for the early-growth stage. The near-infrared region was still proved to be the most significant.

Table 4.21 Useful wavebands and corresponding regression equation parameters for the estimation of various crop-condition indicators and other parameters, prior to the tassle stage for the data acquired from the field spectroradiometer, (July 25, 2000)

Crop parameter	r ²	Wavelength (nm)	Regression equation coefficient*						
			b ₀	b ₁	b ₂	b ₃	b ₄	b ₅	
Leaf area index	0.60	906	-1.324	0.083					
	0.83	765 801	-0.364	-1.985	2.003				
	0.86	763 765 801	-0.016	1.859	-4.089	2.238			
	0.89	763 765 801 878	0.531	2.969	-5.739	3.702	-0.941		
	0.91	763 765 801 878 906	0.065	2.631	-5.345	3.561	-1.379	0.535	
Plant height	0.67	698	182.844	-15.460					
	0.87	716 919	107.260	-7.472	2.355				
	0.92	542 710 919	95.673	36.042	-31.814	2.397			
	0.94	396 406 712 919	80.679	-40.114	47.871	-8.796	2.436		
	0.96	396 406 726 763 862	92.809	-39.738	42.127	-7.824	20.606	-16.051	
Greenness	0.46	705	62.481	-2.620					
	0.58	542 555	54.638	54.681	-53.648				
	0.83	514 526 745	30.054	27.399	-23.581	1.043			
	0.92	514 526 687 914	32.108	51.325	-28.475	-13.983	0.537		
	0.93	512 514 526 687 914	31.681	-39.638	89.803	-29.607	-12.479	0.532	
Total soil moisture	0.10	385	25.749	1.892					
	0.28	379 385	27.333	-3.807	4.297				
	0.46	379 409 413	30.371	-2.567	28.659	-25.875			
	0.55	379 396 409 413	31.398	-3.047	6.703	23.818	-27.134		
	0.68	409 413 418 453 522	26.876	47.862	-60.873	33.282	-22.695	4.906	
Grain yield	0.54	698	10.575	-0.947					
	0.77	515 610	5.777	6.906	-5.761				
	0.84	399 514 611	4.533	-2.606	9.490	-6.491			
	0.88	391 399 515 610	4.524	2.182	-3.774	8.772	-6.503		
	0.93	391 396 427 515 603	2.853	3.825	-2.432	-6.906	13.608	-7.613	
Biomass	0.46	702	2.039	-0.115					
	0.57	528 572	1.459	1.042	-0.976				
	0.78	456 517 898	1.168	1.138	-0.915	0.021			
	0.89	454 512 815 898	1.346	1.365	-1.252	-0.336	0.355		
	0.92	454 511 512 815 898	1.253	1.201	1.740	-2.810	-0.301	0.322	

* Regression equation coefficients of one-, two-, three-, four- and five-variable models
 Note-General form of the equation: crop parameter = $b_0 + b_1S_1 + b_2S_2 + b_3S_3 + b_4S_4 + b_5S_5$, where $S_1, S_2, S_3, S_4,$ and S_5 are the reflectance values at the respective wavelengths listed above.

Table 4.22 Useful wavebands and corresponding regression equation parameters for the estimation of various crop-condition indicators and other parameters at the tassel stage, using aerial spectral measurements (second flight; August 5, 2000)

Crop parameter	r ²	Wavelength (nm)	Regression equation coefficient*						
			b ₀	b ₁	b ₂	b ₃	b ₄	b ₅	
Leaf area index	0.61	932	-2.921	0.167					
	0.64	513 932	-0.440	-0.926	0.167				
	0.71	513 648 932	2.613	-7.110	4.453	0.217			
	0.74	446 513 648 932	4.323	-1.276	-8.519	5.987	0.232		
	0.79	446 483 513 648 932	1.955	-3.973	3.816	-9.037	5.960	0.257	
Plant height	0.59	603	343.350	-46.310					
	0.84	732 770	196.505	-11.635	6.659				
	0.91	747 770 854	166.422	-25.915	54.982	-31.508			
	0.93	739 770 839 854	132.782	-15.112	40.871	37.191	-64.294		
	0.94	747 770 831 839 854	127.526	-24.928	63.078	-41.374	57.455	-55.115	
Greenness	0.83	709	80.685	-4.368					
	0.87	416 709	72.051	5.685	-4.436				
	0.90	416 431 709	83.490	10.861	-11.066	-4.200			
	0.91	416 468 528 709	65.714	9.726	-15.859	30.393	-15.682		
	0.93	416 431 468 528 709	72.179	13.992	-11.358	-13.638	32.620	-16.305	
Leaf chlorophyll content	0.24	595	0.0239	-0.0025					
	0.49	490 656	0.0093	0.0144	-0.0105				
	0.62	610 633 663	0.0193	0.0614	-0.1009	0.0362			
	0.69	610 633 663 694	0.0174	0.0593	-0.1262	0.0328	0.0253		
	0.75	610 633 663 679 694	0.0215	0.0499	-0.1175	0.0525	-0.0207	0.0261	
Total leaf nitrogen	0.68	717	120.715	-4.284					
	0.77	505 603	38.408	56.895	-29.170				
	0.80	453 505 603	35.729	-15.792	75.975	-31.697			
	0.81	409 453 603 603	37.924	6.522	-23.871	78.675	-32.376		
	0.83	453 498 505 588 603	6.068	-26.156	38.431	72.458	74.301	-117.81	
Total soil moisture	0.21	431	51.456	-9.556					
	0.31	431 648	48.648	-13.697	4.256				
	0.49	490 648 694	61.499	-25.729	43.661	-24.909			
	0.75	490 603 663 694	49.616	-24.382	36.307	56.808	-62.828		
	0.80	490 603 663 694 808	36.078	-28.189	38.080	69.846	-69.654	0.229	

* Regression equation coefficients of one-, two-, three-, four- and five-variable models
 Note-General form of the equation: crop parameter = b₀ + b₁S₁ + b₂S₂ + b₃S₃ + b₄S₄ + b₅S₅, where S₁, S₂, S₃, S₄, and S₅ are the reflectance values at the respective wavelengths listed above.

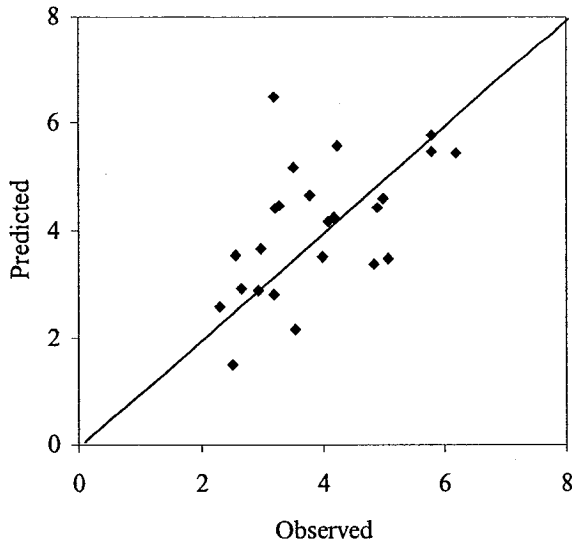
Table 4.22 (cont'd) Useful wavebands and corresponding regression equation parameters for the estimation of various crop-condition indicators and other parameters at the tassel stage, using aerial spectral measurements (**second flight; August 5, 2000**)

Crop parameter	r ²	Wavelength (nm)	Regression equation coefficient*						
			b ₀	b ₁	b ₂	b ₃	b ₄	b ₅	
Grain yield	0.60	565	13.386	-1.506					
	0.73	528 565	2.072	14.224	-11.251				
	0.84	588 709 739	-3.106	8.514	-4.708	0.526			
	0.91	618 709 747 893	-14.344	11.079	-5.116	1.904	-0.933		
	0.93	618 709 770 885 901	-0.815	2.945	-1.698	1.484	-3.757	2.590	
Biomass	0.40	709	2.201	-0.110					
	0.50	543 550	1.583	3.525	-3.414				
	0.60	573 709 747	0.039	1.893	-1.051	0.048			
	0.72	438 573 709 939	0.726	-0.658	2.359	-1.217	0.046		
	0.74	438 498 573 709 939	0.434	-0.870	0.481	1.972	-1.052	0.046	

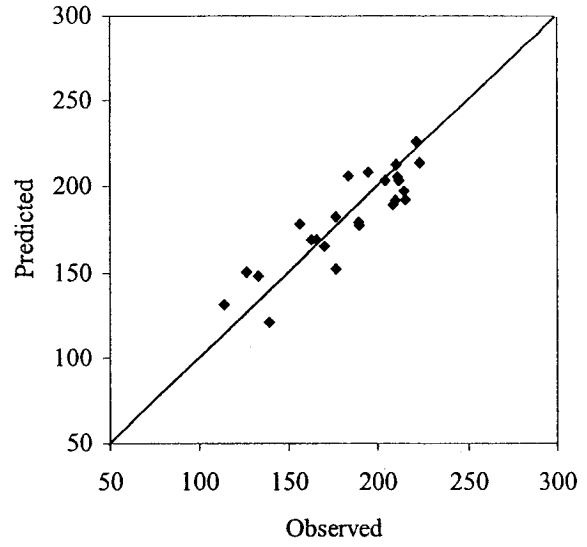
* Regression equation coefficients of one-, two-, three-, four- and five-variable models
 Note-General form of the equation: crop parameter = b₀ + b₁S₁ + b₂S₂ + b₃S₃ + b₄S₄ + b₅S₅, where S₁, S₂, S₃, S₄, and S₅ are the reflectance values at the respective wavelengths listed above.

The model calibration and validation results for the five-waveband models are presented in Table 4.13. The validation ARPE showed a 20% underestimation for biomass, but a prediction within 0.5% for the other parameters (Table 4.13). The magnitude of the calibration ARPE declined from the first to the second spectral data acquisition date for LAI, plant height, leaf nitrogen and grain yield (Table 4.13). As exemplified by higher calibration SSE and ARPE values (Table 4.13), a weaker relationship for soil moisture was observed at the tassel than at the seedling stage, due to greater soil coverage by vegetation. The validation SSE and ARPE and the scatterplots of the observed and predicted values (Figure 4.6) demonstrated an improvement in the predictive abilities of the models, except in the case of biomass. The absolute values of the validation ARPE were no greater than 5.1% except in the case of biomass, for which the ARPE was 20%, whereas those based on data taken during early-growth ranged from -18% to 34%. Although the C_{eff} remained negative (i.e. unacceptable) for all but height, greenness, leaf chlorophyll and leaf N (closely related parameters), the C_{eff} did improve relative to the seedling stage values for all parameters, except soil moisture (Table 4.13). The latter observation is not unexpected because very little soil would remain exposed to direct sunlight at this stage. The observed and predicted values of the various parameters are plotted in Figure 4.6, showing an overall improvement in all models at this stage, with the exception of soil moisture.

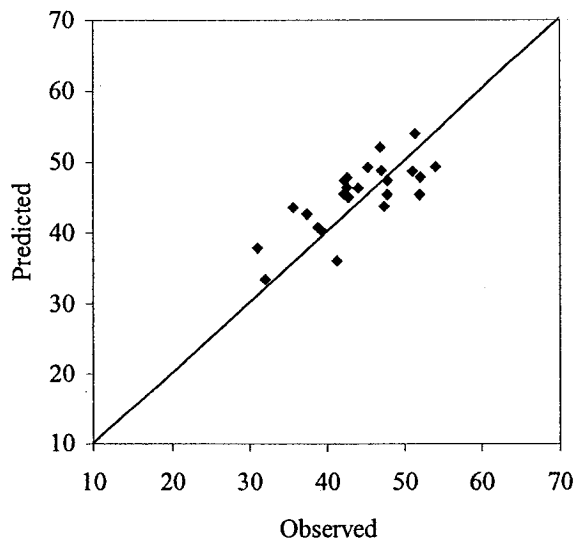
The values for the various crop parameters vs. the best five waveband-derived NDVI are given in Table 4.15. The regression coefficients for the best NDVI models are given in Table 4.16. At this stage, although much higher r^2 values were obtained, they were substantially lower than those of the best five-waveband models. The SSE and ARPE values for the calibration and validation data sets, and the C_{eff} for validation data sets, are presented in Tables 4.17 and 4.14, respectively. The results clearly indicated an improved ability to represent the data and estimate the validation data than was the case for models generated at the early-growth stage. Furthermore, the ARPE values for the validation data set indicate that NDVI-based models were underestimating LAI values by only 2%, and overestimating soil moisture by only 3%. This represented an improvement over the five-waveband models. Except for soil



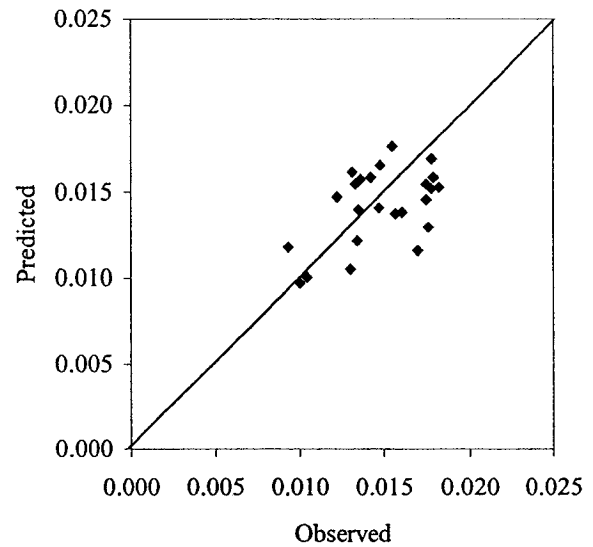
a. Leaf area index (cm^2/cm^2)



b. Plant height (cm)

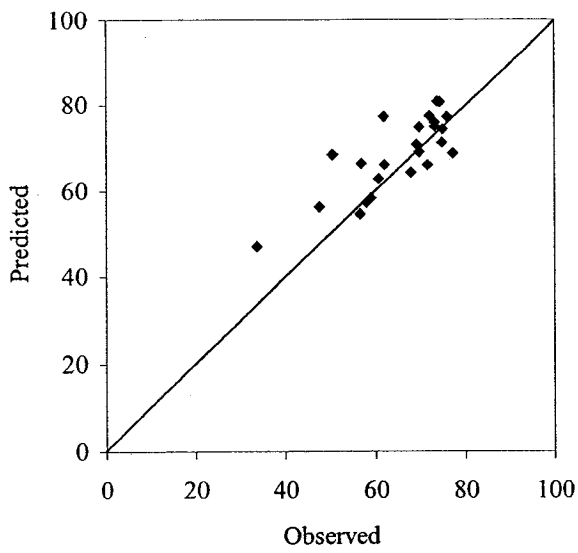


c. Greenness (SPAD reading, unitless)

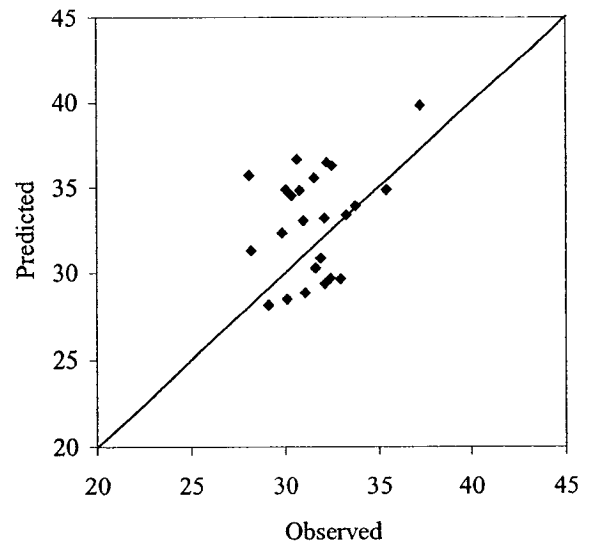


d. Leaf total chlorophyll content (mg/cm^2)

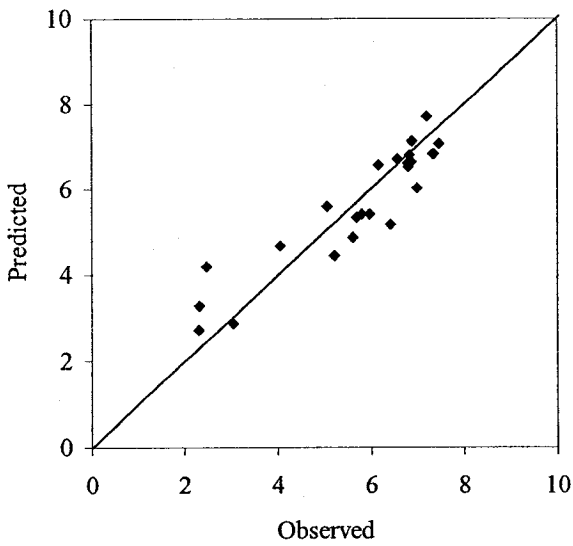
Fig. 4.6 Observed and predicted crop condition parameters and crop yield, based on airborne spectral observations at the tassel stage (August 5, 2000)



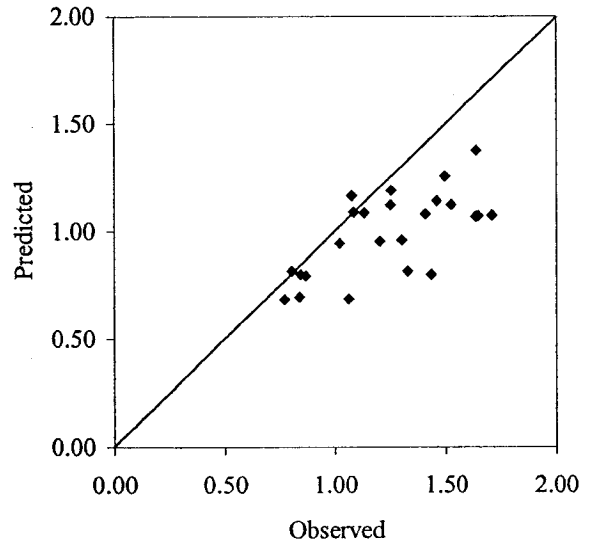
e. Leaf total nitrogen content (g/kg)



f. Total soil moisture content (%)



g. Corn grain yield (t/ha)



h. Dry biomass (kg/m^2)

Fig. 4.6 (cont'd) Observed and predicted crop condition parameters and crop yield, based on airborne spectral observations at the tassel stage (August 5, 2000)

moisture, the C_{eff} values were all positive, thus demonstrating the advantages of NDVI-based models over those based on reflectance alone. Very high C_{eff} values (more than 0.5) for height, greenness, chlorophyll content, and yield clearly justify the use of NDVI-based models. Reflectance at 701 nm was again present in the best models except in the case of LAI. The waveband near 839 nm was also quite prevalent.

4.4.2.3.2 Field spectroradiometer measurements

Details giving r^2 values, useful wavebands, and regression model coefficients for the different predictive models of the various parameters are presented in Table 4.23. The r^2 values were higher for the five-waveband models, with the exception of soil moisture. When these were compared to the models based on aerial measurements, it was observed that slightly better or comparable models could be developed with the field spectral measurements. However, a comparison of the models on two different dates, July 25th and August 5th, revealed that slightly higher or comparable r^2 values were obtained for the earlier data set (with the exception for soil moisture). The ARPE values for the validation data set indicated an underestimation of 10.3% and overestimation of 9.0% in various parameters (Table 4.19). Such findings are reasonable, although the C_{eff} values were unsatisfactory. The C_{eff} values for models based on data from the airborne sensor were higher.

4.4.2.4 Fully-mature stage

4.4.2.4.1 Aerial measurements

The last set of spectral data was acquired 86 days after planting, when the crop was fully matured and grain filling was almost complete. The results of the MAXR analysis (Table 4.24) indicated that, for five-waveband models, the r^2 values ranged from 0.56 for soil moisture to 0.98 for greenness. Once again, no particular waveband was found to be useful for the estimation of all parameters at the fully-mature stage. Models with more independent parameters resulted in better prediction results. Once again, besides the near-infrared region, the blue region was found to be most useful in the development of various models.

Table 4.23 Useful wavebands and corresponding regression equation parameters for the estimation of various crop-condition indicators and other parameters at the tassel stage, for the data acquired from the field spectroradiometer, (second flight; August 5, 2000)

Crop parameter	r ²	Wavelength (nm)	Regression equation coefficient*						
			b ₀	b ₁	b ₂	b ₃	b ₄	b ₅	
Leaf area index	0.44	914	-0.944	0.103					
	0.72	844 858	-0.790	-3.265	3.357				
	0.77	776 844 858	0.158	-1.035	-2.404	3.493			
	0.81	776 803 844 858	0.674	-2.648	3.610	-4.087	3.153		
	0.84	776 803 844 858 909	1.460	-3.477	5.322	-4.896	3.684	-0.635	
Plant height	0.29	822	53.300	2.638					
	0.70	759 765	142.021	-72.362	71.702				
	0.78	486 759 765	100.155	35.408	-80.476	78.872			
	0.88	503 685 759 763	168.362	213.036	-162.017	-80.310	76.689		
	0.91	396 503 685 759 763	185.582	-44.960	295.844	-195.241	-98.006	92.322	
Greenness	0.16	911	24.634	0.372					
	0.54	735 737	36.868	-20.974	20.183				
	0.65	735 737 740	41.384	-105.681	143.401	-39.149			
	0.78	473 492 735 737	36.241	-120.506	124.938	-31.827	29.992		
	0.94	402 471 489 732 734	29.342	-22.452	-111.374	138.268	-31.412	29.018	
Leaf chlorophyll content	0.27	710	0.0223	-0.0008					
	0.54	435 652	0.0177	0.0090	-0.0075				
	0.60	435 437 652	0.0195	0.0321	-0.0237	-0.0075			
	0.83	391 453 460 668	0.0165	0.0079	-0.0562	0.0661	-0.0153		
	0.87	387 391 453 460 668	0.0180	-0.0049	0.0131	-0.0563	0.0646	-0.0147	
Total leaf nitrogen	0.18	713	94.782	-2.694					
	0.52	526 533	67.340	114.079	-97.797				
	0.67	387 526 533	77.658	-22.358	183.607	-153.902			
	0.72	387 525 685 685	80.473	-18.258	191.870	-143.827	-23.216		
	0.83	387 525 534 690 691	96.429	-21.881	194.193	-156.429	-196.295	187.012	
Total soil moisture	0.15	622	25.041	2.226					
	0.34	621 622	27.502	-97.247	99.962				
	0.46	621 622 641	29.976	-118.498	133.032	-13.414			
	0.82	622 647 671 688	23.814	33.060	-38.563	48.232	-35.934		
	0.87	621 622 647 671 688	25.941	-53.094	84.983	-36.455	42.575	-32.105	

* Regression equation coefficients of one-, two-, three-, four- and five-variable models
 Note-General form of the equation: crop parameter = b₀ + b₁S₁ + b₂S₂ + b₃S₃ + b₄S₄ + b₅S₅, where S₁, S₂, S₃, S₄, and S₅ are the reflectance values at the respective wavelengths listed above.

Table 4.23 (cont'd) Useful wavebands and corresponding regression equation parameters for the estimation of various crop-condition indicators and other parameters at the tassel stage, for the data acquired from the field spectroradiometer, (second flight; August 5, 2000)

Crop parameter	r ²	Wavelength (nm)	Regression equation coefficient*					
			b ₀	b ₁	b ₂	b ₃	b ₄	b ₅
Grain yield	0.25	822	-0.673	0.128				
	0.63	751 752	2.924	-8.846	8.775			
	0.74	486 751 752	0.400	2.025	-9.691	9.563		
	0.85	473 486 751 752	1.028	-24.268	26.428	-12.203	11.995	
	0.88	473 475 486 751 752	0.333	-41.084	18.550	24.793	-12.204	12.005
Biomass	0.15	380	0.800	0.293				
	0.31	514 605	0.875	0.798	-0.545			
	0.51	380 592 602	0.870	0.588	2.609	-2.837		
	0.70	380 396 589 605	0.792	0.552	0.194	2.093	-2.419	
	0.76	380 586 589 605 710	1.036	0.407	-4.824	8.517	-3.146	-0.335

* Regression equation coefficients of one-, two-, three-, four- and five-variable models
 Note-General form of the equation: crop parameter = b₀ + b₁S₁ + b₂S₂ + b₃S₃ + b₄S₄ + b₅S₅, where S₁, S₂, S₃, S₄, and S₅ are the reflectance values at the respective wavelengths listed above.

Table 4.24 Useful wavebands and corresponding regression equation parameters for the estimation of various crop-condition indicators and other parameters at the fully- mature stage, using aerial spectral measurements (**third flight; August 25, 2000**).

Crop parameter	r ²	Wavelength (nm)	Regression equation coefficient*					
			b ₀	b ₁	b ₂	b ₃	b ₄	b ₅
Leaf area index	0.44	901	-1.671	0.127				
	0.74	498 901	2.660	-3.157	0.222			
	0.83	498 520 901	3.198	-5.777	1.012	0.282		
	0.87	498 701 808 901	4.496	-4.629	0.311	-0.520	0.748	
	0.91	490 498 701 808 901	3.920	2.318	-6.268	0.314	-0.703	0.906
Plant height	0.57	709	340.213	-16.554				
	0.88	717 901	130.680	-12.178	5.120			
	0.93	550 717 732	50.601	165.192	-105.581	22.562		
	0.94	409 550 717 732	58.359	-16.097	177.259	-111.710	23.81	
	0.97	431 550 573 717 924	50.468	-23.428	377.528	-225.673	-90.27	6.948
Greenness	0.72	709	93.679	-5.116				
	0.95	724 932	53.683	-3.385	1.522			
	0.97	528 618 932	63.382	-29.014	17.906	1.336		
	0.97	453 528 618 932	53.616	7.984	-28.582	15.960	1.193	
	0.98	438 453 528 618 932	52.577	-4.250	11.285	-27.822	15.057	1.263
Total soil moisture	0.15	932	44.6752	-0.3535				
	0.44	424 431	31.9931	12.3377	-12.0062			
	0.52	424 431 468	35.5741	15.8465	-8.0001	-7.9435		
	0.54	424 431 461 468	31.9115	16.8859	-9.1278	3.8478	-10.32	
	0.56	424 431 461 468 490	36.9586	15.9386	-9.1430	5.5742	-8.288	-4.90
Grain yield	0.59	709	14.410	-0.927				
	0.91	724 762	2.060	-0.648	0.383			
	0.93	453 520 916	-0.652	3.683	-4.368	0.325		
	0.94	453 520 916 916	-1.256	3.779	-4.391	-0.442	0.770	
	0.95	453 520 831 847 916	-0.715	3.360	-4.544	1.901	-1.934	0.422
Biomass	0.39	717	2.378	-0.085				
	0.48	550 717	1.886	1.389	-0.660			
	0.63	416 490 656	0.837	-0.657	1.924	-1.002		
	0.72	409 416 490 656	0.606	0.465	-1.118	2.067	-1.026	
	0.78	409 416 490 626 656	0.369	0.588	-1.173	2.910	1.561	-3.41

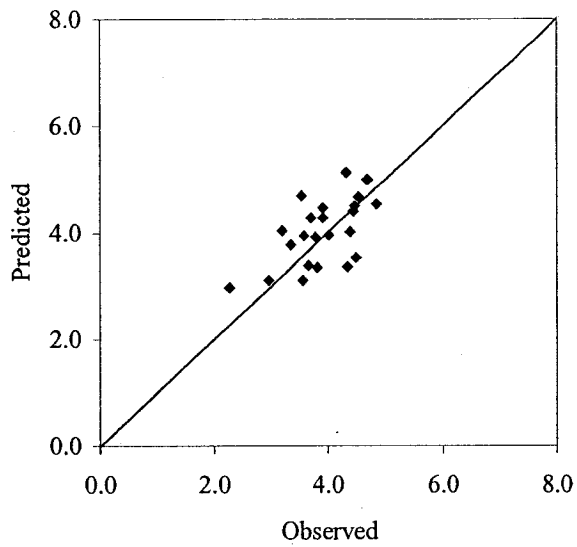
* Regression equation coefficients of one-, two-, three-, four- and five-variable models
 Note-General form of the equation: crop parameter = b₀ + b₁S₁ + b₂S₂ + b₃S₃ + b₄S₄ + b₅S₅, where S₁, S₂, S₃, S₄, and S₅ are the reflectance values at the respective wavelength listed above.

Plots of observed vs. predicted values, from the best five-waveband models for the different parameters, showed a generally good agreement between the observed and predicted values, with the exception of the soil moisture and total biomass predictions (Figure 4.7). The corresponding SSE, ARPE and C_{eff} values are presented in Tables 4.13 and 4.14. All predictions show an absolute value of ARPE of no more than 5.2%. The C_{eff} values for LAI, plant height and grain yield, ranging from 0.189 to 0.382, represent good precision, while the C_{eff} value of 0.680 for greenness represents an excellent predictive ability. The C_{eff} values for moisture and biomass were below -0.7 (unsatisfactory).

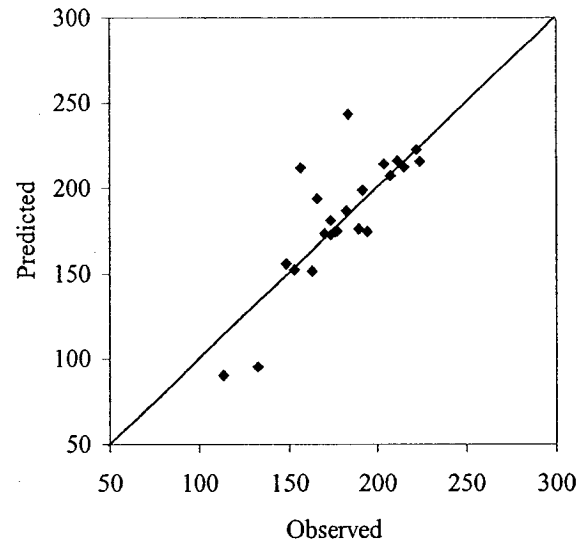
Models based on the NDVI values are summarized in Tables 4.15 and 4.16. Very high r^2 values were obtained for greenness, yield, and height: 0.93, 0.90, and 0.87, respectively; however, these were lower than the values for the corresponding five-waveband models. The ARPE values (-0.06 to 0.05) for the validation data sets indicate that all models performed very well. These values were also higher than those obtained at the previous stages of crop development. At this stage also, the r^2 values could not justify the use of NDVI, over the use of reflectance values in different wavebands, for the estimation of plant parameters. However, when the C_{eff} values were compared (as the most rigorous criterion of model performance), it became evident that the NDVI-based models were more reliable except in the case of LAI.

Although the 701-nm waveband was found to be the most prominent in the best NDVI ratios at the previous growth stages, it only appeared in a few of the best NDVI expressions for the fully-mature stage. The 839-nm waveband was once again represented, but there was not a predominant waveband to explain the crop physiological parameters at this stage. A review of the five-waveband relationships indicated that no particular waveband was particularly useful for estimating a given parameter at different developmental stages, or for estimating different parameters at a single stage. This means that different wavelength regions should be used for the development of such models. Moreover, better results may be expected from models involving more wavebands.

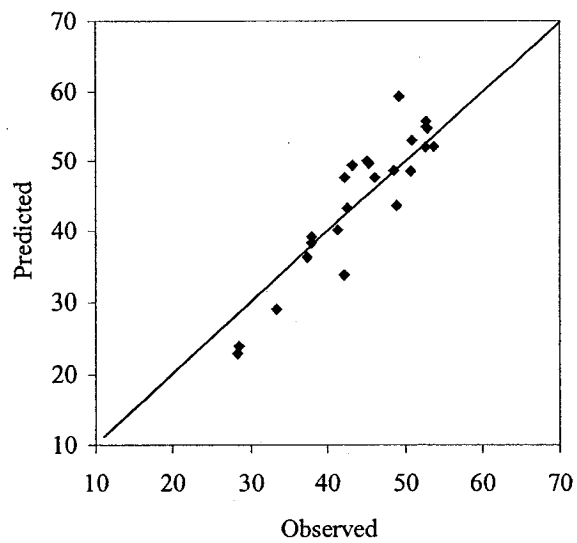
In general, the models obtained in this study performed at an equivalent level



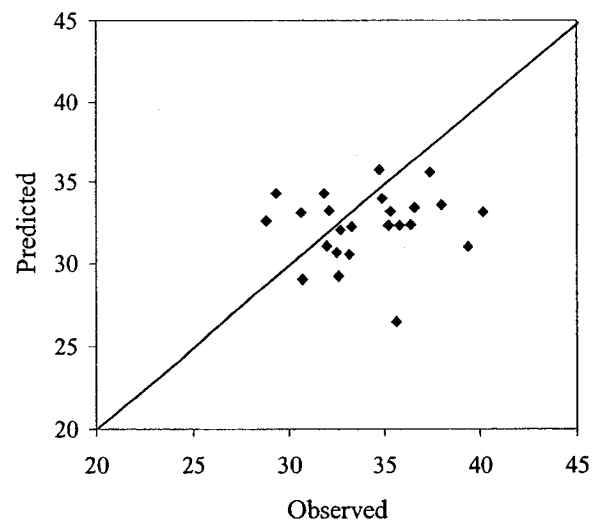
a. Leaf area index (cm²/cm²)



b. Plant height (cm)

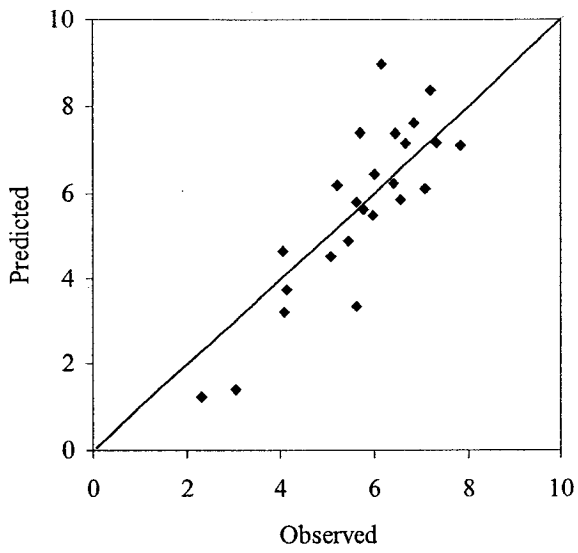


c. Greenness (SPAD reading, unitless)

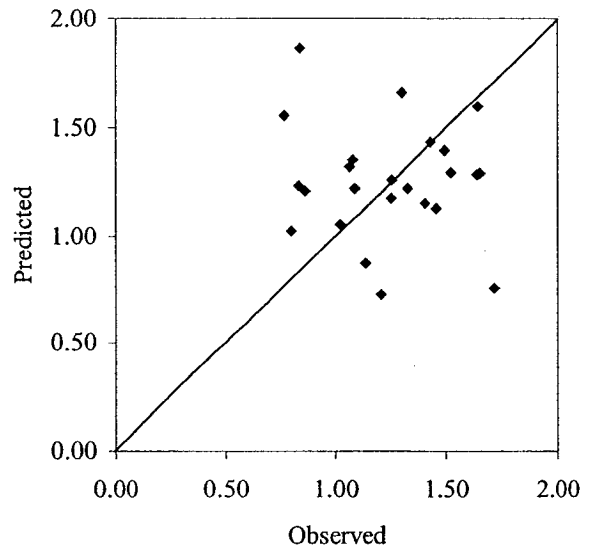


d. Total soil moisture content (%)

Fig. 4.7 Observed and predicted crop condition parameters and crop yield, based on airborne spectral observations at the fully-mature stage (August 25, 2000)



e. Corn grain yield (t/ha)



f. Dry biomass (kg/m²)

Fig. 4.7 (cont'd) Observed and predicted crop condition parameters and crop yield, based on airborne spectral observations at the fully-mature stage (August 25, 2000)

or better than models of these parameters reported in earlier literature. For example, in a most recent study, Thenkabail et al. (2000) based their experiment on a spectral data set acquired from a hand-held spectroradiometer, and obtained r^2 values for four-waveband models of 0.78 and 0.66 for LAI and plant height, respectively, while this study shows the corresponding values of 0.87 and 0.94 for similar models, for the calibration data set. For the NDVI-based models, the obtained values were 0.86 and 0.31 for LAI and height, respectively. In this study, the highest r^2 values were 0.87 and 0.59 for plant height and LAI, respectively. In addition, the values obtained by this study for the NDVI-based models are for a validation data set and based on data from an airborne sensor. Shanahan et al (2001) reported r^2 values of about 0.9 between corn yield and broadband NDVI. They acquired images from an airborne platform in four wavebands over an experiment involving different nitrogen levels. Similarly, in an experiment involving different corn hybrids grown under various nitrogen levels, Blackmer et al. (1996a), using a portable spectroradiometer, presented yield prediction models with r^2 ranging from 0.70 to 0.99 for different growth stages. In the present study, the highest r^2 value obtained on a calibration data set was 0.95 (third flight). It is difficult to make a true comparison of the results with earlier studies because none of them estimated crop parameters on the basis of data acquired from an airborne platform. Moreover, there is no evidence that a researcher has reported the combined effect of weed infestation and nitrogen level on crop reflectance.

4.5 Conclusions

This study has demonstrated the potential of using hyper-spectral airborne remote sensing in the visible and near-infrared regions, in the detection of weed infestations and nitrogen stresses in the corn fields. Statistical analysis of data indicated that the spectral response of corn canopy changed significantly in the presence of weeds and/or varying nitrogen fertilization levels. In addition, spectral response changed significantly over time. In general, the green and near-infrared regions were found to be good indicators of the two stresses in corn. However, the wavebands, permitting discrimination between levels of nitrogen stress, were not the

same as those permitting discrimination between weed control strategies. The best indicators of these stresses and the best representatives of crop physiological parameters were also dependent on the stage of development of the canopy. It was easier to differentiate between treatments on the basis of data acquired from the airborne sensor than the ground-based spectroradiometer, because the lower spatial resolution from high altitude was more than compensated for by a complete image of the study area.

The study also demonstrated that hyper-spectral imagery from airborne or ground-based sensors may be used to estimate several biophysical parameters of corn as well as certain canopy-related parameters. Highly significant regression models were developed based on the stepwise regression technique using the MAXR criterion. More than 70% of the variability in the crop parameters could be explained by models based on reflectance in five wavebands. The ARPE and C_{eff} values for the reflectance-based models indicated that most of the parameters and crop yield could be estimated within 5% from airborne platforms. The performance of models to estimate various crop parameters depended upon the growth stage of the crop. However, there was little consistency in the usefulness of wavelength regions for the estimation of these parameters. Furthermore, different wavebands were found useful in the best models, developed for the estimation of a particular parameter at different growth stages of the crop. There was a generally good agreement between the observed and predicted values of various parameters. Moreover, when the NDVI-based models for aerial measurements were compared with the multiple reflectance waveband-based models, the former were found to be more reliable. Among the three spectral data sets obtained from an airborne platform at different growth stages of corn, best results were generally obtained with data from the second flight (tassel stage).

The proposed approach can be extended to other years by pre-establishing ground control points or calibration plots with known crop growth conditions. Effective wavebands for precision crop management could then be identified, and used for processing full images acquired over larger fields to locate problem areas.

The results of this study were far more encouraging than those of the study

presented in Chapter 3, and tend to confirm suggestions by various authors that higher spectral resolution should be used for weed detection and crop monitoring, as was the case here.

PREFACE TO CHAPTER 5

Although the results of Chapter 4 were encouraging compared to those of Chapter 3, the regression and ANOVA approaches were cumbersome to interpret, and it was difficult to extract much more than tendencies in the data. This led to the exploration of alternative methods of classification of the various growth conditions included in the field experiments.

Although the McGill research group has been involved in developing ANN models for various possible applications to precision farming, including weed recognition systems, a more tangible approach was desired. Such an approach might lead to a clearer identification of direct relationships between reflectance values and growth conditions. Based on the understanding that decision trees partition large data sets according to well-defined statistical rules, this appeared to be a better option than ANNs, insofar as closing in on the specifics of the sought-after relationships. Nevertheless, taking into account the ability of ANNs to recognize patterns implicitly, even in a non-linear system, it seemed appropriate to treat the data with this technique and to compare the classification accuracies of the two methods.

Research papers based on the chapter:

1. Goel, P. K., S. O. Prasher, R. M. Patel, J.-A. Landry, R. B. Bonnell, and A. A. Viau. Classification of hyperspectral data by decision trees and artificial neural networks to identify weed stress and nitrogen status of corn. *Computers and Electronics in Agriculture* 39(2): 67-93.

(Copy of the published paper is given in the attached CD-ROM.)

CHAPTER 5

APPLICATION OF DECISION TREES AND ARTIFICIAL NEURAL NETWORKS TO CLASSIFICATION OF HYPER-SPECTRAL DATA

5.1 Abstract

This study examines the ability of the C&RT decision tree algorithm and of the back-propagation ANN to classify images of experimental corn plots into categories of nitrogen application rate and type of weed present. The images were acquired from an airborne 72-waveband hyper-spectral imaging system (CASI, compact airborne spectrographic imager), having a spatial resolution of 2m x 2m, at three developmental stages - early growth, tassel, and fully mature.

Neither the decision trees nor the ANNs were able to classify the nine treatment combinations adequately at any stage of development, although the best validation results were obtained at the tassel stage. When trees or ANNs were generated to classify the plots according to only one of the factors (weeds or nitrogen), the misclassification rate was reasonable based, on the spectra obtained at the tassel stage (17% misclassified for nitrogen application rates, 21.5% misclassified for weed control strategies). In general, results were slightly better when the ANNs were used to classify the data.

5.2 Introduction

The spatial and spectral resolutions of satellite-borne imaging systems have improved significantly over the last twenty years. This has generated substantial interest in the application of the available information to the management of agro-ecosystems. Given the huge quantity of available data and the complexity involved in optimizing agricultural systems, under an increasing number of environmental constraints, the development of more efficient methods of image analysis has become a priority. Approaches to image analysis should be more automatic, with limited human interaction for such critical evaluations (Soh and Tsatsoulis, 1999).

Classification algorithms should be capable of tackling noise in the data sets, of identifying the best features to discriminate between different classes, and of minimizing confusion among spectral classes (Friedl et al., 1999). Another important issue, related to automated or semi-automated classification algorithms, is that they should be capable of handling different situations in the same domain (Soh and Tsatsoulis, 1999).

A basic requirement for the classification of images into different categories is that differences in one or more features of the images should be detectable within a suitable degree of statistical confidence, and that these differences should be consistent with the criteria used to define the categories. Various statistical methods have been used to identify wavebands, groups of wavebands, or functions of more than one waveband that lead to a proper classification of images. Among these are analysis of variance with tests for separation of means and principal components analysis. Interpretation of the results of these statistical methods can nevertheless be cumbersome when there is a large number of possible predictor variables, as is the case for hyper-spectral images. As a consequence of the aforementioned, there is a trend towards delegating the task to data mining techniques such as artificial neural networks (ANNs) and decision trees (DTs).

The applicability of decision trees to the classification of images has been demonstrated by various authors (Friedl et al., 1999; Soh and Tsatsoulis, 1999; Friedl and Brodley, 1997; Hansen et al., 1996). ANN models have been used, with varying degrees of success, in handling classification problems in agricultural applications (Yang et al., 2000; Wang et al., 1998a; Nakano, 1997; Ghazanfari et al., 1996; Deck et al., 1995) and in remote sensing (Augusteijn and Warrender, 1998; Danaher et al., 1997; Augusteijn et al., 1995; Kanellopoulos et al., 1992; Hepner et al., 1990).

The research described in this chapter concerns the interpretation of hyper-spectral images, taken from an airborne platform, over a set of experimental plots cropped with corn and subjected to various combinations of weed control and nitrogen application rate. Earlier research has indicated that it is possible to determine the nitrogen status of various crops (Lukina et al., 2000; Plant et al., 2000; Blackmer and White, 1998; Gopala Pillai et al., 1998; Sui et al., 1998; Taylor et al., 1998;

Martin and Aber, 1997; Bausch and Duke, 1996; Blackmer et al., 1996a; Ma et al., 1996; Buschmann and Nagel, 1993), and to distinguish between weed species (Medlin et al., 2000; Zwiggelaar, 1998; Lass and Callihan, 1997; Lass et al., 1996; Brown and Steckler, 1995; Hanson et al., 1995; Menges et al., 1985; Everitt et al., (1987, 1995, 1996)) on the basis of certain spectral wavebands in the visible and near-infrared (NIR) regions.

Therefore, it seemed plausible that the treatment combinations set up in the experimental field might be classified correctly by the decision tree and artificial neural network approaches. The aforementioned was based on hyper-spectral images, involving 72 fairly narrow wavebands in the spectral regions, previously identified as being representative of nitrogen status and weed population characteristics. Thus, the objective of this study was to assess and compare the classification accuracies of decision tree and ANN models generated for this purpose.

5.2.1 A brief overview of decision tree and artificial neural networks

To avoid repetition, the reader is referred to sections 2.6.1 and 2.6.2 for details concerning the characteristics of decision trees and artificial neural networks, and also the applications of these data mining methods to the analysis of spectral data.

5.3 Materials and Methods

5.3.1 Experimental details

Already given in section 4.3.1.

5.3.2 Acquisition of spectral data

Aerial spectral measurements were used, details of which are given in section 4.3.2.

5.3.3 Data analysis

The goal of the study was to classify the data into categories representing the treatments applied to the experimental plots, based on the spectral values recorded in different wavebands. This involved different approaches in the use of decision trees

and one approach in the case of ANNs. The decision to use ANNs was made in response to the results of the decision tree approach.

5.3.3.1 Decision trees

Decision trees were generated using Answer Tree 2.1.1, a decision tree classification package developed by SPSS (SPSS Inc., Chicago, IL). The specific algorithm used was the C&RT (Classification and Regression Tree) algorithm developed by Breiman et al. (1984). Different tree-growing mechanisms and validation procedures were used to evaluate the performance of the trees. To determine the classifier accuracy, a 10-fold crossvalidation was used. In a 10-fold crossvalidation, the data set is randomly partitioned into 10 parts. Iteratively, 10 different models are then built, with each iteration involving a different combination of nine parts for the model development and one part for the testing. Risk estimate, for crossvalidation and resubstitution, represents the percentage of the cases incorrectly classified in testing and training data sets, respectively.

As mentioned in Chapter 4, the sub-plots in which only grass weeds were controlled could not be used in the analysis because the broadleaved weed population was negligible in these plots. This may have been due to the absence of weed patches in those locations in the previous year, however, this was not confirmable. Chapter 4 also mentioned the need to exclude data from the 72nd waveband, due to excessive noise in the signal. Thus, data from a total of 36 sub-plots, consisting of four replicates of all combinations of three weed treatments (W1, W3, and W4) and three nitrogen levels (N₆₀, N₁₂₀, and N₂₅₀), were used in the analysis.

First of all, the spectral data from the three different flights were analyzed separately. Recalling that the sub-plots were 20m x 20m, and that the spatial resolution of the hyper-spectral data was 2m x 2m, 20 to 25 pixels could be attributed to each sub-plot after removing pixels involving border effects. Three subsets were then generated from each of the cropped images. One subset consisted of the average values of the wavebands computed over the whole sub-plot. The second consisted of the reflectance values at four randomly chosen pixels in each sub-plot, and these were not averaged. The third consisted of data at 20 points from each sub-plot.

Decision trees were then generated to classify the data into categories representing: (a) the nine combinations of weed control and nitrogen fertilization rate, or (b) the weed control strategies alone, or (c) the nitrogen fertilization rates alone. The 20-point subsets were also pooled, and decision trees were generated to classify the data into categories of type (a), (b) or (c); another was generated to classify the data into stages of crop development. Single-variable best regressors were used to determine the splits at each node. The Gini impurity measure was used to optimize the splits in all cases. Misclassification tables with risk assessments were also generated for all trees.

5.3.3.2 Artificial neural networks

Neural Network Professional II/PLUS (version 5.0), developed by Neural Ware Inc. (Pittsburgh, PA), was used to build ANN models with different architectures. ANNs were developed corresponding to the different decision trees generated using the 20-point subsets, except in the case of the pooled data. The architecture of all the ANN models was a fully connected, multi-layer, feed-forward, consisting of one input layer, one output layer, and one or two hidden layers. The back-propagation learning algorithm, the most widely used approach to tackle non-linear problems (Lacroix et al., 1997), was used for all the ANN models attempted in the study. This algorithm iteratively minimizes an error term by comparing the output and input values during the training period (Schalkoff, 1992). The normalized-cumulative delta learning rule and the sigmoid transfer function were also used. The root mean square (RMS) value was considered as the learning criteria. Models were trained in steps for different numbers of training cycles. The reflectance values in all of the 71 wavebands were used as input to the models, and the number of outputs was dependent on the number of categories in which the data were to be classified.

5.4 Results and Discussion

5.4.1 Decision tree approach

The data were analyzed according to three subsets, as described in section 5.3.3.1, each one of which provided a different number of data records to process,

according to different sets of categories. As a result, it was necessary to find out, in each case, which structure was suitable in terms of the number of tree levels and the maximum and minimum number of cases permitted in parent and child nodes, respectively. Risk summaries were generated for each case in the form of misclassification tables. The misclassification rate is calculated according to the number of case incorrectly classified and total number of cases.

5.4.1.1 Results based on reflectance at each waveband (sub-plot average)

The risk summaries (classification accuracy) for the decision trees, generated on the basis of reflectance at each wavelength averaged over all retained pixels in a sub-plot, are presented in Table 5.1 for the three flights. The wavebands retained as splitting criteria in the final models are listed at the bottom. The risk of classification was calculated according to the number of cases incorrectly classified. Although the best results were obtained for the spectral data acquired at the tassel stage (second flight, August 5th), the results were clearly unsatisfactory. When the whole data set was used, 16.7% of the cases were misclassified (risk estimate for resubstitution=0.167) and the crossvalidation risk estimate was 80.6%.

The next set of decision trees was generated on the same averages, but with fewer categories (i.e. considering only the weed control strategies or only the nitrogen application rates). The risk summaries for these six decision trees are presented in Table 5.2. Although there appears to be a significant improvement in the overall performance of these decision trees, compared to the previous set, the crossvalidation risks were still quite high at 0.750, 0.556, and 0.417 for nitrogen and 0.583, 0.278, and 0.389 for weeds, for the first, second, and third flight, respectively.

At this point, the problem was perceived to be reflecting variability among replicates in each category, whether the treatments were considered together or one at a time. High variability may be representative of high natural variability of the objects being studied, or may be due to unrepresentative data. However, it seemed equally likely that there were simply not enough data points to suit the purpose.

Decision trees were then grown for the subset involving four randomly

Table 5.1 Misclassification matrix (decision tree approach) for the detection of various combinations of weed and nitrogen effects, using the average spectral value of each plot for different flights (crossvalidation method)

a. First flight (June 30th)

		Actual									
		N ₆₀ W1	N ₆₀ W3	N ₆₀ W4	N ₁₂₀ W1	N ₁₂₀ W3	N ₁₂₀ W4	N ₂₅₀ W1	N ₂₅₀ W3	N ₂₅₀ W4	Total
Predicted	N ₆₀ W1	2	1	0	0	0	0	0	1	0	4
	N ₆₀ W3	0	3	0	0	0	1	0	0	0	4
	N ₆₀ W4	0	0	3	1	1	0	1	0	0	6
	N ₁₂₀ W1	0	0	0	3	0	0	0	0	0	3
	N ₁₂₀ W3	0	0	0	0	2	0	0	0	0	2
	N ₁₂₀ W4	0	0	0	0	0	3	0	0	0	3
	N ₂₅₀ W1	0	0	0	0	0	0	2	0	0	2
	N ₂₅₀ W3	0	0	1	0	0	0	0	3	0	4
	N ₂₅₀ W4	2	0	0	0	1	0	1	0	4	8
	Total	4	4	4	4	4	4	4	4	4	36
Risk estimate	Resubstitution					Crossvalidation					
	0.3056					0.8889					
Bands in the final model	409, 446, 588, 641, 717, 878, 932, 939										

b. Second flight (August 5th)

		Actual									
		N ₆₀ W1	N ₆₀ W3	N ₆₀ W4	N ₁₂₀ W1	N ₁₂₀ W3	N ₁₂₀ W4	N ₂₅₀ W1	N ₂₅₀ W3	N ₂₅₀ W4	Total
Predicted	N ₆₀ W1	4	0	1	0	1	0	0	0	0	6
	N ₆₀ W3	0	3	1	0	0	1	0	0	0	5
	N ₆₀ W4	0	0	2	0	0	0	0	0	0	2
	N ₁₂₀ W1	0	0	0	4	0	0	0	0	0	4
	N ₁₂₀ W3	0	0	0	0	3	0	0	0	1	4
	N ₁₂₀ W4	0	0	0	0	0	3	0	0	0	3
	N ₂₅₀ W1	0	1	0	0	0	0	4	0	0	5
	N ₂₅₀ W3	0	0	0	0	0	0	0	4	0	4
	N ₂₅₀ W4	0	0	0	0	0	0	0	0	3	3
	Total	4	4	4	4	4	4	4	4	4	36
Risk estimate	Resubstitution					Crossvalidation					
	0.1667					0.8056					
Bands in the final model	483, 490, 513, 535, 550, 558, 724, 755, 770										

Treatments: W1- no weed control; W3-broadleaf weed control; W4-full weed control; N₆₀-60 kg N/ha; N₁₂₀-120 kg N/ha; N₂₅₀-250 kg N/ha

Table 5.1 (cont'd) Misclassification matrix (decision tree approach) for the detection of various combinations of weed and nitrogen effects, using the average spectral value of each plot for different flights (crossvalidation method)

c. Third flight (August 25th)

		Actual									Total
		N ₆₀ W1	N ₆₀ W3	N ₆₀ W4	N ₁₂₀ W1	N ₁₂₀ W3	N ₁₂₀ W4	N ₂₅₀ W1	N ₂₅₀ W3	N ₂₅₀ W4	
Predicted	N ₆₀ W1	4	1	0	0	0	0	1	1	1	8
	N ₆₀ W3	0	3	0	0	0	0	0	0	0	3
	N ₆₀ W4	0	0	4	0	0	0	0	0	1	5
	N ₁₂₀ W1	0	0	0	4	0	0	0	0	0	4
	N ₁₂₀ W3	0	0	0	0	4	0	0	0	1	5
	N ₁₂₀ W4	0	0	0	0	0	4	0	0	1	5
	N ₂₅₀ W1	0	0	0	0	0	0	3	0	0	3
	N ₂₅₀ W3	0	0	0	0	0	0	0	3	0	3
	N ₂₅₀ W4	0	0	0	0	0	0	0	0	0	0
	Total	4	4	4	4	4	4	4	4	4	36
Risk estimate	Resubstitution						Crossvalidation				
	0.1944						0.8055				
Bands in the final model	409, 416, 431, 461, 543, 565, 701, 739										

Treatments: W1- no weed control; W3-broadleaf weed control; W4-full weed control; N₆₀-60 kg N/ha; N₁₂₀-120 kg N/ha; N₂₅₀-250 kg N/ha

Table 5.2 Misclassification matrix (decision tree approach) for the detection of separate weed and nitrogen effects, using average spectral values of each plot for different flights (crossvalidation method)

a. First flight (June 30th)

		Actual						Actual			
		N ₆₀	N ₁₂₀	N ₂₅₀	Total			W1	W3	W4	Total
Predicted	N ₆₀	11	2	1	14	W1	12	0	3	15	
	N ₁₂₀	0	8	1	9		W3	0	12	0	12
	N ₂₅₀	1	2	10	13			W4	0	0	9
	Total	12	12	12	36		Total		12	12	12
		Risk estimate						Risk estimate			
Resubstitution		0.1944						0.0833			
Crossvalidation		0.7500						0.5833			
Bands in the final model		409, 476, 550, 641, 724, 732, 939						409, 513, 701, 724, 732, 939			

b. Second flight (August 5th)

		Actual						Actual			
		N ₆₀	N ₁₂₀	N ₂₅₀	Total			W1	W3	W4	Total
Predicted	N ₆₀	10	0	1	11	W1	12	1	1	14	
	N ₁₂₀	0	10	0	10		W3	0	11	0	11
	N ₂₅₀	2	2	11	15			W4	0	0	11
	Total	12	12	12	36		Total		12	12	12
		Risk estimate						Risk estimate			
Resubstitution		0.1389						0.0556			
Crossvalidation		0.5556						0.2778			
Bands in the final model		490, 535, 747, 770						424, 446, 732, 739			

c. Third flight (August 25th)

		Actual						Actual			
		N ₆₀	N ₁₂₀	N ₂₅₀	Total			W1	W3	W4	Total
Predicted	N ₆₀	11	0	1	12	W1	12	1	2	15	
	N ₁₂₀	0	12	1	13		W3	0	11	0	11
	N ₂₅₀	1	0	10	11			W4	0	0	10
	Total	12	12	12	36		Total		12	12	12
		Risk estimate						Risk estimate			
Resubstitution		0.0833						0.0833			
Crossvalidation		0.4167						0.3889			
Bands in the final model		409, 424, 558, 701						416, 453, 490, 762			

Treatments: W1- no weed control; W3-broadleaf weed control; W4-full weed control; N₆₀-60 kg N/ha; N₁₂₀-120 kg N/ha; N₂₅₀-250 kg N/ha

selected pixels per sub-plot. This gave a total of 144 sets of reflectance values to represent 36 plots. When the decision trees were grown, considering the nine treatment combinations, the crossvalidation risk estimates improved to about 50% (data not shown), leading to the testing of decision trees based on 20 points per plot at a time.

5.4.1.2 Results based on twenty randomly selected points in each sub-plot

With 20 random points in each plot, 720 sets of reflectance values were available, 80 for each of the nine categories. In this case, several trials led to the conclusion that trees could be grown for a maximum of 20 levels, and that it was sufficient to have a minimum of five cases in the parent node and one case in child node. Because the total number of data points was considered to be sufficient, the data were divided into a training set and a validation set. Sixty-four sets of reflectance values from each sub-plot were randomly associated with training, with the remaining 16 attributed to validation.

Misclassification matrices for the unseen validation data sets are presented in Table 5.3, for each of the three growth stages of the crop. Once again, the best results were obtained from the data acquired at the tassel stage (August 5th). While only 34% of the cases from the second flight data set were misclassified, about 47% from the first and 52% from the third flight were wrongly classified.

A substantial improvement in the results was observed in all categories when treatments were considered one at a time (Table 5.4). Again, the minimum classification risks were obtained at the tassel stage (0.17 for nitrogen application rate and 0.21 for weed control strategy). It is interesting to note that misclassification was mainly the result of the classification of either low or high nitrogen cases into the normal category, rather than due to the classification of low nitrogen into a higher nitrogen category. With respect to the wavebands involved in the dichotomization, despite the fact that many more were involved than in the earlier cases, there did not appear to be much consistency from one model to the next.

A 10-fold crossvalidation approach was then used on this subset. The results for all three flights are summarized in Table 5.5. Out of the three flights, the best

Table 5.3 Misclassification matrix (decision tree approach) for the detection of various combinations of weed and nitrogen effects, using spectral values at 20 points in each plot for different flights (for the unseen data set)

a. First flight (June 30th)

		Actual									Total
		N ₆₀ W1	N ₆₀ W3	N ₆₀ W4	N ₁₂₀ W1	N ₁₂₀ W3	N ₁₂₀ W4	N ₂₅₀ W1	N ₂₅₀ W3	N ₂₅₀ W4	
Predicted	N ₆₀ W1	5	0	1	2	2	1	0	4	3	18
	N ₆₀ W3	2	7	2	0	2	1	0	0	0	14
	N ₆₀ W4	1	1	9	0	0	0	0	0	0	11
	N ₁₂₀ W1	0	5	0	13	0	0	1	0	0	19
	N ₁₂₀ W3	1	2	1	1	4	0	2	1	2	14
	N ₁₂₀ W4	0	0	5	0	0	7	0	2	0	14
	N ₂₅₀ W1	0	0	0	0	1	0	7	0	1	9
	N ₂₅₀ W3	3	0	0	0	2	3	1	7	0	16
	N ₂₅₀ W4	0	0	1	0	2	1	3	0	13	20
	Total	12	15	19	16	13	13	14	14	19	135
Risk Estimate										0.467	
Bands in the final model	409, 416, 424, 431, 446, 453, 468, 483, 490, 498, 505, 513, 528, 543, 550, 558, 565, 595, 633, 648, 679, 694, 701, 709, 717, 724, 732, 739, 747, 755, 762, 770, 778, 801, 816, 824, 839, 847, 862, 870, 893, 901, 916, 932, 939										

b. Second flight (August 5th)

		Actual									Total
		N ₆₀ W1	N ₆₀ W3	N ₆₀ W4	N ₁₂₀ W1	N ₁₂₀ W3	N ₁₂₀ W4	N ₂₅₀ W1	N ₂₅₀ W3	N ₂₅₀ W4	
Predicted	N ₆₀ W1	8	3	0	1	0	0	0	0	0	12
	N ₆₀ W3	2	7	1	0	0	0	0	1	0	11
	N ₆₀ W4	0	1	14	0	0	0	0	2	0	17
	N ₁₂₀ W1	1	0	0	10	0	4	1	0	0	16
	N ₁₂₀ W3	0	3	0	0	10	0	2	1	0	16
	N ₁₂₀ W4	0	0	0	6	0	7	1	0	1	15
	N ₂₅₀ W1	0	0	0	0	0	1	13	1	4	19
	N ₂₅₀ W3	0	0	2	0	3	0	0	10	4	19
	N ₂₅₀ W4	0	0	0	0	0	0	0	0	10	10
	Total	11	14	17	17	13	12	17	15	19	135
Risk Estimate										0.341	
Bands in the final model	409, 416, 424, 431, 446, 461, 468, 476, 483, 490, 505, 513, 543, 573, 588, 610, 618, 656, 671, 679, 686, 701, 709, 717, 724, 770, 801, 816, 831, 839, 847, 854, 870, 885, 893, 901, 916, 924, 932										

Treatments: W1- no weed control; W3-broadleaf weed control; W4-full weed control; N₆₀-60 kg N/ha; N₁₂₀-120 kg N/ha; N₂₅₀-250 kg N/ha

Table 5.3 (cont'd) Misclassification matrix (decision tree approach) for the detection of various combinations of weed and nitrogen effects, using spectral values at 20 points in each plot for different flights (for the unseen data set)

c. Third flight (August 25th)

		Actual									Total
		N ₆₀ W1	N ₆₀ W3	N ₆₀ W4	N ₁₂₀ W1	N ₁₂₀ W3	N ₁₂₀ W4	N ₂₅₀ W1	N ₂₅₀ W3	N ₂₅₀ W4	
Predicted	N ₆₀ W1	12	2	2	0	0	0	0	0	0	16
	N ₆₀ W3	2	6	2	1	2	1	0	1	1	16
	N ₆₀ W4	3	2	3	0	1	4	0	0	0	13
	N ₁₂₀ W1	0	1	0	8	1	0	1	0	0	11
	N ₁₂₀ W3	1	4	0	2	5	1	2	0	2	17
	N ₁₂₀ W4	0	1	1	0	4	5	0	0	0	11
	N ₂₅₀ W1	1	0	2	2	4	1	7	0	3	20
	N ₂₅₀ W3	0	1	0	0	3	1	0	9	4	18
	N ₂₅₀ W4	0	0	0	1	0	0	2	0	10	13
	Total	19	17	10	14	20	13	12	10	20	135
										Risk Estimate	0.518
Bands in the final model	409, 416, 438, 446, 468, 483, 490, 498, 505, 520, 543, 565, 588, 618, 648, 663, 671, 679, 694, 701, 709, 717, 724, 739, 747, 762, 778, 785, 793, 816, 839, 862, 870, 878, 885, 893, 901, 908, 916, 939										

Treatments: W1- no weed control; W3-broadleaf weed control; W4-full weed control; N₆₀-60 kg N/ha; N₁₂₀-120 kg N/ha; N₂₅₀-250 kg N/ha

Table 5.4 Misclassification matrix (decision tree approach) for the detection of separate weed and nitrogen effects, using spectral values at 20 points in each plot for different flights (for the unseen data set)

a. First flight (June 30th)

		Actual				Actual				
		N ₆₀	N ₁₂₀	N ₂₅₀	Total		W1	W3	W4	Total
Predicted	N ₆₀	30	5	5	40	W1	30	5	4	39
	N ₁₂₀	11	29	8	48	W3	7	29	5	41
	N ₂₅₀	3	8	36	47	W4	6	12	37	55
	Total	44	42	49	135	Total	43	46	46	135
Risk Estimate					0.2963	Risk Estimate				0.2889
Bands in the final model	409, 416, 424, 438, 446, 468, 476, 483, 490, 498, 543, 550, 558, 565, 588, 633, 686, 701, 709, 717, 724, 732, 755, 770, 778, 801, 816, 831, 847, 854, 893, 901, 916, 932, 939				409, 416, 424, 446, 453, 468, 476, 483, 490, 498, 535, 550, 558, 595, 663, 694, 709, 717, 747, 770, 839, 854, 870, 901, 924, 932, 939					

b. Second flight (August 5th)

		Actual				Actual				
		N ₆₀	N ₁₂₀	N ₂₅₀	Total		W1	W3	W4	Total
Predicted	N ₆₀	34	7	1	42	W1	36	6	1	43
	N ₁₂₀	5	34	6	45	W3	6	36	13	55
	N ₂₅₀	1	3	44	48	W4	0	3	34	37
	Total	40	44	51	135	Total	42	45	48	135
Risk Estimate					0.1704	Risk Estimate				0.2148
Bands in the final model	409, 446, 453, 490, 498, 505, 513, 543, 558, 565, 595, 610, 656, 671, 709, 709, 724, 739, 747, 755, 762, 778, 839, 885, 901, 908, 916				424, 438, 461, 476, 490, 505, 520, 580, 618, 641, 656, 671, 679, 694, 709, 724, 732, 739, 801, 847, 862, 885, 916, 924, 932					

Treatments: W1- no weed control; W3-broadleaf weed control; W4-full weed control; N₆₀-60 kg N/ha; N₁₂₀-120 kg N/ha; N₂₅₀-250 kg N/ha

Table 5.4 (cont'd) Misclassification matrix (decision tree approach) for the detection of separate weed and nitrogen effects, using spectral values at 20 points in each plot for different flights (for the unseen data set)

c. Third flight (August 25th)

		Actual				Actual				
Predicted		N ₆₀	N ₁₂₀	N ₂₅₀	Total		W1	W3	W4	Total
	N ₆₀	36	13	1	50	W1	33	5	7	45
	N ₁₂₀	6	30	12	48	W3	15	27	8	50
	N ₂₅₀	0	6	31	37	W4	2	8	30	40
Total	42	49	44	135	Total	50	40	45	135	
Risk Estimate					0.2815	Risk Estimate				0.3333
Bands in the final model	409, 424, 438, 446, 453, 461, 468, 490, 513, 520, 543, 558, 565, 610, 618, 648, 656, 679, 694, 709, 717, 724, 739, 747, 785, 824, 854, 878, 885, 893, 901				409, 431, 438, 446, 453, 461, 468, 483, 490, 498, 505, 513, 520, 543, 558, 565, 603, 648, 663, 671, 679, 686, 717, 732, 739, 747, 793, 801, 847, 885, 893, 901, 908, 924					

Treatments: W1- no weed control; W3-broadleaf weed control; W4-full weed control; N₆₀-60 kg N/ha; N₁₂₀-120 kg N/ha; N₂₅₀-250 kg N/ha

Table 5.5 Risk estimate values indicating the performance of different decision trees developed with spectral values at 20 points in each plot

Decision tree evaluation criteria*	Risk estimate value							
	June 30, 2000		August 5, 2000		August 25, 2000		Combined data	
	Resubstitution/ training	Crossvalidation/ testing	Resubstitution/ training	Crossvalidation/ testing	Resubstitution/ training	Crossvalidation/ testing	Resubstitution/ training	Crossvalidation/ testing
1. Combined effect of weed and nitrogen								
a. Cross validation (10 fold)	0.1014	0.4042	0.0667	0.2847	0.1028	0.4083	0.0556	0.2597
b. Cross validation (separate training and test data)	0.0752	0.4667	0.0581	0.3407	0.0855	0.5185	0.0935	0.4315
2. Effect of weed alone								
a. Cross validation (10 fold)	0.0403	0.2347	0.0417	0.1625	0.0556	0.3083	0.0630	0.2593
b. Cross validation (separate training and test data)	0.0632	0.2889	0.0325	0.2148	0.0444	0.3333	0.0572	0.2691
3. Effect of nitrogen alone								
a. Cross validation (10 fold)	0.0514	0.3208	0.0431	0.1889	0.0486	0.2278	0.0556	0.2597
b. Cross validation (separate training and test data)	0.0786	0.2963	0.0427	0.1704	0.0359	0.2815	0.0601	0.3016

*Resubstitution and crossvalidation terms for 10-fold cross validation criteria, training and testing for simple crossvalidation

results were obtained for the second flight (August 5th), giving a risk estimate of 0.2847 for 10-fold crossvalidation and 0.3407 for the unseen validation data set, when both nitrogen and weed factors were considered together. Much better results were obtained when one of the two factors, either weed or nitrogen, was studied alone. At the tassel stage, when only weed control strategies were considered, 21% of the cases in the unseen data set were misclassified, while 17% of cases were misclassified when nitrogen was considered alone.

Finally, the data were pooled from all three flights. First of all, attempts were made to classify the pooled data into three growth categories. As expected, the results indicated that fewer than 1% of the cases (four cases) were misclassified in an unseen data set of 431 cases. This clearly indicated that the spectral responses of the crop canopy were quite different at the three growth stages. Further analysis was carried out to classify pooled data into different nitrogen and weed combinations, and also to separate the categories of weeds and nitrogen. The results are summarized in the far right columns of Table 5.5.

5.4.2 Comparison of the decision tree models with ANN models

A large number of ANN models with different architectures were generated for each case in order to find the best model. All models were based on the 20 point per sub-plot subsets. Simple models with one or two hidden layers were first generated. The number of processing elements (PEs) varied from 10 to 70 in the first hidden layer and from 10 to 40 in the second hidden layer. The selection of these numbers was based on the change in RMS value with the addition or deletion of PEs in a layer. The number of PEs in the input layer was 71, which equaled the number of used wavebands. However, depending upon the output categories, the number of PEs in the output layer was three or nine. The best ANN model was retained for each case. To avoid bias in the development of models, all the data was randomized and divided into three data sets. The models were initially trained with 60% of the data set and tested with 20% of the data. Fully trained models were then validated on a completely unseen data set, consisting of 20% of the cases (about 144 values). Models were also crossvalidated to confirm the results.

The output of the ANNs consisted of factors with three or nine elements, depending on what case a given ANN was trained to classify. Because the elements were continuous (as opposed to 1s and 0's), the input record was assigned to the category represented by the element with the highest value. For example, in a classification of categories for weed control strategy, the first element of the output vector was associated with treatment W1, the second with W3, and the third with W4. If the output vector was (0.7, 0.2, 0.1), the input record was assigned to W1.

ANN models were first trained to classify the aerial spectral data into all nine treatment combinations for each flight separately. There were 432 data records for training and 144 each for testing and validation of models. For the initial growth and tassel stages, the best ANN models had one hidden layer and 41 PEs and 22 PEs, respectively. However, the best model for the fully-mature stage (third flight), had 35 PEs in the first hidden layer and 10 PEs in the second hidden layer.

Results for the ANNs trained to classify the records into categories representing the nine treatment combinations are presented in the form of misclassification matrices in Table 5.6. As was the case for the decision trees, the best results were obtained for the data set at the tassel stage (second flight, August 5th) stage. In total, about 29.9% of the cases were misclassified in all categories in the second flight data set, followed by 36.8% in the third, and 41.7% in the first flight. A closer look at the misclassification matrix indicated that at all three stages, most of the misclassified cases had been classified into the next nearest category. In other words, it was very rare for N₆₀ to be misclassified as N₂₅₀. Diagonal values in the misclassification matrix represent the number of cases correctly classified. The risk estimates were lower than those of the corresponding decision trees (Table 5.3), for all stages of crop development. Nevertheless, the lowest (tassel stage) was 29.9%.

The misclassification matrices for ANNs trained to classify records into one or the other treatment (weed control or nitrogen rate) are given in Table 5.7 for the three flights. Risk estimates were much lower for each flight, compared to the results for the nine treatment combinations, as was the case for the analogous comparison involving decision trees. Again, better classification results were obtained from the aerial data set acquired at the tassel stage. When nitrogen alone was considered,

Table 5.6 Misclassification matrix (Artificial Neural Networks models) for the detection of various combinations of weed and nitrogen effects, using spectral values at 20 points in each plot for different flights (for the unseen data set)

a. First flight (June 30th)

		Actual									Total
		N ₆₀ W1	N ₆₀ W3	N ₆₀ W4	N ₁₂₀ W1	N ₁₂₀ W3	N ₁₂₀ W4	N ₂₅₀ W1	N ₂₅₀ W3	N ₂₅₀ W4	
Predicted	N ₆₀ W1	8	2	1	3	3	5	4	0	1	27
	N ₆₀ W3	1	14	1	6	1	0	1	0	0	24
	N ₆₀ W4	4	2	11	0	1	3	0	0	0	21
	N ₁₂₀ W1	0	0	0	9	1	0	0	0	0	10
	N ₁₂₀ W3	0	1	1	0	7	0	0	1	1	11
	N ₁₂₀ W4	1	0	1	0	1	11	0	1	0	15
	N ₂₅₀ W1	1	0	0	4	0	0	13	1	0	19
	N ₂₅₀ W3	0	0	1	0	3	0	0	4	0	8
	N ₂₅₀ W4	0	1	0	0	1	0	0	0	7	9
	Total	15	20	16	22	18	19	18	7	9	144
Risk Estimate										0.417	

b. Second flight (August 5th)

		Actual									Total
		N ₆₀ W1	N ₆₀ W3	N ₆₀ W4	N ₁₂₀ W1	N ₁₂₀ W3	N ₁₂₀ W4	N ₂₅₀ W1	N ₂₅₀ W3	N ₂₅₀ W4	
Predicted	N ₆₀ W1	8	0	0	1	0	0	0	0	0	9
	N ₆₀ W3	1	20	5	0	0	0	0	0	0	26
	N ₆₀ W4	0	5	10	0	0	0	0	0	0	15
	N ₁₂₀ W1	2	0	0	8	6	0	1	0	0	17
	N ₁₂₀ W3	0	1	0	0	9	0	0	2	2	14
	N ₁₂₀ W4	0	0	1	0	1	9	0	0	0	11
	N ₂₅₀ W1	0	0	0	2	1	0	13	2	0	18
	N ₂₅₀ W3	0	0	0	0	6	0	3	13	1	23
	N ₂₅₀ W4	0	0	0	0	0	0	0	0	11	11
	Total	11	26	16	11	23	9	17	17	14	144
Risk Estimate										0.299	

Treatments: W1- no weed control; W3-broadleaf weed control; W4-full weed control; N₆₀-60 kg N/ha; N₁₂₀-120 kg N/ha; N₂₅₀-250 kg N/ha

Table 5.6 (cont'd) Misclassification matrix (Artificial Neural Networks models) for the detection of various combinations of weed and nitrogen effects, using spectral values at 20 points in each plot for different flights (for the unseen data set)

c. Third flight (August 25th)

		Actual									Total
		N ₆₀ W1	N ₆₀ W3	N ₆₀ W4	N ₁₂₀ W1	N ₁₂₀ W3	N ₁₂₀ W4	N ₂₅₀ W1	N ₂₅₀ W3	N ₂₅₀ W4	
Predicted	N ₆₀ W1	11	2	1	5	0	0	0	0	0	19
	N ₆₀ W3	1	7	0	1	0	0	0	0	0	9
	N ₆₀ W4	0	1	13	0	0	3	0	0	0	17
	N ₁₂₀ W1	1	2	0	2	3	0	0	0	0	8
	N ₁₂₀ W3	0	1	1	5	10	0	3	1	0	21
	N ₁₂₀ W4	0	0	0	0	1	12	0	0	0	13
	N ₂₅₀ W1	0	0	0	3	0	0	12	5	2	22
	N ₂₅₀ W3	0	0	0	0	1	1	3	12	2	19
	N ₂₅₀ W4	0	0	0	0	0	2	1	1	12	16
	Total	13	13	15	16	15	18	19	19	16	144
Risk Estimate										0.368	

Treatments: W1- no weed control; W3-broadleaf weed control; W4-full weed control; N₆₀-60 kg N/ha; N₁₂₀-120 kg N/ha; N₂₅₀-250 kg N/ha

Table 5.7 Misclassification matrix (Artificial Neural Networks models) for the detection of separate weed and nitrogen effects, using spectral values at 20 points in each plot for different flights (for the unseen data set)

a. First flight (June 30th)

		Actual				Actual					
		N ₆₀	N ₁₂₀	N ₂₅₀	Total	W1	W2	W3	Total		
Predicted	N ₆₀	35	17	6	58	W1	42	3	6	51	
	N ₁₂₀	7	30	7	44	W3	2	42	7	51	
	N ₂₅₀	1	6	35	42	W4	1	8	33	42	
	Total	43	53	48	144	Total	45	53	46	144	
Risk Estimate					0.3056	Risk Estimate					0.1875

b. Second flight (August 5th)

		Actual				Actual					
		N ₆₀	N ₁₂₀	N ₂₅₀	Total	W1	W2	W3	Total		
Predicted	N ₆₀	41	4	0	45	W1	38	11	0	49	
	N ₁₂₀	2	35	3	40	W3	2	34	1	37	
	N ₂₅₀	0	8	51	59	W4	0	3	55	58	
	Total	43	47	54	144	Total	40	48	56	144	
Risk Estimate					0.1181	Risk Estimate					0.1181

c. Third flight (August 25th)

		Actual				Actual					
		N ₆₀	N ₁₂₀	N ₂₅₀	Total	W1	W2	W3	Total		
Predicted	N ₆₀	45	4	0	49	W1	45	6	1	52	
	N ₁₂₀	8	42	4	54	W3	0	37	3	40	
	N ₂₅₀	0	5	36	41	W4	3	4	45	52	
	Total	53	51	40	144	Total	48	47	49	144	
Risk Estimate					0.1458	Risk Estimate					0.1181

Treatments: W1- no weed control; W3-broadleaf weed control; W4-full weed control; N₆₀-60 kg N/ha; N₁₂₀-120 kg N/ha; N₂₅₀-250 kg N/ha

the lowest risk estimate value was 0.118 for the second flight, 0.146 for the third, and 0.306 for the first flight. Better results were obtained with the ANN than with the decision tree, with the exception of the first flight. Much better results were obtained from the analysis based on the weed factor. Only 11.8% of the cases from the second and third flights (Risk estimate value = 0.118) were misclassified, whereas 18.8% of the cases from the first flight were misclassified. The best classification result obtained with decision trees was 21.5% misclassification of cases from the second flight.

5.5 Conclusions

Overall, the best classification results from ANN models and decision trees were obtained using data from the second flight (August 5th), reflecting the results of Chapter 4, based on regression models and analysis of variance. Risk estimates were lower in both cases when one treatment was considered at a time. The progression in improvement of results, with the number of data records available to the decision tree, points to a need for better spatial resolution. As noted in Chapter 4, concerning the comparison of results using ground-based and aerial spectral data, there is an interplay between resolution and coverage. It is possible that better results could be obtained at full coverage, with somewhat higher resolution.

An area that could be investigated further is the optimization of inputs to the models. In the case of decision trees, the dichotomization was done on the basis of the best single regressor at each node, i.e. the one waveband that best separated the data in each case. One might obtain better classification accuracy on the data set, even if the data from all three flights were combined. This could be effected by first applying a technique such as principal components analysis to the spectral data, in order to obtain orthogonal functions of the reflectance values at different wavelengths to describe the variability of the data set. Such functions would then serve as the regressors for the C&RT algorithm and might yield better results. Insofar as ANNs are concerned, the best classification accuracies reported in the literature are based on data sets that have been pre-processed to find the optimal descriptors, which in turn serve as inputs for training such models.

The risk estimates associated with the broadest objective of this work (i.e. to classify the data into nine treatment combinations) are modest, being in the vicinity of 0.3 (or 30% misclassification) for ANNs and decision trees. However, pre-processing of these reflectance values using appropriate data reduction and orthogonalization techniques could lead to risk estimates as low as those obtained for the one-treatment-at-a-time models. Furthermore, the most useful wavebands retained in the final models, were generally different.

In conclusion, compared to the results presented in Chapter 3 based on data acquired from a 24-waveband sensor on very small plots, there was a marked improvement in the ability to relate spectral imagery to canopy conditions using equipment with higher spectral resolution. There appears to be some advantage to using ANNs over decision trees or simple regression or correlation analyses, in classifying spectral data into categories of treatment combinations. However, implementation of state-of-the-art pre-processing is needed to make the technology applicable to precision farming.

PREFACE TO CHAPTER 6

The study presented in this section was motivated by the moderate classification accuracies obtained with decision trees and ANNs. For all intents and purposes, the results using these technologies were comparable. There was little consistency in the wavebands used to segment the data into various sets of categories by decision trees, or in the ANN architectures leading to the highest classification accuracies. Therefore, it seemed logical to explore both conventional methods of classifying hyper-spectral imagery as well as relatively new classifiers, such as linear unmixing and the spectral angle mapper.

Research papers based on the chapter:

1. Goel, P. K., S. O. Prasher, J.-A. Landry, R. M. Patel, and A. A. Viau. Hyperspectral image classification to detect weed infestations and nitrogen status in corn. *Transactions of the ASAE* (In press).

(Copy of the published paper is given in the attached CD-ROM.)

CHAPTER 6

IMAGE CLASSIFICATION FOR MAPPING WEEDS AND NITROGEN LEVELS

6.1 Abstract

Hyper-spectral data acquired from an airborne sensor were classified according to categories of weed control strategy and nitrogen application rate by seven different supervised algorithms. The ultimate objective was to produce maps reflecting the combinations of these categories in an experimental field. The data were obtained over a field plot experiment designed to investigate the effects of different weeds on corn (*Zea Mays* L.) growth at three levels of nitrogen fertilization. The images analyzed were obtained at the tassel stage. The following supervised algorithms were applied to the images: maximum likelihood, minimum distance, Mahalanobis distance, parallelepiped, binary encoding, spectral angle mapping and linear spectral unmixing. The algorithms failed to classify the images, into the nine combinations of weed and nitrogen treatment, to an acceptable level of accuracy for precision farming requirements. However, when these algorithms were required to classify images into categories of one or the other treatment, performance was reasonable for practical applications, being 66% for classification to nitrogen levels and 68% to weed control strategies. The best results were obtained in the classification of two levels at a time, of one or the other factor. Not one classifier proved best for all subsets of the complete factorial problem.

6.2 Introduction

The greatest strength of remote sensing lies in the wide spatial coverage that can be obtained in a short time. Ground-truthing is an essential step in the development of a remote sensing system, because it is the step that permits the development of relationships between conditions or objects on the earth's surface and the images. Once relationships with adequate statistical significance are established, specialized maps are produced by classifying each pixel of the image into categories reflecting the absence or presence of one or more features, and then referencing them

to their relative positions in the scanned area.

Many different classification algorithms have been applied to remote sensing data. Most of the earlier methods were developed for the analysis of multi-spectral imagery with relatively few wavebands. These include the maximum likelihood, minimum distance, Mahalanobis distance, parallelepiped and binary encoding classifiers. However, the aforementioned are now considered inadequate for the large data sets that result from the use of hyper-spectral sensors. This is due to the loss in potential information stored in continuous spectra, the need for a greater number of training pixels, and the greater computational requirements of such methods (Lillesand and Kiefer, 2000). Researchers dealing with hyper-spectral data sets have used statistical procedures to select a few suitable wavebands based on class separability or prioritization based on transformation techniques (such as principal component analysis) to reduce the dimensionality of the data (Pu and Gong, 2000). These selected wavebands or transformed components are then used to develop maps by applying multi-spectral image classification algorithms. However, attention has now turned to the development of new procedures, such as spectral matching and spectral unmixing (Staenz, 1996), which are thought to be more effective than the previous methods.

The objective of the study, presented in this chapter, was to compare the classification resulting from seven classifiers, including spectral matching and spectral unmixing. This was carried out using hyper-spectral images of plots cropped with corn, that had been subjected to combinations of weed control strategy and nitrogen application rate.

6.2.1 A brief overview of image classification methods

Image classification is the process of assigning classes to the pixels in a remotely sensed image, and generating a thematic or land cover class map. Thus, a classified image shows the spatial distribution of a particular theme or class of interest. Many approaches are being used to classify remotely sensed data. In general, classification procedures have been grouped into two classes: supervised and unsupervised. In a supervised classification, training pixels or areas are selected for

each category based on some prior or acquired knowledge of the classes in the imagery. The image is then segmented according to spectrally 'similar' pixels for each class. In the unsupervised classification procedure, features are typically separated solely on the basis of spectral properties which are 'similar' in a statistical sense. Some of the supervised classification algorithms, used in the present study are briefly discussed in the following paragraphs.

The maximum likelihood classifier is the most widely used technique to classify remote sensing images. With this technique, the estimates of the probability function of all classes of interest in the image are based on a Gaussian distribution. For classification, the individual pixels in the image are assigned to the class with the highest probability value.

The minimum distance classifier determines the mean vector value of each class. The Euclidean distance of an unknown pixel from each class is determined, and the unknown pixel is assigned to the closest class.

The Mahalanobis classifier is similar to the maximum likelihood classifier, but is a direction-sensitive distance classifier, where covariances of all the classes are considered equal. This classifier is faster than the maximum likelihood procedure. A discussion on these methods is presented by Richard (1994).

The parallelepiped classifier uses a simple approach of classification, based on decision boundaries, by drawing boundaries for a training class using straight lines in each waveband. In the simplest case of two wavebands, the method may be visualized by the boundaries resembling a series of rectangles covering each class. However, for a greater number of wavebands, each class is covered by a multidimensional box or parallelepiped. Unknown pixels are assigned to a class if they fall within the class boundaries; otherwise, they are classified as unknown.

In the binary encoding classification approach, the endmember spectra (spectra known to represent a condition or type of object) and the unknown spectra are coded as 0's or 1's, depending on whether the waveband value falls above or below the spectrum mean. The classification image is then produced by using an 'OR' function to compare each encoded unknown spectral and endmember spectra. Details of this approach are given by Mazer et al. (1988).

The Spectral Angle Mapper (SAM) classification algorithm is based on comparing image spectra to a known library of spectra or endmembers. In this method, the endmember and unknown pixel spectra are treated as vectors, and a calculation is made of the spectral angle between them. The angles between pixel spectra and spectra of different endmembers are compared in different wavebands, and the pixel is assigned to the category having the most similar angle. Because it is only the direction of the vector that is used in this approach, the method is insensitive to differences in illumination (length of the vector). A more detailed discussion is given by Kruse et al. (1993).

The spectral unmixing technique is based on the fact that most surfaces on the earth, geologic or vegetated, are not homogeneous, resulting in a mixture of spectral responses by a single pixel. Thus, this technique is aimed at estimating the proportion of each class in the pixel. The complexity of mathematical models to determine the abundance of each class is based on how these materials are mixing on the surface. Linear unmixing techniques assume that the sum of the fractional proportion of all potential endmembers in each pixel is equal to unity, and may therefore be represented by a linear model.

$$\sum_1^n F_i = F_1 + F_2 + F_3 + \dots + F_n = 1 \quad , \quad (6.1)$$

where F_1, F_2, \dots, F_n are the fractional proportions of each possible endmember, n , in the pixel.

The other main assumption of the unmixing procedure is that the spectral response of each pixel, i.e., recorded digital number (DN_λ) value in a particular waveband, λ , is the weighted sum of the spectral responses of each endmember:

$$DN_\lambda = F_1 DN_{\lambda,1} + F_2 DN_{\lambda,2} + \dots + F_n DN_{\lambda,n} + E_\lambda \quad , \quad (6.2)$$

where F_1, F_2, \dots, F_n are the fractional proportions of each endmember in the pixel; $DN_{\lambda 1}, DN_{\lambda 2}, \dots, DN_{\lambda n}$ are the responses of each endmember, if the pixel is fully covered by that particular endmember, and E_λ is the error term (Lillesand and Kiefer, 2000).

In addition to the above methods, other classification approaches have been used in the field of remote sensing; however, no single classifier is best for all the particular conditions. In general, results from the various classifiers are compared to achieve optimal results (ENVI, Training Manual, 2000).

6.3 Materials and Methods

6.3.1 Experimental details

Refer to section 4.3.1

6.3.2 Acquisition of spectral data

A Compact Airborne Spectrographic Imager (CASI) was used to acquire a hyper-spectral image in 72 narrow wavebands (407 to 949 nm), in the visible and near-infrared regions. The spatial resolution was 2 m. The analyses presented in Chapters 4 and 5, indicates that the images obtained at the tassel stage of the corn crop were easier to classify than the others. Thus, the various classifiers were evaluated for this data set only. More details on the acquisition and processing of the image were given in section 4.3.2.

6.3.3 Data analysis

As explained in Chapter 4, the data associated with the plots in which broadleaved weeds were permitted to grow and grasses were eliminated (W2) was not considered in the analysis. Thus, a total of 36 plots were used in the analysis, with three weed treatments (W1, W3, and W4) and three nitrogen levels (N_{60} , N_{120} , and N_{250}) replicated four times. The reflectance values from waveband 72 could not be used due to excessive noise in the signal. Because each combination of the two factors was replicated four times, data from two of the replicates were used for training the classifiers and the rest were used in validation.

All analyses were performed using the ENVI image processing software (ENVI 3.1, Research System, Inc., Boulder, Colorado, USA). In each sub-plot, a region of interest (ROI) was created to eliminate pixels in which there may be border effects. The ROI consisted of 25 to 30 pixels, depending on the sub-plot (recall that there were approximately 100 pixels associated with the 20m x 20m sub-plots). Only the supervised classification algorithms provided in the ENVI software were used, because all the plots were of known character. Numerous trials were carried out using the various, optional threshold parameters available in each classification module. The classifiers used were: maximum likelihood, minimum distance, Mahalanobis distance, parallelepiped, binary encoding, spectral angle mapper and spectral unmixing.

The first problem presented to these classifiers was to separate all nine combinations of nitrogen application rate and weed treatments, representing a rather complex crop growth scenario in the field. In the next step, the images were classified by taking one factor at a time, which involved the assumption that the variability caused by the levels of the other factor was intrinsic. The classification accuracies of the seven methods were compared on the basis of the validations.

The Kappa coefficient (κ) was also calculated to compare the accuracy of different classifiers. This coefficient is used to measure the accuracy of a classifier by comparing the number of correctly classified pixels with that obtained by a purely random classification. It is defined as follows:

$$\kappa = \frac{n \sum_k X_{kk} - \sum_k X_{k\Sigma} X_{\Sigma k}}{n^2 - \sum_k X_{k\Sigma} X_{\Sigma k}} \quad (6.3)$$

where: n = number of pixels in all groundtruth classes,

k = a particular class,

X_{kk} = sum of the confusion matrix diagonals,

$X_{k\Sigma}$ = sum of the groundtruth pixels in class k , and

$X_{\Sigma k}$ = sum of the pixels attributed to the k^{th} class.

In this experiment, all pixels were ground-truthed with respect to nitrogen.

However, it would be difficult to consider that the weed control strategies were ground-truthed for weed density, even though they were controlled with respect to type of weed population. The between-row LAI measurements taken at ground level could give some indication of differences in weed density, and could conceivably be used to draw inferences regarding the comparative influence on reflectance values of broadleaved and grassy weeds.

6.4 Results and Discussion

A color-infrared image, shown in Figure 6.1, indicated the prevailing variability in corn growth conditions across the various treatments. Qualitatively speaking, the darker colors represent comparatively better growth and higher nitrogen levels. Nitrogen-deficient areas and plots in which growth is poor due to other reasons may be distinguished by their lighter and yellowish color. However, it was difficult to group all plots visually into the nine different treatment categories. A field layout indicating the location of different treatments is given in Figure 6.2.

Attempts were made to classify the whole image based on the nine different categories, representing all the possible combinations of three nitrogen levels and three weed control measures. None of the classifiers performed this task at a satisfactory level, which was also the case with the methods used in Chapters 4 and 5. The classifiers were then trained to categorize the data according to one factor at a time, as described with the decision trees and ANNs (Chapter 5). In the case of nitrogen application rates, classifiers were also trained to distinguish between each possible pair. In the case of weed control strategies, one classifier was trained to distinguish between full weed control (W4) and no weed control (W1), whereas another was trained to categorize images into two categories: (a) no weed control (W1) or control of broadleaves only (W3), or (b) full weed control (W4).

The performances of all seven classifiers with respect to nitrogen are presented in Table 6.1. The confusion matrices for the best 3-level classifier and for the best 2-level classifiers are given in Table 6.2. The comparison of classifiers in the case of weeds is given in Table 6.3. The confusion matrices for the best 3-level and 2-

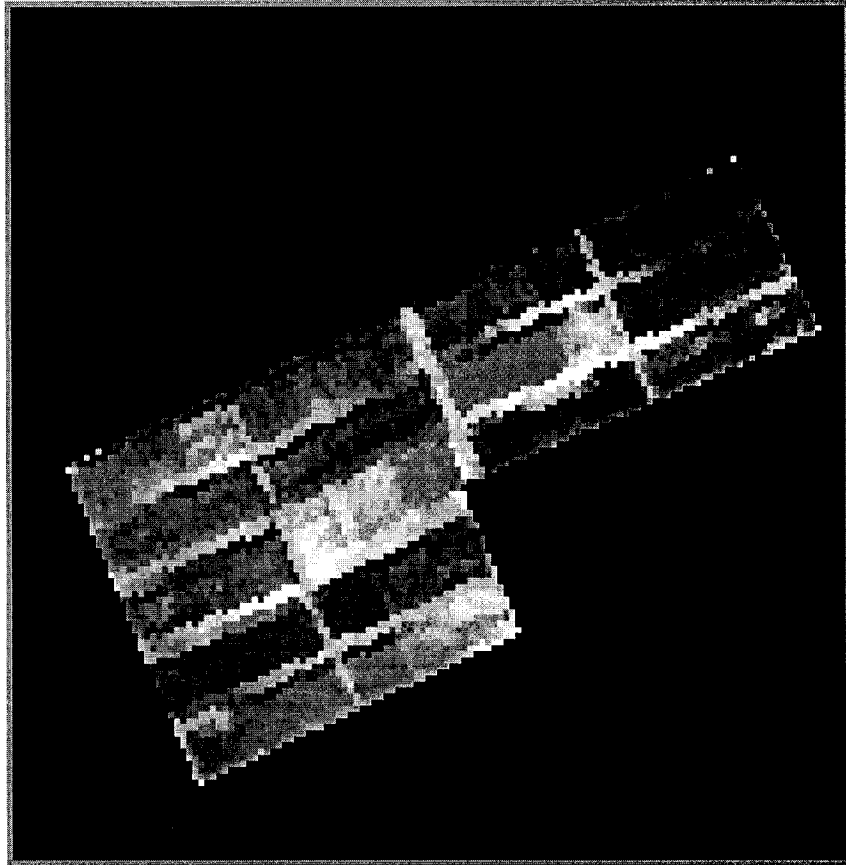
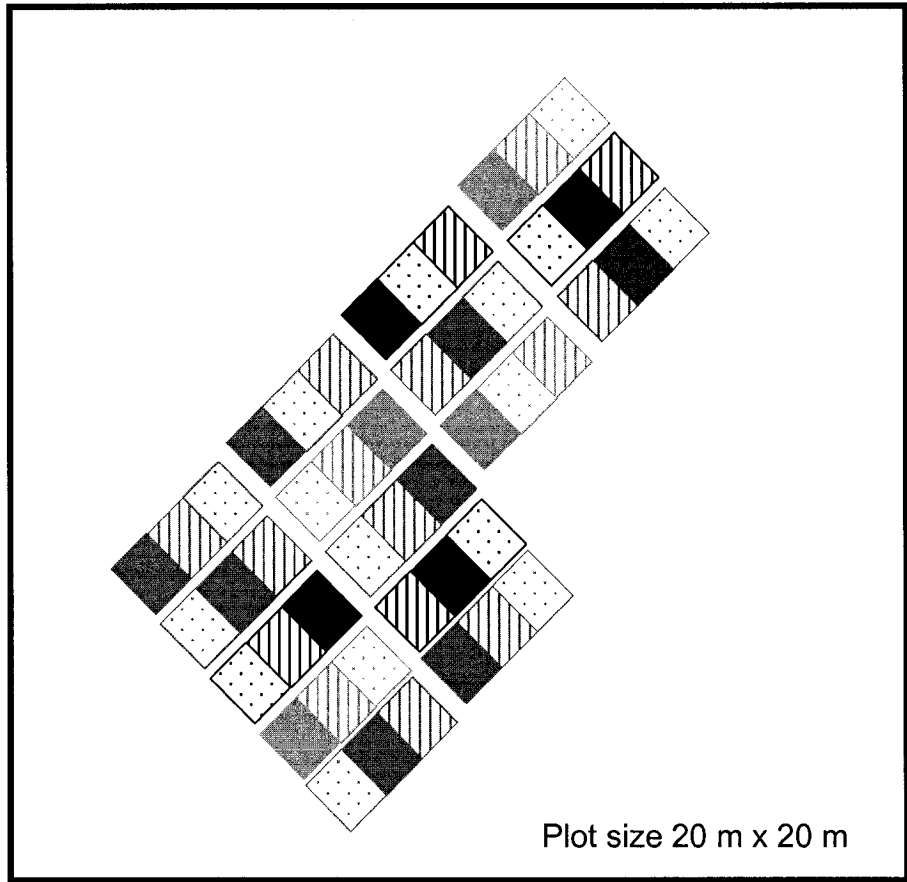


Fig. 6.1 Color-infrared image of experimental plots during the second flight (August 5, 2000, tassel stage). Bands centered at 747 nm, 558 nm, and 490 nm are displayed as red, green, and blue, respectively.



Legend

	N ₂₅₀	N ₁₂₀	N ₆₀	
W ₁				N ₆₀ : Low nitrogen
W ₂				N ₁₂₀ : Normal nitrogen
W ₃				N ₂₅₀ : High nitrogen
W ₄				W ₁ : No weed control
				W ₂ : Grass control
				W ₃ : Broad leaf control
				W ₄ : Full weed control

Fig. 6.2 Field layout indicating the relative location of various weed and nitrogen treatment plots

level cases for weed controls are given in Table 6.4.

The accuracies, for classifying the 36 plots into nitrogen application rates, ranged from 41.77% to 65.84% (Table 6.1). The best results were obtained using the spectral angle mapper (65.84%, $\kappa=0.488$) and binary encoding (65.30%, $\kappa=0.483$). With only two levels of nitrogen considered at a time, binary encoding yielded the best results for the sets (N_{60} vs. N_{250}) and (N_{120} vs. N_{250}); although the SAM and linear unmixing were a close second in the former set. Discrimination between N_{120} and N_{250} appeared to be the most difficult task. This was a small incremental effect on crop productivity as a result of fertilizing at a rate of 250 kg/ha rather than at 120 kg/ha, when compared to the large change resulting from doubling the nitrogen from 60 to 120 kg/ha. This is clearly supported by the yields recorded under various nitrogen levels. Under full weed control (W4), yields in N_{60} , N_{120} , and N_{250} were 4.80 t/ha, 6.11 t/ha, and 6.75 t/ha, respectively.

The classification maps, based on the best classifier for different nitrogen classification approaches, are presented in Figure 6.3. The confusion matrices, representing the accuracy of classification for the best classifiers, are presented in Table 6.2. A closer scrutiny of the confusion matrix for all three nitrogen levels indicated that most of the misclassified pixels were from N_{120} plots. This clearly suggests that high and low nitrogen categories may be classified with very high accuracy; and that good results may be expected when the objective is to separate areas with high or low nitrogen levels.

From the point of view of precision farming, it would be more beneficial to detect differences in the nitrogen status of young plants prior to broadcasting the second application of fertilizer. This would permit a variable rate of application of this nutrient to optimal levels across the field with a lower total dose.

When classified according to the three types of weed control strategy (Table 6.3), the highest accuracy was obtained from the minimum distance classifier (67.83%, $\kappa=0.516$). The maximum likelihood classifier yielded the best accuracy for classification of no weed control (W1) or full weed control (W4). The minimum distance approach was best for the comparison (W1 or W3) vs. (W4). The poorest results for all three sets were associated with binary encoding, which yielded the best

Table 6.1 Accuracy of different image classification methods for nitrogen treatments

Classification Method	Classification accuracy (%)			
	All nitrogen levels (i.e. N ₆₀ , N ₁₂₀ , and N ₂₅₀)	N ₆₀ vs. N ₂₅₀	N ₁₂₀ vs. N ₆₀	N ₁₂₀ vs. N ₂₅₀
Linear Spectral Unmixing	50.44 (0.254)	94.61 (0.892)	73.88 (0.479)	75.53 (0.511)
Spectral Angle Mapper	65.84 (0.488)	94.88 (0.898)	73.61 (0.473)	75.53 (0.511)
Binary Encoding	65.30 (0.483)	99.46 (0.989)	89.18 (0.784)	48.95 (0.0)
Mahalanobis Distance	60.88 (0.415)	88.94 (0.779)	66.23 (0.331)	78.42 (0.569)
Maximum Likelihood	41.77 (0.161)	77.09 (0.557)	58.05 (0.221)	52.34 (0.817)
Minimum Distance	47.43 (0.213)	81.67 (0.633)	61.21 (0.225)	60.53 (0.210)
Parallelepiped	49.20 (0.236)	77.36 (0.556)	70.45 (0.407)	53.42 (0.075)

Note: Kappa coefficient values are given in parenthesis, numbers in bold represent efficiency for best classifier.

Treatments: N₆₀-60 kg N/ha; N₁₂₀-120 kg N/ha; N₂₅₀-250 kg N/ha

Table 6.2 The confusion matrix for nitrogen treatments

a. All nitrogen levels

Predicted category (Number of pixels)	Actual category (Number of pixels)			
	N ₆₀	N ₁₂₀	N ₂₅₀	Total
N ₆₀	146	61	4	211
N ₁₂₀	39	76	32	147
N ₂₅₀	0	57	150	207
Total	185	194	186	565
Classification accuracy (%)		65.84		
Classification method		Spectral angle mapper		

b. Low nitrogen (N₆₀) vs. high nitrogen (N₂₅₀)

Predicted category (Number of pixels)	Actual category (Number of pixels)		
	N ₆₀	N ₂₅₀	Total
N ₆₀	183	0	183
N ₂₅₀	2	186	188
Total	185	186	371
Classification accuracy (%)		99.46	
Classification method		Binary encoding	

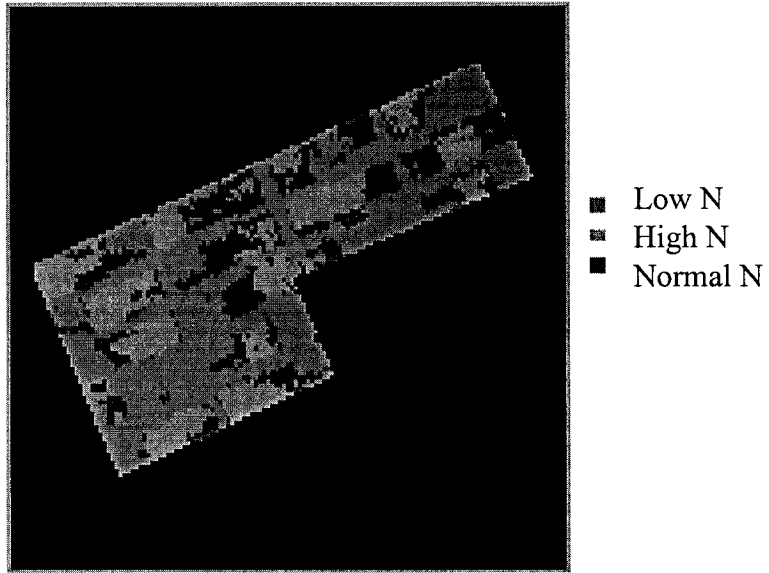
c. Normal nitrogen (N₁₂₀) vs. low nitrogen (N₆₀)

Predicted category (Number of pixels)	Actual category (Number of pixels)		
	N ₆₀	N ₁₂₀	Total
N ₆₀	183	39	222
N ₁₂₀	2	155	157
Total	185	194	379
Classification accuracy (%)		89.18	
Classification method		Binary encoding	

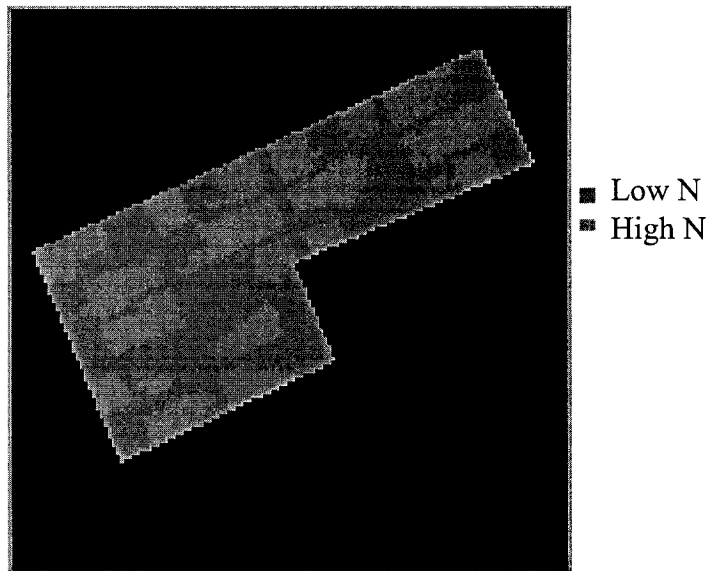
d. Normal nitrogen (N₁₂₀) vs. high nitrogen (N₂₅₀)

Predicted category (Number of pixels)	Actual category (Number of pixels)		
	N ₁₂₀	N ₂₅₀	Total
N ₁₂₀	140	28	168
N ₂₅₀	54	158	212
Total	194	186	380
Classification accuracy (%)		78.42	
Classification method		Binary encoding	

Treatments: N₆₀-60 kg N/ha; N₁₂₀-120 kg N/ha; N₂₅₀-250 kg N/ha

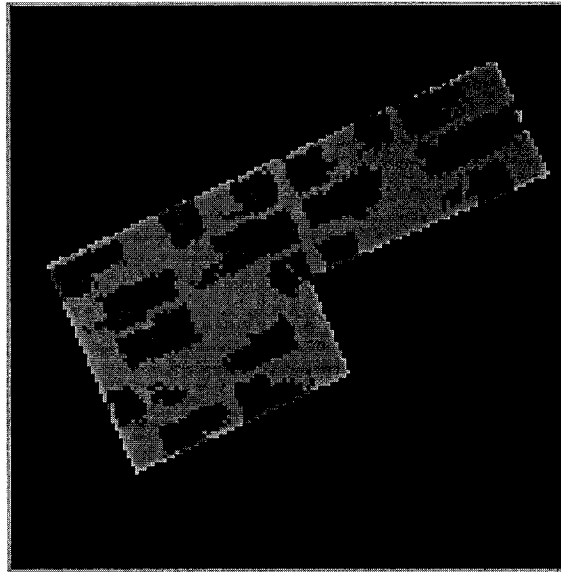


a. All nitrogen level categories, classified with the spectral angle mapper classifier.

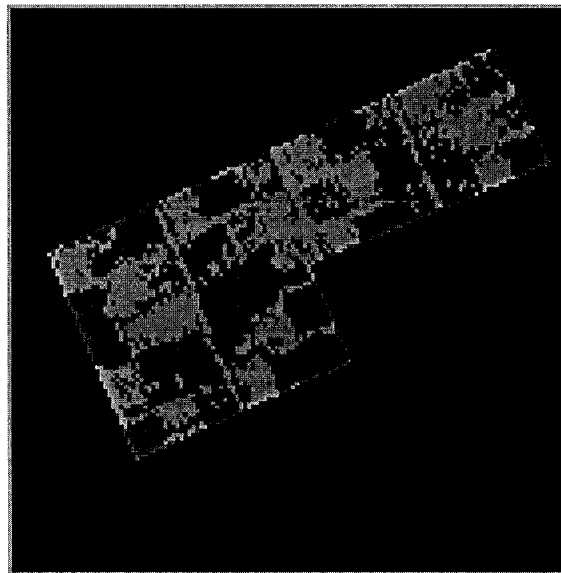


b. High and low nitrogen levels, classified with the binary encoding classifier.

Fig. 6.3 Classification map for nitrogen categories.



c. Normal and low nitrogen level categories, classified with the binary encoding classifier.



d. Normal and high nitrogen level categories, classified with the Mahalanobis distance classifier.

Fig. 6.3 (cont'd) Classification map for nitrogen categories.

Table 6.3 Accuracy of different image classification methods for weed detection

Classification Method	Classification accuracy (%)		
	All weed classes (i.e. W1, W3, and W4)	No weed control vs. full weed control (i.e. W1 vs. W4)	No weed control & Broadleaf control vs. full weed control (i.e. W1 and W3 Combined vs. W4)
Linear Spectral Unmixing	50.82 (0.276)	79.46 (0.587)	80.42 (0.568)
Spectral Angle Mapper	58.74 (0.374)	80.81 (0.614)	81.35 (0.585)
Binary Encoding	33.80 (0.036)	46.46 (0.0)	53.15 (0.0)
Mahalanobis Distance	59.91 (0.399)	87.54 (0.754)	80.19 (0.599)
Maximum Likelihood	63.40 (0.441)	91.25 (0.824)	67.60 (-0.002)
Minimum Distance	67.83 (0.516)	85.86 (0.717)	84.84 (0.661)
Parallelepiped	58.51 (0.389)	83.51 (0.708)	71.79 (0.237)

Note: Kappa coefficient values are given in parenthesis, numbers in bold represent efficiency for best classifier.

Treatments: W1- no weed control; W3-broadleaf weed control; W4-full weed control

Table 6.4 The confusion matrix for weed detection

a. All weed classes

Predicted category (Number of pixels)	Actual category (Number of pixels)			
	W1	W3	W4	Total
W1	116	46	0	162
W3	43	67	30	140
W4	0	19	108	127
Total	159	132	138	429
Classification accuracy (%)	67.83			
Classification method	Minimum distance			

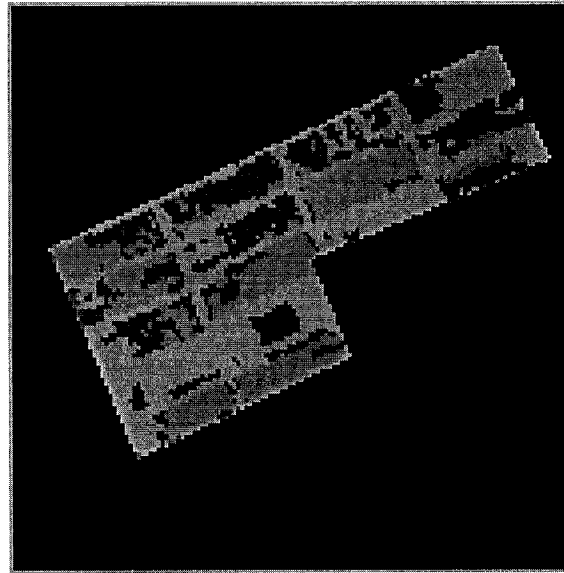
b. No weed control (W1) vs. full weed control (W4)

Predicted category (Number of pixels)	Actual category (Number of pixels)		
	W1	W4	Total
W1	148	15	163
W4	11	123	134
Total	159	138	297
Classification accuracy (%)	91.25		
Classification method	Maximum likelihood		

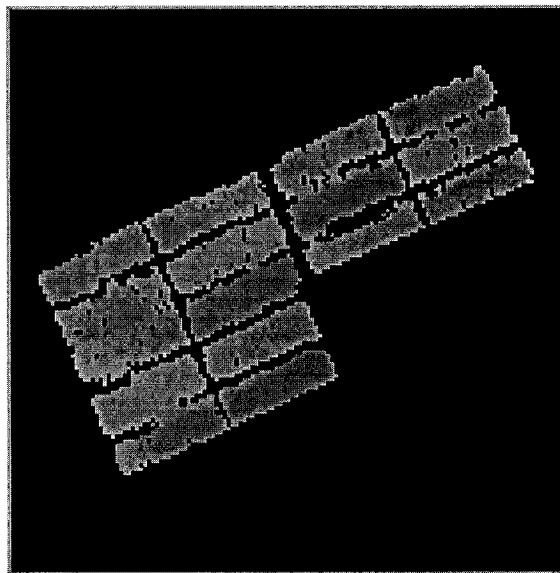
c. No weed control (W1) and broadleaf control (W3) combined vs. full weed control (W4)

Predicted category (Number of pixels)	Actual category (Number of pixels)		
	W1 & W3 Combined	W4	Total
W1 and W3 Combined	252	26	278
W4	39	112	151
Total	291	138	429
Classification accuracy (%)	84.84		
Classification method	Minimum distance		

Treatments: W1- no weed control; W3-broadleaf weed control; W4-full weed control

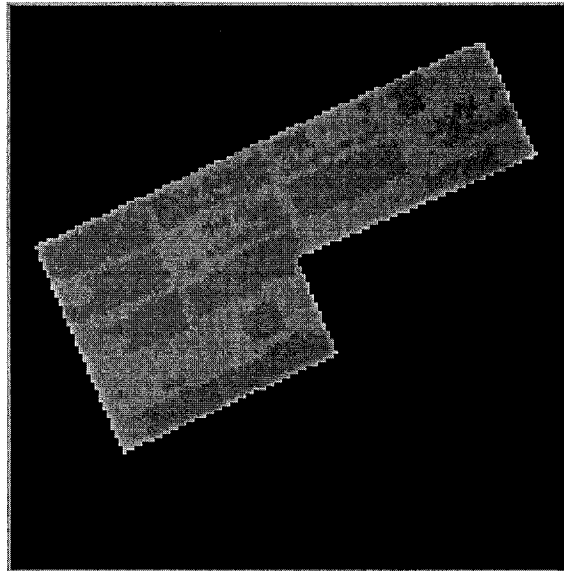


a. All weed classes, classified with the minimum distance classifier.



b. Full weed control and no weed control classes, classified with the maximum likelihood classifier.

Fig. 6.4 Classification map for weed categories.



- Full weed control
- No weed control and broadleaf weed control classes combined

c. Full weed control and combined categories of both no weed control and broadleaf weed control treatments, classified with the minimum distance classifier.

Fig. 6.4 (cont'd) Classification map for weed categories.

results overall for the various nitrogen categories. The confusion matrix for the weed control classifications (Table 6.4a) indicate that the most likely to be misclassified are the pixels from plots having only grassy weeds (W3). Because total biomass is the most dominating factor influencing the reflectance values, maximum misclassification was between W1 and W3. In general, there was not much variability in the distribution of weeds across various plots. The weed maps generated, on the basis of the best classifiers for each case, are presented in Figure 6.4. Visual comparison with Figure 6.2 indicates good concordance not only with areas where weeds were fully controlled but also with the areas where weeds were not controlled.

The results for both weed and nitrogen treatments did not provide one single classifier which performed best under all conditions. However, the results obtained in this study are quite comparable to those reported in the published literature. For example, Bajwa and Tian (2001) reported good accord between a map generated from spectral data and a ground-truth weed map. They used ISODAT, a classification algorithm in MultiSpec software (Purdue University, West Lafayette, Ind., USA), to segment weed patches in multi-spectral aerial images taken over soybean fields. GopalaPillai and Tian (1999) also used ISODAT, in this case to generate maps from multi-spectral aerial images showing soil variability, nitrogen stress and yield levels in corn fields. The reported classification accuracy was 75%, although difficulties were encountered separating out nitrogen levels. Brown and Steckler (1993) used the supervised, maximum likelihood method to map weed patches in a multi-spectral aerial image of a no-till corn field. No attempt was made to distinguish between types of weeds, and a classification accuracy of 82% was obtained for this simplified problem. Lass et al. (1996) used an unsupervised method to classify images of monospecific stands of grasses. They reported classification accuracies ranging from 19% to 72%, depending on the type of weed categories to be identified and the spatial resolution of the images. In a study aimed at detecting rangeland weeds, through CIR aerial photographs, Menges et al. (1985) used the maximum likelihood classifier and achieved classification accuracies of 68% to 100%, depending upon the type of plant. Classification accuracies ranging from 58% to 98% were reported by Staenz (1996) in

a study to identify different crops from hyper-spectral aerial images, using maximum likelihood, logistic, and band-moment procedures. Deguise et al. (1999) used spectral unmixing to identify weeds in hyper-spectral aerial images. A good match was reported between the visually identified weed patches and the hyper-spectral image. However, the accuracy was not reported in quantitative terms.

6.5 Conclusions

The results of this study tend to corroborate the findings of Chapters 4 and 5, in which analysis of variance, decision trees and artificial neural networks were used to classify the hyper-spectral images into treatment combinations or subsets thereof. The classification accuracies of the seven classifiers tested in this chapter, did not produce strikingly better results than the decision trees or ANNs for comparable classification problems. Not one classifier could be identified as the best for all situations.

As was the case for decision trees and ANNs, classification accuracies were significantly better when the original problem of classification, to nine treatment combinations, was reduced to either looking at one treatment at a time, or comparing sets of two levels of a given treatment. As mentioned in the conclusions to Chapter 4, the moderate classification results are more likely to be the result of a spatial resolution that is too low, given the complexity of the problem of classifying the nine treatment combinations.

CHAPTER 7

SUMMARY AND GENERAL CONCLUSIONS

7.1 Summary

At a fundamental level, this research project was motivated by the need to reduce the various impacts of agriculture on the environment. This study was part of a larger effort to develop variable rate technologies for herbicide and fertilizer applications. The basic objective of this study was to investigate the relationships between multi-spectral and hyper-spectral images, acquired from airborne sensors, and specific characteristics of crop canopies, under various combinations of nitrogen and weed stresses. This objective was pursued in two field studies, involving corn and soybean, with different weed control strategies in 1999, and corn at different combinations of weed control and nitrogen fertilization rates in 2000. An aircraft-mounted 24-waveband multi-spectral sensor (475-nm to 910-nm range) was used in the first year, whereas a 72-waveband hyper-spectral sensor (407-nm to 949-nm range) was at the disposal of the project in the second year. In 1999, it was only possible to obtain one image of the experimental field (24 plots, 3m x 3m dimension) from the airborne sensor. The 1999 field season was considered a preliminary study, because many adjustments were made to the methodology, upon critical evaluation of the 1999 data.

Three images were taken in the year 2000; one during early growth, one when the corn had developed tassels, and one at full maturity (kernels filled). Plot dimensions were 20m x 20m (total of 48 plots). Spectral measurements were also made at the canopy level (512-waveband field spectroradiometer) and several crop physiological parameters were measured with specialized instrumentation. Additional work involved weed population assessment.

The ultimate aim of data analysis was to determine whether the accuracy level of aerial imagery could be classified into categories, representing the combinations of the two factors controlled in the field experiments. Regression analysis was used to determine which wavebands and waveband ratios were most closely associated with

canopy conditions. Based on the results of this approach, it was decided to investigate the classification accuracies that might be attained by data mining techniques (specifically, the C&RT decision tree algorithm and back-propagation ANNs), five well-known classifiers, and also two classification techniques that have gained substantial recognition in image analysis and mapping in recent years, that of spectral angle mapping and linear unmixing.

7.2 Conclusions

There are several general conclusions that may be drawn from the work presented here. As such, these will be presented in an order reflecting the chronological order of the work presented in the main chapters of the thesis.

(1) The preliminary study (of 1999), that explored the potential of a multi-spectral airborne system in detecting weed infestations in corn and soybean crops, confirmed several of the opinions expressed in the literature. The results showed the encouraging potential of aerial multi-spectral systems in discriminating between weed-free and weed-infested areas in a crop. However, it was difficult to distinguish velvetleaf and grassy weed treatments from either the mixed weed or weed-free treatments. In general, better results were obtained for the distinction between weed-free and various weed-infested treatments with the ratio of radiance in the red and near-infrared wavebands. Investigations also indicated strong correlations between spectral data and various crop biophysical parameters.

However, a closer visual inspection of the spectra indicated that the radiance spectra obtained over the corn and soybean crops differed primarily in magnitude of radiance, because the shapes of the spectra were very nearly identical. This phenomenon was the case, whether the spectra were compared with respect to weed control strategies within a crop, or with respect to the same control strategy observed for both of the two crops. Thus, spectra obtained during the vegetative growth of vegetation predominantly indicated differences in canopy density rather than type of vegetation. The differences in the spectral signatures of corn, soybean and the weeds involved in this study were too subtle to be detected from images with limited

spectral resolution, and all the more so from images taken at the spatial resolution available, at the altitude measured (1m x 1m), because the proportion of reflected spectrum due to the crop far outweighs that of the weeds.

There is support in the literature for these conclusions, with findings indicating that different weed species could best be discriminated at the flowering stage, because the spectral signatures differed due to color differences in flowers (Lass and Callihan, 1997). Furthermore, several authors, working with spectral measurements obtained at various altitudes or in leaf-scale studies, have suggested that higher spectral resolution would be necessary to provide better discrimination between weeds and crops. It is perhaps best not to venture any further in drawing conclusions from the first year of study, because the aircraft data were essentially limited due to the small plot size and radiance values, and the resultant difficulty posed by the quantitative comparison of results. Suffice it to say that the results from the preliminary study led to an improved methodology in the second year.

(2) The second year of the field experiment was the subject of the material presented in Chapters 4, 5 and 6. The study, using hyper-spectral airborne and field sensors to detect weed infestations and nitrogen stresses, suggested that the reflectance of the corn crop was significantly influenced ($\alpha=0.05$) in certain wavebands by the presence of weeds, the nitrogen rate and the interaction between the two. Aerial observations indicated that the nitrogen effect was detectable in many wavelength regions, at all three growth-stages. However, differences in response due to nitrogen stress were most evident, at 498 nm and 671 nm, in the aerial data set. In these particular wavebands, differences due to nitrogen levels were observed at all growth stages because no interaction effect was found with weeds. From the aerial platform, the influence of weeds was most easily observed at the tasseling stage of the corn crop. Wavelengths from 520 to 603 nm and 701 to 939 nm were useful in detecting different weed infestations. In general, the study suggested that high and low nitrogen effect in corn could easily be differentiated in many spectrum regions. However, the selection of appropriate wavebands was very crucial, in order to separate all three nitrogen levels. Similarly, weed-free corn plots could be separated

from no weed control plots in more spectrum regions. However, in order to separate the presence of more specific weeds in corn, differences in spectral values existed in a few spectral regions. Importantly, the most significant wavelength regions for differentiating weed and nitrogen treatments were different. The choice of optimal wavelength regions also depended upon the growth stage of the crop.

In general, efforts to develop functional relationships, using hyper-spectral observations (aerial and field) and various crop biophysical parameters, indicated that predictive models with $r^2 > 0.9$ could be developed for various crop physiological parameters, based on the spectral data. Highly significant models could also be developed for crop yield estimation using spectral observations. For aerial spectral data sets, linear models were also developed using normalized difference vegetation indices (NDVI). Better results were obtained when NDVI values were utilized for the development of models, rather than using model based on 5-waveband reflectance values. In general, 701-nm and 839-nm wavebands were found to be the most useful for the development of NDVI-based models.

The comparison between models, based on hyper-spectral data acquired from the airborne sensor and those obtained from the ground-based platform (Chapter 4), led to the conclusion that there was a comparative mismatch between resolution and sampling coverage between the two systems. Aerial platforms provided better representative values by averaging out the natural variation across a plot, which resulted in less variation across the same treatment plots. High variation resulted in different plots of the same treatment because of lower sampling coverage of the ground-based system.

The regression models representing the relationships between data obtained from the air and crop physiological parameters were significant for the most part. ANOVA results relating aerial spectral data to the split-plot experiment with weed control strategies and nitrogen fertilization rates were also statistically significant in certain respects. However, neither type of the aforementioned models could be considered adequate for the purposes of precision application of agricultural inputs.

The main problem with the regression models, aside from measurement errors, involving reflectance data or ratios of reflectance, and crop physiological

parameters, is that the pixels associated with specific parts of an image do not have a one-to-one relationship with the ground-truth measurements. Complexity is added, due to the fact that each pixel in the image represents a complex response of a ground parcel, wherein the proportional coverage of crop, weed, and soil vary from pixel to pixel. Thus, the variability among pixels pertaining to a particular sub-plot could not be fully associated with the variability in the samples of a given parameter in the sub-plot. This latter problem leads to a distortion of the relationships. On the other hand, the fact that the relationships tended to be closer when the ratios were used, points to the complexity of the influences of weeds and nitrogen status on the radiation reflected by the canopy. With respect to ANOVA and contrasts, the situation is analogous in that the weed control strategies do not create the perfect conditions (uniform weed density and weed composition) across the replicates associated with a specific nitrogen level, because of natural variation. These considerations lead to the conclusion that a more complete sampling should be carried out at the ground, and that much better results might be obtained if data from pixels were associated with the closest reference measurement taken at canopy level. However, collection of such extensive information (pixel wise) and ensuring proper geo-referencing of each ground sampling point to image pixel, will again be a practical and technological challenge.

(3) With respect to classification by decision trees and ANNs (Chapter 5) and the seven other classifiers described in Chapter 6, the main conclusion drawn is that not one stood out as “better” than the others. Classification accuracy was similar (i.e. poor) when all nine treatment combinations were treated as categories; accuracy was adequate to good when the categories involved levels of individual treatments only; and very good to excellent accuracy when the classification problems involved pairs of levels within a treatment. This points back to the limitations of the data, more specifically to the spatial resolution of the data acquired from the airborne sensor. Ideally, pixels should be associated with weed or crop; however this is impossible in practice unless the aerial imagery is obtained before corn leaves from different rows overlap and imagery is acquired at higher spatial resolution.

On another note, all of the classification techniques explored have strong underlying similarities in terms of the how their respective mathematics or probabilistic criteria are applied to partition the data, and it is therefore not surprising that not one was prominent. However, further exploration with other data processing may lead to refinement in the results.

(4) When considering the results as a whole, in light of the limitations of the methods used, there is sufficient evidence that hyper-spectral data acquired from an airborne sensor, at a spatial resolution of 2m x 2m, may be used to detect nitrogen stress and weed infestations in a corn crop, given appropriate ground-truthing. It is not clear whether this is due to the combined influences on the quantities of biomass in the various sub-plots, or to a detectable change in the spectral signature of the corn. In either case, the practical problem that becomes evident is that the time, during the growing season at which the best discrimination may be obtained, is too late in the growing season (tassel stage). As a result, little flexibility is available in management to improve conditions during the same growing season. However, some studies also suggest that weed aggregations are stable at a specific location over time. In such situations, weed mapping could be useful in site-specific weed management for the following year as well. The detection of weeds at later stages is also important because adopting appropriate measures at this stage for stopping seed production and reproduction could control further propagation and the spreading of weeds in the next year and into newer fields. Furthermore, information on nitrogen status at the latter stage in the season could serve as a guide to investigate the problematic areas in the field.

Thus, it may be concluded that this study clearly demonstrated that multi-spectral and hyper-spectral remote sensing technologies have the definite potential of detecting weed infestations and nitrogen stress in corn. These stresses are detectable even when both are present simultaneously. On a note of caution, that the data acquired from the airborne sensors with the resolution available and analyzed with the methods used in this study, do not fully satisfy the requirements of PCM. However, this study suggests that with an improvement in the following: spatial coordination of

aerial and ground-truth sampling, more refined data analysis, and somewhat better spatial resolution from the airborne sensors, it should be possible to produce maps of nitrogen levels and weed status of sufficient accuracy, to be used to provide control data to the variable rate technologies, required for precision crop management.

CHAPTER 8

CONTRIBUTIONS TO KNOWLEDGE AND SUGGESTIONS FOR FUTURE RESEARCH

8.1 Contributions to Knowledge

The following are specific original contributions to knowledge made from this study:

1. To the author's knowledge, this is the first field study investigating the potential of hyper-spectral airborne sensors to monitor corn growth, under the combined influence of different weed management strategies and nitrogen fertilization rates. A number of useful wavelength regions and ratios have been identified, to provide a more efficient application of remote sensing platforms to differentiate among various weed infestation conditions, and also to detect nitrogen stress. The conclusions of this study could have a direct bearing on the direction of future research on the development of airborne systems capable of providing maps of the variability of factors critical to crop growth. In such a way, this study contributes to the development of systems for precision crop management in eastern Canada.
2. A number of functional relationships were developed between hyper-spectral data and crop biophysical parameters. Such relationships would be important in time-critical and site-specific decision-making, to enable optimal allocation of economically and environmentally crucial resources. These relationships may be coupled with crop growth models for better predictions of crop growth. This study also indicated that, even under variable growth conditions (due to weed and nitrogen), highly significant models may be developed for early yield prediction using hyper-spectral data.

3. Decision trees and artificial neural network algorithms may be used to classify highly complex, hyper-spectral aerial data sets. The results indicated that these algorithms have a strong potential when applied to agricultural remote sensing applications. The literature review indicated that the application of decision tree algorithms, to classify aerial hyper-spectral data sets acquired over an agricultural field, was the first of its kind.

8.2 Suggestions for Further Research

1. There is a need to determine how the spatial resolution of the airborne sensing system needs to be improved to achieve the underlying aim of the research presented here: i.e., to develop accurate maps of the weed and nitrogen status of crop canopies. Should a similar field experiment be set up in the future, it is suggested that the area should be scanned from different altitudes with the airborne hyper-spectral sensor; and that a moving bridge system should be set up to permit full-coverage scanning with a field spectroradiometer just over the tops of the canopies. Efforts should also be made to note the exact positions of all accessory measurements (LAI, greenness, etc.) so as to permit them to be properly referenced to the pixel data. Efforts should also be made to obtain the cooperation of farmers using different cultural techniques to permit flights and ground-truthing in full-scale agricultural productions.
2. There is also a need to obtain accurate spectral signatures of crops and their predominant weeds at various stages of development. This is required in order to achieve a more refined analysis of spectral imagery. With the assumption that there are significant differences between the signatures, it would then be necessary to determine whether the airborne sensor is sensitive enough to detect them. This kind of information was not available at the time of the present study.

3. One of the problems in this study was the difficulty in separating the weed control strategies during ANOVA and classification. This was partly due to the fact that, under field conditions, it is difficult to create perfect homogeneous conditions in the replicates associated with three of the weed control strategies. As seen in the first year, weed density in the corn plots was about double that of the soybean plots. There were also some differences in weed density within crop types, as well as variability among replicates within treatment combinations. It was possible to separate full weed control from no weed control (mixed weeds), but not corn plots with velvetleaf only from corn with no weeds, or corn plots with grassy weeds from corn plots with no weeds, or corn plots with velvetleaf only from corn plots with grasses only. Therefore, it is necessary to develop equivalencies between various types of weed, in order to be able to account for differences in reflectance caused by weed density.
4. Researchers have used various other statistical approaches to analyze remote sensing data; therefore, other data analysis techniques may also be explored to improve upon these results. It is suggested that the data from this study may be statistically pre-processed to find an orthogonal set of discriminators, which can then be used to train decision trees and/or ANNs, in order to classify the data into categories of treatment combinations.
5. Further research is recommended on the sensitivity of remote sensing instruments in the detection of nitrogen stress at the canopy scale, under varying planting densities and changing canopy architectures due to nitrogen levels. Efforts could also be made to develop better relationships with more levels of nitrogen fertilization. It is further recommended to examine the effect of other different factors on reflectance, such as soil moisture, organic matter, and crop residue.

6. Another important area, which could be explored, involves coupling remote sensing systems and ground-based real-time weed or nitrogen sensing systems. Currently, extensive efforts are being made by researchers to develop ground-based systems for weed control and fertilizer applications. Instead of using remote sensing, as a stand-alone system to develop weed or nitrogen variability maps, remote sensing could be used as the secondary source of information, in order to further improve upon the efficiency of ground-based systems.

CHAPTER 9

REFERENCES

- Adams, M. L., W. A. Norvell, W. D., Philpot, and J. H. Peverly. 2000. Spectral detection of micronutrient deficiency in 'Bragg' soybean. *Agronomy J.* 92(2): 261-268.
- Adcock, T. E., F. W. Nutter, Jr., and P. A. Banks. 1990. Mapping herbicides injury to soybean (*Glycine max.*) using a radiometer. *Weed Sci.* 38(6): 625-627.
- Anderson, J. E., R. I. Fischer, and S. R. Deloach. 1999. Remote sensing and precision agriculture: ready for harvest or still maturing. *Photogrammetric Engineering and Remote Sensing* 65(10): 1118-1123.
- AnswerTree 2.0 *User's Guide*. 1998. SPSS Inc., Chicago, IL.
- Arnon, D. I. 1949. Copper enzymes in isolated chloroplasts polyphenoloxidase in *Beta vulgaris*. *Plant Physiology* 24(1): 1-15.
- Asrar, G., E. T. Kanemasu, and M. Yoshida. 1985. Estimation of leaf area index from spectral reflectance of wheat under different cultural practices and solar angle. *Remote Sens. Environ.* 17(1): 1-11.
- Atkinson, P. M., and A. R. L. Tatnall. 1997. Neural networks in remote sensing. *Int. J. Remote Sens.* 18(4): 699-709.
- Augusteijn, M. F., and C. E. Warrender. 1998. Wetland classification using optical and radar data and neural network classification. *Int. J. Remote Sens.* 19(8):1545-1560.
- Augusteijn, M. F., L. E. Clemens, and K. A. Shaw. 1995. Performance evaluation of texture measures for ground cover identification in satellite image by means of a neural network classifier. *IEEE Transactions on Geoscience and Remote Sensing* 33(3): 616-626.
- Bajwa, S. G., and L. F. Tian. 2001. Aerial CIR remote sensing for weed density mapping in a soybean field. *Transactions of the ASAE* 44(6): 1965-1974.

- Bankert, R. L. 1994. Cloud classification of AVHRR imagery in maritime regions using a probabilistic neural network. *Journal of Applied Meteorology* 33:322-333.
- Baret, F., J. G. P. W. Clevers, and M. D. Steven. 1995. The robustness of canopy gap fraction estimate from red and near-infrared reflectance: a comparison of approaches. *Remote Sens. Environ.* 54(2): 141-151.
- Baret, F., S. Jacquemoud, G. Guyot, and C. Leprieur. 1992. Modeled analysis of the biophysical nature of spectral shift and comparison with information content of broad bands. *Remote Sens. Environ.* 41: 133-142.
- Bausch, W. C., and H. R. Duke. 1996. Remote sensing of plant nitrogen status in corn. *Transactions of the ASAE* 39(5): 1869-1875.
- Blackmer, T. M., and J. S. Schepers. 1995. Use of a chlorophyll meter to monitor N status and scheduling fertilization of corn. *J. Prod. Agric.* 8(1): 56-60.
- Blackmer, T. M., and S. E. White. 1998. Using precision farming technologies to improve management of soil and fertilizer nitrogen. *Aust. J. Agric. Res.* 49(3): 555-564.
- Blackmer, T. M., J. S. Schepers, and G. E. Varvel. 1994a. Light reflectance compared with other nitrogen stress measurements in corn leaves. *Agronomy J.* 86(6): 934-938.
- Blackmer, T. M., J. S. Schepers, and G. E. Meyer. 1994b. Remote sensing to detect nitrogen deficiency in corn. In: *Proceeding of Site-Specific Management for Agricultural Systems eds. Robert, P.C., Rust, R. H., Larson, W. E., Second International Conference: ASA, CSSA, SSSA, Madison, WI* pp: 505-512.
- Blackmer, T. M., J. S. Schepers, G. E. Varvel, and E. A. Walter-Shea. 1996a. Nitrogen deficiency detection using reflected shortwave radiation from irrigated corn canopies. *Agronomy J.* 88(1): 1-5.
- Blackmer, T. M., J. S. Schepers, G. E. Varvel, G. E. Meyer. 1996b. Analysis of aerial photographs for nitrogen stress within corn fields. *Agronomy J.* 88(5): 729-733.

- Bouman, B. A. M. 1992. Linking physical remote sensing models with crop growth simulation models, applied for sugar beet. *Int. J. Remote Sens.* 13(14): 2565-2581.
- Breiman, L., J. H. Friedman, R. A. Olshen, and C. J. Stone. 1984. *Classification and Regression Trees*. Belmont, CA:Wadsworth.
- Brisco, B., R. J. Brown, T. Hirose, H. McNairn, and K. Staenz. 1998. Precision agriculture and the role of remote sensing: a review. *Canadian J. of Remote Sensing* 24 (3): 315-327.
- Brown, R. B., and J.-P. G. A. Steckler. 1993. Weed patch identification in no-till corn using digital imagery. *Canadian J. of Remote Sensing* 19(1): 88-91.
- Brown, R. B., and J.-P. G. A. Steckler. 1995. Prescription maps for spatially variable herbicide application in no-till corn. *Transactions of the ASAE* 38(6): 1659-1666.
- Brown, R. B., J.-P. G. A. Steckler, and G. W. Anderson. 1994. Remote sensing for identification of weeds in no-till corn. *Transactions of the ASAE* 37(1): 297-302.
- Brown, R. J., B. Guindon, P. M. Teillet, and D. G. Goodenough. 1984. Crop type determination from multitemporal SAR imagery. *Ninth Canadian Symposium on Remote Sensing, St. John's, Nfld., Aug. 14-17*, pp: 683-692.
- Brown, R. J., H. Staenz, H. McNairn, B. Hopp, and R. van Acker. 1997. Application of high resolution optical imagery to precision agriculture. *20th Canadian Remote Sensing Symposium, Calgary, Canada, May, 1998*.
- Buschmann, C., and E. Nagel. 1993. In vivo spectroscopy and internal optics of leaves as basis for remote sensing of vegetation. *Int. J. Remote Sens.* 14(4): 711-722.
- Cardina, J., D. H. Sparrow, and E. L. McCoy. 1995. Analysis of spatial distribution of common lambsquarters (*Chenopodium album*) in no-till soybean (*Glycine max.*). *Weed Sc.* 43(2): 258-268.
- Carlson, T. N., W. J. Capehart, and R. R. Gillies. 1995. A new look at the simplified method for remote sensing of daily evapotranspiration. *Remote Sens. Environ.* 54(2): 161-167.

- Carr, P. M., G. R. Carlson, J. S. Jacobsen, G. A. Nielsen, and E. O. Skogley. 1991. Farming soils, not fields: A strategy for increasing fertilizer profitability. *J. Prod. Agric.* 4(1): 57-61.
- Chappelle, E. W., M. S. Kim, and J. E. McMurtrey. 1992. Ratio analysis of reflectance spectra (RARS): an algorithm for the remote estimation of the concentration of chlorophyll a, chlorophyll b, and carotenoid in soybean leaves. *Remote Sens. Environ.* 39: 239-247.
- Clevers, J. G. P. W. 1997. A simplified approach for yield prediction of sugar beet based on optical remote sensing data. *Remote Sens. Environ.* 61(2): 221-228.
- Clevers, J. G. P. W., C. Büker, H. J. C. van Leeuwen, and B. A. M. Bouman. 1994. A framework for monitoring crop growth by combining directional and spectral remote sensing information. *Remote Sens. Environ.* 50(2): 161-170.
- Cloutis, E. A., D. R. Connery, and F. J. Dover. 1999. Agricultural crop monitoring using airborne multi-spectral imagery and C-band synthetic aperture radar. *Int. J. Remote Sens.* 20(4): 767-787.
- Cloutis, E. A., D. R. Connery, D. J. Major, and F. J. Dover. 1996. Airborne multi-spectral monitoring of agricultural crop status: effect of time of year, crop type and crop condition parameters. *Int. J. Remote Sens.* 17(13): 2579-2601.
- Crist, E. P. 1984. Effect of cultural and environmental factors on corn and soybean spectral development patterns. *Remote Sens. Environ.* 14: 3-13.
- Curran, P. J. 1985. Aerial photography for the assessment of crop condition: a review. *Applied Geography* 5(4): 347-360.
- Curran, P. J., J. A. Kupiec, and G. M. Smith. 1997. Remote sensing the biochemical composition of slash pine canopy. *IEEE Trans. Geosci. Remote. Sens.* 35(2): 415-420.
- Danaher, S., G. Herries, T. Selige, and M. M. Súirtán. 1997. A comparison of the characterization of agricultural land using singular value decomposition and neural networks. In: *Neurocomputing in Remote Sensing Data Analysis*, eds. I. Kanellopoulos, G. G. Wilkinson, F. Roli, and J. Austin. Springer-Verlag Berlin Heidelberg, New York, pp. 14-27.

- Deck, S. H., C. T. Morrow, D. H. Heinemann, and H. J. Sommer III. 1995. Comparison of a neural network approach. *Transactions of the ASAE* 39(6): 2319-2324.
- Decker, W. L. 1994. Developments in agricultural meteorology as a guide to its potential for the twenty-first century. *Agricultural and Forest Meteorology* 69: 9-25.
- Deguisse, J. C., K. Staenz, and J. Lefebvre. 1999. Agricultural application of airborne hyperspectral data: weed detection. Presented at the Fourth International Airborne Remote sensing Conference and Exhibition/21st Canadian Symposium on Remote Sensing, Ottawa, Ontario, Canada, 21-24 June.
- Delécolle, R., S. J. Maas, M. Guérif, and F. Baret. 1992. Remote sensing and crop production models present trends. *ISPRS J. Photogrammetry and Remote Sensing* 47: 145-161.
- Depenau, J. 1997. Neural networks for classification of ice type concentration from ERS-1 SAR images. *Neurocomputing in Remote Sensing Data Analysis*, eds. I. Kanellopoulos, G. G. Wilkinson, F. Roli, and J. Austin. Springer-Verlag Berlin Heidelberg, New York, pp. 71-78.
- Dwyer, L. M., M. Tollenaar, and L. Houwing. 1991. A nondestructive method to monitor leaf greenness in corn. *Can. J. Plant Sci.* 71(April): 505-509.
- Everitt, J. H., D. E. Escobar, M. A. Alaniz, M. R. Davis, and J. V. Richerson. 1996. Using spatial information technologies to map Chinese tamarisk (*Tamarix chinensis*) infestations. *Weed Sc.* 44(1): 194-201.
- Everitt, J. H., G. L. Anderson, D. E. Escobar, M. R. Davis, N. R. Spencer, and R. J. Andrascik. 1995. Use of remote sensing for detecting and mapping leafy spurge (*Euphorbia esula*). *Weed technology* 9(3): 599-609.
- Everitt, J. H., J. V. Richerson, M. A. Alaniz, D. E. Escobar, R. Villarreal, and M. R. Davis. 1994. Light reflectance characteristics and remote sensing of Big Bend loco (*Astragalus mollissimus* var. *earlei*) and Wooton loco (*Astragalus wootonii*). *Weed Sci.* 42(1): 115-122.

- Everitt, J. H., R. D. Pettit, and M. A. Alaniz. 1987. Remote sensing of Broom snakeweed (*Gutierrezia sarothrae*) and spiny aster (*Aster spinosus*). *Weed Sci.* 35(2): 295-302.
- Everitt, J. H., S. J. Ingle, H. W. Gausman, and H. S. Mayeux, Jr. 1984. Detection of false broomweed (*Ericameria austrotexana*) by aerial photography. *Weed Sci.* 32(5): 621-624.
- Fisher, R. A. 1936. The use of multiple measurements in taxonomic problems. *Annals of Eugenics* 7: 179-188.
- Foody, G. M., M. B. McCulloch, and W. B. Yates. 1994. Crop classification from C-band polarimetric radar data. *Int. J. Remote Sens.* 15(14): 2871-2885.
- Frazier, B. E., C. S. Walters, and E. M. Perry. 1997. Role of remote sensing in site-specific management. In: *The State of Site Specific Management for Agriculture*, eds. F. J. Pierce, and E. J. Sadler. ASA Misc. Publ., ASA, CSSA, and SSSA, Madison, WI. pp. 149-160.
- Friedl, M. A., and C. E. Brodley. 1997. Decision tree classification of land cover from remotely sensed data. *Remote Sens. Environ.* 61(3): 399-409.
- Friedl, M. A., C. E. Brodley, and A. H. Strahler. 1999. Maximizing land cover classification accuracies produced by decision trees at continental to global scales. *IEEE Transactions of Geoscience and Remote Sensing* 37(2): 969-977.
- Gausman, H. W. 1974. Leaf reflectance of near-infrared. *Photogrammetric Engineering and Remote Sensing* 60(2): 183-191.
- Gausman, H. W. 1977. Reflectance of leaf components. *Remote Sens. Environ.* 6:1-9.
- Gausman, H. W., and W. A. Allen. 1973. Optical parameters of leaves of 30 plant species. *Plant Physiology* 52(1): 57-62.
- Ghazanfari, A., J. Irudayaraj, and A. Kusalik. 1996. Grading pistachio nuts using a neural network approach. *Transactions of the ASAE* 39(6): 2319-2324.
- Goel, N. S. 1988. Models of vegetation canopy reflectance and their use in estimation of biophysical parameters from reflectance data. *Remote Sensing Review* 4(1):1-212.

- GopalaPillai, S., and L. Tian. 1999. In-field variability detection and spatial yield modeling for corn using digital aerial imaging. *Transactions of the ASAE* 42(6): 1911-1920.
- GopalaPillai, S., L. Tian, and J. Beal. 1998. Detection of nitrogen stress in corn using digital aerial imagery. 1998 ASAE Annual International Meeting at Orlando, Paper No. 98-3030. ASAE, 2950 Niles Road, St. Joseph, MI 49085-9659 USA.
- Guyot, G. 1990. Optical properties of vegetation canopies. In *Application of Remote Sensing in Agriculture*, eds. M. D. Dteven, and J. A. Clark. Butterworths, London.
- Hall, J. C., L. L. V. Eerd, S. D. Miller, M. D. K. Owen, T. S. Prather, D. L. Shaner, M. Singh, K. C. Vaughn, and S. C. Weller. 2000. Future research directions for weed science. *Weed Technology* 14(3): 647-658.
- Hansen, M., R. Dubayah, and R. DeFries. 1996. Classification trees: an alternative to traditional land cover classifiers. *Int. J. Remote Sens.* 17(5): 1075-1081.
- Hanson, L. D., P. C. Robert, and M. Bauer. 1995. Mapping wild oat infestations using digital imagery for site-specific management. In: *The State of Site Specific Management for Agriculture*, eds. F. J. Pierce, and E. J. Sadler. ASA Misc. Publ., ASA, CSSA, and SSSA, Madison, WI. pp. 495-504.
- Hatfield, J. L., and P. J. Pinter, Jr. 1993. Remote sensing for crop protection. *Crop Protection* 12(8): 403-413.
- Hayes, M. J., and W. L. Decker. 1998. Using satellite and real-time weather data to predict maize production. *International Journal of Biometeorology* 42(1): 10-15.
- Hepner, G. F., T. Logan, N. Ritter, and N. Bryant. 1990. Artificial neural network classification using a minimal training set: comparison to conventional supervised classification. *Photogrammetric Engineering and Remote Sensing* 56(5): 469-473.
- Hill, M. J., G. E. Donald, P. J. Vickery, and E. P. Furnival. 1996. Integration of satellite remote sensing, simple bioclimatic models and GIS for assessment of

- pastoral development for a commercial grazing enterprise. *Australian Journal of Experimental Agriculture* 36(3): 309-321.
- Hill, M. J., G. E. Donald, P. J. Vickery, A. D. Moore, and J. R. Donnelly. 1999. Combining satellite data with a simulation model to describe spatial variability in pasture growth at a farm scale. *Australian Journal of Experimental Agriculture* 39(3): 285-300.
- Holben, B. N., C. J. Tucker, and Cheg-Jeng Fan. 1980. Spectral assessment of soybean leaf area and leaf biomass. *Photogrammetric Engineering and Remote Sensing* 46(5): 651-656.
- Horler, D. N. H., M. Dockray, and J. Barber. 1983. The red edge of plant leaf reflectance. *Int. J. Remote Sens.* 4(2): 273-288.
- Hruschka, W. R. 1987. Data analysis: wavelength selection methods. In: *Near-Infrared Technology in the Agricultural and Food Industries*, eds. P. C. Williams and K. H. Norris. St. Paul, MN: American Association of Cereal Chemists, pp. 35-55.
- Ingleby, H. R., and T. G. Crowe. 2000. Reflectance models for predicting organic carbon on Saskatchewan soils. *Canadian Agricultural Engineering* 42(2): 57-63.
- Inoue, Y., and S. Morinaga. 1995. Estimating spatial distribution of plant growth in a soybean field based on the remotely-sensed spectral imagery measured with a balloon system. *Jpn. J. Crop. Sci.* 64(1): 156-158
- Inoue, Y., S. Morinaga, and A. Tomita. 2000. A blimp-based remote sensing system for low-altitude monitoring of plant variables: a preliminary experiment for agriculture and ecological applications. *Int. J. Remote Sens.* 21(2): 379-385.
- Jackson, R. D., and A. R. Huete. 1991. Interpreting vegetation indices. *Prevent. Vet. Med.* 11: 185-200.
- Jackson, R. D., and P. J. Pinter Jr. 1986. Spectral response of architecturally different wheat canopies. *Remote Sens. Environ.* 20(1): 43-56.
- Jago, R. A., M. E. J. Cutler, and P. J. Curran, 1999. Estimating canopy chlorophyll concentration from field and airborne spectra. *Remote Sens. Environ.* 68(3): 217-224.

- James, L. D., and S. J. Burges. 1982. Selection, calibration, and testing of hydrologic models. In: *Hydrologic Modeling of Small Watersheds*, eds. C. T. Haan, H. P. Johnson, and D. L. Brakensiek. ASAE Monograph No. 5, ASAE, St. Joseph, MI, pp. 437-472.
- Jin, Y.-Q, and C. Liu. 1997. Biomass retrieval from high-dimensional active/passive remote sensing data by using artificial neural networks. *Int. J. Remote Sens.* 18(4): 971-979.
- Joel, G., J. A. Gamon, and C. B. Field. 1997. Production efficiency in sunflower: the role of water and nitrogen stress. *Remote Sens. Environ.* 62(2): 176-188.
- Johnson, G. A., J. Cardina, and D. A. Mortensen. 1997. Site-specific weed management: current and future direction. In: *The State of Site Specific Management for Agriculture*, eds. F. J. Pierce, and E. J. Sadler. ASA-CSSA-SSSA, Madison, WI53711, USA, 131-147.
- Johnson, L. F., C. A. Hlavka, and D. L. Peterson. 1994. Multivariate analysis of AVIRIS data for canopy biochemistry estimation along the Oregon transect. *Remote Sens. Environ.* 47(2): 216-230.
- Kanellopoulos, I., A. Varfis, G. G. Wilkinson, and J. Mégier. 1992. Land-cover discrimination in SPOT HRV imagery using an artificial neural networks: a 20-class experiment. *Int. J. Remote Sens.* 13(5): 917-924.
- Kimes, D. S., B. N. Holben, J. E. Nickeson, and A. McKee. 1996. Extracting forest age in a pacific northwest forest from thematic mapper and topographic data. *Remote Sens. Environ.* 56(2): 133-140.
- Kimes, D. S., K. J. Ranson, and G. Sun. 1997. Inversion of a forest backscatter model using neural networks. *Int. J. Remote Sens.* 18(10): 2181-2199.
- Kimes, D. S., R. F. Nelson, M. T. Manry, and A. K. Fung, 1998. Attribute of neural networks for extracting continuous vegetation variables from optical and radar measurements. *Int. J. Remote Sens.* 19(14): 2639-2663.
- Klemm, J., and E. Fagerlund. 1987. Influence of different nitrogen and irrigation treatments on the spectral reflectance of barley. *Remote Sens. Environ.* 21(1): 1-14.

- Knipling, E. B. 1970. Physical and physiological basis for the reflectance of visible and near-infrared radiation from vegetation. *Remote Sens. Environ.* 1: 155-159.
- Krause, G. H., and E. Weis. 1991. Chlorophyll fluorescence and photosynthesis: the basics. *Annu. Rev. Physiol. Plant Mol. Biol.* 42: 313-349
- Kruse, F. A., A. B. Lefkoff, J. B. Boardman, K. B. Heidebrecht, A. T. Shapiro, P. J. Barloon, and A. F. J. Goetz. 1993. The Spectral Image Processing System (SIPS)- interactive visualization and analysis of imaging spectrometer data. *Remote Sens. Environ.* 44: 145-163.
- Lacroix, R., F. Salehi, X. Z. Yang and K. M. Wade. 1997. Effects of data processing on the performance of artificial neural networks for dairy yield prediction and cow culling classification. *Transactions of the ASAE* 40(3) : 839-846.
- Lamb, D. W. 1998. Opportunity for satellite and airborne remote sensing of weeds in Australian crops. In: *Precision Weed Management in crops and Pasture*, eds R.W. Medd, and J.E. Pratley. Proceedings of a workshop, 5-6 May, 154 pp. (CRC for Weed Management Systems, Adelaide).
- Lamb, D. W. 2000. The use of qualitative airborne multispectral imaging for managing agricultural crops-a case study in south-eastern Australia. *Australian Journal of Experimental Agriculture* 40(5): 725-738.
- Lamb, D. W., and M. Weedon. 1998. Evaluating the accuracy of mapping weeds in fallow fields using airborne digital imaging: *Panicum effusum* in oilseed rape stubble. *Weed Research* 38(6): 443-451.
- Lamb, D. W., and R. B. Brown. 2001. Remote-sensing and mapping of weeds in crops. *J. Agric. Engng Res.* 78 (2): 117-125.
- Lamb, D. W., M. M. Weedon, and L. J. Rew. 1999. Evaluating the accuracy of mapping weeds in seedling crops using airborne digital imaging: *Avena spp.* in seedling triticale. *Weed research* 39(6): 481-492.
- Lass, L. W., and R. H. Callihan. 1997. The effect of phenological stage on detectability of Yellow Hawkweed (*Hieracium pratense*) and Oxeye Daisy (*Chrysanthemum leucanthemum*) with remote multispectral digital imagery. *Weed Technology* 11(2): 248-256.

- Lass, L. W., H. W. Carson, and R. H. Callihan. 1996. Detection of yellow starthistle (*Centaurea solstitialis*) and common St. Johnswort (*Hypericum perforatum*) with multispectral digital imagery. *Weed Technology* 10 (3): 466-474.
- Lee, J., R. C. Weger, S. K. Sengupta, and R. M. Welch. 1990. A neural network approach to cloud classification. *IEEE Transactions on Geoscience and Remote Sensing* 15: 3263-3270.
- Lillesand, T. M., and R. W. Kiefer. 2000. Remote Sensing and Image Interpretation. John Wiley and Sons, Inc., 605 Third Avenue, New York.
- Lukina, E. V., W. R. Raun, M. L. Stone, J. B. Solie, G. V. Johnson, H. L. Lees, J. M. LaRuffa, and S. B. Phillips. 2000. Effect of row spacing, growth stage, and nitrogen rate on spectral irradiance in winter wheat. *J. Plant Nutrition* 23(1): 103-122.
- Ma, B. L., M. J. Morrison, and L. M. Dwyer. 1996. Canopy light reflectance and field greenness to assess nitrogen fertilization and yield of maize. *Agronomy J.* 88(6): 915-920.
- Martin, M. E., and J. D. Aber. 1997. High spectral resolution remote sensing of forest canopy lignin, nitrogen, and ecosystem processes. *Ecological Applications* 7(2): 431-443.
- Matson, P., L. Johnson, C. Billow, J. R. Miller, and R. Pu. 1994. Seasonal patterns and remote spectral estimation of canopy chemistry across the Oregon transect. *Ecological Applications* 4(2): 280-298.
- Mazer, A. S., M. Martin, M. Lee, and J. E. Solomon. 1988. Image processing software for imaging spectrometry analysis. *Remote Sens. Environ.* 24(1): 201-210.
- Medlin, C. R., D. R. Shaw, P. D. Gerard, and F. E. LaMastus. 2000. Using remote sensing to detect weed infestation in *Glycine Max*. *Weed Sci.* 48(3): 393-398.
- Menges, R. M., P. R. Nixon, and A. J. Richardson. 1985. Light reflectance and remote sensing of weeds in agronomic and horticultural crops. *Weeds Sci.* 33(4): 569-581.

- Miller, J. R., E. W. Hare, and J. Wu. 1990. Quantitative characterization of the vegetation red edge reflectance 1. An inverted-Gaussian reflectance model. *Int. J. Remote Sens.* 11(10): 1755-1773.
- Moran, M. S., S. J. Mass, and P. J. Pinter Jr. 1995. Combining remote sensing and modeling for estimating surface evaporation and biomass production. *Remote Sensing Reviews* 12: 335-353.
- Moran, M. S., Y. Inoue, and E. M. Barnes. 1997. Opportunities and limitations for image-based remote sensing in precision crop management. *Remote Sens. Environ.* 61(3): 319-246.
- Moulin, S., A. Bondeau, and R. Delecolle. 1998. Combining agriculture crop models and satellite observations: from field to regional scale. *Int. J. Remote Sens.* 19(6): 1021-1036.
- Munden, R., P. J. Curran, and J. A. Catt. 1994. The relationship between red edge and chlorophyll concentration in the Broadbalk winter wheat experiment at Rothamsted. *Int. J. Remote Sens.* 15(3): 705-709.
- Nakano, K. 1997. Application of neural networks to the color grading of apples. *Computer and Electronics in Agriculture* 18: 105-116.
- O'Neill, N. T., F. Zagolski, M. Bergeron, A. Royer, J. Miller, and J. Freemantle. 1997. Atmospheric correction validation of CASI images acquired over the BOREAS Southern study area. *Canadian Journal of Remote Sensing* 23(2): 143-162.
- Panda, S. S., and S. Panigrahi. 2000. Analysis of remotely sensed aerial images for precision farming. Presented at the 2000 ASAE annual international meeting at Milwaukee, Wisconsin, Paper No. 003055, 2950 Niles road, St. Joseph, MI 49085-9659 USA.
- Patel, N. K., C. Patnail, S. Dutta, A. M., Shekh, and A. J. Dave. 2001. Study of crop growth parameters using airborne imaging spectroradiometer. *Int. J. Remote Sens.* 22(12): 2401-2411.
- Peñuelas, J., J. A. Gamon, A. L. Fredeen, J. Merino, and C. B. Field. 1994. Reflectance indices associated with physiological changes in nitrogen- and water-limited sunflower leaves. *Remote Sens. Environ.* 48(2): 135-146.

- Perry Jr., C. R., 1984. Functional equivalence of spectral vegetation indices. *Remote Sens. Environ.* 14(1-3): 169-182.
- Peterson, D. L., J. D. Aber, P. A. Matson, D. H. Card, N. Swanberg, C. Wessman, and M. Spanner. 1988. Remote sensing of forest canopy and leaf biochemical contents. *Remote Sens. Environ.* 24(1): 85-108.
- Pierce, F. J., and P. Nowak. 1999. Aspects of precision agriculture. *Advances in Agronomy* 67: 1-85.
- Pierce, L. E., K. Sarabandi, and F. T. Ulaby. 1994. Application of an artificial neural network in canopy scattering inversion. *Int. J. Remote Sens.* 15(16): 3263-3270.
- Plant, R. E. 2001. Site-specific management: the application of information technology to crop production. *Computer and Electronics in Agriculture* 30(1-3): 9-29.
- Plant, R. E., D. S. Munk, B. R. Roberts, R. L. Vargas, D. W. Rains, R. L. Travis, and R.B. Hutmacher. 2000. Relationship between remotely sensed reflectance data and cotton growth and yield. *Transactions of the ASAE* 43(3): 535-546.
- Ponzoni, F.J., and J. L. de M. Goncalves. 1999. Spectral feature associated with nitrogen, phosphorous, and potassium deficiencies in *Eucalyptus saligna* seedling leaves. *Int. J. Remote Sens.* 20(11): 2249-2264.
- Pu, R., and P. Gong. 2000. Band selection from hyperspectral data for conifer species identification. *Geographic Information Sciences* 6(2): 137-142.
- Quinlan, J. R. 1993. C4.5: Programs for Machine Learning. San Mateo, CA: Morgan Kaufmann.
- Reichenberger, L., and J. Russnogle. 1989. Farm by the foot. *Farm J.* 113(6): 11-15.
- Rew, L. J., B. Whelan, and A. B. Mcbratney. 2001. Does kriging predict weed distribution accurately enough for site-specific weed control? *Weed Research* 41(3): 245-263.
- Richard, J. A. 1994. Remote Sensing Digital Image Analysis. Springer-Verlag, Berlin.

- Saha, S. K., and S. Jonna. 1994. Paddy acreage and yield estimation and irrigated cropland inventory using satellite and agrometeorological data. *Asian Pasific Remote Sensing Journal* 6(2): 79-87.
- Schalkoff, R. J. 1992. Pattern Recognition: Statistical, Structural and Neural Approach. J. Wiley, New York.
- Schepers, J. S., D. D. Francis, M. F. Vigil, and F. E. Below. 1992. Comparison of corn leaf nitrogen concentration and chlorophyll meter reading. *Commun. Soil Sci. Plant Anal.* 23(17-20): 2173-2187.
- Schilfgaard, J. V. 1999. Is precision agriculture sustainable? *American Journal of Alternative Agriculture* 14(1): 43-46.
- Senay, G. B., A. D. Ward, J. G. Lyon, N. R. Fausey, and S. E. Nokes. 1998. Manipulation of high spatial resolution aircraft remote sensing data for use in site-specific farming. *Transactions of the ASAE* 41(2): 489-495.
- Serrano, L., I. Filella, and J. Peñuelas. 2000. Remote sensing of biomass and yield of winter wheat under different nitrogen supplies. *Crop Science* 40(3): 723-731.
- Shanahan, J. F., J. S. Schepers, D. D. Francis, G. E. Varvel, W. W. Wilhelm, J. M. Tringe, M. R. Tringe, M. R. Schlemmer, and D. J. Major. 2001. Use of remote-sensing imagery to estimate corn grain yield. *Agronomy J.* 93(3): 583-589.
- Singh, R. K., B. Engel, and M. Provancha. 1998. Remote sensing image analysis using a neural net classification scheme. Presented at the 1998 ASAE annual international meeting at Orlando, Florida, Paper No. 983038, 2950 Niles road, St. Joseph, MI 49085-9659 USA.
- Smith, J. A. 1993. LAI inversion using a back-propagation neural network trained with multiple scattering model. *IEEE Transactions on Geoscience and Remote Sensing* 31(5):1102-1106.
- Soh, L. K., and C. Tsatsoulis. 1999. Segmentation of satellite imagery of natural scenes using data mining. *IEEE Transactions on Geoscience and Remote Sensing* 37(2): 1086-1099.
- Stafford, J. V. 1997. Precision Agriculture '97 vol. 1: Spatial variability in Soil and Crop. Oxford: Bios Scientific Publishers Ltd.

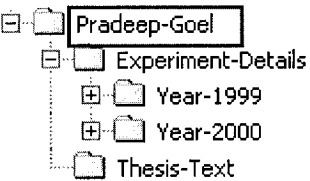
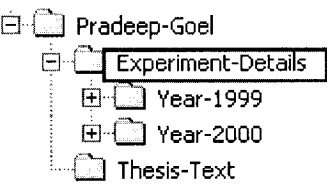
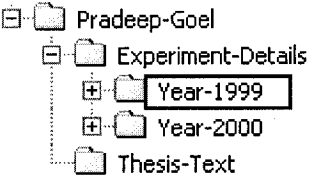
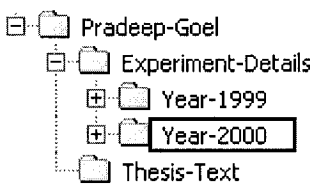
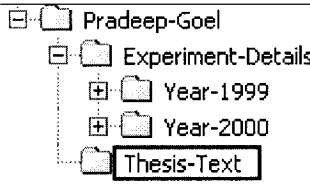
- Staenz, K. 1996. Classification of a hyperspectral agricultural data set using band moments for reduction of the spectral dimensionality. *Canadian Journal of Remote Sensing* 22(3): 248-257.
- Steckler, J.-P. G. A., and R. B. Brown. 1993 Prescription maps for herbicide spray control. ASAE paper No. 93-1070. St. Joseph, Mich., ASAE.
- Steel, R.G. D., J. H. Torrie, and D. A. Dickey. 1997. Principles and Procedures of Statistics: a Biomedical Approach. McGraw Hill, New York.
- Stevens, M. D. 1993. Satellite remote sensing for agricultural management: opportunities and logistic constraints. *ISPRS J. Photogrammetry and Remote Sensing* 48: 29-34.
- Stombaugh, T. S., and S. Shearer. 2000. Equipment technology for precision agriculture. *Journal of Soil and Water Conservation* (First Quarter): 6-11.
- Stone, M. L., J. B. Solie, W. R. Raun, R. W. Whitney, S. L. Taylor, and J. D. Ringer. 1996. Use of spectral radiance for correcting in-season fertilizer nitrogen deficiencies in winter wheat. *Transactions of the ASAE* 39(5): 1623-1631.
- Sui, R., J. B. Wikerson, W. E. Hart, and D. D. Howard. 1998. Integration of neural networks with a spectral reflectance sensor to detect nitrogen deficiency in cotton. Presented at the 1998 ASAE Annual International Meeting at Orlando, Florida, Paper No. 983104, ASAE, 2950 Niles Road, St. Joseph, MI 49085-9659 USA.
- Swain, P. H., and S. M. Davis. 1978. *Remote Sensing: The Quantitative approach*, McGraw-Hill, New-York.
- Takebe, M., T. Yoneyama, K. Inada, and T. Murakami. 1990. Spectral reflectance ratio of rice canopy for estimating crop nitrogen status. *Plant and Soil* 122(2): 295-297.
- Taylor, S. L., W. R. Raun, J. B. Solie, G. V. Johnson, M. L. Stone, and R. W. Whitney. 1998. Use of spectral radiance for correcting nitrogen deficiencies and estimating soil test variability in an established bermudagrass pasture. *J. Plant Nutrition* 21(11): 2287-2302.

- Thenkabail, P. S., R. B. Smith, and E. D. Pauw. 2000. Hyperspectral vegetation indices and their relationships with agricultural crop characteristics. *Remote Sens. Environ.* 71(2):158-182.
- Thomas, J. R., and G. F. Oerther. 1972. Estimating nitrogen content of sweet pepper leaves by reflectance measurements. *Agronomy J.* 64(1): 11-13.
- Thomas, J. R., and H. W. Gausman. 1977. Leaf reflectance vs. leaf chlorophyll and carotenoid concentration for eight crops. *Agronomy J.* 69(5): 799-802.
- Tomer, M. D., J. L. Anderson, and J. A. Lamb. 1997. Assessing corn yield and nitrogen uptake variability with digitized aerial infrared photographs. *Photogrammetric Engineering and Remote Sensing* 63(3): 299-306.
- Tucker, C. J., I. Y. Fung, C. D. Keeling, and R. H. Gammon. 1980. Remote sensing of leaf water content in the near infrared. *Remote Sens. Environ.* 10: 23-32.
- Vogelmann, T. C. 1993. Plant tissue optics. *Annu. Rev. Plant Physiol. Plant Mol. Biol.* 44: 231-251.
- Walburg, G., M. E. Bauer, C. S. T. Daughtry, and T. L. Housley. 1982. Effect of nitrogen on the growth, yield, and reflectance characteristics of corn canopies. *Agronomy J.* 74(4): 677-683.
- Wang, D., F. E. Dowell, and R. E. Lancey. 1998a. Single wheat kernel color classification using neural networks. *Transactions of the ASAE* 42(1): 233-240.
- Wang, N., N. Zhang, F. E. Dowell, and J. Kurtz. 1998b. Potential use of plant spectral characteristics in weed detection. Presented at 1998 ASAE Annual International Meeting at Orlando, Florida, Paper No. 983059, ASAE, 2950 Niles Road, St. Joseph, MI 49085-9659 USA.
- Wessman, C. A., J. D. Aber, D. L. Peterson, and J. M. Melillo. 1988. Remote sensing of canopy chemistry and nitrogen cycling in temperate forest ecosystems. *Nature* 335(8 September): 154-156.
- Wiegand, C. L., A. J. Richardson, and R. J. Nixon. 1986. Spectral component analysis: a bridge between spectral observations and agrometeorological crop models. *IEEE Trans. Geosci. Remote Sens.* GE-24: 83-88.

- Wilkinson, G. G. 1997. Open question in neurocomputing for earth observation. In: *Neurocomputing in Remote Sensing Data Analysis*, eds. I. Kanellopoulos, G. G. Wilkinson, F. Roli, and J. Austin. Springer-Verlag Berlin Heidelberg, New York, pp. 3-13.
- Yang, C.-C., S. O. Prasher, J. A. Landry, and A. DiTommaso. 2000. Application of artificial neural networks in image recognition and classification of crop and weeds. *Canadian Agricultural Engineering* 42(3): 147-152.
- Zhang, J., and G. M. Foody. 2001. Fully-fuzzy supervised classification of sub-surban land cover from remotely sensed imager: statistical and artificial neural networks approaches. *Int. J. Remote Sens.* 22(4):615-628.
- Zwiggelaar, R. 1998. A review of spectral properties of plants and their potential use for crop/weed discrimination in row-crops. *Crop Protection* 17(3): 189-206.

APPENDIX-A

Details of the content of the CD-ROM are briefly given in the table.

Directory/Subdirectory	Content
 <pre> graph TD Pradeep-Goel --> Experiment-Details Pradeep-Goel --> Year-1999 Pradeep-Goel --> Year-2000 Pradeep-Goel --> Thesis-Text </pre>	<p>The root directory contains a subdirectory <i>Pradeep-Goel</i> which is divided into two subdirectories, <i>Experiment-Details</i> and <i>Thesis-Text</i>.</p>
 <pre> graph TD Pradeep-Goel --> Experiment-Details Pradeep-Goel --> Year-1999 Pradeep-Goel --> Year-2000 Pradeep-Goel --> Thesis-Text </pre>	<p>This directory is further divided into two subdirectories. Details concerning the first year (1999) and the second year (2000) of the experiment are given in two subdirectories <i>Year-1999</i> and <i>Year-2000</i>, respectively.</p>
 <pre> graph TD Pradeep-Goel --> Experiment-Details Pradeep-Goel --> Year-1999 Pradeep-Goel --> Year-2000 Pradeep-Goel --> Thesis-Text </pre>	<p>In this directory, all the relevant details of the experiment and collected data during the first year of the study are given. The image collected from AISA sensor and collected ground data is given in the subdirectories <i>AISA-Image</i> and <i>Ground-Data</i>, respectively. Further details on these are given in the <i>readme</i> file.</p>
 <pre> graph TD Pradeep-Goel --> Experiment-Details Pradeep-Goel --> Year-1999 Pradeep-Goel --> Year-2000 Pradeep-Goel --> Thesis-Text </pre>	<p>All the details related to the second year of the study are given in the <i>Year-2000</i> directory. Hyperspectral CASI images, ASD spectral data, and other ground data are given in the subdirectories <i>CASI-Image</i>, <i>ASD-Data</i>, and <i>Ground-Data</i>, respectively. These directories are further divided into various sub-subdirectories. The names of these subdirectories are self explanatory. Further details on these are given in the <i>readme</i> file.</p>
 <pre> graph TD Pradeep-Goel --> Experiment-Details Pradeep-Goel --> Year-1999 Pradeep-Goel --> Year-2000 Pradeep-Goel --> Thesis-Text </pre>	<p>This directory contains the thesis document in MS-WORD format. Various tables and figures are given in separate files and are named according to the chapter number. Copies of the published papers are also given various subdirectories.</p>



30 April 2003

Our ref: HW/lt/May03.J001
Your ref:

Pradeep Kumar Goel
McGill University
Department of Agricultural and Biosystems Engineering

Dear Dr Goel

COMPUTERS AND ELECTRONICS IN AGRICULTURE, Vol 38, No 2, 2003, pp 99-124, Goel et al: "Potential of airborne ...": Vol 39, No 2, Goel et al: "Classification of hyperspectral .."

As per your letter dated 29 April 2003, we hereby grant you permission to reprint the aforementioned material at no charge **in your thesis** subject to the following conditions:

1. If any part of the material to be used (for example, figures) has appeared in our publication with credit or acknowledgement to another source, permission must also be sought from that source. If such permission is not obtained then that material may not be included in your publication/copies.
2. Suitable acknowledgment to the source must be made, either as a footnote or in a reference list at the end of your publication, as follows:
"Reprinted from Publication title, Vol number, Author(s), Title of article, Pages No., Copyright (Year), with permission from Elsevier".
3. Reproduction of this material is confined to the purpose for which permission is hereby given.
4. This permission is granted for non-exclusive world **English** rights only. For other languages please reapply separately for each one required. Permission excludes use in an electronic form. Should you have a specific electronic project in mind please reapply for permission.
5. This includes permission for the National Library of Canada to supply single copies, on demand, of the complete thesis. Should your thesis be published commercially, please reapply for permission.

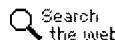
Yours sincerely

Helen Wilson
Rights Manager

Your future requests will be handled more quickly if you complete the online form at
www.elsevier.com/locate/permissions



Yahoo! - My Yahoo! - Help



Search

Go on a romantic get away



BOOK NOW

UNITED.COM

Mail Addresses Calendar Notepad

gn Out]

Check Mail

Compose

Mail Upgrades - Search Mail - Mail Options

Folders [Add]

Previous | Next | Back to Messages

Printable View - Full

Inbox

Draft

Sent

Bulk [Empty]

Trash [Empty]

Delete

Reply

Reply All

Forward

as attachment

Move to folder..

This message is not flagged. [Flag Message - Mark as Unread]

From: [this is spam | Add to Address Book]

To:

Subject: Urgent request for copyright permission

Date: Tue, 29 Apr 2003 10:22:31 -0500

How bad is your credit?

Save Air-Car-Hotel

United Escapes

FREE Fax Number

For Your Y! Mail

View Homes

for Sale &

Compare

REALTORS®

Pradeep, ASAE is pleased to grant permission. If you have any questions, please don't hesitate to contact me.

Thanks

Sandy

Sandy Rutter
American Society of Agricultural Engineers - (ASAE)
Publications Department

USA

Phone:

Fax:

E-mail:

Internet:

-----Original Message
From: Pradeep Goel
Sent: Tuesday, April 29, 2003 2:14 AM

To:
Subject: Urgent request for copyright permission

Hi!

I will be grateful if you could arrange to send me a copyright permission to include my following papers in my Ph.D. thesis. Today at the time of final submission of my thesis, I realized that as per the McGill university, this permission is necessary to accept the final copy of the thesis. Since the deadline for the final submission is very close, I will appreciate if you could either fax me at 514-398-8387 or send me as an email attachment.

I am extremely sorry for submitting this urgent request at the last moment.

1. Goel, P. K., S. O. Prasher, R. M. Patel, D. L. Smith, and A. DiTommaso. 2002. Use of airborne multi-spectral imagery for weed detection in field crops. Transactions of the ASAE 45(2): 443-449.
2. Goel, P. K., S. O. Prasher, J.-A. Landry, R. M. Patel, and A. A. Viau. 2003. Estimation of crop biophysical parameters through airborne hyper-spectral remote sensing. Transactions of the ASAE (In press, IET-600).
3. Goel, P. K., S. O. Prasher, J.-A. Landry, R. M. Patel, and A. A. Viau. Hyperspectral image classification to detect weed infestations and nitrogen status in corn. Transactions of the ASAE (In press, IET-602).

Thanks,
With regards,
Pradeep Kumar Goel

=====
Pradeep Kumar Goel
Ph.D. Candidate
Department of Agricultural and Biosystems Engineering
Macdonald Campus of McGill University

Phone:

Do you Yahoo!?
The New Yahoo! Search - Faster. Easier. Bingo.
<http://search.yahoo.com>